CYSTEINE METABOLIC REMODELING: A METABOLIC MARKER FOR CANCER AGGRESSIVENESS AND A NOVEL PUTATIVE TARGET IN ONCOLOGICAL MANAGEMENT

ANA RITA CRISPIM HIPÓLITO

Tese para obtenção do grau de Doutor em Ciências da Saúde na Especialidade de Biomedicina na Faculdade de Ciências Médicas | NOVA Medical School da Universidade NOVA de Lisboa

Setembro, 2023

Campo Mártires da Pátria, 130
1169-056 Lisboa · Portugal

www.nms.unl.pt

CYSTEINE METABOLIC REMODELING: A METABOLIC MARKER FOR CANCER AGGRESSIVENESS AND A NOVEL PUTATIVE TARGET IN ONCOLOGICAL MANAGEMENT

ANA RITA CRISPIM HIPÓLITO

Orientadores: Jacinta Serpa, Professora Auxiliar da NOVA Medical School - FCM|NMS/UNL; Investigadora voluntária do Instituto Português de Oncologia de Lisboa Francisco Gentil - IPOLFG

João B. Vicente, Investigador Auxiliar do Instituto de Tecnologia Química e Biológica António Xavier – ITQB/UNL

Vasco Bonifácio, Professor Auxiliar do Instituto Superior Técnico

Tese para obtenção do grau de Doutor em Ciências da Saúde na Especialidade de Biomedicina

Setembro, 2023

The experimental data included in this thesis are sourced from manuscripts that have been previously published or are currently undergoing preparation for publication. I hereby state that I have fully participated in the conception, execution and in the validation of the experimental work, in the analysis and interpretation of the collected data as well as in the preparation of the manuscripts.

The experimental work developed in the course of this thesis was approved by the Ethics Research Committee of NMS|FCM-UNL (74/2020/CEFCM) and by the Ethics Committee of IPOLFG (UIC/1188).

Table of Contents

Abstract

Cancer remains a major health issue and one of the most frequent causes of death.

The present work explores the central role of cysteine metabolic remodeling, an often overlooked yet pivotal phenomenon with substantial implications, in the field of carcinogenesis and cancer response.

The central objective of this thesis was to clarify the intricate role of cysteine metabolic remodeling in highly prevalent and lethal forms of cancer that lack effective therapeutic solutions against resistance and advanced disease. Results indicate the significance of cysteine metabolic rewiring, under the regulatory influence of *BRD9* status, in shaping the aggressiveness of cutaneous melanoma (CM) through MST modulation. Furthermore, this thesis underscores the value of metabolic profiling, specifically focused on cysteine metabolism, in stratifying patients for tailored therapy in non-small cell lung cancer (NSCLC) and demonstrates the feasibility of inhibiting cysteine metabolism as a novel therapeutic avenue for NSCLC, colorectal cancer (CRC), and breast cancer (BC).

Overall, this work offers prospects for identifying cysteine metabolism as a new and complex therapeutic target and reveals the hidden potential of cysteine metabolic remodeling in the intricate landscape of cancer biology.

Keywords

Cysteine, Metabolic remodeling, Cutaneous melanoma, Non-small cell lung cancer, Colorectal cancer, Breast cancer, Cancer therapy.

Sumário

O cancro é definido como um vasto e heterogéneo grupo de patologias caracterizadas pela proliferação descontrolada de células cancerígenas que apresentam várias alterações a nível das suas características celulares e moleculares, o que lhes confere capacidades e comportamentos aberrantes.

Atualmente, o cancro é um preocupante problema de saúde pública, sendo responsável por milhões de mortes por ano em todo o mundo, estando o cancro colorretal, cancro da próstata, cancro do pulmão e cancro da mama (maioritariamente presente nas mulheres) no topo do *ranking* dos cancros mais incidentes e fatais na Europa.

A carcinogénese tem por base mutações e alterações epigenéticas em genes específicos, que induzem, não só a expressão anormal das proteínas codificadas pelos mesmos como também alterações na atividade e na função da própria proteína. Estas alterações estão na base do processo de transformação carcinogénica e promovem a ativação *quasi* constitutiva de importantes vias de sinalização que contribuem para a manutenção das características e capacidades anormais das células cancerígenas. As características implícitas ao processo de carcinogénese originadas por estas alterações e associadas à instabilidade genómica presente nestas células estão descritas na literatura como *Hallmarks of Cancer (Hannahan and Weinberg, 2000).* Embora tenham sido inicialmente considerados seis principais *Hallmarks of Cancer*, evidências científicas demonstraram outras características essenciais ao processo de carcinogénese que foram entretanto consideradas como *Hallmarks of Cancer,* incluindo assim atualmente oito principais características de malignidade: capacidade proliferativa descontrolada, evasão a sinais de supressão de crescimento, competências de resistência ao processo de morte celular, capacidade replicativa ilimitada, promoção da angiogénese e invasão da vasculatura, desenvolvimento de capacidades invasivas e metastáticas, remodelação metabólica e evasão ao sistema imune. No contexto desta tese, ir-nos-emos focar especificamente na capacidade de remodelação metabólica que estas células apresentam. O conceito de remodelação metabólica foi inicialmente introduzido em 1924 por Otto Warburg, que defendia que as células malignas tinham as suas necessidades metabólicas sustentadas maioritamente pela glicólise, independentemente da disponibilidade de oxigénio no microambiente – o *Efeito Warburg*. Atualmente, sabe-se que, embora a glicólise possa ser utilizada pelas células cancerígenas, a maioria destas células preferencialmente utiliza a fosforilação oxidativa como forma de satisfazer as suas

necessidades energéticas. A glucose é um composto central no metabolismo das células cancerígenas e funciona também como um substrato para a via dos fosfatos de pentose, uma via essencial na síntese de nucleótidos e no controlo do *status* redox das células através da produção de NADPH e glutatião (GSH). O GSH é um importante sistema de eliminação das espécies reativas de oxigénio (ROS), cujos níveis estão especialmente aumentados nas células cancerígenas dada a sua elevada atividade metabólica, sendo responsável, portanto, pela manutenção do *status* redox celular. Este interveniente metabólico é um tripéptido composto por glutamato, cisteína e glicina.

Além da glucose, a glutamina, cujo metabolismo tem um grande impacto a nível da produção de GSH através da produção de glutamato, é também considerada um interveniente central na remodelação metabólica em cancro, atuando como um precursor de intermediários para o ciclo do ácido tricarboxílico (TCA), sustentando a produção de ATP.

As células cancerígenas dependem assim da disponibilidade de recursos antioxidantes para que possam resistir ao dano oxidativo que advém da sua aumentada atividade metabólica. A cisteína, um aminoácido não-essencial, é um componente do GSH e um interveniente central no metabolismo celular cancerígeno. Este aminoácido pode ser obtido a partir do catabolismo do GSH ou de proteínas, da síntese *de novo* através da via de transulfuração, que usa como substrato a homocisteína derivada do ciclo da metionina, ou através da dieta. Evidências científicas têm vindo a apontar a cisteína como um interveniente central na remodelação metabólica em cancro, sendo o seu transporte e catabolismo cruciais na manutenção das necessidades metabólicas das células cancerígenas. Este aminoácido participa ativamente na produção de biomassa e energia como fonte de carbono através da produção de compostos como o piruvato que pode ser convertido em acetil-CoA e entrar no ciclo TCA ou ser direcionado para a síntese de ácidos gordos, e o α-cetoglutarato, um precursor de glutamato e interveniente no ciclo TCA. Além disso, a cisteína participa ainda na estimulação bioenergética e controlo do stress oxidativo celular através da produção de sulfureto de hidrogénio (H_2S), produto do seu catabolismo. A cisteína pode ser metabolizada através de duas vias: pela ação de enzimas sintetizadoras de H_2S, com a sua consequente libertação juntamente com outros metabolitos; ou pela ação da enzima cisteína dioxigenase (CDO), seguindo o metabolismo oxidativo. O grupo de enzimas sintetizadoras de H_2S inclui as enzimas cistationina β-sintase (CBS) e cistationina γ-liase (CSE), que possuem uma dupla função, podendo funcionar como enzimas sintetizadoras de cisteína ou como enzimas

catabolizantes, levando à produção de H_2S e compostos orgânicos. Este grupo de enzimas engloba ainda o eixo composto pelas enzimas cisteína aminotransferase (CAT): 3-mercaptopiruvato sulfurtransferase (MST), cuja ação resulta na degradação da cisteína e α-cetoglutarato pela CAT, levando à formação de 3-mercaptopiruvato e glutamato, sendo o primeiro de seguida metabolizado pela MST, com produção de H_2S e piruvato. A relevância das enzimas sintetizadoras de H_2S e da enzima CDO está cientificamente comprovada em vários tipos de cancro, incluindo melanoma, cancro do pulmão, cancro colorretal e cancro da mama, nos quais a expressão destas enzimas se encontra frequentemente alterada. Isto provoca consequentemente alterações na produção de H_2S, o que pode induzir graves danos celulares. Concentrações intracelulares subtóxicas de H_2S estão descritas como estimuladoras da bioenergética celular, por doação de eletrões através da sulfureto:quinona oxidoredutase para a cadeia transportadora de eletrões mitocondrial (mETC), estimulando a produção de ATP. No entanto, concentrações mais altas de H_2S estão descritas como inibidoras da enzima citocromo c oxidase, promovendo assim o efeito reverso e inibindo a produção de ATP pela mETC. Além disto, o efeito do H_2S contribui para uma melhor adaptação das células cancerígenas do microambiente tumoral (TME), incluindo a fatores como a hipoxia, stress oxidativo e ativação da neoangiogénese, favorecendo ainda a regulação do ciclo celular e evasão à apoptose. Além das enzimas envolvidas no metabolismo da cisteína, o anti-portador cistina/glutamato (xCT, codificado pelo gene *SLC7A11*) e o transportador de aminoácidos excitatórios 3 (EAAT3, codificado pelo gene *SLC1A1*) estão descritos como intervenientes cruciais na remodelação metabólica e manutenção de características malignas num extenso painel de cancros, incluindo melanoma, cancro colorretal, cancro do pulmão e cancro da mama, através da alteração da sua expressão.

Além do papel da remodelação metabólica da cisteína na manutenção das características malignas de um tumor, este fenómeno está também associado ao desenvolvimento de resistência à terapêutica oncológica, uma vez que este aminoácido apresenta um elevado potencial antioxidante por si próprio ou como parte do tripéptido GSH. Os fármacos alquilantes e oxidativos são altamente utilizados na terapêutica oncológica, no entanto, alterações ao nível do potencial antioxidante celular, promove resistência a estas terapias por haver uma melhor resposta celular ao aumento dos níveis de ROS, o que leva à proteção das células cancerígenas contra os fármacos que utilizam estes mecanismos de ação. Alterações ao nível dos intervenientes que participam no metabolismo da cisteína estão assim associadas ao desenvolvimento de quimioresistência

através de um aumento da produção de H_2S e também através de alterações na dinâmica intracelular de cisteína.

Embora o papel da enzima CBS esteja amplamente estudado em vários tipos de cancro, as enzimas CSE e MST têm recebido menos atenção por parte da comunidade científica.

O objetivo central desta tese foi clarificar o complexo papel da remodelação do metabolismo da cisteína em tipos de cancro altamente prevalentes e letais, cujas opções de tratamento são ainda pouco eficientes no que toca a ultrapassar a resistência à terapia e evitar o avanço da doença. Desta forma, esta tese pretendeu explorar o papel das enzimas CBS, CSE, CAT:MST, e dos transportadores xCT e EAAT3 na remodelação metabólica que ocorre em melanoma, cancro do pulmão, cancro colorretal e cancro da mama, tendo em consideração a sua expressão e função. Os resultados aqui apresentados indicam a importância da reconfiguração metabólica da cisteína, sob regulação do *status* do gene *BRD9*, na agressividade do melanoma cutâneo através da modulação da enzima MST. Além disso, este trabalho salienta o valor da elaboração de perfis metabólicos, focados especificamente no metabolismo da cisteína, na estratificação de doentes para terapia personalizada no cancro do pulmão de células não pequenas e demonstra a viabilidade da inibição do metabolismo da cisteína como uma nova via terapêutica para o cancro do pulmão de células não pequenas, cancro colorretal e cancro da mama.

Este trabalho oferece assim dados relevantes que sublinham o potencial do metabolismo da cisteína como um novo alvo terapêutico altamente complexo, e reforça a relevância da dependência da cisteína no contexto da remodelação metabólica no panorama da biologia do cancro.

Palavras-chave

Cisteína, Remodelação metabólica, Melanoma cutâneo, Cancro do pulmão de células não pequenas, Cancro colorretal, Cancro da mama, Terapia oncológica.

Figure Index

Table Index

Acknowledgments/Agradecimentos

Não consigo expressar por palavras o quanto estes longos quatro anos de doutoramento enriqueceram a minha vida. Quero dedicar esta página da minha tese a algumas pessoas que foram elementos-chave neste percurso e a quem devo um especial agradecimento.

A primeira pessoa a quem quero dirigir o meu sincero agradecimento é a Doutora Jacinta Serpa, minha orientadora principal. A investigadora que me fez querer seguir o caminho do doutoramento pelas suas palestras interessantíssimas a que assisti durante o mestrado, durante as quais partilhava conhecimento de uma forma que acredito que pouca gente conseguisse. Obrigada por acreditar em mim, mesmo quando não me conhecia, e abrir portas que me permitiram chegar onde estou hoje, e por toda a orientação ao longo destes anos e todo o conhecimento que me transmitiu. Embora tenham existido muitos momentos difíceis, estes anos sob a sua orientação foram de crescimento profissional e pessoal intensivos e isso moldou-me na pessoa que sou hoje e, por isso, estar-lhe-ei sempre agradecida. Aos meus orientadores Doutor João Vicente e Doutor Vasco Bonifácio, agradeço terem aceitado orientar-me ao longo destes anos e estarem sempre disponíveis para discutir resultados e protocolos, sempre com uma palavra amiga a cada problema. Devo ainda um agradecimento ao Doutor Luís Gafeira Gonçalves pelos ensinamentos ao nível da técnica de ^{1}H-NMR e, neste contexto, à instituição ITQB-NOVA pelo acesso ao equipamento (CERMAX) que enriqueceu bastante este trabalho.

Às minhas colegas de laboratório e amigas, que merecem um parágrafo só para elas nesta página. À Filipa Coelho, à Cindy Mendes e à Filipa Martins. Obrigada por serem as "mãos extra" sempre que o protocolo é exigente. Obrigada pela partilha de conhecimento, por toda a entre ajuda e por fazerem de nós, CMM, uma verdadeira equipa. Obrigada, Filipa Coelho, por tudo o que me ensinaste a todos os níveis ao longo destes anos. Obrigada por todos os momentos de amizade e de apoio, que se estenderam à vida fora do laboratório e que, espero, se prolongue durante muitos anos. À Cindy. Por todos os momentos, todas as gargalhadas, todos os vídeos do Youtube que eu não conhecia e trouxeram mais diversão aos meus dias, pelo nível básico de francês que trago destes anos e todos os artistas musicais, filmes e séries que desconhecia e que enriqueceram o meu

conhecimento cultural a um nível a que nunca tinha chegado. Mas, acima de tudo, por todo o apoio, disponibilidade e amizade. À Filipa Martins. Por todas as palavras doces (e pelas mais azedas, quando a gémea má vem à superfície), pela orientação no percurso da vida enquanto *curly girl*, pelo apoio incansável, por estar sempre disponível, e por tantas outras coisas. Espero levar esta amizade para a vida, celebrar convosco todas as vossas conquistas e ser ombro amigo quando assim precisarem.

A todos os meus colegas da UIPM, que me fazem adorar trabalhar lá por formarem a equipa mais divertida da biologia molecular, independentemente da sua função. Quero agradecer em particular às mamocas Sofia Fragoso e Sidónia, à Joaquina Sequeira, a todos os elementos LHO sem exceção e à Doutora Lúcia Roque. Obrigada por toda a ajuda nos momentos-chave e por todos os conselhos e amizade. À Teresa e à Ana Magalhães, duas amizades profundas que também a UIPM me trouxe em anos anteriores. Teresa e Ana, obrigada por toda a amizade e todos os momentos de alegria. Obrigada pelo vosso apoio constante em todos os momentos ao longo dos anos, por terem sempre um conselho amigo quando é preciso. Teresa, obrigada ainda pelos teus conhecimentos de mestre em ambiente MS Office, valeu! Obrigada também ao Hugo Lisboa, que ao longo destes anos se tornou uma presença e amizade importante.

Às minhas amigas de uma década Bárbara e Sara que, embora longe, estão sempre perto ao longo desta caminhada que é a vida.

Ao meu ombro amigo e companheiro de todas as horas e de todas as lutas, Íven, devo um especial agradecimento por estes anos de planos cancelados e noites de trabalho tardias que requereram muita paciência e compreensão. Sem ti as conquistas não teriam o mesmo sabor.

Por fim, mas não menos importante, aos meus pais, irmão e avós, que ouviram todos os meus desabafos ao longo destes anos e acreditaram sempre nas minhas capacidades para alcançar todos os meus objetivos, obrigada!

É o fim de uma etapa que me fez crescer exponencialmente enquanto profissional e enquanto pessoa e que nunca irei esquecer.

List of publications

Ana Hipólito, Renato Ferreira, Cheila Brito, *et al*. *BRD9* status is a major contributor for cysteine metabolic remodeling through MST and EAAT3 modulation in malignant melanoma. Submitted for publication.

Ana Hipólito, Cindy Mendes, Filipa Martins, *et al.* H_2S-synthesizing enzymes are putative determinants in lung cancer management toward personalized medicine. Submitted for publication.

Ana Hipólito, Cindy Mendes, Filipa Martins, *et al*. Cystathionine β-Synthase Inhibition: Pioneering a New Era in Colorectal Cancer Therapeutics with Selenium-Chrysin Polyurea Dendrimer Nanoformulation. Submitted for publication.

Ana Hipólito, Cindy Mendes, Isabel Lemos, *et al*. Cystathionine β-synthase (CBS) and xCT (*SLC7A11*) targeting by selenium-chrysin (SeChry) triggers different types of cell death in breast cancer. Manuscript in preparation.

Lopes-Coelho F, Martins F, **Hipólito A**, *et al*. A Metabolic Signature to Monitor Endothelial Cell Differentiation, Activation, and Vascular Organization. Biomedicines. 2022;10(9).

Lopes-Coelho F, Martins F, **Hipólito A**, *et al.* The Activation of Endothelial Cells Relies on a Ferroptosis-Like Mechanism: Novel Perspectives in Management of Angiogenesis and Cancer Therapy. Front Oncol. 2021;11.

Hipólito A, Martins F, Mendes C, *et al*. Molecular and Metabolic Reprogramming: Pulling the Strings Toward Tumor Metastasis. Front Oncol. 2021;11.

Hipólito A, Mendes C, Serpa J. The Metabolic Remodeling in Lung Cancer and Its Putative Consequence in Therapy Response. Adv Exp Med Biol. 2020;1219:311-333.

Hipólito A, Nunes SC, Vicente JB, *et al.* Cysteine Aminotransferase (CAT): A Pivotal Sponsor in Metabolic Remodeling and an Ally of 3-Mercaptopyruvate Sulfurtransferase (MST) in Cancer. Molecules. 2020;25(17).

Santos I, Ramos C, Mendes C, *et al*. Targeting Glutathione and Cystathionine β-Synthase in Ovarian Cancer Treatment by Selenium-Chrysin Polyurea Dendrimer Nanoformulation. Nutrients. 2019;11(10).

Lopes-Coelho F, Silva F, **Hipólito A**, *et al*. Acetylation drives hepatocyte nuclear factor 1β stability by blocking proteasome-mediated degradation. J Cell Biochem. 2019;120(6):9337-9344.

Posters in conferences

Ana Hipólito, João B. Vicente and Jacinta Serpa, Metabolic remodeling in cancer centered at the cysteine/H_2S axis, 2023 USA-Portugal Leaders in Cancer Research, Champalimaud Foundation, Lisboa, 2023.

Ana Hipólito, Cheila Brito, Ana Tomás, *et al*., MST and EAAT3 are key players in the metabolic reliance on cysteine in BRD9-c.183G>C melanoma cells, Cutaneous Melanoma: from where to where?, Liga Portuguesa Contra o Cancro, Lisbon, 2021.

Ana Hipólito, Sofia C. Nunes, João B. Vicente., *et al*, H_2S-synthesizing enzymes are putative determinants in lung cancer chemoresistance, Webinar Cancer biology: from basic to translational research, Liga Portuguesa Contra o Cancro, Lisboa, 2020.

List of abbreviations

^{1}H-NMR – Proton nuclear magnetic resonance

3-SP - 3-sulphinopyruvate

AA – Antibiotic-antimycotic

AAT- aspartate aminotransferase

ALK- Anaplastic lymphoma kinase

ANOVA – Analysis of variance

AOAA – Aminooxyacetic acid

AOE- Antioxidant enzyme

APC- Adenomatous polyposis coli

ARE - Antioxidant responsive element

ASCT2- Alanine/serine/cysteine transporter 2

ATCC - American type culture collection

ATP – Adenosine triphosphate

Akt- Ak strain transforming

AzMC – 7-Azido-4- methylcoumarin

BC – Breast cancer

BRAF – Proto-oncogene serine/threonine-protein kinase variant B

BRCA1 – Breast cancer 1 gene

BRCA2 – Breast cancer 2 gene

BRD9 - Bromodomain-containing protein 9

BSA – Bovine serum albumin

CAF- Cancer-associated fibroblast

CAT – Cysteine aminotransferase

CBS – Cystathionine-β-synthase

CDK4 – Cyclin dependent kinase 4

CDKN2A – Cyclin-dependent kinase inhibitor 2A

CDO1 – cysteine dioxygenase type 1

CIMP – CpG island methylation phenotype

CIN – Chromossomal instability

CM – Cutaneous melanoma

COX2 - Cyclooxygenase 2

CRC – Colorectal cancer

CSA – Cysteinesulphinate

CSD – Cysteinesulphinate decarboxylase

CSE/CTH – Cystathionine-γ-lyase

CTLA4 – Cytotoxic T-lymphocyte associated protein 4

CTNNB1 – Catenin beta 1

Cys – Cysteine

CysGly – Cysteinylglycine

CysGlySSP – S-cysteinylglycinylated proteins

CysSSP – S-cysteinylated proteins

DHI – 5,6-Dihydroxyindole

DHICA – 5,6-Dihydroxyindole-2-carboxylic acid

DNA – Deoxyribonucleic acid

DOPA – L-3,4-Dihydroxyphenylalanine

dPP – Dipeptidase

EAAT3 – Excitatory amino acid transporter 3

EC – Endothelial cell

ECACC - European Collection of Authenticated Cell Cultures

ECM – Extracellular matrix

EDTA – Ethylenediaminetetraacetic acid

EGFR – Epidermal growth factor receptor

EMT – Epithelial-to-mesenchymal transition

ER – Estrogen receptor

ERK – Extracellular signal-regulated kinases

FACS – Fluorescence-activated cell sorting

FBS – Fetal bovine serum

FITC – Fluorescein isothiocyanate FOXM1 forkhead box M1

GCL – Glutamate-cysteine ligase

GLUT – Glucose transporter protein type

GOT1 – Glutamic-oxaloacetic transaminase 1

GOT2 – Glutamic-oxaloacetic transaminase 2

GPX4 – Glutathione peroxidase 4

GSH – Glutathione

GSS – Glutathione synthetase

GluCys – Glutamylcysteine

H_2S – Hydrogen sulphide

HER2 – Human epidermal growth factor receptor 2

HRAS – Harvey rat sarcoma virus

hT – Hipotaurine

ICI – Immune checkpoint inhibitor

KEAP1 – Kelch-like ECH associated protein 1

KRAS – Kirsten Rat Sarcoma viral oncogene homolog

LC – Lung cancer

LCLC – Lung large cell carcinoma

LD – Lipid droplets

LKB1 – Liver kinase B1

LUAD – Lung adenocarcinoma

LUSC – Lung squamous cell carcinoma

MAPK – mitogen-activated protein kinase

MC1R – Melanocortin 1 receptor

MEK – Extracellular signal-regulated kinase

MET – Mesenchymal-epithelial transition factor tyrosine kinase

mETC – Mitochondrial electron transport chain

MITF – Microphthalmia-associated transcription factor

MLH1 – MutL homolog 1

MMR – Mismatch repair

mRNA – Messenger RNA

MS – Microsatellite

MSH2 – MutS homolog 2

MSH6 – MutS homolog 6

MSI – Microsatellite instability

MST/MPST – 3-mercaptopyruvate sulphurtransferase

mtDNA – Mitochondrial DNA

mTOR – Mammalian target of rapamycin

MYC – Myc proto-oncogene protein

NADPH – Nicotinamide adenine dinucleotide phosphate hydrogen

NF1 – Neurofibromin 1

NFkB – Nuclear factor-kappaB

NP-40 – Nonidet P-40

NRAS – Neuroblastoma RAS viral oncogene homolog

NRF2 – Nuclear factor erythroid 2-related factor 2

NSCLC – Non small cell lung cancer

Nrf2 – Nuclear factor-erythroid 2

OXPHOS – Mitochondrial oxidative phosphorylation

PAG – DL-Propargylglycine

PBS – Phosphate-buffered saline

PCR – Polymerase chain reaction

PD1 – Programmed cell death protein 1

PDL1 – Programmed cell death ligand-1

PFA – Paraformaldehyde

PI – Propidium iodide

PI3K – Phosphatidylinositol-4,5-Bisphosphate 3-Kinase

PLP – Pyridoxal 5'-phosphate

PMS2 – Postmeiotic segregation increased 2

POT1 – Protection of telomeres 1

PPP – Pentose phosphate pathway

PR – Progesterone receptor

PSAT1 – Phosphoserine aminotransferase 1

PTEN – Phosphatase and tensin homolog

RAF – Rapidly accelerated fibrosarcoma

RAS – Rat sarcoma vírus protein

RET – Rearranged during transfection Proto-Oncogene

RNA – Ribonucleic acid

ROS – Reactive oxygen species

ROS1 – Proto-oncogene tyrosine-protein kinase

SCLC – Small cell lung carcinoma

SD – Standard deviation

SeChry - Selenium-containing chrysin

SGLT – Sodium/glucose cotransporter protein

SHMT – Serine hydroxymethyltransferase 1

SLC1A1 – Solute carrier family 1 member 1

SLC7A11 – Solute carrier family 7 member 11

SMAD2 – Mothers against decapentaplegic homolog 2

SMAD4 – Mothers against decapentaplegic homolog 4

SWI/SNF – SWItch/Sucrose Non-Fermentable

Snail – Zinc finger protein

TCA – Tricarboxylic acid cycle

TERT – Telomerase reverse transcriptase

TKI – Tyrosine kinase inhibitor

TME – Tumor microenvironment

TNBC – Triple negative breast cancer

TP53 – Tumor protein p53

TYRP1 – Tyrosinase related protein 1

TYRP2 – Tyrosinase related protein 2

UDP-GlcNAc – Uridine diphosphate N-acetylglucosamine

UV – Ultraviolet

UVR – Ultraviolet radiation

VEGF – Vascular endothelial growth factor

VEGFA – Vascular endothelial growth factor A

Wnt – Wingless-related integration site

xCT - Cystine/glutamate antiporter

α-KG - α-Ketoglutarate

γ-GT - γ-Glutamyl transpeptidase

γ-GluCys - γ-Glutamylcysteine

Chapter I

General Introduction

This chapter is partially supported by the following publications:

Hipólito A, Martins F, Mendes C, *et al*. Molecular and Metabolic Reprogramming: Pulling the Strings Toward Tumor Metastasis. Front Oncol. 2021;11:656851.

Hipólito A, Mendes C, Serpa J. The Metabolic Remodeling in Lung Cancer and Its Putative Consequence in Therapy Response. Adv Exp Med Biol. 2020;1219:311-333.

Hipólito A, Nunes SC, Vicente JB, *et al.* Cysteine Aminotransferase (CAT): A Pivotal Sponsor in Metabolic Remodeling and an Ally of 3-Mercaptopyruvate Sulfurtransferase (MST) in Cancer. Molecules. 2020;25(17):3984.

I.I. Cancer Biology

Cancer is defined as a large and heterogeneous group of diseases characterized by uncontrolled proliferation of abnormal cells that present a number of rewired cellular and molecular features, conferring them aberrant competences that ultimately allows them to survive and thrive.[1–4] Cancer is considered a major public health issue, accounting for millions of deaths *per* year worldwide[5–9], with colorectal (CRC), prostate, lung (LC) and breast (BC) (mostly in women) cancers leading the ranking of cancer burden in Europe.[6,8] Carcinogenesis develops from driver mutations and epigenetic alterations in key genes, inducing aberrant expression of the coding proteins and alterations in their functioning. These abnormal functioning is the basis for the transformation of normal cells into malignant cells and leads to chronic and aberrant signaling of critical pathways, favoring cancer cell proliferation and sustaining tumor growth.[10] Malignant cells thus require the plasticity to adapt to hostile environments to sustain their survival. This adaptation capacity allows tumors to develop more aggressive phenotypes with ability to invade surrounding and, eventually, long distance tissues, leading to metastasis and colonization of other organs. All of these adaptations are based on the regulation of several molecular and cellular mechanisms that provide the necessary conditions for cancer cells to thrive.[10,11]

Although tumors can occur in a variety of tissues and organs, with distinctive molecular features and tissue-specific origins, the carcinogenesis process involves a series of recognized abilities that normal cells acquire in their process of becoming malignant independently of tumor specifications, originated by enabling capacities as genome instability and tumor-induced inflammation – the Hallmarks of Cancer.[1,4,12] Even though Hannahan and Weinberg initially considered the existence of six hallmarks of cancer[1,12], as scientific evidence accumulated, other cellular traits were considered as hallmarks of cancer and, thus, currently the hallmarks of cancer comprise eight features: ability to sustain proliferative signaling, evading growth suppressors, competence to escape cell death, limitless replicative potential, angiogenesis promotion and accessing vasculature, developed invasive and metastatic skills, metabolic reprogramming and avoiding immune annihilation (Figure I.1).[4]

The maintenance of these cancer-associated phenotypic characteristics is supported by abnormal physical properties of the microenvironment, which can induce wide alterations in the epigenome[4], and soluble molecules which are secreted by tumor and surrounding cells acting in an autocrine, paracrine or endocrine manners to regulate cell migration, proliferation, differentiation and cell death.[13]

Tumor microenvironment (TME)-associated cells, as cancer-associated fibroblasts (CAFs), immune cells, endothelial cells (ECs) and pericytes, are thought to suffer epigenetic remodeling upon their recruitment, thus functionally contributing for a convenient TME.[14]

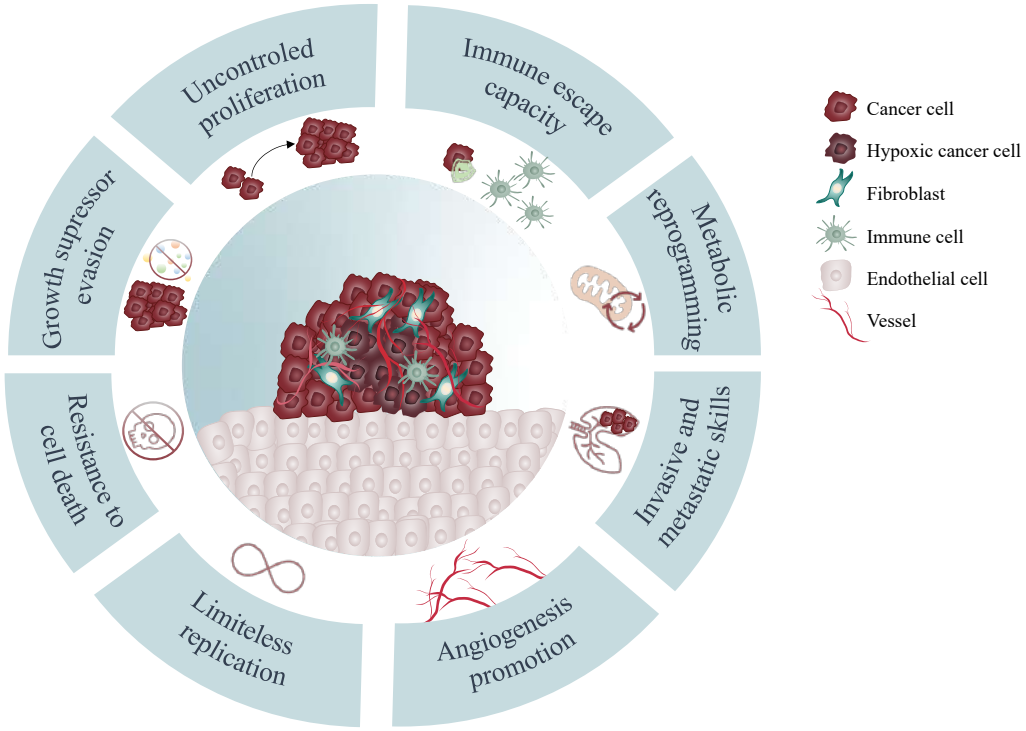

Figure I.1- The Hallmarks of Cancer. Currently the Hallmarks of Cancer comprise eight features: ability to sustain proliferative signaling, evading growth suppressors, competence to escape cell death, limitless replicative potential, angiogenesis promotion and accessing vasculature, developed invasive and metastatic skills, metabolic reprogramming and avoiding immune annihilation.

Hypoxia is a known feature of tumors, which arises as a consequence of insufficient or deficient vascularization, thus limiting nutrient bioavailability, which is a factor described to inhibit mRNA translation and, thus, interfere in protein synthesis in a breast cancer cellular model.[15] Moreover, this form of metabolic stress is further described to prompt selective translation of cytokine and inflammatory mRNAs, inducing a pro-inflammatory behavior.[15] The influence of microenvironment conditions and secreted factors by TME-associated cells is also described to induce epithelial-to-mesenchymal transition (EMT), prompting the invasiveness of tumors.[4,16,17] EMT involves the

transformation of a immotile epithelial cell into a mesenchymal phenotype, acquiring the ability to invade surrounding tissues.[16,17] The epigenetic switch associated to EMT stimulation is described for several players, as the Snail family, which are master transcription factors mediators of EMT[18,19], whose activation is reported to induce several chromatin modifiers, resulting in significant changes to the chromatin landscape, thus contributing for the maintenance of EMT.[20] The physical and molecular composition of the extracellular matrix (ECM) further contributes to the maintenance of cancer hallmarks.[21]

Within the scope of this thesis, the biological aspects of cutaneous melanoma (CM), colorectal cancer (CRC), lung cancer (LC), and breast cancer (BC) will be focused and explored below.

I.I.I. Cutaneous Melanoma

Melanoma, the most worrisome form of skin cancer, can be categorized into three types based on the location of malignant melanocytes: cutaneous (acral and nonacral), uveal, and mucosal melanoma.[22–28] Cutaneous melanoma (CM), which constitutes approximately 90% of all melanoma cases, develops in the skin, affecting epidermis and dermis.[22,26,27] Uveal melanoma, on the other hand, arises in the ocular stroma and accounts for around 3-5% of cases[24–26], while mucosal melanoma is found in mucous membranes, comprising approximately 1.5% of cases.[23,26] In the context of this thesis we will particularly focus on CM.

CM is a type of skin cancer, which represents the most common, invasive and deadly melanoma subtype, affecting around 90% of diagnosed melanoma patients by promoting lesions in the skin due to the malignant transformation of melanocytes. Although CM affects both men and women, CM incidence is directly related to age, with median age onset settled at 64 years.[22,29,30] CM is a very aggressive cancer due to the high mobility and invasive capacity of malignant cells, which allows metastatic colonization at early stages and frequent relapse events after primary tumor excision.[22] CM belongs to the group of cancers that arise due to chronic mutagenic exposure, in this case to ultraviolet radiation (UVR), and it is, as expected, one of the tumors that shows the highest mutational frequency, largely attributed to the significant rise in the occurrence of cytidine to thymidine (C>T) transitions, which are known as a distinctive mutational

signature resulting from exposure to UV light.[31–33] Exposure to UVR is, in fact, the major known risk factor associated to CM, including natural exposure and tanning bed use, accounting for about 70% of all CM cases due to extensive genome damage, in a wavelength-dependent manner, leading to apoptosis or cellular transformation of melanocytes.[29,34–36] Melanocytes are responsible for producing the pigment melanin and transfer it to neighboring keratinocytes, where it protects the nuclei content of these cells against UVR-induced damage, acting in a photo protective way by forming supranuclear caps and scavenging absorbed radiation.[37,38] Melanin can be produced in two forms: brownish-black eumelanin and red/orange pheomelanin, the latter associated to the fair skin with a lower ability to tan, freckles and red hair phenotype.[39] The photo lability of pheomelanin facilitates the generation of reactive oxygen species (ROS)[28,40] potentiating the mutational character of UVR. Both forms of melanin derive from a common precursor: DOPAquinone, which is produced from the oxidation of tyrosine by tyrosinase to L-3,4-dihydroxyphenylalanine (DOPA) and then to DOPAquinone. Eumelanin is then formed by the conversion of DOPAchrome to 5,6-dihydroxyindole-2-carboxylic acid (DHICA) and oxidation of 5,6-dihydroxyindole (DHI) and DHICA, catalyzed by two other tyrosinase-related proteins (TYRP1 and 2). Pheomelanin is spontaneously produced, requiring only cysteine to form 2, 5- or 5, 5-cysteinylDOPA that leads to the formation of cysteinylDOPAquinones, and then benzothiazine and benzothiazole.[38,39,41–45] Skin cancer incidence is directly correlated to skin pigmentation, thus individuals that produce higher levels of pheomelanin present a lower protection, thus are more prone to develop CM.[38–40,44]

Mutations in *BRAF* and *NRAS* are frequently identified in benign melanocytic neoplasms and, so, these mutations are thought to be involved in the initial steps of the malignant transformation of melanocytes[28,46–48], which may then acquire secondary mutations.[49] Interestingly, the most common mutations occurring in *BRAF* and *NRAS* are not UV typical C>T transitions, which may indicate a key role of these alterations as driver mutations non-related to UV exposure.[32] *BRAF* and *NRAS* mutations, commonly found in a variety of human cancers, particularly melanoma, have been associated with poor prognosis in melanoma, with *NRAS* indicating poorer outcomes in metastatic disease.[50–52]

Mutations in the RAS family are also frequently found in melanoma, particularly in *NRAS*, but also in *HRAS* and *KRAS* [48,52–54], leading to constitutive activation of these proteins, which causes multiple oncogenic downstream signaling events as MAPK

signaling through the RAS/RAF/MEK/ERK / MAPK/ERK signaling cascade and phosphorylation and activation of PI3K and the PI3K/AKT pathway. Mutations in *BRAF*, which are the most frequently found in CM, cause the constitutive activation of *BRAF* kinase, another key intervenient in the RAS/RAF/MEK/ERK / MAPK/ERK signaling pathway, and are associated to clinical and pathological features of CM tumors.[32,55,56] Interestingly, *BRAF* mutations tend to occur in cancer types that present significant rates of mutated *NRAS*, which is the case of CM.[53,55] This may suggest that the RAS/RAF/MEK/ERK / MAPK/ERK signaling pathway is a pivotal event in CM and may be activated in a significant percentage of cases, being its role redundant and achieved by different routes.[55] Gene loss or mutations in the tumor suppressor gene *PTEN* (a negative regulator of PI3K signaling) are also described in melanoma, more frequently associated to *BRAF* than *NRAS*-mutant tumors, which most likely occurs since *NRAS* mutations, but not *BRAF* mutations, also result in activation of the PI3K/AKT pathway.[57–59] PI3K/AKT as well as the MAPK and mTOR signaling pathways are further regulated by tumor suppressor gene *NF1* (a negative regulator of RAS-dependent pathways) status, which is also found mutated in CM and, when inactivated, leads to the activation of these pathways.[60–62] *NF1* is further described as a significative player in *BRAF*-mutant CM tumors, being associated with resistance to *BRAF* and *MEK* inhibitors.[62,63]

Family history is an important factor to take in account in CM susceptibility, with the genetic factor accounting for up to 15% of all CM cases.[28,64,65] *CDKN2A*, a gene responsible for cell cycle control, is not only the most frequently mutated gene in hereditary cases of melanoma[66,67], but also the most frequently altered tumor suppressor gene in sporadic cases, commonly through gene loss but also through inactivating mutations or gene silencing by promoter methylation.[57–59,68] In addition to *CDKN2A*, *CDK4* is another gene involved in regulating the cell cycle, which is implicated in familial melanoma.[69–71] Mutations in genes responsible for maintaining and safeguarding telomeres, such as *TERT* and *POT1*, also play a role in hereditary melanoma.[72–78] *TERT* mutations are believed to be associated with the early stages of malignant transformation and can be found in both sporadic and hereditary melanomas.[79] Furthermore, mutations in the promoter region of *TERT* are linked to a poorer prognosis, leading to shorter overall survival.[80] Nevertheless, *POT1* mutations are more commonly observed in hereditary melanoma compared to *TERT* mutations. Hereditary melanoma is further characterized by mutations in genes involved in melanin production, such as *MC1R* and *MITF*.[81–84] Notable, *MC1R* variants were further identified as a risk factor for melanoma, enhancing the penetrance of

CDKN2A mutations.[85] Even though CM germline mutations were already identified in key genes, most CM familial cases remain without an identified genetic cause.[47,65,72,86–88] Several studies, thus, have focused on uncovering other genes that can promote genetic susceptibility to CM.[64,65,89,90] In that context, *BRD9* was identified as a promising susceptibility gene involved in the pathogenicity of familial CM.[89] BRD9 protein defines different sub-complexes of SWI/SNF and it works as an epigenetic reader that can selectively identify and bind, through its bromodomain, acetylated lysine residues belonging to histone or non-histone proteins.[91] BRD9 functions as a gene expression modulator by remodeling chromatin and recruiting the transcriptional machinery for genes involved in cellular functions, such as proliferation, migration and invasion.[91–94]

Targeted therapies and immune checkpoint inhibitors changed the gold standard care for advanced and metastatic CM, which used to be based on chemotherapy regimens (*e. g.* dacarbazine)[95,96]. Targeted therapies include inhibitors towards MAPK/ERK signaling kinases, including BRAF and MEK, which can be used combined.[96] Anti-tumor immune response is another key clinical tool that has changed the CM clinical management panorama through immune checkpoint inhibitors (ICIs), which include monoclonal antibodies for CTLA4, ipilumab, and for PD1, nivolumab and pembrolizumab.[36,95,96] However, resistance to therapy remains a concerning issue and tumors can develop subsequent genetic alterations, among other resistance mechanisms, that abrogate, at least partially, the effect of both targeted therapies and immune checkpoint inhibitors, leading to relapse events.[95–99]

I.I.II. Lung Cancer

LC is a highly deadly disease, affecting both men and women around the world with concerning 5-year survival rates of about 19%.[100,101] LC is actually the most frequently diagnosed cancer globally with higher incidence in men than women. Additionally, even though LC is a highly study subject and despite the medical and scientific advances that allow earlier diagnosis and the development of novel and targeted therapies, LC survival has only slightly improved over the last decades, remaining a leading cause of cancer-related deaths.[101–104] LC can be categorized in two main histological groups: small cell lung carcinoma (SCLC, 15% of all LC) and non-small cell lung carcinoma (NSCLC, 85% of all LC), the latter is subcategorized into large cell carcinoma (LCLC), adenocarcinoma (LUAD), squamous cell carcinoma (LUSC), being LUAD and LUSC the most frequently

diagnosed types of NSCLC.[103,105] Although LC carcinogenesis arises from multiple key factors, with the individual genetic and epigenetic background, that comprises multiple inherited and acquired mechanisms of susceptibility, representing a determinant factor, lifestyle choices, continued exposure to polluted or toxic environments and chronic infections are further associated to LC carcinogenesis. In line with this, 90% of LC are caused by smoking habits and the use of tobacco products.[102,105,106] Though lung tumors are known to show an intratumoral heterogeneity and variable genetic landscape, LUAD, but not LUSC, is characterized by driver mutations in *KRAS* and *EGFR,* usually presenting a mutually exclusive pattern, consistent with a similar role of both these proteins in LC tumorigenesis.[107–109] Besides these, *HER*2, *MET RET, TP53, KEAP1, LKB1, and NF1* are also frequently found altered.[108,109] Moreover, LUAD is also known to present fusions involving *ALK* and *ROS1*.[108–111] As LUAD, LUSC frequently presents alterations in tumor suppressor genes, namely, *TP53* and *CDKN2A,* both associated with tumor progression.[31,109,112] Although LC is highly associated to smoking habits, as stated before, a smaller percentage of LC cases occur in never smokers. Interestingly, non-smoker related lung tumors present a distinct molecular signature from those that arise in smokers, presenting not only a much lower mutational burden with a tendency to present *EGFR*-activating mutations and/or *ALK* and *ROS1* translocations, while the mutational background of lung tumors occurring in smokers are characterized by a high proportion of *KRAS* and *TP53* mutations.[31,109–113] Molecular targeted therapies have been the clinical focus in terms of therapeutic options in LC. Indeed, several specific inhibitors have been proposed for clinical use, targeting key oncogenic proteins present in lung tumors. The most prevalent targeted therapies are tyrosine kinase inhibitors (TKIs), which are commonly used to target EGFR (*e.g.* gefitinib and erlotinib) and ALK rearrangements (*e.g*. crizotinib, also targeting *ROS1* and *MET* mutations). Still, these treatments only benefit patients that harbor these driver mutations, which are a small percentage of all LC. Moreover, although *KRAS* and *EGFR* mutations are usually mutually exclusive, some tumors upon the exposure to *EGFR*-targeted therapy acquire *KRAS* mutations and the coexistence of *KRAS* and *EGFR* alterations becomes possible, which confers resistance to *EGFR* inhibitors to these tumors. Additionally, resistance can also occur by secondary mutations in *EGFR*, alternative activations or histological changes.[114–116] However, due to lung tumors heterogeneity the possibility that resistant clones might exist prior to therapy cannot be excluded. The standard treatment for patients who do not fit the molecular profile for targeted therapies is still based on radiation and cytotoxic/cytostatic

therapy with platinum-based regimens (*e.g.* cisplatin, carboplatin) with or without bevacizumab, an anti-angiogenic monoclonal antibody.[116] Moreover, immunotherapy with ICIs have been clinical groundbreaking therapies with impressive results in terms of NSCLC patients' survival. Monoclonal antibodies targeting PD-1 receptor (*e.g.* nivolumab and pembrolizumab) or its ligand PD-L1 (*e.g.* atezolizumab and durvalumab) have occupied an important position as NSCLC therapy options, being a first line option in advanced disease.[116–121]

I.I.III. Colorectal Cancer

CRC is a leading cancer-related deaths pathology, accounting for about 10% of all annually diagnosed cancers worldwide, being more frequently diagnosed in women than men and showing higher incidence rates in the most developed countries.[6,122] CRC etiology is related to sporadic and hereditary genetic alterations, with familial history accounting for about 10–20% of all patients.[123] Other important factors include environmental aspects, such as dietary composition rich in saturated fats and red meat, excessive total energy intake, alcohol and tobacco consumption, and sedentary lifestyle.[122,124] Hereditary CRC syndromes can be categorized in non-polyposis and polyposis syndromes, the latter more easily recognized as it is characterized by the presence of a high number of polyps.[122] CRC tumorigenesis can arise due to several genomic instability pathways, resulting in distinct molecular signatures. CRC tumors can, however, exhibit features of multiple pathways, since the definitions of each one are not mutually exclusive.[125–128]

The chromosome instability pathway (CIN) is responsible for the majority of sporadic colorectal tumors (65-70%). CIN arises due to altered cellular function due to defects in chromosome segregation, being further related to defects in cell cycle checkpoints, telomere dysfunction and DNA damage deficient response, due to mutations in genes such as *KRAS, CTNNB1, APC, TP53, SMAD4* and *SMAD2*.[125,126,129] CIN is, thus, defined by an accelerated rate of gains and/or losses of whole or large portions of chromosomes, resulting in karyotypic variability from cell to cell and leading to imbalances in chromosome number (aneuploidy), subchromosomal genomic amplifications and, frequently, loss of heterozygosity.[125,126,129,130] Microsatellite instability pathway (MSI), on the other hand, is characterized by the presence of mutations, deletions or insertions in short tandem repeat DNA sequences located throughout the entire genome that are

related to the regulation of transcription and other genomic processes - microsatellite sequences (MS).[125,131] Overall, this molecular phenomenon is caused by mutations in DNA mismatch repair (MMR) genes (*MLH1, MSH2, MSH6, PMS2*), which lead to a deficient MMR with lower efficiency in recognizing and excising frameshifts.[125] MMR works as a proofreading machine that assures the fidelity of DNA replications by identifying and repairing mismatched nucleotides. Mutations in these genes leads to non-repaired mutated MS, leading to MSI.[131] These defective cells, which continue to accumulate mutations, are then replicated, leading to a hypermutation phenotype.[125,126,129] MSI areas, thus, accumulate alterations (mutator phenotype) since DNA polymerase cannot efficiently bind to these sequences.[125] A third molecular pathway, the CpG island methylation phenotype (CIMP), consists of aberrant hypermethylation of CpG sequences, which are commonly found in promoter regions of key genes involved in the regulation of vital cellular processes, as cell cycle, apoptosis, angiogenesis, DNA mismatch repair, among others.[127,132]

CRC treatment is based on surgery, targeted therapy, neoadjuvant radiotherapy and adjuvant chemotherapy. Overall, advanced CRC management relies on regimens that include chemotherapy agents, targeted therapy (BRAF/MEK inhibitors) and/or immunotherapy. The regimen applied depends, of course, on the molecular profile as well as stage of the tumor. Therapy regimens usually combine different agents. Chemotherapy agents usually used in CRC regimens are 5-fluorouracil, oxaliplatin and irinotecan, which can be combined together or with other targeted therapies.[122] A triplet of all three, FOLFOXIRI, is actually used as backbone, in combination with targeted agents.[133] Targeted therapy with monoclonal antibodies binding to EGFR (*e.g.* Cetuximab), or the VEGF inhibitor (*e.g.* Bevacizumab) is currently considered to be standard of care for first-line treatment of metastatic CRC.[122,133] Resistance to therapy remains, however, a great obstacle to surpass.[134–140]

I.I.IV. Breast Cancer

BC is a common cancer among women from all ages around the world, though is can also affect men.[141] BC is a heterogenous disease, with multiple molecular entities that define distinct phenotypes and clinical responses. Identification of primary tumor histological and molecular characteristics such as the expression of hormone receptor ER

or PR and HER2 are key features with predictive value of response to therapy and prognosis. Interestingly, PR expression correlates with ER expression, being the functional link between PR and ER in BC intricate and complex.[142–145] In fact, even though PR is estimated to be expressed in more than 50% of positive ER breast tumors, it is rarely expressed in ER^- tumors. PR, thus constitutes itself a marker for functional ER pathway[143,146,147] and has, in fact, been suggested as a ER pathway determinant.[145] Both ER^+ and PR^+ tumors are overall associated with better prognosis than ER/PR^- tumors.[143,148] HER2 overexpression is underlined by *HER2* gene amplification and is associated to uncontrolled proliferation of cancer cells and is indeed described to be an early event on BC tumorigenesis, occurring in about 15-30% of all invasive BC, maintaining its status from tumorigenesis to metastasis.[146,149–151] Thus, HER2 status has a predictive value that not only guide therapy regimen decision but also informs on prognosis, recurrence probability and overall survival.[146,149–156] Although it seems like a relatively poor characterization, this expression pattern remains one of the main indicatives for clinical management, with triple-negative tumors (TNBC) indicating a poorer prognosis.[141,157–160] Besides these markers, Ki-67, a proliferation marker which reflect tumor growth capacity, as well as expression and mutation profiling of other genes of interest are tools with clinical significance in stratifying invasive BC patients across the considered molecular subtypes. The molecular classification of BC tumors relies mainly on the expression of hormone receptors ER/PR and/or HER2 expression (when amplified), being TNBC classification attributed to BC tumors lacking ER, PR and HER2 expression [141,146,160–162].

Metastases remain the leading cause of death in BC patients, mostly affecting lung, liver, brain and bone tissue, though with different preference patterns according to the molecular subtype.[163,164] HER2-enriched and TNBC are the most prone subtypes to local and distant metastasis, showing the worst overall survival rates and, thus, most aggressive phenotypes.[162]

BC therapy regimens are based on the molecular classification of the tumor as well as its stage and are overall integrated regimens that can comprise (neo)adjuvant chemotherapy with cytotoxic agents as doxorubicin, paclitaxel and cyclophosphamide, platinum-based salts (eg. carboplatin, cisplatin), monoclonal antibodies (*e.g.* tocilizumab and trastuzumab), TKIs (*e.g.* tivozanib and lapatinib), histone deacetylase inhibitors (HDACis; *e.g.* vorinostat), radiotherapy, surgery and endocrine therapy (estrogen receptor inhibitors; *e.g.* tamoxifen).[163,165]

I.II. Tumor Microenvironment: A Tumor's Finest Ally

Cancer has been recognized over time as a multifactorial entity in which cancer cells play a major role but are not a single agent behind cancer's pathogenicity. The TME plays crucial roles in sustaining cancer cell survival, tumor growth and dissemination. Cancer cells emerge, indeed, in a complex environment, where they coexist and partner through dynamic cellular interactions with several different cell types and molecules or metabolites (Figure I.2).[166,167]

The TME comprises several non-tumoral cells that associate with cancer cells, such as CAFs, ECs and immune cells, as well as other components that allow the tumor to thrive, as the ECM, abnormal stroma and vasculature, and molecules that further support tumor growth as cytokines, growth factors and several metabolites that sustain the tumor's metabolic needs (Figure I.2). These environmental settings are responsible for tumor progression and for the maintenance of the hallmarks of cancer, described above.[166–169] It has become clear that TME plays a critical role in selectively pressuring cancer cells, inducing their adaptability skills at the genetic and molecular level, thus shaping its metabolic phenotype through metabolic reprogramming, further supporting cancer progression as well as resistance do adverse conditions.[167,169–171]

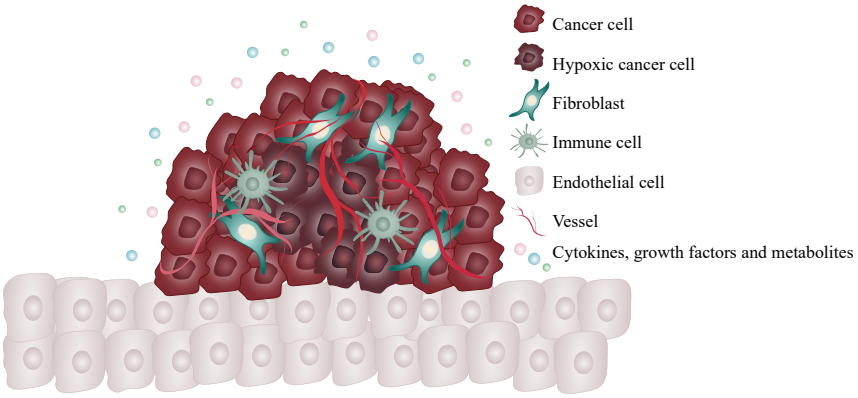

Figure I.2 – Tumor progression is supported by TME players. Cancer cells arise within a complex environment characterized by dynamic interactions with various cell types and molecules, including numerous non-cancerous cells, as cancer-associated fibroblasts (CAFs), endothelial cells (ECs), and immune cells, which coexist and collaborate with cancer cells. Additionally, there are other components in the TME that promote tumor growth, such as the extracellular matrix (ECM), abnormal stroma, and vasculature, which, together with various molecules, including cytokines, growth factors, and metabolites, provide essential support for meeting the metabolic requirements of the tumor and drive tumor progression by sustaining the hallmarks of cancer.

I.II.I. Metabolic Remodeling: From the Warburg Effect to Sustained Bioenergetics

One of the pioneer evidences of the metabolic remodeling occurring in cancer cells was published in 1924 by Otto Warburg, who stated that cancer cells would mainly rely on glycolysis to sustain energy demands, independently of oxygen availability – the Warburg Effect.[172–174] Nowadays it is known that although cancer cells can use glycolysis as an energy source, most cells rather employ oxidative phosphorylation (OXPHOS) and not always resort to glucose.[175]

Independently of these coexisting metabolic routes, cancer cells must adapt to sustain their survival and expansion and so, the high glycolytic rate of these cells implies the increased expression of glycolytic transporters, which mainly belong to the Na^+-coupled glucose transporters (SGLT) and glucose transporter facilitators (GLUT) families.[176] Besides glucose, glutamine is considered a central metabolite in cancer context, acting as a supplier for the tricarboxylic acid (TCA) cycle and supporting ATP production.[176–178] In fact, highly proliferating cells primarily rely on glucose and glutamine as their two main carbon sources.[179] Glucose is a core organic compound and its degradation, through glycolysis, also sustains the functioning of pentose phosphate pathway (PPP). PPP is a biosynthetic pathway crucial in the production of pentoses (ribose 5-phosphate- R5P) for nucleotides synthesis and in the control of redox cellular state.[180] Therefore, in cancer, PPP sustains proliferation and the metabolic flow through the production of NADPH and glutathione (GSH) regeneration.[181,182] GSH is a ROS scavenger which, besides keeping cell metabolism under redox balanced conditions, also contributes for chemoresistance.[182]

Glutamine is an amino acid that can be synthesized in human cells, which holds relatively constant levels in the circulation, its concentrations rising to higher values than any other amino acid.[178,183,184] Maintenance of these glutamine levels provides a readily available source of carbon and nitrogen, which cancer cells can then potentially utilize to fuel tumor growth by supporting biosynthesis, cellular homeostasis, and energy production.[178,179,183,185] Glutamine can be taken up by cells by specific transporters, as ASCT2, and support nucleotide biosynthesis and uridine diphosphate N-acetylglucosamine (UDP-GlcNAc) synthesis or can be transformed by glutaminase into glutamate, another important amino acid in cancer settings.[179,185] Glutamate can then be converted to α-ketoglutarate (α-KG) by the action of two types of enzymes: glutamate dehydrogenases or aminotransferases.[186] Glutamine, as a source of serine and glycine, is also an important supplier of one-carbon metabolism, a core metabolic pathway ensuring

the needs for compounds to support epigenetics and purines and pyrimidines syntheses and ultimately contributing for nucleotides and nucleic acids production as well as the modulation of gene expression.[187] Glutamate and glycine further contribute for the synthesis of the already mentioned most abundant and important antioxidant in the cell – GSH.[188]

Glutamine metabolism impacts directly on antioxidant response on cancer cells by yielding glutamate which can, other than combining with cysteine in the first step of GSH synthesis, participate in glycine synthesis through its transamination. This reaction leads to phosphoserine and α-KG production and is catalyzed by phosphoserine aminotransferase 1 (PSAT1). The subsequent conversion occurs through serine hydroxymethyltransferase (SHMT) towards the final product glycine, as a part of the one-carbon metabolism. Glycine can, though, be obtained from a variety of other sources, including threonine, choline, betaine, dimethylglycine, among others.[189,190]

I.II.II. Antioxidant Sources in Cancer Cells

As stated before, cancer cells accelerate and remodel their metabolic activity in order to sustain tumor aberrant growth, and this occurs through different metabolic routes, among them mitochondrial metabolism, which is a major source of ROS.[188,191] Thus, cancer cells must rely on higher availability of antioxidant resources (even more than non-malignant cells) to counterbalance the damaging effects of oxidative stress.[188] GSH is a tripeptide composed of the amino acids glutamate, cysteine and glycine. GSH synthesis occurs in 2 reaction steps non-redundantly catalyzed by specific enzymes. The first and limiting step of GSH production involves the condensation of glutamate and cysteine through glutamate-cysteine ligase (GCL), producing γ-glutamylcysteine (γ-GluCys). Next, glutathione synthetase (GSS) catalyzes the condensation of glycine, which can be synthesized *de novo* or taken up, to γ-GluCys (Figure I.3).[178,188] Conversely, for GSH degradation, GSH is transformed into cysteinylglycine (CysGly) by γ-glutamyl transpeptidase (γGT) and then again to cysteine by dipeptidase (dPP).[192]

Moreover, glutamate can also be exchanged for cystine (the oxidized form of cysteine), through the cystine/glutamate transporter (xCT), cystine being then rapidly intracellularly reduced to cysteine under physiological conditions.[193,194]

I.II.III. Cysteine Metabolic Reprogramming in Cancer

Cysteine is a sulfur-containing nonessential amino acid. In the extracellular space, free cysteine can easily form disulfide bridges by oxidation of its thiol groups, resulting in the formation of cystine.[195,196] Cysteine is a key player in cellular metabolism, as it can serve as a carbon and sulfur source to sustain both bioenergetics and biosynthesis. In the last decade, new insights have pointed out cysteine as crucial in cancer metabolic remodeling, its uptake and catabolism arising as the main courses to supply the cancer cell metabolic needs.[192,197]

xCT (encoded by *SLC7A11*) is a widely studied antiporter, which along the years has been suggested to play a crucial role in cancer progression and invasion, as well as in multidrug resistance[193,198–205], being overexpressed across a panel of cancers, including BC, NSCLC and CRC and CM.[205–215] Cysteine, besides contributing for protein and GSH synthesis, is also an essential energy and biomass source, thus playing distinct roles in the metabolic remodeling of cancer cells.[192,194,197] This includes the maintenance of oxidative stress control, stimulation of cellular bioenergetics by the production of hydrogen sulfide (H_2S) during its catabolism, and in biomass and energy production as a carbon source.[192,194,197] Cysteine role as a carbon source arises from its ability to generate compounds as pyruvate, which can be converted into acetyl-CoA and enter the TCA cycle or be used for fatty acid synthesis, and α-KG, a precursor of glutamate and also a TCA intermediate.[192,194,197] Thus, cysteine contributes for cancer cell evasion and adaptation to harmful stimuli, such as cytotoxic agents or TME conditions as hypoxia.[192,194,197] Cysteine can be originated from GSH or protein degradation, *de novo* synthesis through the reverse transsulfuration pathway from the methionine cycle-derived homocysteine, or by dietary intake (Figure I.3).[192,216–219] While xCT is described as a main cyste(i)ne transporter, several other important transporters are described for cysteine uptake, among them the excitatory amino acid transporter 3 (EAAT3, encoded by *SLC1A1*),[220–222] which is further associated with different cancer types.[223–225] Cysteine can be degraded via distinct pathways: through the action of H_2S-synthesizing enzymes, with the subsequent release of H_2S and other intermediates; by oxidative catabolism via the action of cysteine dioxygenases (CDO); and by the NFS1 cysteine desulfurase, using its sulfur for iron-sulfur cluster synthesis and assembly (Figure I.3).[192] Additionally, the mitochondria tRNA-cysteinyl synthase 2 (CARS2) has been shown to use cysteine as a substrate for cysteine persulfide synthesis or co-translational insertion of persulfidated cysteine into

nascent polypeptides.[226] The enzymes cystathionine β-synthase (CBS) and cystathionine γ-lyase (CSE) have a double role in cysteine metabolism and its action can be directed towards cysteine synthesis, from homocysteine, or degradation, with organic compounds and H_2S generation (Figure I.3).[227] Cysteine can alternatively be catabolized through the CAT:MST axis, with a first reaction catalyzed by cysteine aminotransferase (CAT, also named glutamic oxaloacetic transaminase-GOT and aspartate aminotransferase-AAT) which has two isoforms, classified according to their cellular localization as cytoplasmic (cCAT) and mitochondrial CAT (mCAT) - generating the metabolites 3-mercaptopyruvate and glutamate from α-KG and cysteine. The resulting 3-mercaptopytuvate is then a substrate for 3-mercaptopyruvate sulfurtransferase (MST), which incorporates a sulfane sulfur into the active site Cys248 with pyruvate release (Figure I.3).[228–231] This persulfide (Cys-SSH) then reacts with a sulfane sulfur acceptor which can be a monothiol (as GSH, cysteine and homocysteine) or a dithiol (as dihydrolipoic acid and thioredoxin), eventually leading to H_2S production.[231–234] Alternatively, cysteine catabolism can be catalyzed by CDO1, leading to cysteine oxidation by CDO1 to cysteinesulphinate (CSA), which is then converted by cysteinesulphinate decarboxylase (CSD) into hypotaurine (hT), producing taurine. Instead, CSA can be transaminated by AAT/CAT to 3-sulphinopyruvate (3-SP), generating pyruvate and sulfite/sulfate (Figure I.3).[192,235–238] Several studies have proven the relevance of H_2S-synthesizing enzymes in cancer cell metabolic remodeling and in cancer progression, with its expression levels frequently found increased across a wide panel of cancers, including BC, NSCLC and CRC, as well as CM.[239–251] Moreover, CDO1 has also been reported to be involved in tumor progression.[252–256] H_2S, one of the catabolic products of cysteine metabolizing enzymes CBS, CSE and MST, is under tight physiological regulation, since imbalances in H_2S levels can induce severe toxic cellular consequences. At subtoxic intracellular concentrations, H_2S is a well-known stimulator of cell bioenergetics, both as a source of electron equivalents for the mitochondrial electron transport chain (mETC) by reducing quinone to quinol via sulfide:quinone oxidoreductase (SQR), and through persulfidation of ATPase, thus stimulating mitochondrial ATP production; however, higher H_2S levels lead to toxic effects by inhibiting cytochrome c oxidase, thereby impairing ATP production (Figure I.3).[257–263] Although the role of cysteine-derived H_2S in cancer progression is not fully disclosed, studies have shown that H_2S contributes to cancer cell ability to adapt to TME conditions. Other than ATP production, H_2S effects seem to extend to hypoxia adaptation, antioxidant

response to oxidative stress, neoangiogenesis, cell cycle regulation and apoptosis evasion.[192,245,264–271]

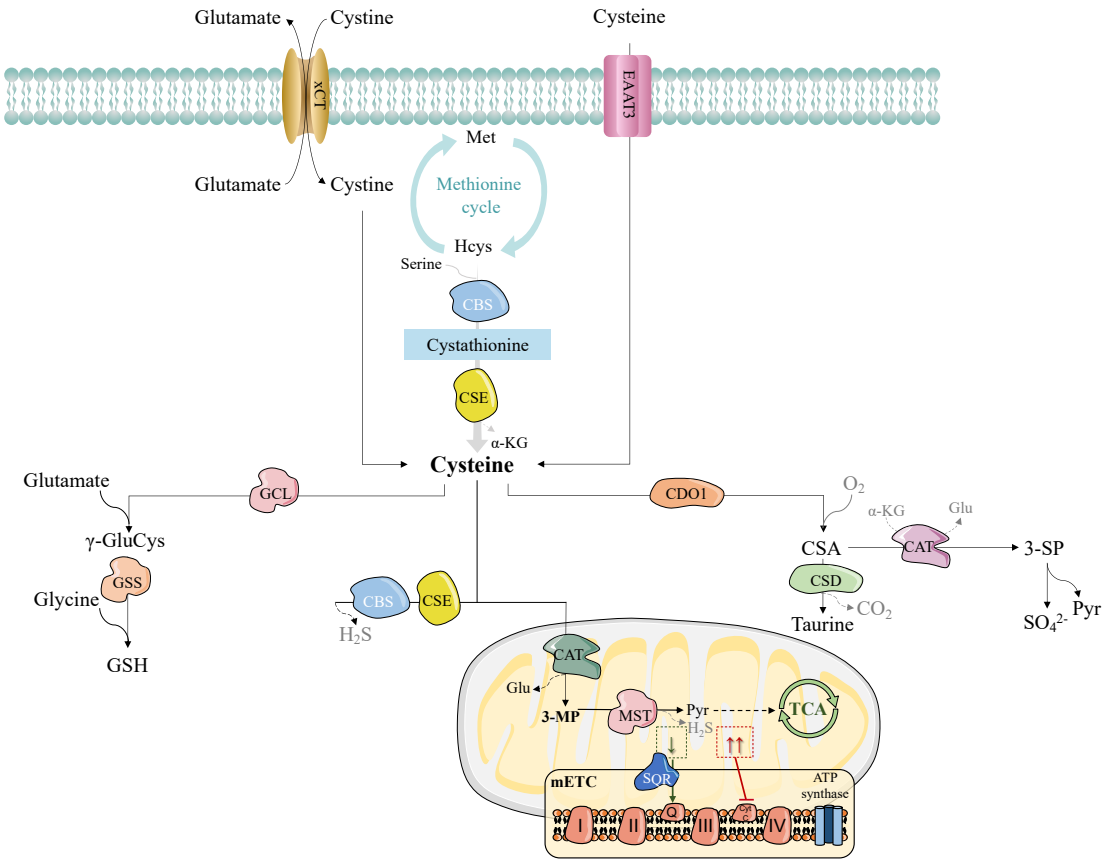

Figure I.3 – *Cysteine metabolic remodeling in cancer.* Cysteine can be uptaken by different transporters, as xCT system, which uptakes cysteine in its oxidized form (cystine) in exchange for glutamate, or EAAT3. Cysteine can then be metabolized through the H_2S-synthesizing enzymes CBS or CSE, which can perform the dual function of synthesizing cysteine from the methionine (Met) cycle-derived homocysteine (Hcys) or degrading available cysteine. MST is a third H_2S-synthesizing enzyme which, within the CAT:MST axis can catabolize cysteine with pyruvate release (Pyr). The produced H_2S, depending on its concentration can then have different effects on cellular bioenergetics: At subtoxic intracellular concentrations, H_2S is a well-known stimulator of cell bioenergetics, both as a source of electron equivalents for the mitochondrial electron transport chain (mETC), stimulating mitochondrial ATP production; however, higher H_2S levels lead to toxic effects by inhibiting cytochrome-c oxidase, thereby affecting the mETC complex IV and impairing ATP production.[257–263] Cysteine can also be metabolized through an oxidative pathway involving CDO1, which oxidizes cysteine to cysteinesulphinate (CSA), which is then converted by cysteinesulphinate decarboxylase (CSD) into hypotaurine (hT), producing taurine. Instead, CSA can be transaminated by AAT/CAT to 3-sulphinopyruvate (3-SP), generating pyruvate and sulfite/sulfate.[192,235–238] Cysteine can also contribute for GSH synthesis, which is a 2-step reaction involving the condensation of glutamate (Glu) and cysteine through glutamate-cysteine ligase (GCL), producing γ-glutamylcysteine (γ-GluCys). Next, glutathione synthetase (GSS) catalyzes the condensation of glycine, which can be synthesized *de novo* or up taken, to γ-GluCys.[178,188]

As mentioned earlier, CBS is an extensively characterized and researched mammalian enzyme, whose expression and activity undergo changes in various types of cancer. However, CSE and especially MST are enzymes that have received less attention in terms

of research. Therefore, it is crucial to delve deeper into understanding the role of these enzymes in cancer progression. CBS and CSE are thought to have a role in melanoma metastasis.[272] Interestingly, *CTH* (encoding CSE) is reported to mediate cellular senescence in melanoma cells.[273] Moreover, MYC, a known oncogene and tumor-associated transcription factor can regulate *CTH* expression in melanoma cells.[273] Another study reports *CTH* upregulation correlation with melanoma progression, with CSE levels increasing from nevi to primary melanoma but with low expression in metastasis while CBS expression was not found in dysplastic nevi and only found in a small percentage of primary melanoma tumors, reinforcing the role of CSE in melanoma progression.[241] Moreover, *CTH* overexpression in melanoma cell lines is associated to significantly decreased cell proliferation.[241,274] Additionally, MST is also reported to be expressed in melanoma cell lines, with higher enzymatic activity levels comparing to CSE, which may indicate a preferred route regarding cysteine metabolism in melanoma cell lines. [274]

The H_2S-synthesizing enzymes CBS, CSE and MST were found upregulated in NSCLC cell lines and tumor tissue and inhibition of these enzymes led to cell migration and invasion impairment while endogenous H_2S bioavailability induced EMT and increased cell migration.[270] Additionally, H_2S was further found to promote the production of pro-angiogenic factors, as VEGFA, indicating a role of H_2S synthesizing enzymes in NSCLC tumor progression, sustaining EMT and angiogenesis.[270] LUAD cells are reported to remodel H_2S biosynthesis to, besides support cellular bioenergetic demands, increase their ability to repair mtDNA[275], which is essential for OXPHOS.[276] Moreover, inhibition of H_2S production with AOAA, a common inhibitor of CBS/CSE[277], induces sensitivity of LUAD cells to chemotherapy agents, which is thought to be due to mitochondrial dysfunction as an effect of the inhibition of H_2S production.[275] This further indicates a crucial role of CBS/CSE in LUAD cellular homeostasis, fulfilling bioenergetic demands, which is further described in other studies.[270,278,279]

CBS is thought to be implicated in CRC carcinogenesis, since its expression was found to increase significantly in the transition from healthy colonic tissue to adenocarcinoma formation.[280] In fact, several studies described an overall CBS overexpression in CRC tumors, comparing to surrounding healthy tissue[280–282], thus suggesting an impact of CBS overexpression in tumor bioenergetics and growth.[283]

Moreover, CBS upregulation is believed to be linked to cancer progression and metastasis[284], as demonstrated in CRC metastasis-competent circulating tumor cells[246], further reinforcing the significance of CBS in these processes. Even though studies have focused particularly on CBS role in cancer overall, both CSE and MST have been described as altered in CRC as well. AOAA, a common inhibitor of CBS/CSE[277], was found to sensitize CRC cell lines to chemotherapeutic agents.[285]Interestingly, the Wnt/β-catenin pathway, an extremely conserved signaling pathway that is one of the most representative driver pathways in CRC[286], was found to regulate *CTH* expression, which is also recognized to play important roles in CRC.[287] Moreover, MST is described to associate with more aggressive CRC phenotypes, through regulation of cell proliferation, migration and bioenergetics.[288–291] However, MST role in CRC remains controversial, since MST is also described to be downregulated in CRC, with the extent of downregulation correlating with the depth of invasion.[292]

Finally, H_2S-synthesisizing enzymes are also described to participate in BC promotion.[293,294] CBS is overexpressed in BC tissue comparing to adjacent normal tissue and, interestingly, expression score correlates with BC progression.[239,295] Both CBS and CSE expression in BC seems to associate with more aggressive phenotypes, suggesting both enzymes can have prognostic value.[239,293,295] Moreover, CBS and CSE inhibition impairs cell proliferation, survival, invasion, and migration in BC.[293,296] BC cell death induced by H_2S inhibition has been associated to a disrupted PI3K/AKT/mTOR pathway.[296] CSE expression in BC seems to correlate with STAT3 expression, which is shown to be a transcriptional regulator of CSE, with the ability to directly bind to the *CTH* promoter.[248,249] Additionally, CSE is reported to be upregulated in BC tumors with lymph node metastasis comparing to non-metastatic BC tumors and this was further described in BC cell lines. CSE overexpression was also found to promote BC metastasis *in vivo* via VEGF signaling pathway, while *CTH* knockdown *in vivo* impairs lung metastasis promoted by the TNBC cell line MDA-MB-231, reinforcing the vital role of H_2S-synthesizing enzymes in BC progression.[297] Moreover, MST is also reported to be upregulated in BC cell lines.[298]

As mentioned above, cysteine can be oxidatively metabolized, involving CDO1, leading to the formation of either pyruvate and sulfite or taurine. Although several studies have focused on the role of CDO1 in cancer pathophysiology, few have focused on the

specific role of cysteine metabolism by CDO1 with pyruvate as an end product. CDO1 downregulation is reported for several human cancers.[299] This downregulation can enhance the antioxidant capacity of cancer cells by increasing cysteine bioavailability.[300] The metabolic role of CDO1 in CM biology remains to be explored, and even its association as a tumor suppressor gene or a biomarker for disease progression is unknown. In CRC, promoter methylation and *CDO1* downregulation is described, being considered a tumor suppressor gene and the epigenetic status of *CDO1* serves as marker for disease progression and response to therapy.[301–303] However, few studies have been developed on the metabolic role of CDO1 in CRC subsets of patients. CDO1 has been implicated in LC pathogenesis as a metabolic liability for LC tumors that exhibit elevated levels of intracellular cysteine, especially in tumors displaying *NRF2/KEAP1* mutations.[254] As described for other tumors[299], *CDO1* is preferentially found downregulated in NSCLC[254,304], particularly in tumors mutated for *KEAP1*, a major repressor of NRF2, which controls transcription of genes encoding antioxidant enzymes (AOEs) and is associated to oncogenic signaling and stress response, enhancing cancer cells response to oxidative stress.[254,305,306] Thus, *CDO1* silencing sustains NSCLC cell proliferation and viability by restricting cysteine degradation to wasteful and toxic metabolites as CSA and sulfite but, instead, leading to cysteine accumulation or redirection.[254] In BC, CDO1 expression seems to be related to the BC molecular type, CDO1 levels being lower in TNBC cases than in $HER2^+$ and luminal cases.[307,308] Studies indicate *CDO1* as a tumor suppressor gene in BC, its epigenetic status being a biomarker for prognosis.[307,309] *CDO1* silencing favors BC chemoresistance to anthracyclines and a predictor to distant metastasis in luminal BC.[253,310]

The epigenetic modulation of *CDO1* is the main parameter explored in cancer, but little is known about the biological and functional implications of CDO1 in cancer overall. Therefore, more studies are needed to explore the metabolic role of CDO1 in cancer, which can serve as a distinguisher and a marker in certain cancer subsets of patients.

I.III. The Role of Cysteine Metabolic Remodeling in Chemoresistance

Undoubtedly, one of the most fascinating abilities of a tumor is its plasticity to adapt to a hostile TME. Without this ability, cancer cells would not be able to survive and thrive.

Molecular characteristics of the tumor, gathered with the interaction between therapy agents, cancer cells and TME play a vital role in therapy success.

Cancer cells can either show certain molecular traits that will make them intrinsically resistant to a treatment (intrinsic resistance) or can acquire, upon selective pressure by cytotoxic agents, features that will allow them to become resistant and lead to tumor unresponsiveness to a certain therapy - acquired resistance.[311] The multifactorial process of chemoresistance involves the strengthening or *de novo* acquiring of cancer features that allow the resistance to therapy.[311,312]

Cysteine is pivotal for cancer cells to evade drug toxicity since it is itself a powerful antioxidant and is a limiting part of GSH, another scavenger of free radicals. Thus, cysteine remodeled metabolism contributes as a major mechanism of resistance, mostly for the abrogation of oxidative or alkylating drugs commonly used in cancer therapy regimens.[205,313–317] This occurs by direct binding to or reacting with the cytotoxic agents, inhibiting ROS and preventing cellular damage to proteins or DNA.[205,313–317]

H_2S-synthesizing enzymes have been associated to chemoresistance: increased H_2S levels in cancer cells associated with increased cysteine flux have been, in fact, associated with chemoresistance response in several cancer types.[192,244,264,318–320] Moreover, inhibiting H_2S synthesis restores sensitivity to chemotherapy.[281,285] Increased antioxidant capacity in cancer cells further decreases ferroptosis, a newly recognized form of programmed cell death, which involves the promotion of lipid oxidation through a Fenton-like reaction by iron ions (Fe^{2+}). This reaction leads to increased levels of ROS and depletion of GSH, subsequently hindering the activity of glutathione peroxidase 4 (GPX4), a GSH-dependent hydroperoxidase, responsible for the elimination of lipid peroxides.[321,322] Ferroptosis thus, correlates with increased ROS input, GSH depletion, abrogation of cyst(e)ine import and lipid peroxide accumulation, and can be induced by several compounds, including inhibitors of cystine transport, as Erastin.[323–325] This creates an additional potential route for anticancer approaches aiming to overcome resistance. Our team has previously reported that, not only cysteine serves as an adaptative and cytoprotective tool in hostile TME conditions, as hypoxia, in ovarian cancer cells, but also allows resistance to platinum-based chemotherapy. We have identified high cysteine concentrations in ascitic fluids and serum from advanced stage ovarian cancer patients.[256] Furthermore, the capacity of cancer cells to metabolize and uptake cysteine may serve as a predictive indicator for the risk of resistance development to platinum-based therapy.[256]

Considering the ubiquitous occurrence of H_2S, the presence of elevated expression and enhanced activity of H_2S-generating enzymes strongly supports the involvement of cysteine metabolism in therapy response. This also indicates the potential value of utilizing stratification tools based on cysteine-related metabolic profiles in clinical settings, allowing for the customization and repurposing of oncological treatments. Furthermore, it suggests the potential use of H_2S-based chemo-preventive drugs as a viable approach against various malignancies.

Hypothesis, Aims and Thesis Outline

Tumor metabolic remodeling has acquired a main focus as a central hallmark of cancer along the years.[1,4,12] However, strategies aiming to take advantage of tumor metabolic profiles are still scarce, even though it has the potential to be a powerful tool in stratifying patients and aiding in clinical decisions. Cysteine metabolic remodeling, in particular, has been reported to be a crucial event in carcinogenesis and tumor progression due to cysteine's role as carbon and sulfur source, thus sustaining tumor bioenergetics and biosynthesis.[192] Additionally, cysteine metabolic remodeling is further associated with resistance to therapy due to its antioxidant properties and its limiting role in the synthesis of GSH. In cancer cells, cysteine metabolic remodeling increases its antioxidant potential giving these cells the ability to evade oxidative and alkylating drugs commonly used in cancer therapy.[205,313–317] In this context, the main players involved in cysteine metabolism are frequently found altered in the context of cancer, namely CBS, CSE, CAT:MST, the central H_2S-producing enzymes responsible for cysteine metabolism, and CDO1, responsible for cysteine oxidative catabolism.[239–251] [252–256] These enzymes, as well as the main cysteine transporters, xCT[193,198–205] and EAAT3[220–225], are important players in cysteine metabolic circuitries.

Additionally, the metabolite H_2S resulting from cysteine catabolism by CBS, CSE and MST is a well-known stimulator of cell bioenergetics, as a source of electron equivalents for the mETC and through persulfidation of ATPase, thus stimulating mitochondrial ATP production. Moreover, H_2S displays a powerful antioxidant ability as well.[257–263] So, it is expected that increased cysteine flux by alterations in cysteine transporters as well as altered expression and activity of H_2S-synthesizing enzymes can be directly linked to chemoresistance in several cancer types.[203–205,239,244,281,318,320,326] Among those are CM, CRC, LC and BC, some of the cancer types with higher incidence and mortality worldwide.[6–8,35,100,106]

Therefore, our overall hypothesis is that leveraging metabolic profiles, particularly related to cysteine metabolism, can be utilized as means of patient stratification and tumor characterization. Additionally, we propose that targeting cysteine metabolism could enhance cancer cell susceptibility to chemotherapy and overcome resistance. With this hypothesis in mind, we have formulated the following specific objectives, which are closely tied to the experimental and results chapters of our study:

1. To disclose the impact of mutated *BRD9* on cysteine metabolic remodeling in cutaneous melanoma (Chapter II);

2. To study the expression of cysteine metabolic players, characterize metabolic reliance on cysteine and test a metabolic approach using SeChry@PURE$_{G4}$-FA in non-small cell lung cancer (Chapter III);

3. To explore SeChry@PURE$_{G4}$-FA as a potential approach in colorectal cancer (Chapter IV);

4. To study the importance of cysteine metabolic remodeling and test the feasibility of a metabolic approach targeting cysteine metabolism with SeChry@PURE$_{G4}$-FA in breast cancer (Chapter V).

This thesis consists of seven chapters. Chapter I serves as a comprehensive introduction, offering an overview of the theoretical concepts explored in the subsequent chapters. Chapters II to V present the experimental findings derived from the PhD project. Each of these chapters includes an abstract, a brief introduction, materials and methods, as well as results, discussion and conclusion sections. Chapter VI encompasses the general discussion and key conclusions of the PhD project, emphasizing the significant contributions made in comprehending the impact of cysteine metabolic remodeling on CM, CRC, NSCLC and BC, and in testing innovative anti-tumoral strategies to enhance cancer treatment. Chapter VII discusses future perspectives related to the work presented in this thesis.

Chapter II

The Metabolic Impact of Mutated *BRD9* in Cutaneous Melanoma

This chapter is based on the following publication:

Ana Hipólito, Renato Ferreira, Cheila Brito, *et al*. *BRD9* status is a major contributor for cysteine metabolic remodeling through MST and EAAT3 modulation in malignant melanoma. Submitted for publication.

II.I. Abstract

CM is the most aggressive skin cancer, showing globally increasing incidence. Hereditary CM accounts for a significant percentage (5-15%) of all CM cases. However, most familial cases remain without a known genetic cause. Even though, *BRD9* has been associated to CM as a susceptibility gene. Still, the molecular events following *BRD9* mutagenesis are not completely understood. In this chapter, we disclosed *BRD9* as a key regulator in cysteine metabolism and associated altered *BRD9* to increased cell proliferation, migration and invasiveness, as well as to altered melanin levels, inducing higher susceptibility to melanomagenesis.

Data show novel molecular mechanisms based on *BRD9* status that potentially account for the increased risk of developing CM and enhancing CM aggressiveness. Moreover, the findings comprised in this chapter emphasize the role of cysteine metabolism remodeling in melanoma progression.

Keywords

Cutaneous melanoma, *BRD9*, Cysteine metabolism, Metabolic remodeling

II.II. Introduction

CM is the malignant transformation of skin melanocytes and the most hostile and invasive amongst skin cancers, accounting for most skin cancer-related deaths. Increased incidence of malignant CM is directly related to age, with median age of CM onset settled at 64 years.[29,30,327] Malignant CM aggressiveness is grounded on the higher invasive capacity of CM cells, causing metastatic colonization at early stages and frequent relapse events after primary tumor excision.[327] Importantly, metastasis is reported to decrease median overall survival of late stage CM patients. Nevertheless, recent studies reported an increase in overall survival numbers, which is probably a result of the implementation of more efficient therapies and higher clinical survaillance.[327–332] Since CM belongs to the group of cancers that arise due to chronic mutagenic exposure, in this case to UVR, it is, as expected, one of the tumors that shows the highest mutational frequency.[31] In fact, exposure to UVR is the major known risk factor associated to CM, including natural

exposure and tanning bed use, accounting for about 70% of all CM cases due to extensive genome damage, in a wavelength-dependent manner. [29,34–36] This causes UVR-exposed melanocytes to undergo apoptosis or transformation, losing their initial morphology and function and becoming malignant.[34,35] Other risk factors for melanomagenesis are phenotypical characteristics as fair skin, as well as family history.[29] Hereditary CM covers 5 to 15% of all CM cases, and is associated with germline mutations in a range of identified CM susceptibility genes.[47,72,86,87,333–336] However, among all familial CM cases, most remain without an identified genetic cause, which highlights the importance of identifying novel susceptibility genes in hereditary CM.[89] *Bromodomain-containing protein 9 (BRD9)* was previously identified as a promising susceptibility gene in the development of familial CM.[89] BRD9 defines different sub-complexes of SWI/SNF[91] and it works as an epigenetic reader that can selectively identify and bind, through its bromodomain, acetylated lysine residues belonging to histone or non-histone proteins. BRD9, thus, functions as a gene expression modulator by remodeling chromatin and recruiting the transcriptional machinery for certain genes involved in cellular functions, such as proliferation, migration and invasion, as well as metabolic adaptation as the HIF target genes[337], through SWI/SNF(BAF) chromatin remodeling complexes.[91–94,338] Interestingly, *BRD9* was found to be overexpressed in several types of cancer.[339–343]

In the skin, melanocytes produce the pigment melanin and transfer it to neighboring keratinocytes, where it protects the nuclei content of these cells against UVR-induced damage, acting in a photo protective way by forming supranuclear caps and scavenging absorbed radiation.[37,38] Melanin can be produced in two forms: brownish-black eumelanin and red/orange pheomelanin, the latter associated to the fair skin with a lower ability to tan, freckles and red hair phenotype.[39] The photolability of pheomelanin facilitates the generation of ROS[4028], potentiating the mutational character of UVR. It is known that the incidence of skin cancer is directly correlated to skin pigmentation, thus individuals that produce higher levels of pheomelanin are more prone to develop CM.[36,39,344] Both forms of melanin derive, though, from a common precursor: dopaquinone, which is produced from the oxidation of tyrosine by tyrosinase to DOPA and then to dopaquinone.[38,43–45] Eumelanin is then formed by the conversion of DOPAchrome to 5,6-dihydroxyindole-2-carboxylic acid (DHICA) and oxidation of 5,6-dihydroxyindole (DHI) and DHICA, catalyzed by two other tyrosinase-related proteins (TYRP1 and 2).[38,43–45,345] On the other hand, pheomelanin is spontaneously produced, requiring only cysteine to form 2, 5- or 5, 5-cysteinylDOPA that leads to the formation

of cysteinylDOPA-quinones, and then benzothiazine and benzothiazole.[38,41–45,345] Besides cysteine, it is known that GSH, a tripeptide formed by cysteine, glutamate, and glycine, can further combine with DOPAquinone to form pheomelanin.[346,347] Therefore, the metabolism of cysteine in melanocytes is deeply related to melanin synthesis and its UVR-protective role.

Interestingly, along with the high-rate mutational signature, CM is further described to display metabolic reprogramming features resultant from that mutational status.[348] Metabolic rewiring in crucial pathways such as glycolysis and amino acid metabolism are associated with increased CM malignancy and resistance.[348] However, little is known about cysteine metabolism in CM. In cancer, cysteine metabolic rewiring contributes to a better adaptation of cancer cells to hostile microenvironments, leading to tumor progression and resistance.[176] Rewired cysteine metabolism induces alterations in free radical scavenging and redox maintenance through its antioxidant properties by itself or as a glutathione constituent, altering the detoxifying potential in the microenvironment and constituting a severe chemoresistance mechanism.[176,182,313,349]

Cysteine metabolic remodeling further interferes in the production of biomass as a carbon source, and in the production of energy as a key player in sulfur metabolism, but also through its reductive catabolism by the enzymes CBS, CSE, and MST, the latter working together with CAT, leading to H_2S production.[231,264,350] H_2S, besides working as an antioxidant, can also supply the mETC, leading to ATP production and so, it is not surprising that H_2S levels are described to impact on cancer cell proliferation and bioenergetics.[264,283] Cyst(e)ine uptake occurs through specific transporters and exchangers, as EAAT3 or the cystine/glutamate antiporter xCT.[176] Both cysteine metabolic enzymes and transporters are described to be overexpressed in several cancer types.[225,247,264,351–356]

BRD9, as described above, is a key player in chromatin remodeling, and it can interfere with the action of several transcription factors. NRF2 is a transcription factor described to regulate the expression of AOEs.[357] NRF2 binds to specific DNA regions designated by antioxidant responsive element (ARE) sequences, which are conserved genomic regions, involved in orchestrating cellular responses to oxidative stress, maintaining cellular redox balance.[358] Moreover, NRF2 has been described to regulate the *SCL1A1* expression encoding EAAT3, which is able to transport cysteine.[359] The role of SWI/SNF and BRD9 in NRF2 action is controversial and it seems to be tightly dependent on the cellular and disease context. In NSCLC, the loss of function of

SWI/SNF, is associated with the activation of NRF2/KEAP1 pathway.[360] However, some SWI/SNF sub complexes can also potentiate the expression of NRF2 target genes[361], in renal cell carcinoma. Furthermore, in chronical lymphocytic leukemia, the expression of Nrf2 and downstream targets are significantly decreased upon BRD9-silencing.[362]
In this study, the putative regulatory role of *BRD9* in cysteine metabolism remodeling in CM was analyzed. Moreover, these results disclosed a putative mechanism linking mutated forms of *BRD9* to susceptibility to melanomagenesis.

II.III. Materials and Methods

Cell line culture

Human malignant melanoma cell lines A375 (American Type Culture Collection (ATCC), CRL-1619) and WM115 (Rockland code WM115-01-0001, BRAF V600E mutated, USA) were cultured according to the supplier's instructions. Both cell lines were maintained in Dulbecco's Modified Eagles Medium (DMEM) (41965-039, Life Technologies), supplemented with 10% fetal bovine serum (FBS) (S 0615, Merck), 1% Antibiotic-Antimycotic (AA; P06-07300, PAN Biotech) and 50 µg/mL Gentamicin (15750-060, Life Technologies). Cell cultures were maintained at 37°C in a humidified environment of 5% CO_2. Cells were detached with 0.05% Trypsin-EDTA 1× (25300-054, Thermo Fisher Scientific) at 37°C for approximately 5 min and split to new plates according to the experimental standard procedures. Cells were metabolically synchronized under starvation prior the exposure to experimental conditions.

Primary cell culture

Human epidermal keratinocytes isolated from neonatal foreskin (HEKns) (C-0015C, Thermofisher) were cultured in EpiLife medium (M-EPIcf-500, Gibco) supplemented with 1% commercial mix of human keratinocyte growth factors (S-001-5, Gibco), 0.06 mM calcium chloride (J62905.K2, Gibco) and 1% PenStrep (15070063, Gibco). Human dermal fibroblasts isolated from neonatal foreskin (HDFns) (C-004-5C, Gibco) were grown in DMEM (11960, Gibco) supplemented with 10% FBS (10500064, Gibco), 2 mM L-alanyl-L-glutamine dipeptide (35050038, GlutaMAX, Gibco) and 1%

PenStrep (15070063, Gibco). HEKn were used until passage 4 and HDFn until passage 13. Both HEKns and HDFs were grown in a humidified incubator at 37 °C with 5% CO_2.

BRD9 overexpression and *BRD9* c.183 G>C transfection

A375 and WM115 cell lines were transfected with three distinct expression plasmids: pCMV6-Empty (CAT# PS100001, Origene Technologies), pCMV6-*BRD9* WT (CAT# RC229303, Origene Technologies; *BRD9* - NM_023924 - Human Tagged ORF Clone) and pCMV6-*BRD9* c.183G>C (CAT#CW305250, Origene Technologies). pCMV6-*BRD9* c.183G>C contains the mutant open reading frame of RC229303 at nucleotide 183 from G to C leading to a E61D amino acid change. The transfection was performed with Lipofectamine 2000 Transfection Reagent (11668019, Thermo Fisher Scientific), following manufacturer's instructions. Stable transfected clones expressing neomycin resistance marker were selected using 1500 μg/mL of G-418 geneticin (10131035, Thermo Fisher Scientific). Validation of transfection was confirmed using Sanger sequencing, reverse transcription and quantitative real-time PCR and western blot, as described.

Sanger sequencing

Validation of transfection of_A375 and WM115 cell lines, using cDNA, was performed upon amplification by PCR and Sanger sequencing, using primers forward 5′ ACGAGGATTATGCCGACAAG 3′ and reverse 5′ CGTCCAGATGCTTCTCCTTC 3' and the protocol proposed by Big Dye™ Terminator v1.1 Cycle Sequencing RR-100 Kit (4336768, Thermo Fisher Scientific). Afterwards, samples were purified using Exonuclease I 20 U/μl (EN0582, Thermo Fisher Scientific) and FastAP Thermosensitive Alkaline Phosphatase 1 U/μl (EF0654, Thermo Fisher Scientific), and analyzed in an automatic sequencer 3500 Genetic Analyzer (Thermo Fisher Scientific).

Reverse Transcription and Quantitative Real-Time PCR (RT-qPCR)

RNA from A375 and WM115 cell variants, cDNA synthesis and relative quantitative Real-Time PCR was performed as described elsewhere[363] and carried out in a LightCycler 480 instrument (Roche). Primers are presented in in Table II.1.

Table II.1 – Primers used in gene expression analysis. Detailed characterization of the primers used in RT-qPCR assays.

RT-qPCR

Gene	Primer	Primer sequence (5'→3')	Size (nt)	Ta (°C)	G/C %	Fragment size (bp)
BRD9	Forward	*GCGACTTGAAGTCGGACGAGAT*	22	62	55	128
	Reverse	*GTCCACCACTTTCTTGCTGTAGC*	23		52	
CBS	Forward	*GAGCTCTTGGCCAAGTGTG*	19	60	58	232
	Reverse	*GCACGTCCACCTTCTCGG*	18		67	
CTH	Forward	GCAGCCACTGTAACTATTACCC	22	60	50	175
	Reverse	CTGGTGTAATTGCTGCCTCTAG	22		50	
MPST	Forward	CTTCATCAAGACCTACGAGGAC	22	60	50	134
	Reverse	GGTAGTGGCCAGGTTCAATG	20		55	
GOT-1	Forward	*GAGAAGAGAGGATTGGACCTC*	21	60	52	147
	Reverse	*CATGACAGAAGCAATCTGCTTCC*	23		48	
GOT-2	Forward	*CCAGAGCCAGCTCCTGGT*	18	61	67	171
	Reverse	*CTGCCTTGCGGACGCTAG*	18		67	
SLC7A11	Forward	*GGTCCTGTCACTATTTGGAGC*	21	61	58	136
	Reverse	*GAGGAGTTCCACCCAGACTC*	20		59	
SLC1A1	Forward	*GTATCACGGCCACATCTGCC*	20	61	60	121
	Reverse	*GCAATGATCAGGGTGACATCC*	21		52	
HPRT1	Forward	*TGACACTGGCAAAACAATGCA*	21	58	43	94
	Reverse	*GGTCCTTTTCACCAGCAAGCT*	21		52	
	Reverse	GCTATTGTGCGCTGGGCTC	19		63	

Western blotting

Western blotting was performed to confirm the expression of BRD9 protein variants. A375 or WM115 cells were seeded in T-25 cm^2 flasks (6.5×10^5 cells/flask; 2.2×10^5 cells/mL) and collected by scraping and lysed for 1 h using ice-cold radioimmunoprecipitation assay (RIPA) lysis buffer (89900, Thermo Fisher Scientific) with protease and phosphatase inhibitor mixture (PPC1010, Sigma Aldrich). Protein concentration in cell extracts was determined using Pierce BCA protein assay kit (23225, Thermo Fisher Scientific). Cell extracts (25 µg) were resuspended in Laemmli buffer,

consisting of 250 mM Tris-HCL (pH=6.8), 10% Sodium dodecyl sulfate (SDS), 0.5% bromophenol blue and 50% glycerol, was added to each sample in a 1:5 dilution and previously mixed with β-mercaptoethanol in a 1:20 dilution. The protein extracts were separated in a 10% SDS-polyacrylamide gel electrophoresis and transferred onto methanol-activated polyvinylidene difluoride membranes (1620177, Bio-Rad) using the Trans-Blot® Turbo Bloting System (Bio-Rad). The membrane processing, immunoblot and development were performed as described elsewhere.[364] The primary antibodies were anti-BRD9 (dilution 1:7500; overnight incubation at 4°C; ab137245, Abcam), and anti α-tubulin, clone B-5-1-2 (dilution 1:4000; 1 h incubation at room temperature; T5168, Merck KGaA).

Proliferation assay

To study cellular proliferative rate, A375 or WM115 cells were plated in 24-well plates (5×10^4 cells/well; 1×10^5 cells/mL) in supplemented DMEM and left to adhere for 24 h in normal culture conditions. Cells were exposed or not to 0.402 mM L-cysteine (102839, Merck). At each time-point, cells were detached as described (supernatant was also collected) and cells were centrifuged for 5 min at 155 × *g*. Supernatant was discarded and total cells were counted, using a Neubauer improved cell counting chamber.

Wound healing assay

The migratory capacity of A375 or WM115 cells was evaluated using the wound healing assay. Cells were plated in 12-well plates (1×10^5 cells/well/mL) until the formation of a confluent monolayer. Cells were exposed or not to 0.402 mM L-cysteine (102839, Merck). Once confluent, cells were incubated for 3 h with 5 μg/mL mitomycin-C (M4287, Sigma Aldrich) and a linear scratch in each monolayer was made with a 20 μL pipette tip, creating a wound across the well diameter. The media was replaced to remove debris and cells in suspension. Bright-field images of each well were acquired on the Olympus IX53 Inverted Microscope at each time-point. The wound closure was quantified using the ImageJ software (imagej.nih.gov/ij/).

Nuclear Magnetic Resonance Analysis (^{1}H-NMR)

Metabolic profiles were addressed by ^{1}H-NMR. Briefly, cells were seeded in 175 cm^2 culture flasks (6.5 ×1 0^6 cells/flask; 5 × 10^5 cells/mL) and cultured in control conditions or exposed to 0.402 mM L-cysteine (102839, Merck). Cell extracts were performed and samples were prepared as described.[194] The ^{1}H-NMR (noesypr1d) was obtained at 25°C in an Avance 500 II+ (Bruker) spectrometer operating at 500.133 MHz, equipped with a 5 mm TCI(F)-z H-C/N Prodigy cryo-probe. The chemical shifts in aqueous sample were referred to the TSP. Topspin 4.0.7 (Bruker) was used for acquisition and spectra analysis. Compound identification was performed by resorting to the Human Metabolome database (HMDB) and Chenomx NMR suite software version 8.1 (Chenomx Inc.). Metabolites' concentrations were determined using Chenomx NMR suite software version 8.1 for ^{1}H-NMR spectra (Chenomx Inc.).

Immunofluorescence

Cells were seeded in glass coverslips in 24-well plates coated with 0.2% gelatin from porcine skin (G-1890, Sigma-Aldrich) (1 × 10^5 cells/well; 2 × 10^5 cells/mL), and cultured as previously described. Once adherent, cells were fixed with 4% paraformaldehyde for 15 min at 4°C and permeabilized with 0.1% saponin in PBS-BSA (0.5%, w/v, BSA in PBS) for 15 min at room temperature. Cells were then incubated overnight, 4°C with anti-MPST (1:100, HPA001240, Sigma-Aldrich) and anti-EAAT3 (1:100, 14501S, Cell Signaling Technology) and then incubated with secondary antibody for 2 h at room temperature (Alexa Fluor® 488 anti-rabbit, A-11034, Thermo Fisher Scientific). Slides were mounted in VECTASHIELD media with 4′-6-diamidino-2-phenylindole (DAPI, H-1200-10, Vector Labs) and examined by standard fluorescence microscopy (Zeiss Imajer.Z1 AX10 microscope). Images were acquired and processed with CytoVision software (Leica Biosystems).

Promoter activity by luciferase reporter gene assay

A fragment of 5' UTR region (-870 to -28) of *MPST* gene were amplified by PCR (Table II.2) and inserted in pGL3-Basic vector (E1751, Promega) using *Mlu*I and *Hind*III restriction sites and standard techniques.[365] Cells were transfected with 0.5 μg of each

pGL3-*MPST* promoter construct, positive control (pGL3-Control; E1741; Promega) or negative control (pGL3-Basic), and co-transfected with 0.1 µg Renilla vector (E2810; Promega). Luciferase activity of constructs, Firefly and Renilla luciferases were measured using the Dual Luciferase Assay System (E1910, Promega) according to the manufacturer's protocol and results were acquired and analyzed as described.[366]

Table II.2 – Primers used in *MPST* promoter constructs. Detailed characterization of the primers used in pGL3-*MPST* promoter constructs.

pGL3- *MPST* promoter constructs			**Size (nt)**	**Ta (°C)**	**G/C %**
MPST 5'UTR (-870-28)	Forward *Mlu*-I restriction	ATGACGCGTCACCATGTTGGCCAGACTGG	29	67	52
	Reverse *Hind*-III restriction	ATGAAGCTTGCGACAGGGAGGATGTCAG	29		48

H_2S quantification in cell homogenates

Cells were seeded in 6-well plates (5×10^5 cells/well, 2.5×10^5 cells/mL) and cultured in control conditions or exposed to 0.402 mM L-cysteine (102839, Merck) and/or 30 µM NaHS (161527, Sigma-Aldrich) for 16 h. Then, cells were scraped in PBS and centrifuged at 210 × *g* for 5 min. The cell pellet was homogenized in NP40 lysis buffer (1% NP40, 150 mM NaCl, 50 mM Tris-Cl, pH 8.0) on ice for 30 min and centrifuged for 5 min at 20000 g at 4 °C. Cell homogenates (20 µL) were incubated in black 96-well plates with 10 µM 7-Azido-4-Methylcoumarin probe (AzMC, L511455, Sigma Aldrich) in the absence or presence of 1 mM o-(carboxymethyl)hydroxylamine hemihydrochloride (AOAA, C13408, Sigma Aldrich) and 3 mM DL-propargylglycine (PAG, P7888, Sigma Aldrich). H_2S production was monitored following the fluorescent signal of AzMC probe (λ_{exc}: 355 nm; λ_{em}: 460 nm) every 30 min for 2 h, in a VICTOR3 instrument from PerkinElmer/Wallac 1420 v3.0 software. The protein concentration of each lysate was determined with the Bradford method using protein assay dye reagent concentrate (500-0006, Bio-Rad). The H_2S production activities were normalized to the total protein concentration and to a blank sample (cellular lysates without probe).

ATP quantification

Cells were seeded in 6-well plates (5×10^5 cells/well, 2.5×10^5 cells/mL) and cultured in control conditions or exposed to 0.402 mM L-cysteine (102839, Merck) and/or 30 µM NaHS (161527 Sigma Aldrich) for 16 h. Then, cells were scraped in PBS containing 2 mM EDTA, centrifuged at 210 × *g* for 5 min and homogenized in 1% NP40 lysis buffer (1% NP40, 150 mM NaCl, 50 mM Tris-HCl, pH 8.0) with 5% protease inhibitor (S8830, Sigma) on ice for 30 min and centrifuged at 20000 g for 5 min at 4 °C. Protein concentration was quantified using the Bradford method, as described previously. ATP determination kit (A22066, Molecular probes) was used in accordance with the manufacturer's instructions, using an ATP calibration curve, within the range 0 to 30 µM. The measurements were performed using the Luciferase protocol in a VICTOR3 (PerkinElmer), using the Wallac 1420 software.

Chromatin immunoprecipitation (ChIP) analysis

To analyze potential interactions between the transcription factor NRF2 and ARE sequences in *MPST and SLC1A1* promoters, ChIP was employed. We identified two putative ARE sequences recognized by NRF2 in the *MPST* promoter and one in the *SCL1A1* promoter, and designed primers for those regions to perform ChIP analysis. Cell preparation and ChIP assay were performed using the OneDay ChIP kit (kch-onedIP-060, Diagenode) according to the manufacturer's protocol. The chromatin complexes were immunoprecipitated with 1 µg/mL of specific anti-human NRF2 antibody (ab31163; Abcam). The relative occupancy of the immunoprecipitated factors at a specific promoter region was performed by absolute qPCR, using primers for *MPST* and *SLC1A1* promoter (Table II.3) and calculated using the following formula:

$$\text{Relative occupancy}=2^{(\text{CtNegCtl}-\text{CtTarget})}$$

Table II.3 – Primers used in relative occupancy quantification. Detailed characterization of the primers used in ChIP assay.

ChIP assay

Gene	Primer	Primer sequence (5'→3')	Size (nt)	Ta (°C)	G/C %	Fragment size (bp)
MPST (a)	Forward	GCATACTCATGTGGGTAGGG	20	61	55	240
	Reverse	GAGGAAACTGAGGCTCAGAGG	21		57	
MPST (b)	Forward	CTGCTCACACAGATGCTAGG	20	61	55	396
	Reverse	GCCACCCGGTGACATCCG	18		72	
SLC1A1	Forward	GCAAAACTACCGGGCTGG	18	60	61	202
	Reverse	GCTATTGTGCGCTGGGCTC	19		63	

Melanin quantification

Melanin content was measured through spectrophotometry as described elsewhere.[367] Cells were exposed or not to 0.402 mM L-cysteine (102839, Merck) for 16 h after 16 h of starvation. Briefly, A375 and WM115 cell variants were collected with no phenol red 2.5% Trypsin 10 × (15090046, Thermo Fisher Scientific) as described previously, and counted using a Neubauer improved cell counting chamber. Cells were suspended in 1 M NaOH and the melanin content was measured at 490 nm. Melanin concentration was determined through a standard curve (range 0 to 200 µg/mL) obtained with synthetic melanin (M0418, Sigma Aldrich).

Metabolic viability assays

All variants of A375 and WM115 were plated in 96-well clear plates (2×10^4 cells/well; 2×10^5 cells/mL) and treated with a commercial MST inhibitor (I3MT-3, HY-128206, CAS No.459420-09-8, MedChemExpress) at increasing concentrations (0, 30 µM, 100 µM, 300 µM, 600 µM and 900 µM). Upon 48 h of exposure, metabolic viability assays were performed by colorimetry using Cell Proliferation Reagent WST-1 (11644807001, Roche), according to the manufacturer's instructions.

Cell death analysis by flow cytometry

All variants of A375 and WM115 were seeded in 24-well plates (1×10^5 cells/well; 2×10^5 cells/mL). After exposure to MST inhibitor (I3MT-3, HY-128206, CAS No.459420-09-8, MedChemExpress), cells were collected and labeling with FITC-labeled Annexin V (640906, BioLegend) and propidium iodide (PI; P4170, Sigma Aldrich Aldrich) was performed as described.[364] Results were analyzed by flow cytometry (BD FACSCanto II). FlowJo X v10.0.7 software (https://www.flowjo.com/) was used to analyze data.

Three-dimensional (3D) *in vitro* melanoma skin model

To establish the three-dimensional melanoma skin model used, we adapted the protocols published elsewhere.[368,369] Essentially, porous polystyrene scaffolds (Alvetex®, AVP005-48, REPROCELL Europe Ltd.) with an area of 1.13 cm^2 were inserted in 6-well plates and pretreated with 70% ethanol for 30 min to render them hydrophilic properties. The scaffolds were washed twice with phosphate-buffered saline (PBS) and 2×10^6 HDFns were seeded onto the scaffolds in 100 µL of HDFn medium, followed by incubation in a humidified incubator at 37 °C with 5% CO_2 for 1.5 h to allow cell adhesion. Next, the scaffolds containing HDFns were submerged with 9 mL of HDFn medium supplemented with 100 µg/mL L-ascorbic acid (11487487, Fisher Scientific) and maintained up to a further 15 days at 37°C in a 5% CO_2 humidified incubator. The culture medium was renewed every 5 days to allow the formation of a dermal equivalent. After this, 5×10^4 A375 or 1×10^5 WM115 melanoma cells were seeded on the dermis equivalents in 2 mL of melanoma culture medium supplemented or not with 0.402 mM L-cysteine (102839, Merck). After incubating for 3 days at 37°C and 5% CO_2, 1×10^6 HEKns were added in 2 mL of HEKn medium containing the final concentration of 1.5 mM calcium chloride (Gibco) without L-cysteine (102839, Merck). Finally, after further 3 days of incubation, keratinocytes were exposed to air-liquid interface and the culture medium was changed to HEKn medium containing the final concentration of 1.5 mM calcium chloride (Gibco), 10 ng/µL keratinocyte growth factor (K1757, Sigma), 50 µg/mL L-ascorbic acid (11487487, Fisher Scientific) and 0.402 mM L-cysteine (102839, Merck) or not. The medium was changed every 2 days for 18 days to allow HEKn

differentiation in the several epidermis *strata*, as well as melanoma cell invasion into the dermis. The tissues were fixed overnight in 10% neutral buffered formalin (Formalin 10%, Cat. number 9713.9010, VWR) and embedded in paraffin. Sections (4 μm) were stained with hematoxylin and Eosin staining (H&E, Hematoxylin, Cat. Number CS700, Dako; and Eosin, Cat. Number CS701, Dako). Melanoma thickness was measured in 20 different spots in two biological replicates using Aperio ImageScope software (https://www.leicabiosystems.com/en-pt/digital-pathology/manage/aperio-imagescope/).

Immunohistochemistry

The invasion of melanoma cells, in 3D skin model, was evaluated upon immunodetection of S-100 protein, which is expressed in neural crest-derived cells, being considered an efficient melanoma marker.[370,371] Immunohistochemistry analysis was performed using anti–S100 (Cat. Number 760-2523, Roche Diagnostics), pre-diluted for 16 min; pretreatment CC1 - 48 min; Ventana Medical Systems) with appropriate positive and negative controls samples, on the BenchMark ULTRA IHC/ISH Automatic staining platform (Ventana Medical Systems) using OptiView DAB IHC Detection Kit with diaminobenzidine as the chromogen to detect antigen expression. Tissue sections were counterstained with Mayer's hematoxylin before mounting.

Statistical Analysis

Statistical analyses and half maximal effective concentration (EC_{50}) values were performed in GraphPad Prism 8.0 software (www.graphpad.com). Data are presented as mean ± SD. Assays were performed with at least three biological replicates (with at least 3 independent n). For comparisons of two groups, a two-tailed unpaired t-test was used. For more than two groups, one-way and two-way analyses of variance (ANOVA) were used. Statistical significance was established as $p < 0.05$.

II.IV. Results

Overexpression of *BRD9* and *BRD9* c.183G>C induces a less proliferative but more migratory phenotype in A375 cutaneous melanoma cells.

Given that the c.183G>C SNV had been already identified in a Portuguese cohort[89], we hypothesized that, although it was predicted to have benign effects by *in silico* analysis[372], this variant could induce alterations in CM cells that could correlate with hereditary CM features. To test this hypothesis, we transfected A375 melanoma cells with a *BRD9*-encoding plasmid (A375 *BRD9* WT), as well as *BRD9* (c.183G>C)-encoding plasmid. In addition, we transfected the empty pCMV6 vector as a negative control. We then obtained A375 clones successfully overexpressing *wild-type* (WT) or c.183G>C *BRD9* at mRNA and protein levels (Figure II.1 A, B and C). To disclose the cellular effects of both *BRD9* forms in A375 cells, we studied the proliferation rate of these clones over 48 h and found that both A375 *BRD9* WT or *BRD9* c.183 G>C showed a significant reduction in proliferation from 6 h, and substantial reduction of proliferative capacity at 48 h, when comparing to control even in the presence of cysteine (Figure II.1 D and E). We then wondered if these *BRD9* alterations could also affect the migratory capacity of these cells. We assessed cell migration by wound healing over a period of 48 h, in the presence of mitomycin to exclude the interference of cell proliferation on the wound closure. Interestingly, we found that both A375 *BRD9* WT or *BRD9* c.183 G>C showed a significant increase in migration capacity, when comparing with control, starting at 10 h, in the absence and presence of cysteine (Figure II.1 F and G). We can, then, conclude that overexpression of *BRD9* in its WT or c.183G>C variants promotes a shift in cellular features, inducing a less proliferative but more migratory phenotype in A375 cells.

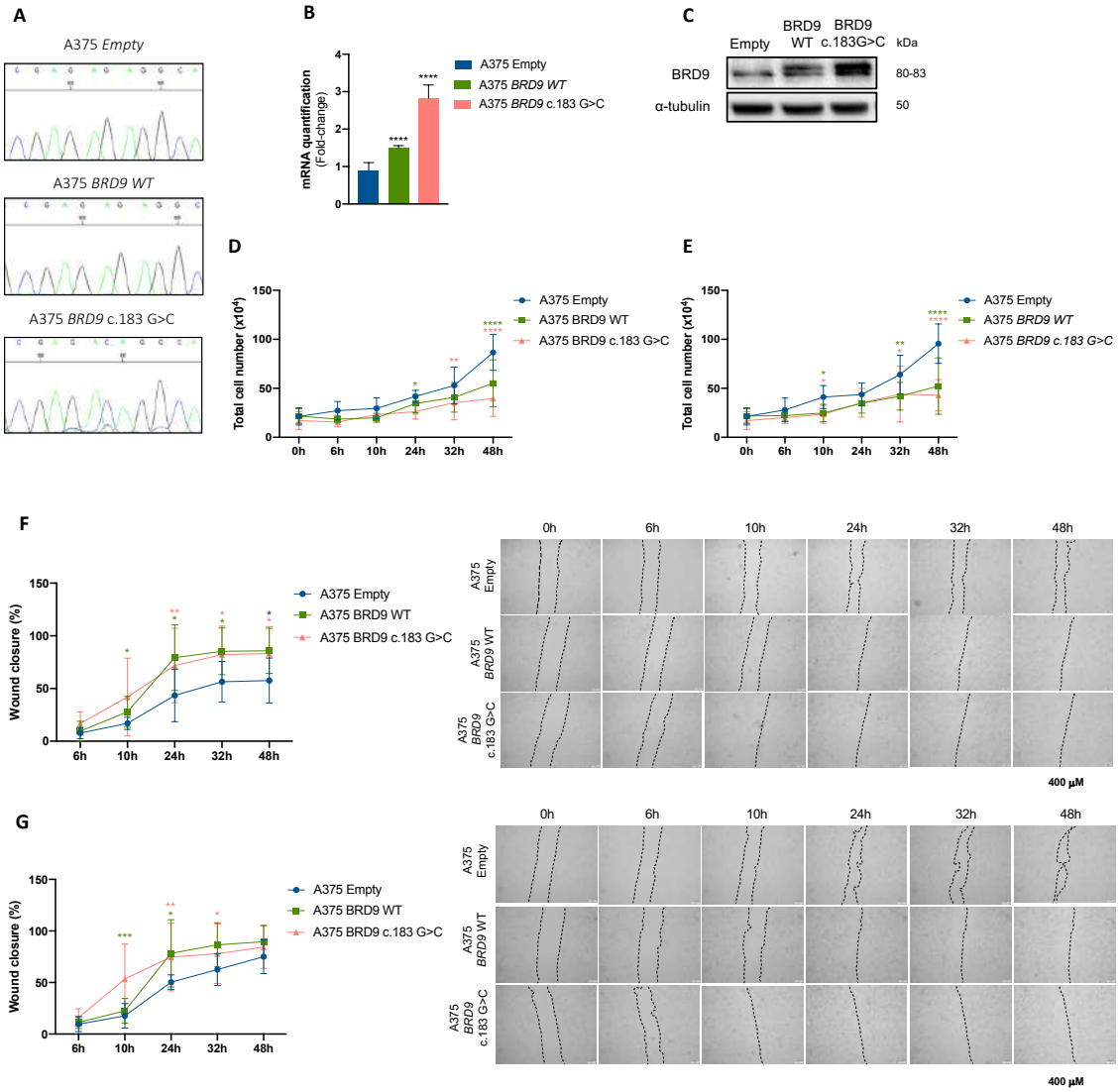
A
A375 Empty
A375 BRD9 WT
A375 BRD9 c.183 G>C
B
mRNA quantification (Fold-change)
A375 Empty
A375 BRD9 WT
A375 BRD9 c.183 G>C
C
Empty
BRD9 WT
BRD9 c.183G>C
kDa
BRD9
80-83
α-tubulin
50
D
Total cell number (x10⁴)
A375 Empty
A375 BRD9 WT
A375 BRD9 c.183 G>C
0h
6h
10h
24h
32h
48h
E
Total cell number (x10⁴)
A375 Empty
A375 BRD9 WT
A375 BRD9 c.183 G>C
F
Wound closure (%)
A375 Empty
A375 BRD9 WT
A375 BRD9 c.183 G>C
400 µM
G
Wound closure (%)
A375 Empty
A375 BRD9 WT
A375 BRD9 c.183 G>C
400 µM

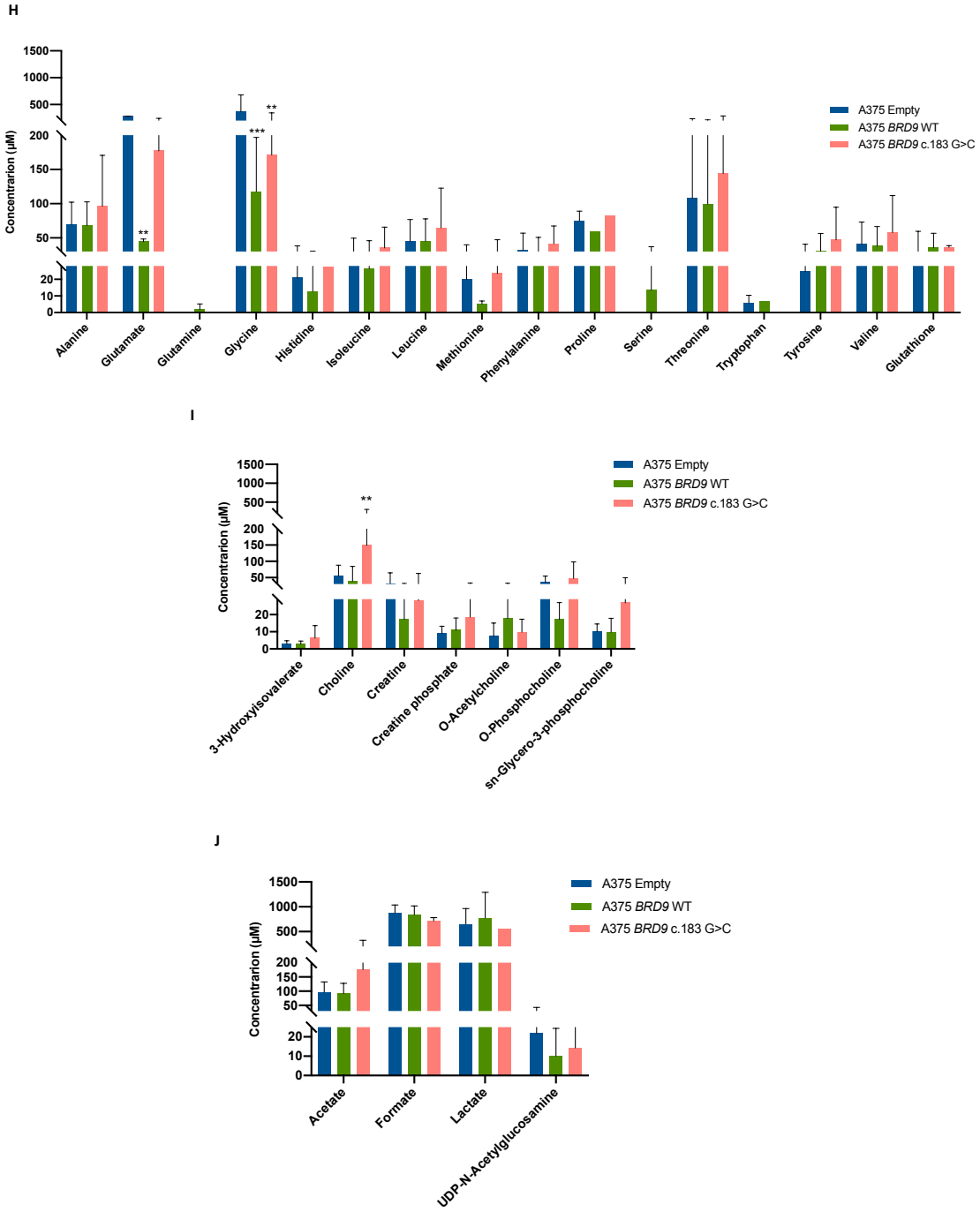

Figure II.1 - *BRD9* wild-type and *BRD9 c.183G>C* overexpression induces a less proliferative but more migratory phenotype and rewires amino acid metabolism in A375 melanoma cells. By Sanger sequencing the sequence mRNA was confirmed **(A)** and by qPCR **(B)** and western blotting **(C)** the transfection of A375 melanoma cells and the expression of the BRD9 variants was confirmed**.** A375 cells transfection with *wild-type* overexpression and *BRD9* c.183G>C (over)expression vectors induced increased mRNA and protein levels of *BRD9*, comparing to empty vector. Overexpression of *BRD9* WT or *BRD9* c.183 G>C induced a decreased proliferation rate in A375 cells, comparing to empty vector, in the absence **(D)** and presence **(E)** of cysteine. Overexpression of *BRD9* WT or *BRD9* c.183 G>C induced an increased migration capacity in A375 cells, by wound healing, comparing to empty vector, in the absence **(F)** and in the presence **(G)** of cysteine. **(H-J)** Nuclear magnetic resonance spectroscopy of transfected A375 melanoma cells extracts in the absence of cysteine indictes that *BRD9* WT and *BRD9* c.183G>C overexpression induces a metabolic remodeling in several key metabolic pathways. Data is represented as mean ± SD. *p<0.5, **p<0.01, ***p<0.001, ****p<0.0001. Experiments were performed with biological triplicates.

BRD9 wild-type and *BRD9* c.183G>C overexpression induces metabolic remodeling in A375 cutaneous melanoma cells

Alterations in cellular features induced by overexpression of *BRD9* and *BRD9* c.183G>C in this cell line, led us to wonder if A375 altered phenotype could be due to metabolic shifts induced by these genetic alterations.

^{1}H-NMR analysis showed that several amino acids show contrasting trends, when comparing to control (A375 empty) levels (Figure II.1 H). Glutamate tended to decrease in A375 *BRD9* WT and A375 *BRD9* c.183G>C. The same tendency was observed for glycine, which presents more prominently in A375 *BRD9* c.183G>C than in A375 *BRD9* WT. Glutamine levels appear to be low and are only noteworthy in A375 *BRD9* c.183G>C. Interestingly, methionine levels seemed to decrease only in A375 *BRD9* c.183G>C, which indicates that a downstream rewiring in cysteine production may be occurring. While cysteine was not detected in the analysis of any cell variants, the levels of reduced GSH were similar between them, which may indicate that cysteine is being rapidly consumed to maintain glutathione availability, since it is a rate-limiting amino acid for glutathione synthesis (Figure II.1 H). Moreover, we also found different metabolic patterns concerning sugar and organic acids metabolism (Figure II.1 I and J), as for acetate and choline, which seem to increase in A375 *BRD9* c.183G>C, and creatine, which decreases in A375 *BRD9* WT (Figure II.1 I and J). Notably, upon cysteine exposure, all A375 cell variants presented a trend to decrease the availability of glutamate and glycine. Accordingly, the GSH levels also tended to decrease upon cysteine exposure in A375 cells overexpressing WT or mutated *BRD9*, which indicates that this metabolic remodeling may require GSH consumption in order to keep the metabolic rate upon accelerating glutathione turnover. Moreover, cysteine canalization as a supplier for other pathways can also be an explanation, since cysteine catabolism dependent on MST seem to be active. Cysteine exposure further induced alterations in sugar and organic acids levels, as well as in other relevant metabolites, as creatine and creatine phosphate (Figure II.2 A, B and C). Metabolic profiling led to the conclusion that both A375 *BRD9* WT and A375 *BRD9* c.183G>C present metabolic variations.

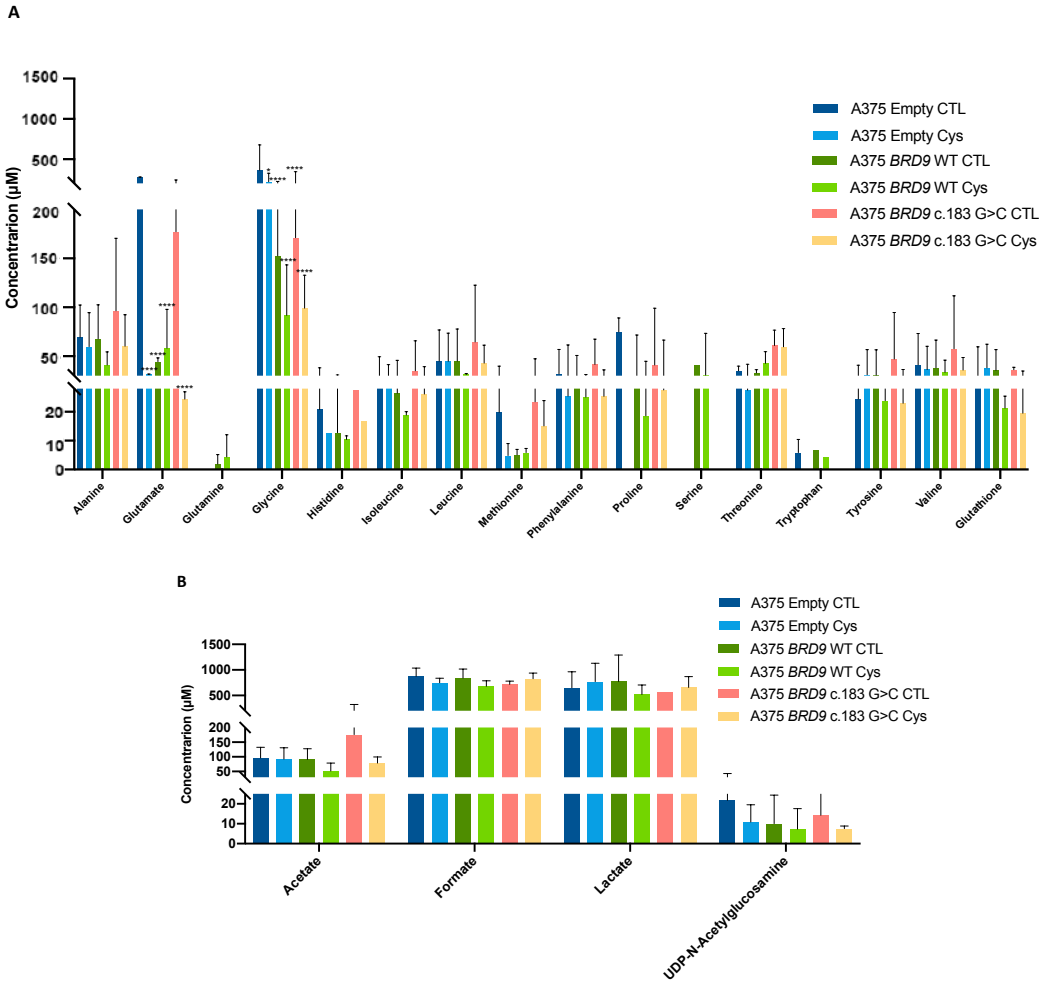
A
Concentrarion (µM)
1500
1000
500
200
150
100
50
20
10
0
A375 Empty CTL
A375 Empty Cys
A375 BRD9 WT CTL
A375 BRD9 WT Cys
A375 BRD9 c.183 G>C CTL
A375 BRD9 c.183 G>C Cys
Alanine
Glutamate
Glutamine
Glycine
Histidine
Isoleucine
Leucine
Methionine
Phenylalanine
Proline
Serine
Threonine
Tryptophan
Tyrosine
Valine
Glutathione
B
Concentrarion (µM)
Acetate
Formate
Lactate
UDP-N-Acetylglucosamine

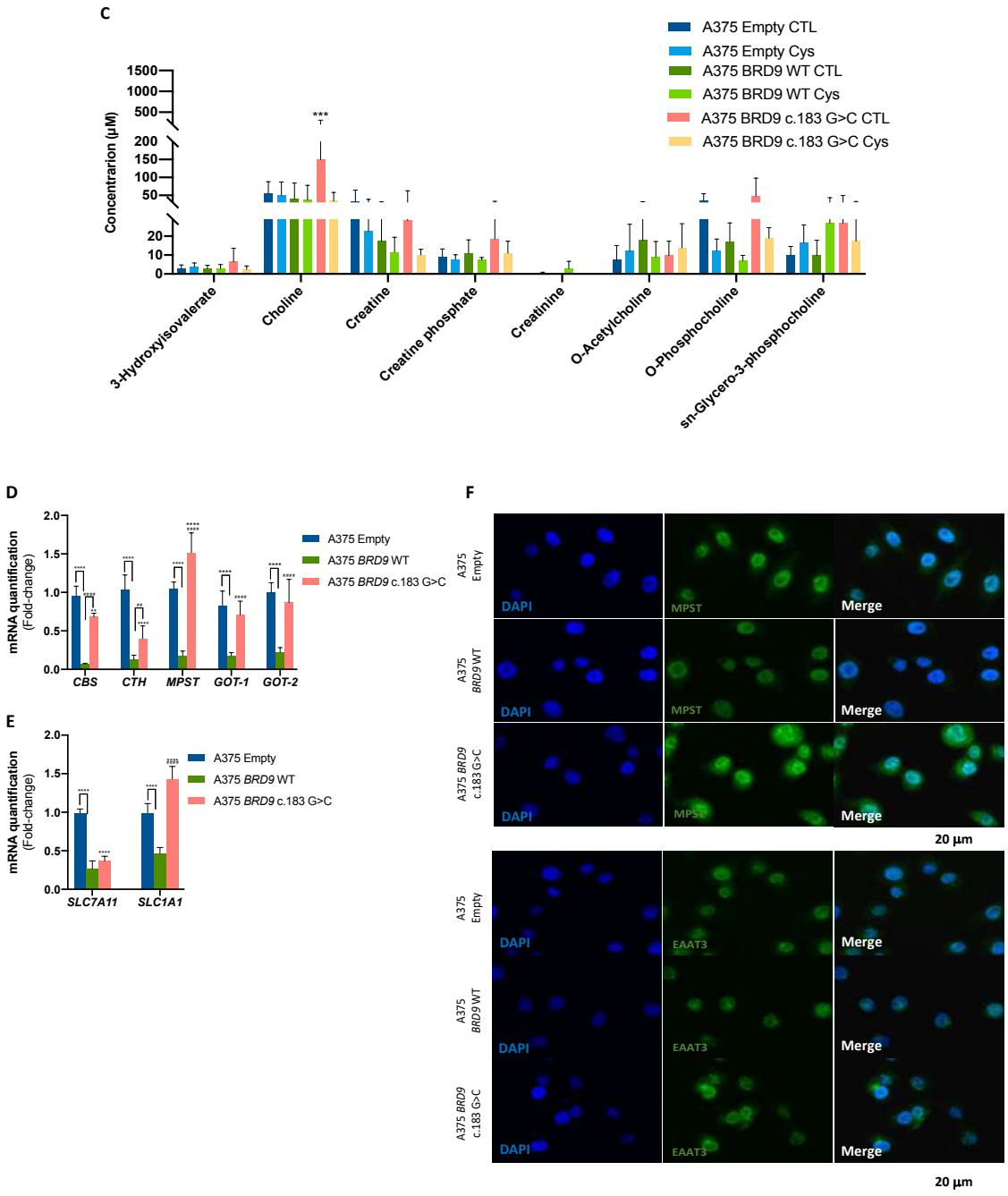

Figure II.2 – *BRD9 wild-type and BRD9 c.183G>C* overexpression alters the metabolic response of A375 cells to cysteine availability and modulates cysteine metabolic enzymes and transporters mRNA and protein expression. (A-C) Nuclear magnetic resonance spectroscopy of transfected A375 melanoma cells extracts in the presence (Cys) or absence (CTL) of cysteine indicates that BRD9 wild-type and BRD9 c.183G>C overexpression modulates the metabolic response to cysteine exposure, regarding intracellular amino acid, sugars and organic acids metabolism and other metabolic compounds. **(D)** By qPCR, mRNA levels of genes encoding enzymes *CBS*, *CTH*, *MPST*, *GOT-1* and *GOT-2*, as well as **(E)** genes encoding cyst(e)ine transporters *SLC7A11* and *SLC1A1* in A375 transfected cells were quantified and it was observed that induction of *BRD9* WT and c.183G>C variants overexpression regulates the expression of cysteine enzymes and transporters. A375 *BRD9* c.183 G>C induces an upregulation of both *MPST* and *SLC1A1,* analyzed by qPCR. **(F)** Protein expression of MST and EAAT3 show upregulation of both proteins induced by *BRD9* c.183 G>C induction, evaluated by immunofluorescence. Magnification 400 X, scale 20 µm. Data is represented as mean ± SD. *p<0.5, **p<0.01, ***p<0.001, ****p<0.0001 (* in relation to Empty; # in relation to *BRD9* WT). Experiments were performed with biological triplicates.

BRD9 wild-type and *BRD9* c.183G>C overexpression modulates cysteine metabolism in A375 cutaneous melanoma cells

The impact of *BRD9* WT and *BRD9* c.183G>C overexpression on the modulation of cysteine synthesis and reductive degradation in A375 cells, was assessed by the quantification of mRNA expression of key enzymes and transporters, namely: CBS (*CBS* gene), CSE (*CTH* gene), MST (*MPST* gene), cytosolic CAT (*GOT-1* gene), mitochondrial CAT (*GOT-2* gene), xCT (*SLC7A11*), and EAAT3 (*SLC1A1*). Interestingly, the overexpression of *BRD9* WT strongly repressed the expression of the entire panel of studied genes, comparing to control. Moreover, overexpression of *c.183G>C BRD9* exhibited a similarly repressive, yet highly attenuated, pattern regarding *CBS*, *CTH*, *GOT-1*, *GOT-2* and *SLC7A11* expression. Surprisingly, A375 *BRD9* c.183G>C appeared to induce *MPST* and *SLC1A1* expression, comparing to control (Figure II.2 D and E). These results were confirmed at the protein level (MST and EAAT3, Figure II.2 F).

We then studied the effect of these expression shifts in cysteine related enzymes and transporters on the production of H_2S, which, as stated above, is produced through cysteine reductive degradation by CBS, CSE and/or CAT/MST. In these assays, we analyzed H_2S levels in the absence or presence of AOAA and PAG, inhibitors of the reverse transsulfuration enzymes CBS and CSE, to estimate their relative roles with respect to MST (or other H_2S sources). A375 cells overexpressing either *BRD9* WT or *BRD9* c.183G>C presented an increase in H_2S levels, which were not altered by CBS/CSE inhibitors (Figure II.3 A). While the increase in H_2S levels in *BRD9* c.183G>C-overexpressing cells matched the increase in MST expression, the same correlation was not observed with *BRD9* WT-overexpressing cells (Figure II.3 A). It cannot be excluded that the capacity of cells to disposing of H_2S may have also been affected.

Pre-incubation of the cells with cysteine did not induce any change in steady-state H_2S levels between the three cell lines. Moreover, cysteine seems to have abrogated the *BRD9*-induced increase in H_2S levels, as compared to the control conditions (Figure II.3 A). Pre-incubation with the polysulfides-containing H_2S donor NaHS increased H_2S levels in every cell line, irrespectively of co-incubation with cysteine, in the absence of inhibitors (Figure II.3 A). The extent of H_2S levels decrease in the presence of AOAA+PAG was more evident in NaHS-incubated cells.

Since H_2S can serve as a source of electron equivalents to the mETC, we checked the effect of *BRD9* overexpression on the ATP levels. In control conditions, overexpression of *BRD9* WT or c.183G>C did not significantly change ATP levels. Incubation with NaHS in the absence or presence of cysteine resulted in a mild increase in ATP levels in all cell lines, whereas co-incubation with cysteine alone showed no significant effect comparing to control (Figure II.3 B). In the presence of AOAA+PAG, in comparison with control cells bearing the empty vector and with control conditions, ATP levels were significantly lower for *BRD9* c.183G>C expressing A375 cells pre-incubated with cysteine and for cells expressing either *BRD9* variant pre-incubated with cysteine (Figure II.3 B).

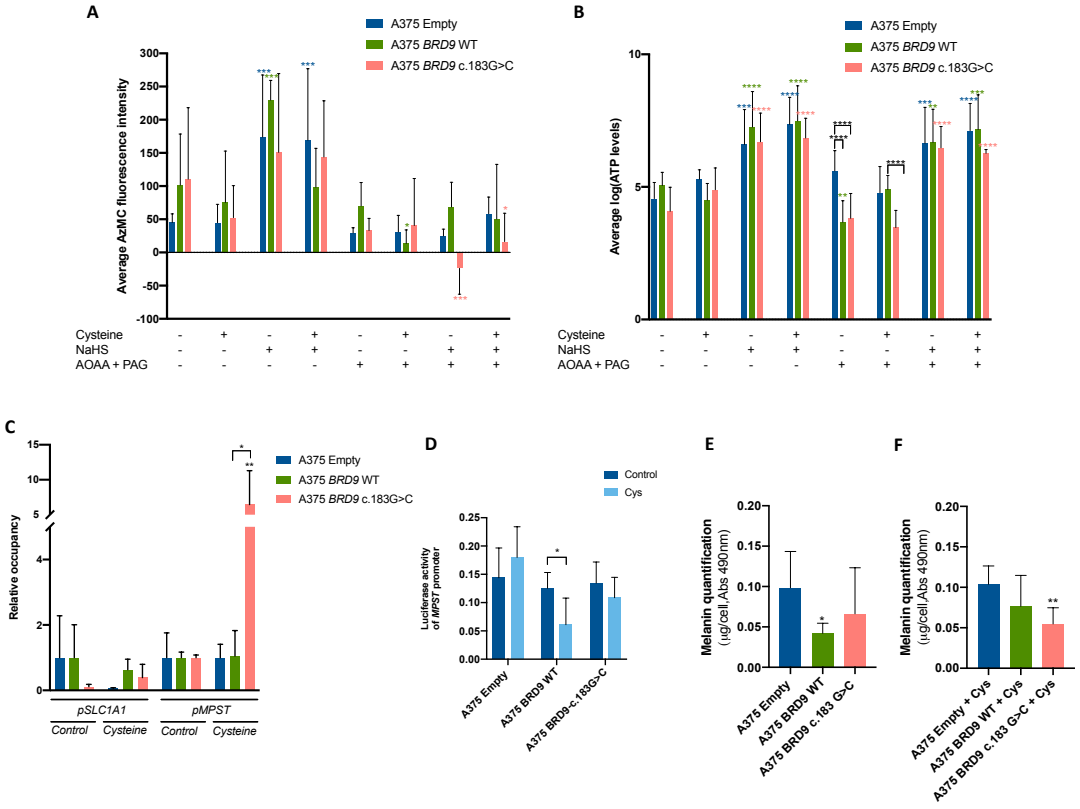

Figure II.3 – *BRD9 wild-type and BRD9 c.183G>C* overexpression induces a more efficient H_2S-producing phenotype, which does not always correspond to accumulated ATP levels in A375 melanoma cells, and modulates MST and EAAT3 activity through NRF2, inducing a remodeling in the melanin production pathway. (A) H_2S quantification following 7-Azido-4-Methylcoumarin probe (AzMC) signal indicates that A375 cells overexpressing *BRD9* WT and *BRD9* c.183 G>C, despite cysteine availability, show higher H_2S production, comparing to A375 Empty, independently of o-(carboxymethyl)hydroxylamine hemihydrochloride (AOAA) and dl-propargylglycine (PAG) treatment. NaHS treatment further increased H_2S levels in every cell line tested, irrespectively of co-incubation with cysteine. **(B)** ATP measurement in transfected A375 cells did not show a modulation of energy production by neither *BRD9* WT nor *BRD9* c.183 G>C overexpression, despite increased H_2S levels. NaHS alone or in combination with cysteine but not cysteine alone led to increased ATP levels across the three cell lines. **(C)** ChIP analysis show a high binding of *NRF2* to *MPST* promoter in the presence of cysteine. **(D)** Transfection of A375 melanoma cells with *BRD9* WT induces decreased *MPST* promoter activity in the presence of cysteine. Melanin quantification in the absence **(E)** and presence **(F)** of

cysteine was performed and cysteine exposure. Melanin quantification show decreased levels in A375 overexpressing-*BRD9* WT in the absence of cysteine, but also decrease A375 *BRD9* c.183 G>C melanin production in the presence of cysteine. Data is represented as mean ± SD. *p<0.5, **p<0.01, ***p<0.001, ****p<0.0001. Experiments were performed with biological triplicates.

BRD9 status modulates *MPST* but not *SLC1A1* through NRF2, inducing a remodeling in the melanin production pathway

Since *BRD9* can modulate the action of NRF2, which is described to modulate *SLC1A1* expression, and MST is an H_2S-producing AOE, we hypothesized that NRF2 regulates not only *SLC1A1* but also *MPST* expression. ChIP analysis revealed that NRF2 does not seem to bind to *SLC1A1* promoter not even in the presence of cysteine nor among the different variants of *BRD9* expressed in A375. We found, however, that NRF2 binding to *MPST* promoter in A375 *BRD9* c.183 G>C is increased and stimulated by cysteine (Figure II.3 C). Luciferase activity studies of *MPST* promoter in all A375 cell variants were performed, in the presence or absence of cysteine. Our results indicate that cysteine significantly decreased *MPST* promoter activity in A375 *BRD9* WT cells (Figure II.3 D). No significant changes were seen in A375 empty nor in A375 *BRD9* c.183 G>C (Figure II.3 D).

We further evaluated the effect of overexpressing WT or c.183 G>C *BRD9* in A375 melanin production. In control culture conditions, A375 *BRD9* WT presented the lowest level of melanin production, while cysteine prompted the decrease of melanin levels in A375 *BRD9* c.183G>C (Figure II.3 E and F).

BRD9 wild-type and BRD9 c.183G>C overexpression in WM115 cell line does not modulate *MPST*/MST and *SLC1A1*/EAAT3 expression

To study if our results could be replicated in another melanoma cell line and if *BRD9* status was the only factor inducing these metabolic and expression alterations, we chose to transfect WM115 cells with the *BRD9*-encoding plasmids. We then successfully obtained WM115 clones overexpressing *BRD9* WT or *BRD9* c.183G>C (Figure II.4 A). This was confirmed at mRNA (Figure II.4 B) and protein levels (Figure II.4 C). We then studied the expression of both *MPST* and *SLC1A1* in the transfected WM115 control, WM115 *BRD9* WT or WM115 *BRD9* c.183G>C variants. WM115 *BRD9* WT presented

decreased *MPST* and *SLC1A1* mRNA, comparing to WM115 transfected with the empty vector. However, WM115 *BRD9* c.183G>C also showed a significant decrease in *MPST* and *SLC1A1* expression, comparing to control (Figure II.4 D). The same trend was found in protein expression of both MST and EAAT3 (Figure II.4 E). Notably, the WM115 cell line expresses high basal levels of *MPST*/MST and *SLC1A1*/EAAT3, but no alteration was seen concerning the effect of *BRD9* variants. WM115 *BRD9* WT or WM115 *BRD9* c.183G>C did not present significant differences in cell migration capacity in the absence or presence of cysteine (Figure II.4 F and G). We also analyzed melanin production in these variants, and found that, although no differences were found in the absence of cysteine, in the presence of cysteine, WM115 *BRD9* c.183G>C significantly increased melanin production (Figure II.4 H and I).

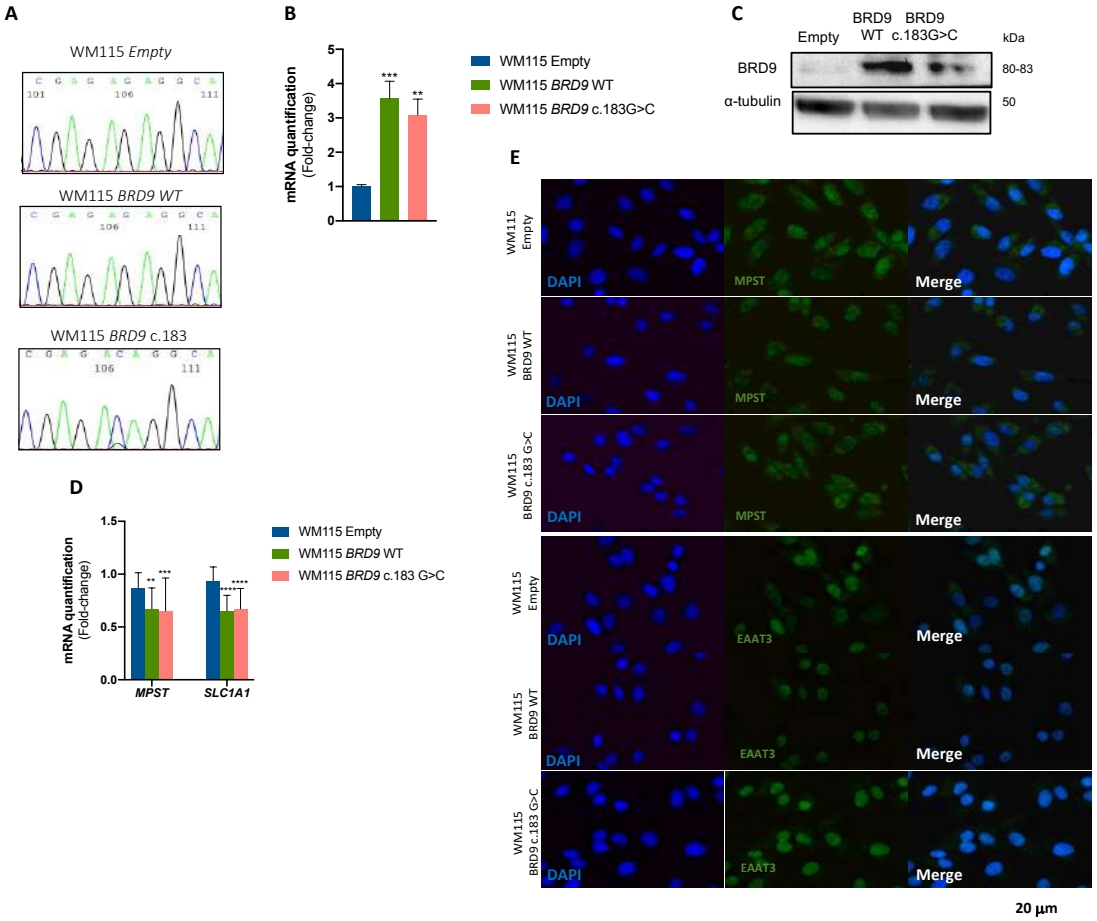

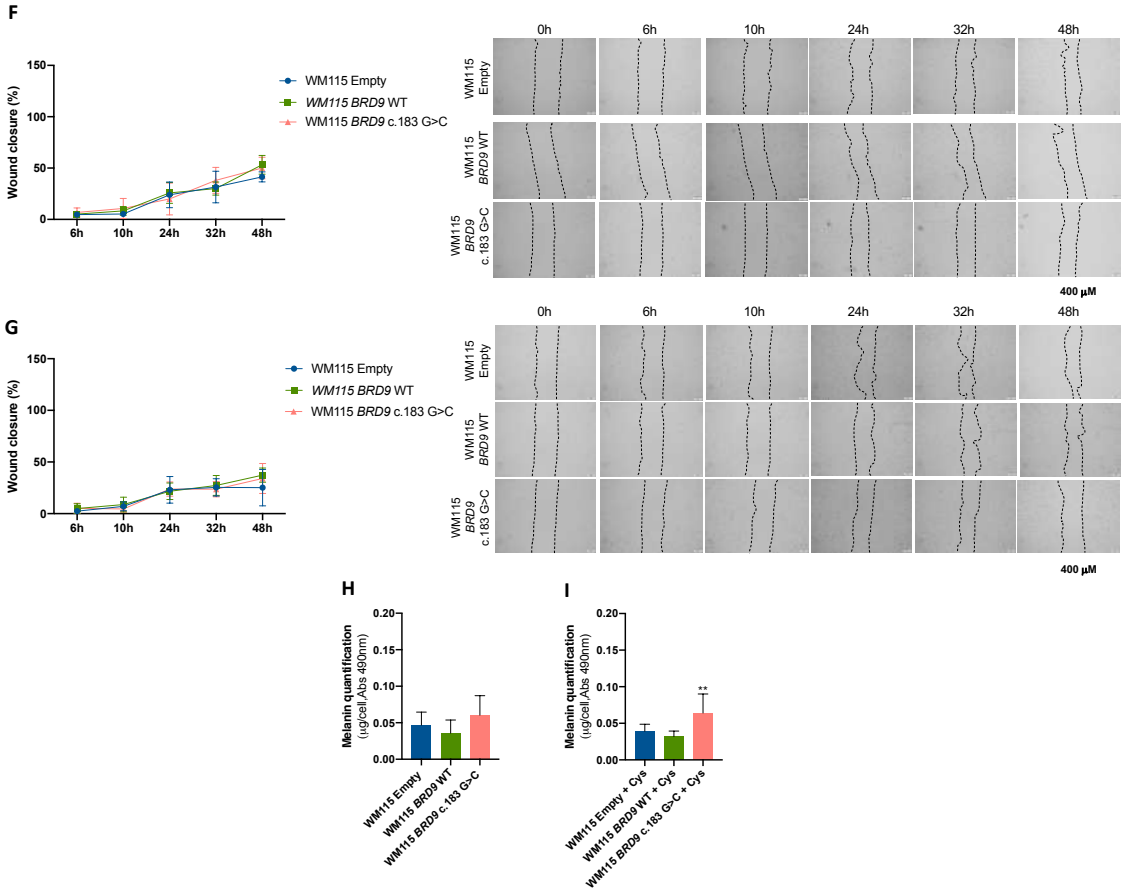

Figure II.4 – Overexpression of *BRD9* WT and *BRD9* c.183G>C was successfully induced in WM115 cells and modulates the expression of MPST/MST and *SLC1A1*/EAAT3, leading to deregulated melanin production in the presence of cysteine. By Sanger sequencing the sequence mRNA was confirmed **(A)** and by qPCR **(B)** and western blotting **(C)** the transfection of WM115 melanoma cells and the expression of the *BRD9* variants was confirmed WM115 cells transfection with *wild-type* overexpression and *BRD9* c.183G>C (over)expression vectors induced increased mRNA and protein levels of *BRD9*, comparing to empty vector. **(D-E)** qPCR and immunofluorescence analysis indicate that *BRD9 WT* and c.183G>C overexpression induces decreased *MPST*/MST and *SLC1A1*/EAAT3 expression in WM115. **(F)** *BRD9 WT*/ c.183G>C overexpression do not induce effects in WM115 migration, by wound healing, in the absence of cysteine. **(G)** *BRD9 WT*/ c.183G>C overexpression does not induce effects in WM115 migration, by wound healing, in the presence of cysteine. Melanin quantification in the absence **(H)** and presence **(I)** of cysteine was performed and cysteine exposure increased melanin levels in *BRD9* c.183G>C WM115 cells. Magnification 400 X, scale 20 µm. Data is represented as mean ± SD. *p<0.5, **p<0.01, ***p<0.001, ****p<0.0001. Experiments were performed with biological triplicates.

BRD9 c.183 G>C increases invasiveness of A375 cutaneous melanoma cell line in a 3D *in vitro* skin model

To address the role of *BRD9* (WT and c.183 G>C) in melanoma aggressiveness, the capacity of invasion of A375 and WM115 cell line variants was tested in a 3D *in vitro* skin model. As observed in Figure II.5 A and B, a higher invasive capacity of A375 cells, comparing to WM115 cells, was verified, since WM115, although presenting primary

tumors, does not invade. However, upon cysteine exposure, WM115 control and *BRD9* WT formed statistically significant thicker tumors than in the absence of cysteine. Considering the A375 variants, the exposure to cysteine did not affect the development of tumors but the overexpression of *BRD9* c.183 G>C induced tumors with statistically significant higher thickness and marked invasion edge comparing to A375 control and *BRD9* WT.

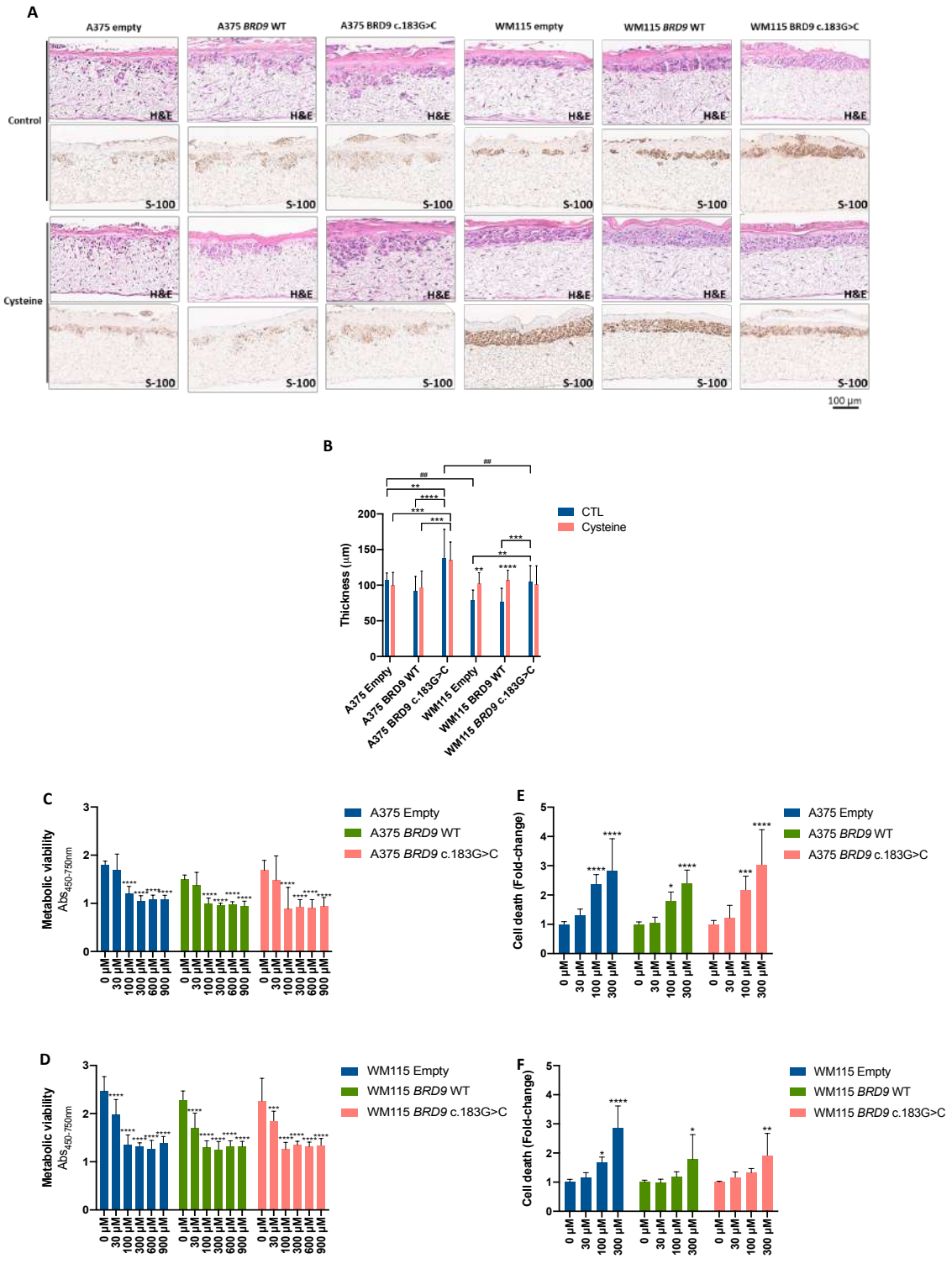

Figure II.5 – *BRD9* c.183G>C increased the invasiveness of A375 in a 3D *in vitro* skin model, and MST inhibition impacts on metabolic viability in all variants of A375 and WM115 cells. The effect of *BRD9* WT and *BRD9* c.183G>C overexpression in melanoma cell lines was evaluated in a 3D *in vitro* skin model. **(A)** Representative images of *in vitro* tumors in hematoxylin and eosin (H&E) staining and S-100 protein immunohistochemistry to specifically detect melanoma cells, and **(B)** the quantification of tumor thickness are presented, considering 20 imaging spots *per* slide of the 2 biological replicates. The impact of MST inhibition was assessed in A375 and WM115 *BRD9 WT* and *BRD9* c.183G>C variants. Statistical significance between different conditions within each cell line (*) and between cell lines (#) were considered. By WST-1 assay (subtracting the absorbance measured at 480nm and 760 nm), it was verified that MST inhibitor (I3MT-3) induces a significant decrease in metabolic viability of A375 **(C)** and WM115 **(D)** *BRD9 WT and BRD9* c.183G>C variants, upon 48 h of exposure, with more significant viability decrease between the concentrations of 30 to 100 μM of the inhibitor. The cell death, measured by flow cytometry (Annexin V-FITC and PT labeling), induced by I3MT-3 in all A375 **(E)** and WM115 **(F)** variants upon 48 h of exposure show differences in resistance to this treatment between A375 and WM115 empty variants *versus* variants overexpressing *BRD9 WT and BRD9* c.183G>C: empty variants of both A375 and WM115 showed more resistance to the inhibitor and presented higher EC_{50} values comparing to *BRD9* WT/c.183 G>C variants. Data is represented as mean ± SD. *p<0.5, **/$^{\#\#}$p<0.01, ***p<0.001, ****p<0.0001. Experiments were performed with biological triplicates.

Inhibition of MST induces a significant decrease in A375 and WM115 cell viability

Since our results pointed to MST as a crucial player in the rewiring of metabolic and cellular features of A375 overexpressing *BRD9* WT and *BRD9* c.183 G>C; and also WM115 express high basal levels of MST independently of *BRD9* status, we supposed that MST can be a target in these melanoma models. Therefore, Empty, *BRD9* WT and *BRD9* c.183 G>C variants of A375 and WM115 were exposed to increasing concentrations of an MST inhibitor for 48 h. A375 *BRD9* WT/c.183 G>C and WM115 *BRD9* WT/c.183 G>C showed similar responses to the inhibitor, with a more significant viability decrease between the concentrations of 30 to 100 μM of the inhibitor (Figure II.5 C, D, E and F).

II.V. Discussion

Hereditary CM constitutes a significant part of all CM cases, in which most of the diagnoses remain without a known genetic familial cause. It is, thus, crucial to explore and acknowledge novel genetic targets that can be associated with CM familial history and that can explain increased susceptibility. To our knowledge, this is the first study exploring the molecular effects of the *BRD9* c.183G>C variant in melanoma. Our study indicates that this variant, even though predicted to be benign rather than disease-

causing[372], induces different alterations in the CM cell lines tested, A375 and WM115. According to Sanger COSMIC database[373] A375 cells present a different genetic background from WM115, presenting mutated *BRAF* (c.1799T>A, p.V600E) and *CDKN2A* (c.181G>T, p.E61*; c.205G>T, p.E69*), while WM115 presents mutated *BRAF* (c.1799_1800TG>AT, p.V600D), *CDKN2A* (c.1_150del150, p.?) and *PTEN* (c.493_634del142, p.?), presenting deletions in both *CDKN2A* and *PTEN*. The significantly different genetic background of A375 and WM115 cells can explain the distinct effect of overexpressing *BRD9* WT and mutated variants. In fact, it is already described that coexisting *BRAF* and *PTEN* mutations are directly linked to metastatic melanoma.[374] Importantly, in this study we disclosed *BRD9* role as a regulator of cysteine metabolism. The involvement of NRF2 in the increased expression of MPST gene, as we verified that NRF2 binding to *MPST* promoter in A375 *BRD9* c.183 G>C is increased and stimulated by cysteine (Figure II.3 C); is in agreement with BRD9 and SWI/SNF loss of function, already described in NSCLC.[360] Importantly, new studies are needed to determine the impact of c.183 G>C in BRD9 structure and function, in order to understand the way this BRD9 mutant variant can interfere with SWI/SNF complex function and somehow differentially modulated the expression of genes. Indeed, both *BRD9* WT and c.183G>C induced distinct metabolic profiles, with emphasis on amino acid metabolism (Figure II.1 H, I and J; Figure II.2 A, B and C). Different genetic backgrounds induce cellular diversity, and our *in vitro* models can represent two distinct melanoma profiles: a cysteine remodeled metabolic profile by *BRD9* with increased MST expression leading to a more invasive phenotype, and a molecular profile with decreased expression of MST induced by *BRD9* altered status, with no influence in cell migration. Therefore, the *BRD9* c.183G>C variant associates to a significantly more migratory phenotype in A375 cells (Figure II.1 G), but not in WM115 cells, which maintained their migratory capacity independently of the *BRD9* status (Figure II.4 F). The role of mutant in melanoma was confirmed in the increased invasive capacity exhibited by A375 *BRD9* c.183G>C variant (Figure II.5 A and B). This highlights the possibility that *BRD9* may not be so relevant in terms of migration in WM115 cells comparing to A375 cells. A detail that likely accounts for this observation is the fact that WM115 cells have the deletion of the E-cadherin encoding gene. It was previously shown that E-cadherin re-expression in melanoma cells decreases the migratory and invasive capacity of cells and rescues the ability of cell-to-cell binding.[375] Despite the fact that A375 cells show higher migration rates in their basal state than WM115 cells (Figure II.1 G, Figure 5 F), WM115

cells have loss of E-cadherin function, hampering finding differences between the migratory capacities of this cell line variants. Furthermore, and looking at the interference of cysteine metabolic adaptation in cell migration, all WM115 cell variants migrate at a lower rate in the presence of cysteine comparing to control conditions (Figure II.4 F and G). The opposite was observed in A375 cell line, in which A375 *BRD9* c.183G>C cell variant exposed to cysteine migrates at a higher rate than in control conditions (Figure II.1 F and G). The 3D skin model revealed that A375 cell line is more invasive than WM115 cell line, which besides presenting tumors, cells do not invade (Figure II.5 A and B). However, upon cysteine exposure, WM115 control and *BRD9* WT formed statistically significant thicker tumors than in the absence of cysteine. By comparing the metabolic viability of all cell variants, it was verified that WM115 cells present higher values than A375 variants, in control conditions. This possibly indicates that WM115 cells proliferate at a higher rate than A375 cells (Figure II.5 C and D), and this will contribute for the increased thickness of WM115 melanomas in 3D skin model, suggesting that cysteine exposure may stimulate WM115 proliferation. Considering the A375 variants, the exposure to cysteine did not affect the development of tumors but the overexpression of *BRD9* c.183 G>C induced tumors with statistically significant higher thickness and marked invasion edge comparing to A375 control and *BRD9* WT (Figure II.5 A and B).
Cysteine exposure induced decreased levels of glutamate in both A375 Empty and *BRD9* c.183G>C, which was accompanied by undetectable glutamine levels. However, in A375 *BRD9* WT, cysteine led to an increasing tendency of glutamate and glutamine levels (Figure II.2 A). Decreased levels of glutamate and glutamine can be explained by increased synthesis of glutathione, as described in ovarian cancer.[313] Glutathione's antioxidant role depends on cysteine's reactive thiol group.[376] Indeed, we found increased GSH levels in A375 Empty but not in A375 *BRD9* c.183G>C. Instead, this variant showed a tendency towards decreased GSH levels in the presence of cysteine, as observed in cells expressing the A375 *BRD9* WT variant (Figure II.2 A). Decreased glutathione levels can derive from a slow glutathione synthesis and/or fast GSH consumption. However, the results point towards increased metabolic demands of *BRD9* expressing cell variants, presenting a more demanding redox turnover, prompting the consumption of reduced glutathione, in contrast to a lower metabolic flow of A375 Empty cells. This is also supported by the evident signs of oxidative stress presented by A375 *BRD9* c.183G>C cells, such as increased expression of the antioxidant enzyme MST[377] and EAAT3 transporter (Figure II.2 D, E and F). This is in line with our results regarding the

enzymatic activity study in all three variants of A375. In fact, we found that A375 *BRD9* c.183G>C cells exhibit increased steady-state levels of H_2S comparing to A375 Empty, in control conditions. Interestingly, A375 *BRD9* WT, even though showing significant decreased expression of antioxidant enzymes and transporters, show similarly increased H_2S levels, comparing to A375 *BRD9* c.183G>C (Figure II.3 A), which can either indicate an increased H_2S production or a lower detoxifying ability. H_2S is described to act in two equally important ways: either as a potent antioxidant or as source of electron equivalents to the mETC, leading to ATP production.[264,378] In our results, increased H_2S levels do not translate in increased ATP levels (Figure II.3 B). This may mean that *BRD9* overexpression whether in its WT or mutated form can further induce imbalances in H_2S production as a distinct way to overcome oxidative stress.

Since complete culture medium contains glutamine, we expected to detect this amino acid in our metabolomics study. Low (A375 *BRD9* WT) or inexistent (A375 Empty and A375 *BRD9* c.183 G>C) levels of glutamine, independently of cysteine availability, further indicate high uptake and consumption of this amino acid (Figure II.2 A). Decreased glutamine is associated with a necessity for redox control within the cell, and is usually found during catabolic stress and antioxidant imbalance.[379] Glutamine can act either as a positive or negative redox status modulator, depending on the activation of specific transcription factors triggered by stressful microenvironments.[379] In this case, high consumption of glutamine may act as an attempt by the cell to compensate the decreased GSH production due to cysteine diversion to other pathways, since these cells probably show increased ROS levels. Decreased glutathione levels are also described to be associated with decreased proliferation rates[379], which is in accordance with our results (Figure II.1 D and E). Glycine levels drastically decrease in the presence of cysteine (Figure II.2 A). Again, decreased availability of glycine may indicate a cellular response to oxidative stress since glycine is also a component of glutathione. Moreover, the decreased levels of serine may indicate increased glycine synthesis and altogether highlight that glycine turnover is in operation in A375 *BRD9* c.183 G>C cell variant.

We further observed a decrease in methionine levels in A375 Empty and *BRD9* c.183 G>C when exposed to cysteine and in A375 *BRD9* WT, independently of cysteine presence (Figure II.2 A). Decreased methionine levels in the presence of cysteine suggest that exogenous cysteine stimulates methionine demethylation, with the resulting homocysteine either being remethylated back to methionine or entering the reverse transulfuration pathway (RTP, comprising CBS and CSE). The observation that both

A375 Empty and *BRD9* c.183 G> variants express high levels of EAAT3, CBS and CSE-encoding genes favors the latter fate involving the RTP and leading to cysteine production (Figure II.2 D, E and F). A375 *BRD9* WT show low levels of methionine, unaffected by cysteine availability (Figure II.2 A), probably related to low CBS expression by this variant. This A375 variant likely relies on a different source of cysteine, since H_2S steady-state levels are comparable to A375 *BRD9* c.183 G>C in control conditions (Figure II.3 A). Decreased levels of acetate (Figure II.2 B) are in agreement with decreased proliferation rate[380,381] in cells overexpressing *BRD9* (Figure II.1 D and E), independently of the mutational status. Indeed, the average number of cells between time point 10 h and 16 h is significantly lower in A375 *BRD9* c.183 G>C comparing to A375 *BRD9* WT. Decreased levels of cholin and phosphocholin can also be indicative of a decreased proliferation rate[382,383] (Figure II.2 C; Figure II.1 D and E). Additionally, high levels of formate and lactate may be related to increased invasion, independently of cysteine presence[384,385](Figure II.2 B; Figure II.1 F and G).

Cysteine metabolism is deeply associated with increased tumor aggressiveness as described before, and so, we hypothesize that *BRD9*-induced cysteine metabolic remodeling may be an extremely relevant feature to further disclose in cutaneous malignant carcinoma. Cysteine, besides being able to supply energy to cancer cells, can also provide them with the resistance mechanisms to overlap standard therapy regimens applied to cancer patients. Moreover, it is a pivotal intervenient in pheomelanin production. Thus, increased cysteine metabolism and uptake can intervene in different ways, all of them contributing to tumorigenesis and/or tumor progression. We postulate that overexpression of WT or c.183G>C *BRD9* can contribute to imbalances in melanin production, deregulating the eumelanin/pheomelanin ratio, thus leading to a higher susceptibility to CM development. In fact, while eumelanin exerts a photo/radioprotection role, pheomelanin can be a source of mutagenic events upon radiation exposure.[38,386] Several studies have uncovered that, indeed, pheomelanin can be associated with increased production of ROS upon UVR exposure.[386–389] Moreover, imbalances in this ratio are already described in uveal melanoma cells, which show much higher levels of pheomelanin than eumelanin.[390]

Metabolic rewiring has become clear to have a central role in tumor development, progression and resistance and has, in fact, been considered a core hallmark of cancer.[4] Thus, it is essential to further explore the role of *BRD9* as a CM susceptibility gene but also as a metabolic regulator. The present work opens a new door towards understanding

hereditary melanoma as a complex entity, in which tumor, not only genetic but also metabolic profiling may be a central piece to disentangle familial history and cancer susceptibility, as well as an important therapy response predictor. Additionally, this study supports a broad role of MST enzyme as a crucial player in CM, not only in tumors presenting alterations in *BRD9*. In fact, our results show that inhibition of MST leads to a decrease in cell viability in both A375 and WM115 cell lines, with a significantly more pronounced effect in A375 and WM115 variants overexpressing *BRD9* WT or c.183 G>C, presenting lower EC_{50} values for the latter (Figure II.5 C, D, E and F). Indeed, increasing evidence points towards MST as a player in cancer metabolic remodeling and its encoding gene, *MPST*, though constitutively expressed in normal differentiated cells, is also often found overexpressed in several different cancer cell lines as well as across a wide range of tumors.[231,391] Moreover, studies have correlated increased expression of MST with chemoresistance in different cancer types[318,392] and have revealed the crucial role of MST in cancer cell proliferation.[282,393] We have previously suggested a critical role for MST expression and activity in cancer according to cancer type and metabolic context, with emphasis on its role in carcinogenesis and/or cancer progression.[231]

In this study, we disclosed a putative role of MST in the metabolic reliance of *BRD9*-mutated CM. MST elevated expression can define a parameter regarding CM aggressiveness, being associated with more migratory and invasive but less proliferative phenotypes, with low melanin production, thus characterizing a specific subset of CM.

II.VI. Conclusion

BRD9 is a CM-associated gene with yet much potential to be further explored. This study highlights that not only the mutational status of *BRD9* but also its expression level can be used as a marker for CM aggressiveness. Here, *BRD9* was disclosed as a regulator of cysteine metabolism in a CM cell model. Overexpression of *BRD9* in its WT or c.183G>C variants can induce metabolic remodeling, leading to altered cellular features. *BRD9* c.183G>C, thus, introduces cysteine metabolism as a putative central player in CM susceptibility, as well as in CM progression. Therefore, MST can be a suitable marker for CM aggressiveness and a potential target, since it correlates with increased migratory and invasive potential and decreased production of melanin,

accounting for an increased risk of accumulating mutations due to decreased DNA protection against radiation.

Chapter III

Cysteine Metabolic Profiling is a Putative Determinant in NSCLC Management and a Step Forward in Personalized Medicine

This chapter is based on the following publication:

Ana Hipólito, Cindy Mendes, Filipa Martins, *et al.* H_2S-synthesizing enzymes are putative determinants in lung cancer management toward personalized medicine. Submitted for publication.

III.I. Abstract

Lung cancer is a lethal disease with no specific therapeutical management, and metabolic profiling can be a way of stratifying patients who may benefit from new therapies. The present study is dedicated to profiling cysteine metabolic pathways players in NSCLC cell lines and tumor samples, analyzing H_2S and ATP levels, mRNA and protein expression patterns of cysteine catabolic enzymes and transporters, and metabolomics analysis by NMR spectroscopy. Selenium-containing chrysin (SeChry) was tested as a therapeutic alternative, aiming at affecting cysteine catabolism, with promising results. NSCLC cell lines presented different cysteine-metabolic patterns, with A549 and H292 presenting a higher reliance on CBS and CSE to maintain H_2S levels, while PC-9 cell line presented an adaptive behavior based on the use of MST and CDO1, both contributing to the role of cysteine as a pyruvate source.

The analyses of human specimens corroborate this variability in profiles, meaning that the expression of certain genes may be informative to define prognosis and new targets. Heterogeneity points out individual profiles and the identification of new targets among metabolic players is a step forward in cancer management towards personalized medicine.

Keywords

Cysteine metabolism; CBS; CSE; MST; CDO1; metabolic plasticity; NSCLC metabolism; metabolism-based therapies

III.II. Introduction

Lung cancer is a lethal disease, responsible for 1.59 million deaths *per* year worldwide, according to the WHO.[394] Although lung tumors are overall molecularly and histologically considered very heterogeneous entities, even within histological subtypes, lung cancer can be classified into two groups: SCLC and NSCLC, the latter accounting for around 85% of all lung cancer cases, while SCLC accounts for 15%. [103,395] NSCLC is further generally subcategorized as LUAD, LUSC and LCLC, the first two being the most

commonly diagnosed subtypes.[103] Different factors account for this high mortality, including late diagnosis, molecular heterogeneity and the development of resistance mechanisms to chemotherapy and targeted therapy.[396,397] Therefore, it is crucial to determine the molecular signatures underlying this chemotherapy response heterogeneity, to identify appropriate targets and markers to create new treatments and stratify patients. In this line, cancer metabolic remodeling is a hub of information amongst which pivotal players and pathways can be posited as pawns in the design of novel, more specific and efficient therapies in the scope of personalized medicine.

Metabolic remodeling is employed by cancer cells to adapt and thrive in the organ and TME, and in the last two decades this field has received attention from the scientific community worldwide.[1,4] Cancer cells rewire their cellular metabolism to sustain the energetic and biosynthetic demands of an elevated proliferation rate, together with the increased capacity of redox control allowing the metabolic flow.[176,398] Albeit cancer cells may present different metabolic profiles, they share several characteristics that make specific metabolic pathways important, such as glycolysis, glutamine catabolism, one-carbon metabolism and redox homeostasis, including cysteine metabolism.[102,176,399] These pathways are dependent on the genetic background of cancer cells, conditioning oncogenic signaling and gene expression. However, the role of TME in the control of nutrients and signaling molecules availability is fundamental.[399,400] Very recently, our team demonstrated the relevance of glucose and lactate dynamics in NSCLC, proving that different subsets of NSCLC present distinct metabolic profiles, including glucose *versus* lactate reliance.[401] Lactate is increasingly accepted as a valuable metabolic source, which is produced due to the high glycolytic rates and managed by cancer cells as a metabolic substrate for oxidative metabolism and gluconeogenesis.[102,402–406]

The ability to avoid oxidative stress-related damage is a powerful skill of cancer cells, which mostly present a metabolic profile ensuring an efficient free-radical scavenging capacity, involving cysteine-dependent pathways. Our team has disclosed that cysteine bioavailability is pivotal in chemoresistance, and cysteine metabolism is crucial for cancer cell survival.[194,256,326]Cysteine's impact on cancer cell survival is mainly associated with its role as a component of GSH [407,408] and as a substrate for H_2S production.[241,409,410] More recently, we documented that cysteine is also a valuable carbon source, being converted into different amino acids, pyruvate and lactate, pointing out its

usefulness as a carbon source for energy and biomass production.[194] CBS, CSE and MST, besides catabolizing cysteine, also catalyze the cyst(e)ine-dependent production of cysteine persulfide (CysSSH), which in several (patho)physiological contexts affords protection from damaging cysteine oxidation.[260,350,411] In addition, to these pathways of cysteine enzymatic breakdown to produce H_2S and organic intermediates, cysteine can be directed to the oxidative metabolism through CDO1. Thus, cysteine is converted into cysteine sulfinic acid, leading to the production of taurine, pyruvate and sulfate, which can be channeled to several other metabolic pathways.[237,238]

All of these enzymes have been somehow implicated in cancer malignancy and poor prognosis, as reviewed by Bonifácio *et al*.[192] From these enzymes, CBS is the most well-studied in cancer context: it acts on cysteine synthesis and degradation, being an important contributor to cancer biology, by degrading cysteine and producing H_2S, which presents pro-tumoral roles, stimulating bioenergetics and angiogenesis, inhibiting apoptosis and promoting cell cycle progression. [412–414] CBS has, in fact, been reported to be aberrantly expressed, accompanied by increased H_2S levels in lung cancer[279,415] and other types of cancer[280,281], being associated with carcinogenesis support and chemoresistance.[318] CBS targeting sensitizes cancer cells to conventional therapy and induces cell death.[363]

The aim of this study was to explore the status of central players in cysteine metabolism specificity in different NSCLC *in vitro* models, to better understand disease heterogeneity and to find important candidates to be used as therapeutic targets and prognosis or therapy response markers. Furthermore, we explored the potential of SeChry as a drug to disturb cysteine availability and metabolism, as we reported in ovarian cancer.[363]

III.III. Materials and Methods

Cell lines and culture conditions

Human adenocarcinoma cell line A549 (CCL-185™), mucoepidermoid carcinoma cell line H292 (CRL-1848™), tubular renal cell line HK2 (CRL-2190™) and keratinocyte cell

line HaCaT (PCS-200-011™) were obtained from ATCC (Manassas, VA, USA) and adenocarcinoma cell line PC-9 (90071810) was obtained from European Collection of Authenticated Cell Cultures (ECACC, Porton Down, Salisbury, United Kingdom). The selected NSCLC cell lines present different mutational profiles for *EGFR* and *KRAS*: A549 cells (*EGFR* WT (*wild-type*) and *KRAS* c.34G>A (p.Gly12Ser); H292 cells (*EGFR* WT and *KRAS* WT), and PC-9 cells (*EGFR* exon 19 deletion (Ex19Del; Glu746-Ala750 deletion) and *KRAS* WT). The cell lines represent the main NSCLC histological types LUAD (A549 and PC-9) and LUSC (H292). Cells were cultured in Dulbecco's Modified Eagle's Medium 1× (DMEM) (41965-039, Gibco, Life Technologies) supplemented with 10% fetal bovine serum (FBS; S 0615, Merck), 1% Antibiotic-Antimycotic (AA; P06-07300, PAN Biotech) and 50 µg/mL Gentamicin (15750-060, Gibco, Life Technologies). Cells were maintained at 37°C in a humidified environment with 5% CO_2. Cells were cultured until an optical confluence of 75–100% and detachment was performed with 0.05% trypsin-EDTA 1× (25300-054, Invitrogen). Before *in vitro* experiment, cells were synchronized under starvation (FBS free culture medium) overnight, except for cytotoxic experiments. All experiments were then conducted using 1% FBS medium with the additional supplements stated above. Cells were kept in control conditions or exposed to 0.402 mM L-Cysteine (102839, Merck).

WST-1 assay for cell metabolic viability

The WST-1 based colorimetric assay (Roche Applied Science, Indianapolis, IN, USA) was performed to quantify cell metabolic viability. Cells were seeded in 96-well clear bottom tissue culture plates and treated at different concentrations. Cells were incubated with WST-1 reagent for 1 h at 37°C with 5% CO_2, according to the manufacturer's instructions. In actively metabolizing cells, the WST-1 reagent is cleaved to formazan by cellular enzymes. The presence of formazan was assessed through spectrophotometric quantification (450 nm) in a Bio-Rad Laboratories iMark™ Microplate Absorbance Reader (1681130).

Measurement of H_2S in cell homogenates

Cells (5×10^5 cells/well) were seeded in 6-well plates, cultured in control condition and

exposed to experimental conditions: 0.402 mM L-cysteine; 50 μM bromopyruvic acid (BPA; 16490, Sigma-Aldrich), and 30 μM sodium hydrosulfide (NaHS;161527, Sigma-Aldrich) for 24 h. Cells were scraped in PBS 1× and homogenized in NP40 lysis buffer (1% NP40, 150 mM NaCl, 50 mM Tris-Cl, pH 8.0) on ice for 30 min and centrifuged at 20000 g for 5 min at 4°C. Cell homogenates (20 μL) were incubated in black 96-well plates with 80 μL of 10 μM 7-azido-4- methylcoumarin (AzMC, L511455, Sigma-Aldrich) with and without 1 mM aminooxyacetic acid (AOAA, C13408, Sigma-Aldrich) and/or 3 mM DL-propargylglycine (PAG, P7888, Sigma-Aldrich), inhibitors of CBS and CSE enzymes. AOAA is an inhibitor of both CBS and CSE, whereas PAG is selective towards CSE.

Protein concentration was determined with the Bradford method (500-0006, Bio-Rad) against a BSA calibration curve. The H_2S measurements were subsequently normalized to total protein concentration and to a blank sample (cellular lysates with and without AOAA, PAG or both without a probe).

H_2S levels were monitored following the AzMC probe emission wavelenght (λ_{exc}: 355 nm; λ_{em}: 460 nm) in a VICTOR3 instrument from PerkinElmer and using the *Wallac 1420 v3.0* software (Umbelliferone, 0.1 s protocol).

ATP quantification

Cells were seeded in 6-well plates (5×10^5 cells/well) and cultured in control conditions or exposed to L-cysteine (0.402 mM), and/or 50 μM BPA, and/or 30 μM NaHS for 24 h. Then, cells were scraped in PBS containing 2 mM EDTA, centrifuged at 210 × *g* for 5 min and homogenized in 1% NP40 lysis buffer with 5% protease inhibitor (Protease inhibitor cocktail tablets S8830, Sigma-Aldrich) on ice for 30 min. Samples were then centrifuged at 20000 g for 5 min at 4 °C. Protein was quantified with the Bradford method. ATP determination kit (A22066, Molecular probes) was used in accordance with the manufacturer's instructions, in the presence of 1 mM AOAA and/or 3 mM PAG. The measurements were performed using the Luciferase protocol in a VICTOR3 instrument from PerkinElmer/, using the *Wallac 1420 v3.0* software (Luminometry, Luciferase FIR protocol). ATP concentration was determined against an ATP calibration curve, within the range between 0 and 30 μM. Assays were performed in biological triplicates.

Quantitative real-time PCR (qPCR)

Total RNA was extracted using RNeasy Mini Extraction kit (74104, Qiagen, Hilden, Germany) and cDNA synthesized from 1 μg RNA by SuperScript II Reverse Transcriptase (18080044, Thermo Fisher Scientific), both according to the manufacturer's protocol.

RNA was extracted from formalin-fixed paraffin-embedded (FFPE) NSCLC samples collected in Instituto Português de Oncologia de Lisboa Francisco Gentil, EPE (IPOLFG, EPE), using semi-automatic isolation with the Maxwell purification system (Maxwell RSC RNA FFPE Kit, AS1440, Promega) and cDNA was synthesized as mentioned above. qPCR was performed using SYBR Green PCR Master Mix (04707516001, Roche), according to the manufacturer's protocol and the specific primers and genes are presented in Table III.1.

Real-time PCR was carried out during 40 amplification cycles, according to the manufacturer's instructions, using a Lightcycler® 480 System instrument (05015243001, Roche). *HPRT* was used as a housekeeping gene (Table III.1). Experiments were performed in biological triplicates.

Table III.1 - Primers used in gene expression analysis. Detailed characterization of the primers used in RT-qPCR assays.

Gene	Primer	Sequence (5'→3')	Length (nt)	AT (°C)	GC %	Fragment (bp)
CBS	Forward	*GAGCTCTTGGCCAAGTGTG*	19	60	58	232
	Reverse	*GCACGTCCACCTTCTCGG*	18		67	
CTH	Forward	GCAGCCACTGTAACTATTACCC	22	60	50	175
	Reverse	CTGGTGTAATTGCTGCCTCTAG	22		50	
MPST	Forward	CTTCATCAAGACCTACGAGGAC	22	60	50	134
	Reverse	GGTAGTGGCCAGGTTCAATG	20		55	
GOT-1	Forward	*GAGAAGAGAGGATTGGACCTC*	21	60	52	147
	Reverse	*CATGACAGAAGCAATCTGCTTCC*	23		48	
GOT-2	Forward	*CCAGAGCCAGCTCCTGGT*	18	61	67	171
	Reverse	*CTGCCTTGCGGACGCTAG*	18		67	
SLC7A11	Forward	*GGTCCTGTCACTATTTGGAGC*	21	61	58	136
	Reverse	*GAGGAGTTCCACCCAGACTC*	20		59	
SLC1A1	Forward	*GTATCACGGCCACATCTGCC*	20	61	60	121
	Reverse	*GCAATGATCAGGGTGACATCC*	21		52	
HPRT1	Forward	*TGACACTGGCAAAACAATGCA*	21	58	43	94
	Reverse	*GGTCCTTTTCACCAGCAAGCT*	21		52	
CDO1	Forward	GAGACATTATTTGCCTGGC	19	56	47	149
	Reverse	CTCACAGCAGGTTCCGTAT	19		53	

Immunofluorescence

Immunofluorescence was used to detect the expression of proteins. Cells (1×10^5 cells/well) were seeded in glass cover slips in 24-well plates coated with 0.2% gelatin from porcine skin (G-1890, Sigma-Aldrich) and then fixated with 2% paraformaldehyde for 15 min at 4ºC. After fixation, cells were incubated with 50 mM NH_4Cl for 10 min. Blocking and antibodies dilution were performed with PBS 1× - 0.5% BSA - 0.1% saponin-PBS (w/v/v). Between incubations, cells were rinsed twice with PBS 1×, for 5 min. After blocking for 1 h, cover slips were incubated with primary antibodies (Table III.2), overnight at 4°C. Cells were incubated with secondary antibody for 2 h at room temperature (1:1000; Alexa Fluor® 488 goat anti-rabbit, A-11034, Thermo Fisher

Scientific; 1:1000; Alexa Fluor® 488 goat anti-mouse, A-11001, Thermo Fisher Scientific).

The slides were mounted in VECTASHIELD media with DAPI (H-1200-10, Vector Labs) and examined by standard fluorescence microscopy under a Zeiss Imager.Z1 AX10 microscope. Images were acquired and processed with CytoVision software and quantified with ImageJ software.

Table III.2 – Antibodies used in immunofluorescence analysis. Proteins detected by immunofluorescence and the antibodies used.

Target protein	Antibody reference
CBS	WH0000875M1, Sigma-Aldrich
CSE	SAB1403711, Sigma-Aldrich
MST	HPA001240, Sigma-Aldrich
xCT	ab175186, Abcam
EAAT3	14501S, Cell Signaling Technology

Proliferation curves

Cell proliferation rate was determined by the establishment of proliferation curves. Cells were seeded in 24-well plates (5×10^4 cells/well) in complete DMEM, synchronized under starvation and exposed to the experimental conditions. At each time-point (0, 6, 10, 24, 32 and 48 h), cells were detached as described (supernatant was also collected) and cells were centrifuged for 5 min at 155 × *g*. The supernatant was discarded and cells were counted by staining with Trypan Blue Stain 0.4% (15250061, Thermo Fisher Scientific) to identify cells with a compromised cell membrane, hence indicating cell death, using a Neubauer improved cell counting chamber.

Bioinformatics analysis

LUAD and LUSC RNA-Seq data from the The Cancer Genome Atlas (TCGA)[416] were analyzed using the cBio Cancer Genomics Portal (http://cbioportal.org)[417,418] to explore LUAD and LUSC genomic data set which included *CBS*, *CTH*, *MPST*, *GOT1*, *GOT2*, *CDO1*, *SLC1A1*, and *SLC7A11*.

Statistical analysis

Statistical analysis and EC_{50} calculation were performed using GraphPad Prism 8.0 software (www.graphpad.com). Sample data were presented as mean (normal distribution) ± SD. Assays were performed with at least three biological replicates per treatment (with at least 3 independent n). Comparisons between data from each group were statistically analyzed by a two-tailed unpaired Student's t-test and multiple comparisons were performed using one-way or two-way ANOVA. To assess differences in gene expression levels in samples from NSCLC tumors, 2-sided independent samples Kruskal-Wallis One-way ANOVA with multiple comparisons or Mann-Whitney test was performed, where the adjusted significance was considered. In this context, the existence of a linear relationship between two variables was investigated using a two-tailed Spearman correlation test. Differences between experimental conditions were considered statistically significant at $p < 0.05$.

III.IV. Results

NSCLC cell lines rely on cysteine for H_2S and ATP production

Cysteine catabolism is an important pathway in biomass and energy production, and metabolic routes accounting for the generation of H_2S and organic compounds are the most explored in cancer.[192] Thus, we started by evaluating the efficacy of NSCLC cell lines in reductive cysteine catabolism, through the measurement of H_2S levels. Interestingly, all cell lines presented similar basal H_2S levels (Figure III.1 A). As an attempt to correlate H_2S levels with reductive cysteine degradation, the inhibition of CBS

and CSE enzymes by AOAA and PAG was analyzed, revealing no significant differences. An absent effect was also observed when NSCLC cells were also cultured in the presence of an H_2S donor (NaHS) alone and in combination with cysteine (Figure III.1 B).

Since NaHS may have prevented fully appreciating the effect of cysteine, H_2S levels were also measured in cells exposed to cysteine supplementation in the absence of NaHS (Figures III.1 C and D). In A549 and H292, cysteine supplementation tended to decrease the H_2S levels at time 0 h (T=0 h), whereas PC-9 remained practically unaltered (Figure III.1 C). Notably, cysteine supplementation in the presence of AOAA increased H_2S levels at T=0 h in all cell lines as compared to cysteine alone. The same was observed for cysteine supplementation in the presence of PAG for the A549 and H292 lines. Despite these differences in H_2S levels at T=0 h, the steady-state average levels remained unaltered between culture conditions (Figure III.1 D). Importantly, since H_2S can be an electron donor to the mETC via sulfide:quinone oxidoreductase, accounting for ATP production [419], ATP levels were measured. Considering both the ATP production at T=0 h and the steady-state average levels, A549 cells increased the production of ATP upon cysteine supplementation independently of the presence of inhibitors (Figures III.1 E and F). H292 and PC-9 were able to maintain ATP levels in all experimental conditions (Figures III.1 E and F). Thus, all cell lines presented a high metabolic adaptive capacity.

In order to understand if cysteine metabolism is a core energetic circuitry in NSCLC, and because we recently documented that glucose-dependent pathways were pivotal in NSCLC[401], experiments blocking glycolysis with BPA with and without cysteine supplementation were performed, measuring H_2S and ATP levels. A549 and H292 cell lines presented decreased H_2S levels in the presence of cysteine with and without glycolysis inhibition with BPA (Figure III.1 C). This decrease was even more evident when comparing BPA alone with control conditions. PC-9 cell line presented no statistically significant changes in all conditions (Figures III.1 C and D). Interestingly, A549 cells tended to increase ATP levels upon BPA and/ or cysteine supplementation (Figures III.1 E and F), and H292 and PC-9 cells maintained the ATP levels in all culture conditions independently of glycolysis inhibition (Figures III.1 E and F). Therefore, these results suggest that glucose-dependent energetic pathways, which are abrogated by BPA, can be compensated in part by cysteine-dependent H_2S production or that glycolysis is preferably employed for synthetic pathways instead of energetic ones.

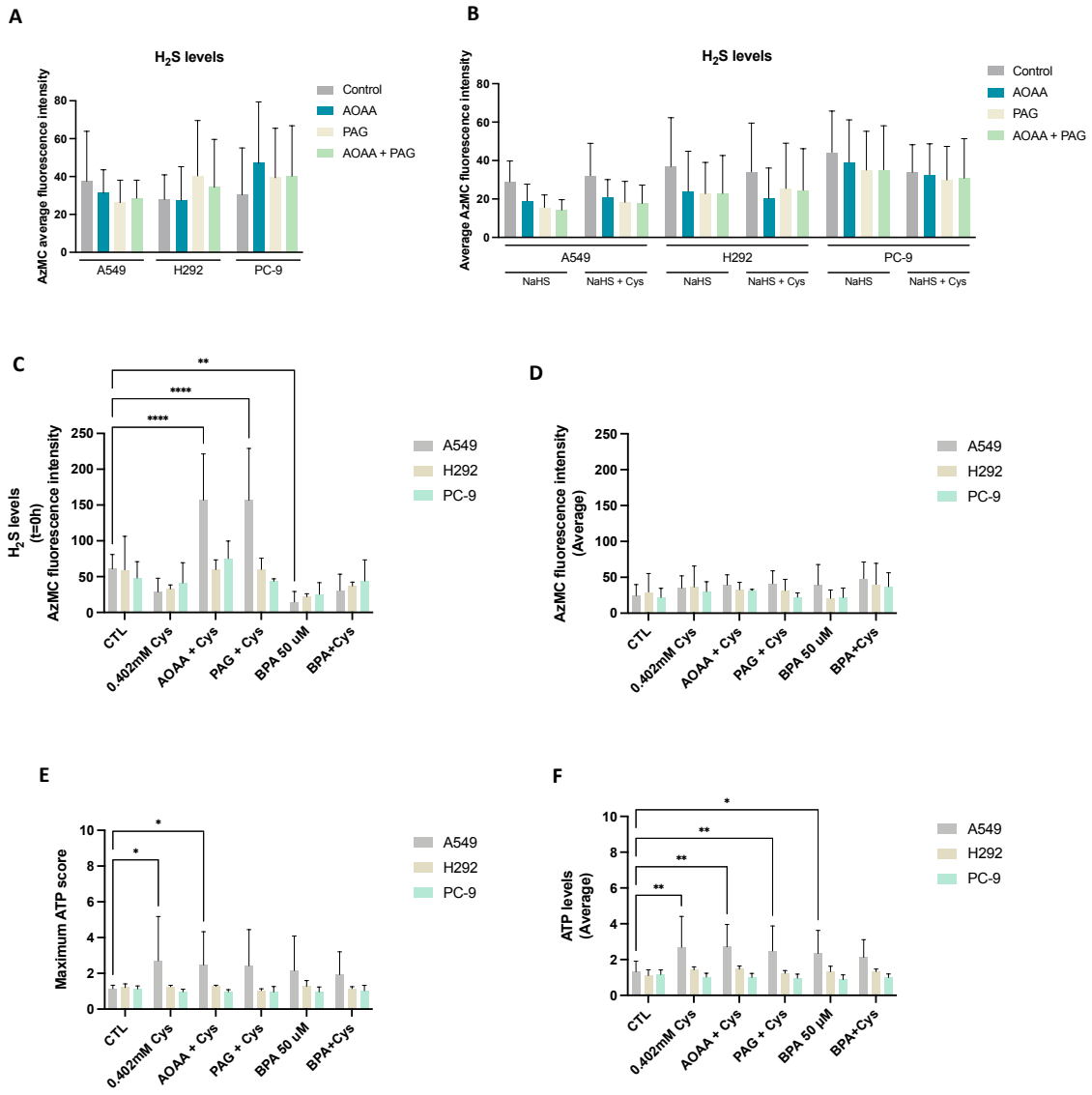

Figure III.1 – NSCLC cell lines present cysteine reliance on H_2S production. (A) NSCLC cell lines show similar basal levels of H_2S production. As an attempt to verify if H_2S production was directly dependent on cysteine degradation, cells were exposed to AOAA/PAG treatment. **(B)** NSCLC cells cultured in the presence of the H_2S donor NaHS, alone and in combination with cysteine show, when exposed to AOAA and PAG, decreased levels of H_2S. PC-9 upon cysteine treatment show a tendency to decrease the average levels of H_2S in control conditions and compensated production of H_2S upon the exposure to inhibitors. **(C)** NSCLC cell lines upon cysteine supplementation tended to decrease the H_2S production at T=0 h, but compensated the CBS and CSE inhibition, maintaining (H292 and PC-9) or increasing (A549) the H_2S levels upon AOAA and PAG exposure. **(D)** Analysis of H_2S levels show that H292 cells present higher H_2S basal production levels, which seems to be dependent on CBS/CSE activity. A549 and PC-9 cells show similar basal ability to produce H_2S. **(E)** Maximum score or **(F)** the average levels of ATP production indicate that A549 cells increased the production of ATP upon cysteine supplementation independently of the presence of inhibitors, while H292 and PC-9 were able to maintain ATP levels in all experimental conditions. Maximum ATP score and average levels indicate that A549 cells increased the levels of ATP upon BPA and/ or cysteine supplementation and H292 and PC-9 cells maintained the ATP levels in all culture conditions independently of glycolysis inhibition. All data are normalized to the control condition and represented as mean ± SD. *p<0.5, **p<0.01, ***p<0.001, ****p<0.0001.

The differential expression of cysteine metabolic players corroborates NSCLC heterogeneity

The expression of *CBS*, *CTH*, *MPST*, *GOT1*, *GOT2*, *CDO1*, *SLC1A1*, and *SLC7A11* genes was evaluated by quantification of the relative mRNA (Figure III.2 A). Additionally, the expression of CBS, CSE and MST enzymes, as well as EAAT3 and xCT transporters was measured by immunofluorescence (Figure III. 2 B). While *CBS* transcriptional levels were higher in H292, the protein levels detected by immunofluorescence were similar among cell lines. Moreover, CBS appeared to be both diffusely localized, but also in small punctae. *CTH* mRNA levels were significantly lower in PC-9 than in the other cell lines, which was not translated into the protein levels. While CSE appeared diffusely expressed in A549 and H292 cells, in PC-9 the protein appeared to localize closer to the membrane. *MPST* mRNA levels were highest in A549 with respect to the other cell lines, with PC-9 exhibiting the lowest mRNA levels. MST expression was similar to CBS (diffuse and in punctae), with comparable protein levels among the three cell lines. *SLC1A1* and *SLC7A11* mRNA levels were relatively low in all cell lines and, similarly to *CTH*, much lower in PC-9 as compared to A549 and H292. However, this did not translate to EAAT3 and xCT protein levels, which were similar in all cell lines and equally exhibited enriched signal in punctae. While *GOT1* had higher mRNA levels in A549 as compared to PC-9 and particularly H292, *GOT2* had lowest levels in A549 (Figure III.2 C). *CDO1* had overall relatively low mRNA levels in all lines, with PC-9 exhibiting the highest levels and *CDO1* mRNA being practically undetectable in H292.

Overall, these expression and localization patterns indicate that heterogeneous metabolic profiles may be found among these NSCLC cell lines, with cysteine metabolism relying on different routes, likely to serve different metabolic requirements.

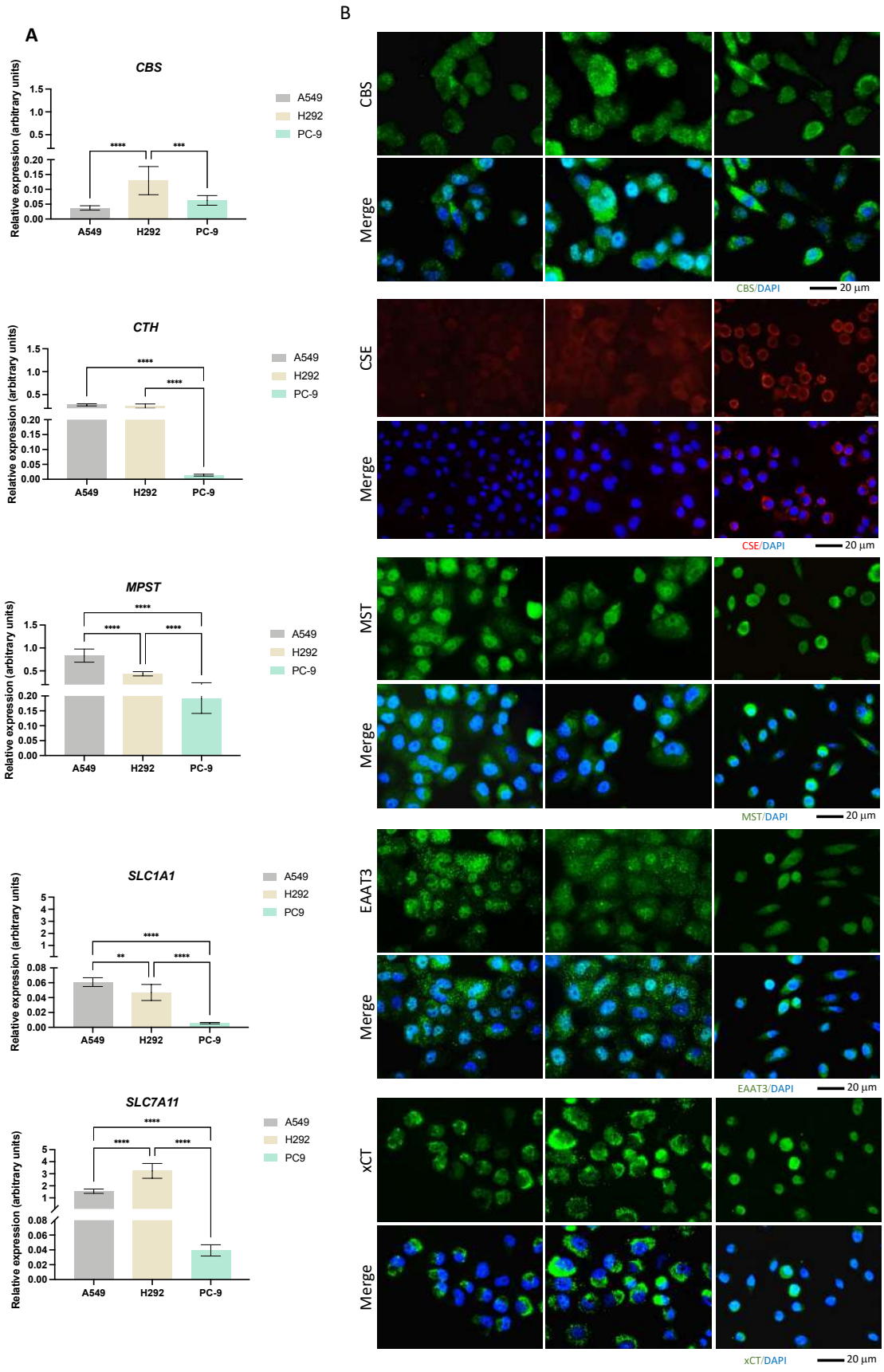
A
B
CBS
Relative expression (arbitrary units)
A549
H292
PC-9
CTH
MPST
SLC1A1
PC9
SLC7A11
CBS
Merge
CBS/DAPI
20 μm
CSE
CSE/DAPI
MST
MST/DAPI
EAAT3
EAAT3/DAPI
xCT
xCT/DAPI

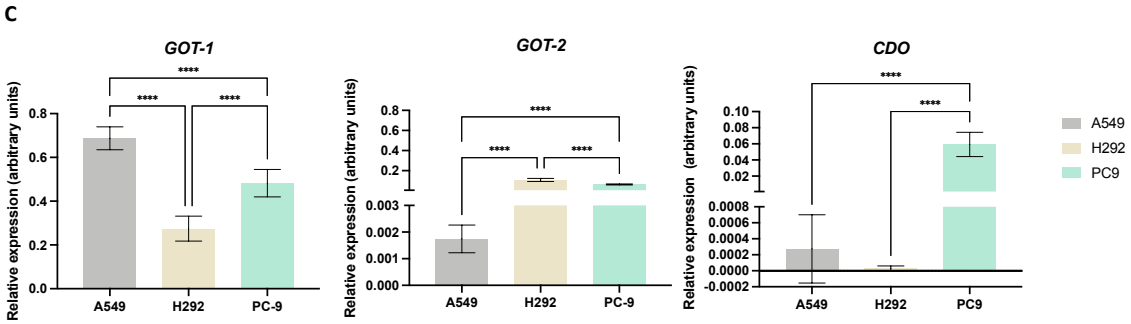

Figure III.2 – NSCLC cells express distinct expression patterns of enzymes and transporters involved in cysteine metabolism. (A) mRNA expression levels analysis show that H292 cells express noteworthy levels of *CBS* and *SLC7A11* comparing to A549 cells, while PC-9 cell show low overall expression of *CTH*, *MPST*, *SLC1A1* and *SLC7A11* **(B)** Immunofluorescence analysis show that protein expression follows mRNA expression patterns, reporting similar differences. **(C)** mRNA expression levels analysis further shows that H292 cells highly express *GOT2*, while PC-9 show high expression levels of *GOT2* and *CDO1*, comparing to A549 cells. All mRNA expression level data are normalized to A549 and represented as mean ± SD. Magnification 400 X, scale 20 µm. *p<0.5, **p<0.01, ***p<0.001, ****p<0.0001.

NSCLC cell lines are chemoresistant and SeChry reduces the metabolic viability of A549 and H292 cells, which seem to present a higher metabolic reliance on cysteine degradation by CBS

Knowing that cysteine metabolism impairs conventional drugs' anti-cancer efficacy[256], metabolic viability was evaluated in NSCLC cell lines exposed to the most commonly used drugs in clinical regimens to NSCLC. Interestingly, cisplatin was the most deleterious drug, in all cancer cell lines, having a higher impact on cell viability loss (Figure III.3 A). Because all cell lines present resistance to at least 3 drugs used in conventional NSCLC therapy, they were considered chemoresistant (Figure III.3 A).

Our previous studies in ovarian cancer showed that SeChry anti-cancer effects were related to cysteine metabolic disruption, due to CBS inhibition and GSH depletion.[363] Thus, metabolic viability assays were performed to evaluate the impact of SeChry on cysteine metabolic reliance in NSCLC cell lines. SeChry was tested in a free form and encapsulated in a nanoparticle, a polyurea dendrimer generation 4, surface functionalized with folic acid ($PURE_{G4}$-FA) to target cancer cells (SeChry@$PURE_{G4}$-FA), as described previously.[363,420]

In order to disclose putative cytotoxic effects on non-cancer cells, tubular renal cells (HK2) and keratinocytes (HaCaT) were also tested in parallel with NSCLC cell lines. All NSCLC cell lines, except PC-9, were quite sensitive to SeChry and SeChry@$PURE_{G4}$-

FA (Figure III.3 B). Amongst NSCLC cell lines, PC-9 presented the highest half-maximum effective concentration (EC_{50}) for SeChry and SeChry@PURE$_{G4}$-FA (Figure III.3 B), suggesting PC-9 may not have a metabolic reliance on cysteine involving CBS, which fits with H_2S and ATP levels described above. EC_{50} values regarding the SeChry effect on non-cancer cells were quite high, whereas EC_{50} for SeChry@PURE$_{G4}$-FA was impossible to determine, nd (Figure III.3 C). Regarding the expression of folate receptor alpha (FR-α), A549 and H292 express high levels, while PC-9 cells show low levels of FR-α, and it was almost undetectable in non-malignant cells (Figure III.3 D). The empty nanoparticles did not have any effect on the metabolic viability of any NSCLC (Figure III.3 B) and non-cancer (Figure III.3 C) cell lines. Free and encapsulated SeChry also decreased all NSCLC cell lines and HK2 proliferation, while no effect was observed in HaCaT (Figure III.3 E).

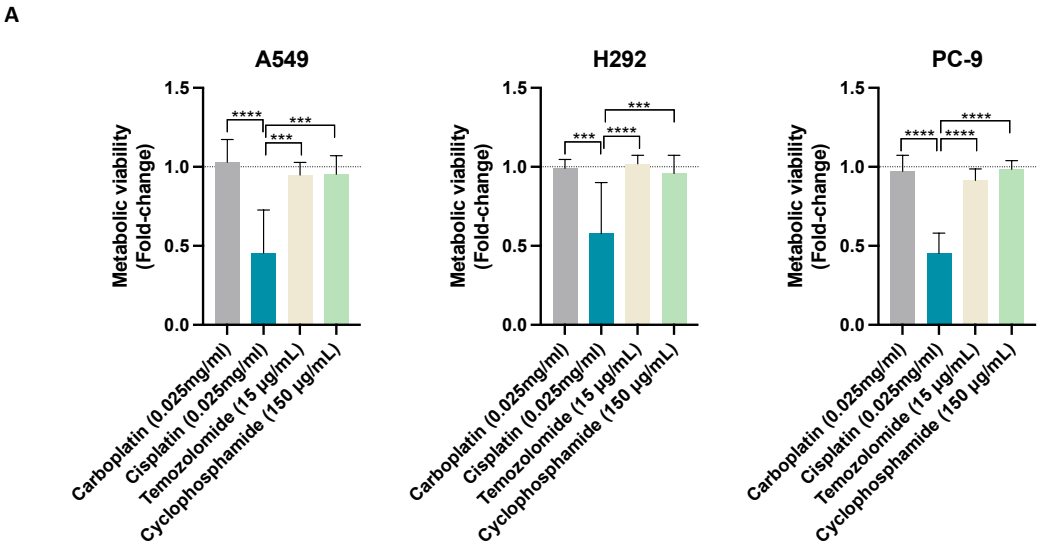

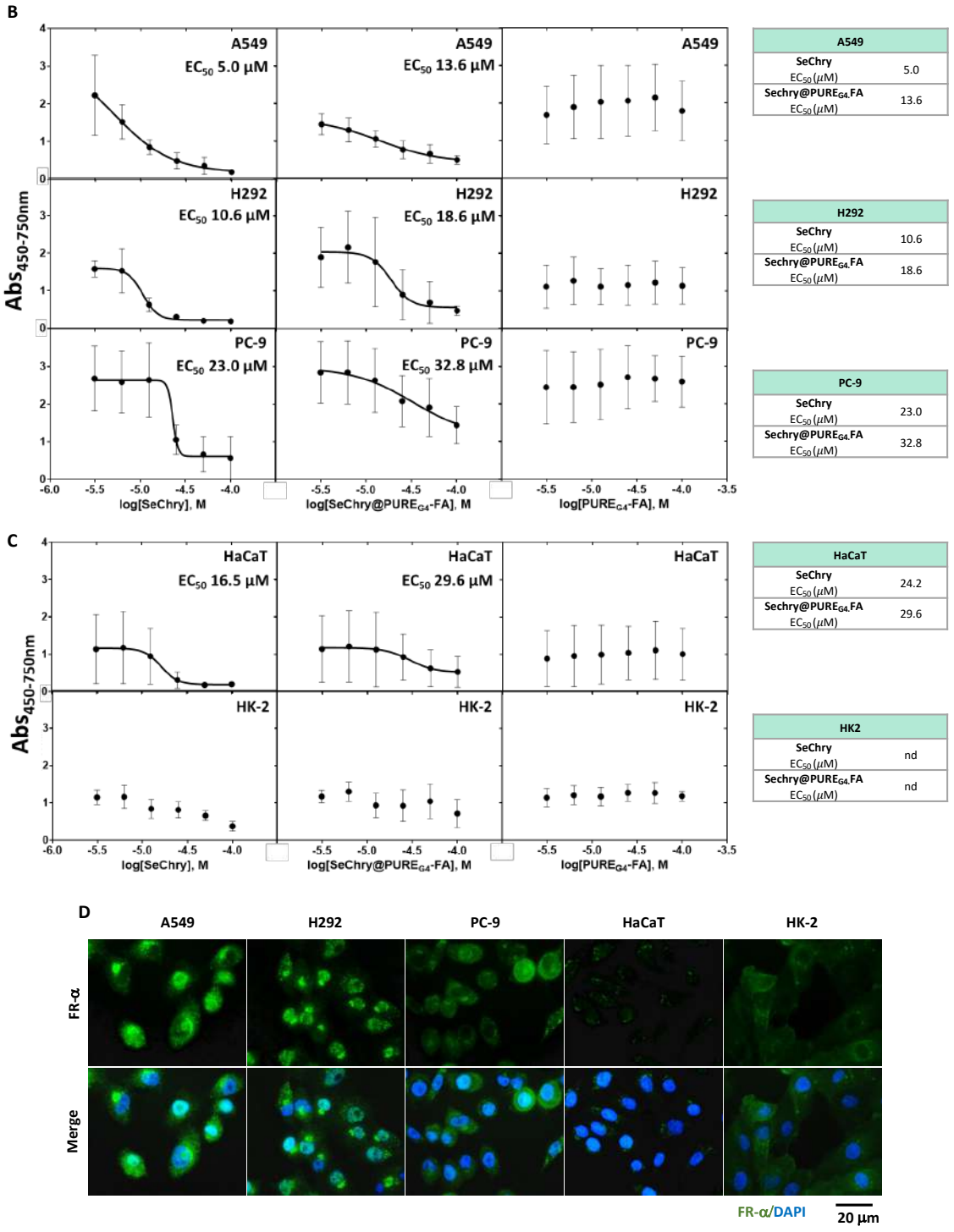
B
A549
EC50 5.0 μM
A549
EC50 13.6 μM
A549
H292
EC50 10.6 μM
H292
EC50 18.6 μM
H292
PC-9
EC50 23.0 μM
PC-9
EC50 32.8 μM
PC-9
Abs450-750nm
log[SeChry], M
log[SeChry@PUREG4-FA], M
log[PUREG4-FA], M
A549
SeChry EC50 (μM) 5.0
Sechry@PUREG4.FA EC50 (μM) 13.6
H292
SeChry EC50 (μM) 10.6
Sechry@PUREG4.FA EC50 (μM) 18.6
PC-9
SeChry EC50 (μM) 23.0
Sechry@PUREG4.FA EC50 (μM) 32.8
C
HaCaT
EC50 16.5 μM
HaCaT
EC50 29.6 μM
HaCaT
HK-2
HK-2
HK-2
Abs450-750nm
log[SeChry], M
log[SeChry@PUREG4-FA], M
log[PUREG4-FA], M
HaCaT
SeChry EC50 (μM) 24.2
Sechry@PUREG4.FA EC50 (μM) 29.6
HK2
SeChry EC50 (μM) nd
Sechry@PUREG4.FA EC50 (μM) nd
D
A549
H292
PC-9
HaCaT
HK-2
FR-α
Merge
FR-α/DAPI
20 μm

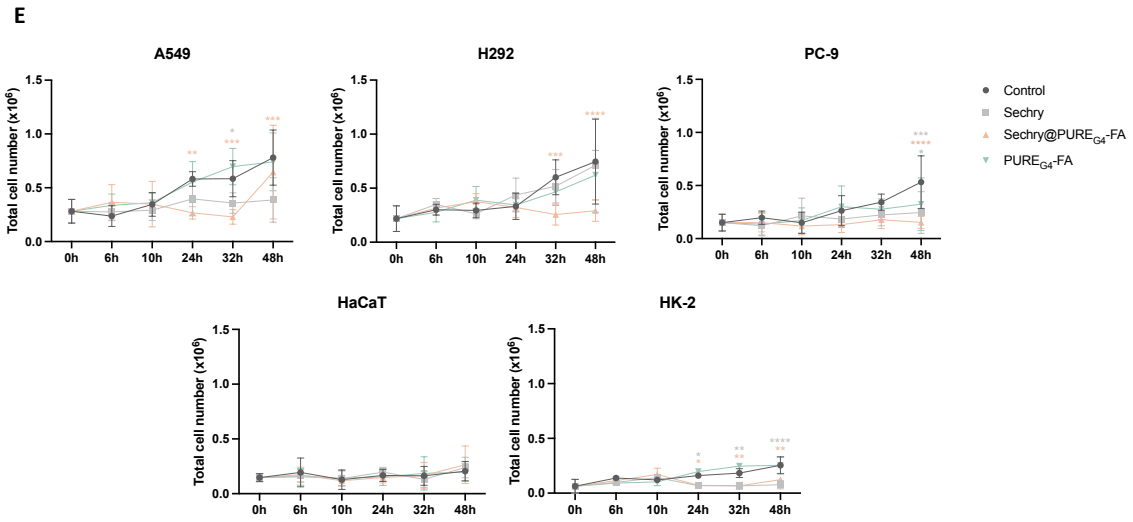

Figure III.3– NSCLC cell lines are chemoresistant and SeChry@PURE$_{G4}$-FA induces decreased cell viability in NSCLC cells, with specificity towards tumor cells rather than non-tumoral cells. **(A)** NSCLC cell lines exposed to the most commonly used therapy regimens showed overall resistance to these drugs, except for cisplatin. **(B,C)** EC_{50} curves and values for SeChry, Sechry@PURE$_{G4}$-FA and PURE$_{G4}$-FA in NSCLC indicate a higher sensitivity of A549 and H292 to the treatment than PC-9. Empty nanoparticles (PURE$_{G4}$-FA) did not induce relevant toxic on cell viability. EC_{50} curves and values for SeChry, Sechry@PURE$_{G4}$-FA and PURE$_{G4}$-FA in non-cancer cell lines (HaCaT and HK2) indicate no effect on cell viability. Empty nanoparticles (PURE$_{G4}$-FA) did not induce relevant toxic on cell viability. **(D)** Detection of FR-α by immunofluorescence indicates high protein levels in in NSCLC but not in non-tumoral cell lines. FR- α is labeled in green and nuclei were counterstained with Dapi (blue). **(E)** SeChry and SeChry@PURE$_{G4}$-FA induced significant decrease in cell proliferation across the NSCLC panel used. All data are normalized to the control condition and represented as mean ± SD. Magnification 400 X, scale 20 µm. *p<0.5, **p<0.01, ***p<0.001, ****p<0.0001.

Expression profile of genes involved in cysteine metabolism can help stratifying patients

We explored TCGA transcriptomic data, considering the two most prevalent groups of NSCLC, LUAD and LUSC, and normal lung tissue to evaluate the expression dynamics of genes involved in cysteine metabolism. Regarding the genes encoding enzymes, the analysis indicated that the expression of *CBS, GOT1* and *GOT2* is increased in LUAD and LUSC comparing to normal lung (Figure III.4 A and B). *CTH* is overexpressed in LUAD, comparing to normal lung (Figure III.4 A and B). No differences were found in *MPST* expression in NSCLC groups compared to normal lung tissue (Figure III.4 A and B). The expression of genes encoding the transporters EAAT3 (*SLC1A1*) and xCT, (*SLC7A11*) are respectively decreased and increased in both LUAD and LUSC, comparing to normal lung (Figure III.4 A and B). *CDO1* was found

downregulated in both LUAD and LUSC, in comparison to normal tissue (Figure III.4 A and B).

The mRNA from a cohort of 55 NSCLC patients, followed in IPOLFG, was used to quantify the expression of *CBS*, *CTH*, *MPST*, *GOT1*, *GOT2*, *CDO1*, *SLC1A1*, and *SLC7A11* genes. Correlations and associations between gene expression, tumor histotypes and somatic mutations were explored. Regarding genes encoding H_2S-producing enzymes (*CBS*, *CTH* and *MPST*), *MPST* was the most expressed gene comparing to *CBS* and *CTH* (Figure III.4 C). *GOT1* showed higher expression levels than *GOT2*, and *CDO1* was detected in most cases (Figure III.4 C). The genes encoding EAAT3 (*SLC1A1*) and xCT (*SLC7A11*) transporters were expressed in quite similar levels among cases (Figure III.4 C). Comparing the expression of genes in NSCLC primary tumors and metastases, only *CDO1* mRNA levels were significantly increased in metastatic samples (Figure III.4 D). Considering the correlation between the expression of the cysteine-related genes, it was observed a significant Spearman correlation between the expression of *CBS* with *CTH, MPST, GOT1, GOT2* and *CDO1; CTH* with *MPST, GOT1, GOT2, CDO1* and *SLC7A11; MPST* with *GOT1, GOT2, CDO1* and *SLC1A1,* and *GOT1* with *GOT2* (Table III.3). A very strong association was found between *CBS* and *GOT1* (r=0.7198); *MPST* and *CTH* (r=0.7013) as well as *CTH* and *GOT1* (r=0.7040). In an attempt to associate particular metabolic profiles with genetic status, correlations between cysteine-related genes were explored in cases presenting mutations in *EGFR* and *KRAS* genes. In the $EGFR^{Mut}$ group, a significant Spearman correlation was found between the expression of *CBS* with *MPST, GOT1* and *GOT2; MPST* with *GOT2, SLC1A1, CTH* with *MPST* and *GOT2* and *SLC7A11,* and *GOT1* with *SLC1A1* and *SLC7A11* (Table III.3). A very strong correlation was observed between *MPST* and *CTH* (r=0.7868); *CTH* and *GOT2* (r=0.7521) as well as *SLC7A11* and *GOT1* (r=0.7455). In the $KRAS^{Mut}$ group, a significant Spearman correlation was found between the expression of *CBS* with *CTH, MPST* and *GOT1; CTH* with *MPST, GOT1* and *CDO1; MPST* with *GOT1* and *SLC1A1,* and *GOT1* with *CDO1* (Table III.3). Very strong Spearman correlations were found between *CBS* and *CTH* (r=0.9031); *CBS* and *GOT1* (r=0.8901), and *CTH* and *GOT1* (r=0.9198).

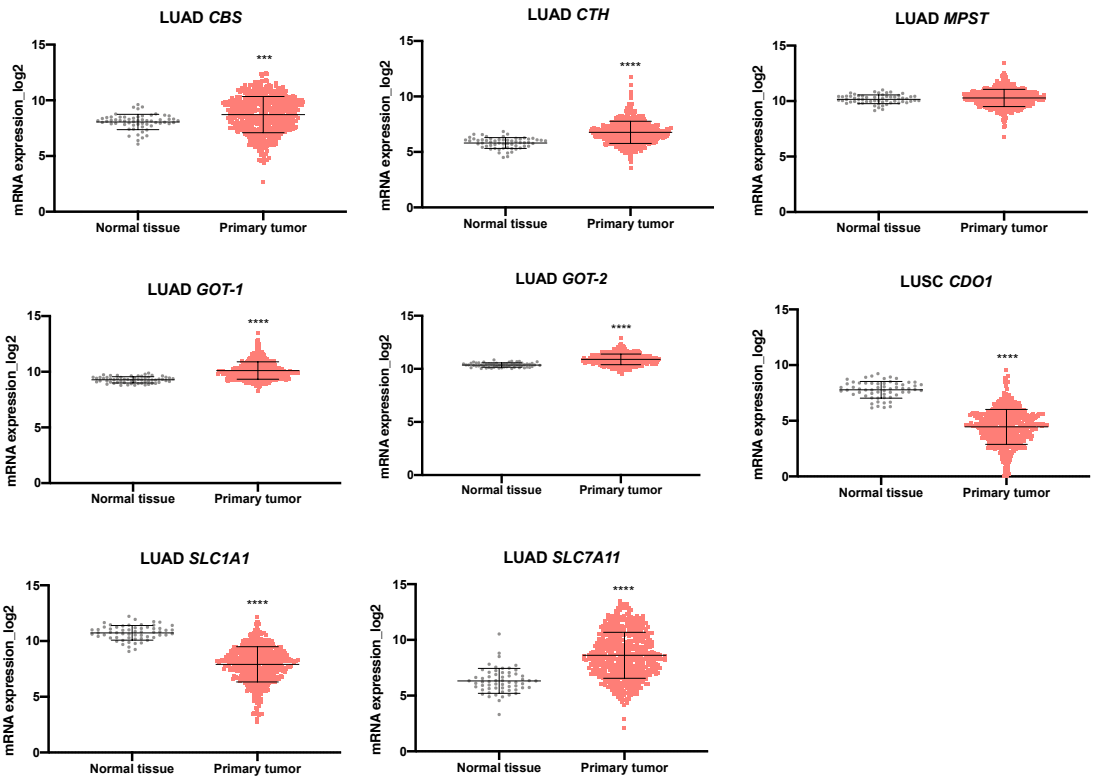
LUAD CBS
LUAD CTH
LUAD MPST
LUAD GOT-1
LUAD GOT-2
LUSC CDO1
LUAD SLC1A1
LUAD SLC7A11
mRNA expression_log2
Normal tissue
Primary tumor

B

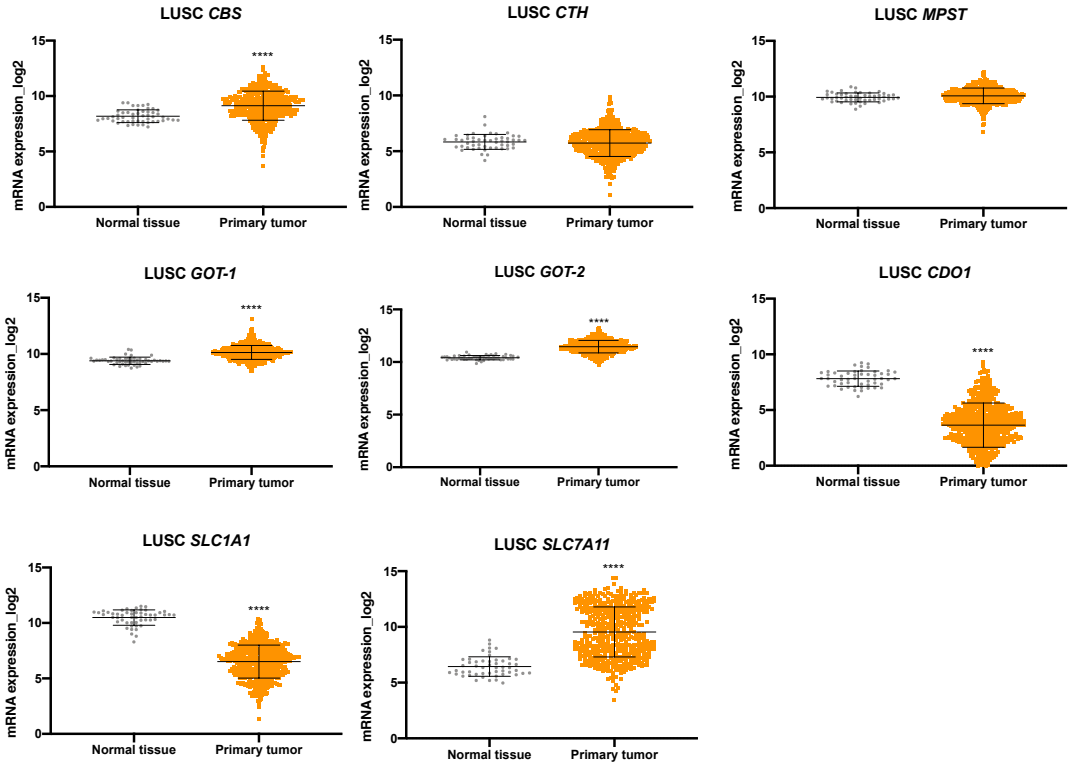
LUSC CBS
LUSC CTH
LUSC MPST
LUSC GOT-1
LUSC GOT-2
LUSC CDO1
LUSC SLC1A1
LUSC SLC7A11
mRNA expression_log2
Normal tissue
Primary tumor

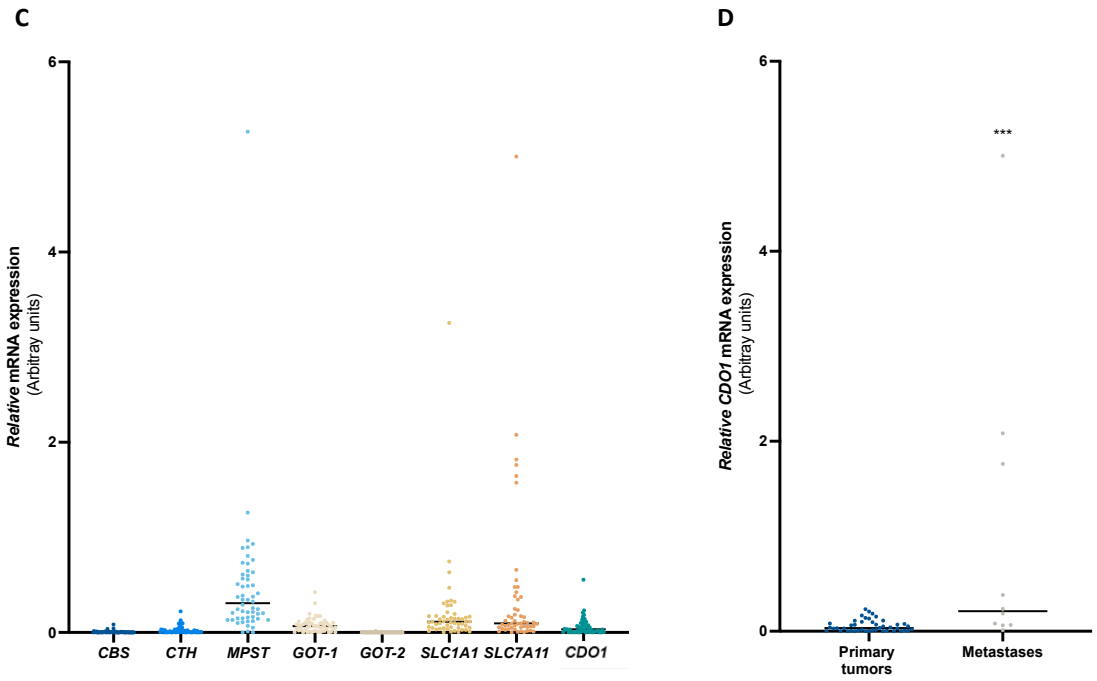

Figure III.4 – Enzymes and transporters of cysteine metabolism are overexpressed in NSCLC patients. (A) Analysis of mRNA levels show upregulation of *CBS, CTH, GOT1, GOT2* and *SLC7A11* and a significant downregulation of *SLC1A1* and *CDO1* in NSCLC primary tumors of the LUAD TCGA cohort. **(B)** Analysis of mRNA levels show upregulation of *CBS*, *GOT1, GOT2* and *SLC7A11* and a significant downregulation of *SLC1A1* and *CDO1* in NSCLC primary tumors of the LUSC TCGA cohort. **(C)** Analysis of the expression of genes encoding H_2S producing enzymes in the IPOLFG NSCLC cohort indicates that *MPST* was the most highly expressed gene; *GOT1* gene was expressed in higher levels than *GOT2*; *CDO1* gene was detected in most cases; *SLC1A1* and *SLC7A11* were expressed in similar levels. **(D)** *CDO1* mRNA expression was found increased in NSCLC metastatic samples comparing to primary tumors. Statistical significance is represented as mean ± SD. *p<0.5, **p<0.01, ***p<0.001, ****p<0.0001.

Table III.3 - Spearman correlation between the expression of metabolic genes in NSCLC samples, considering the total cases and cases presenting *EGFR* and *KRAS* mutations, $EGFR^{Mut}$ and $KRAS^{Mut}$. Significant correlation was considered at $p<0.05$.

NSCLC total cases

Gene	*CBS*	*CTH*	*MPST*	*GOT-1*	*GOT-2*	*SLC1A1*	*SLC7A11*	*CDO1*
	CBS	$r = 0.6885$ $p = <0.0001$	$r = 0.6405$ $p = <0.0001$	$r = 0.7198$ $p = <0.0001$	$r = 0.3672$ $p = 0.0068$	ns	ns	$r = 0.4127$ $p = 0.0021$
		CTH	r = 0.7013 p = <0.0001	$r = 0.7040$ $p = <0.0001$	$r = 0.5951$ $p = <0.0001$	ns	$r = 0.3608$ $p = 0.0080$	$r = 0.4596$ $p = 0.0005$
			MPST	r = 0.6183 p = <0.0001	$r = 0.4593$ $p = 0.0005$	$r = 0.6254$ $p = <0.0001$	ns	$r = 0.4255$ $p = 0.0015$
				GOT-1	$r = 0.4537$ $p = 0.0006$	ns	$r = 0.4574$ $p = 0.0006$	ns
					GOT-2	ns	ns	ns
						SLC1A1	ns	ns
							SLC7A11	ns
								CDO1

NSCLC *EGFR*^{Mut} and *KRAS*^{Mut} cases

	Gene	$EGFR^{Mut}$							
		CBS	*CTH*	*MPST*	*GOT-1*	*GOT-2*	*SLC1A1*	*SLC7A11*	*CDO1*
$KRAS^{Mut}$	*CBS*		ns	ns	$r = 0.5947$ $p = 0.0352$	ns	ns	ns	ns
	CTH	$r = 0.9031$ $p = <0.0001$		$r = 0.7868$ $p = 0.0021$	ns	$r = 0.7521$ $p = 0.0041$	ns	ns	ns
	MPST	$r = 0.6481$ $p = 0.0027$	$r = 0.6466$ $p = 0.0028$		ns	$r = 0.6437$ $p = 0.0202$	$r = 0.6429$ $p = 0.0208$	$r = 0.5604$ $p = 0.0499$	ns
	GOT-1	$r = 0.8901$ $p = <0.0001$	$r = 0.9198$ $p = <0.0001$	$r = 0.6980$ $p = 0.0009$		ns	$r = 0.6355$ $p = 0.0224$	$r = 0.7455$ $p = 0.0047$	ns
	GOT-2	ns	ns	ns	ns		ns	ns	ns
	SLC1A1	ns	ns	$r = 0.6326$ $p = 0.0048$	ns	ns		ns	ns
	SLC7A11	ns	ns	ns	ns	ns	ns		ns
	CDO1	ns	$r = 0.5564$ $p = 0.0165$	ns	$r = 0.5308$ $p = 0.0234$	ns	ns	ns	

III.V. Discussion

Cancer metabolism is a rediscovered research area, and it encloses several queues to better understand cancer biology and find disease specificities, which can be targeted in novel and more personalized therapies. Cysteine metabolic circuitries have been highlighted in recent years as being pivotal in cancer metabolic rewiring, contributing to cancer cells' survival and chemoresistance.[192,197] In this study, new insights into the metabolic players' adaptation and heterogeneity of NSCLC cells are presented, accounting for a more profound knowledge of different subsets of the disease. Common cancer features can go side by side with cancer cell specificities, constituting useful targets and markers.

The metabolic reliance on cysteine was confirmed in three NSCLC cell lines, although specificities have been observed and will be further discussed. All cell lines presented similar H_2S levels (Figure III. 1 A). Our results indicate that whereas A549 and H292 may rely mostly on CBS and CSE to generate H_2S, PC-9 appears to rely mostly on the CAT/MST axis for H_2S generation. Since H_2S steady-state levels result from a balance of its synthesis and consumption, it remains to be established whether the sulfide

oxidation pathway (not directly involved in cysteine metabolism) also operates differently between cell lines.

Beyond the production of lactate, glycolysis is a supplier of other glucose-dependent pathways, such as the PPP which plays a role in biosynthesis and redox control.[176] PC-9 dependence on glucose appears to be lower comparing with A549 and H292 cell lines.[401] This observation is in accordance with the results showing that glycolysis inhibition by BPA can be compensated by the addition of cysteine, in order to generate H_2S to maintain the ATP intracellular content (Figures III.1 C-F), and PC-9 cells sustain higher H_2S levels upon BPA exposure (Figures III.1 C-F). Moreover, PC-9 cells express higher levels of *CDO1* than the other cell lines (Figure III.2 C), reinforcing that cysteine may be a source of pyruvate and glutamate. CDO1 participates in the synthesis of pyruvate from cysteine and in this pathway glutamate is generated from α-ketoglutarate [235,237,238] under the action of CAT/GOT enzymes. This way, CDO1 may complement the action of MST, since these two enzymes work in partnership with CAT enzymes, encoded by *GOT1* and *GOT2* genes, and *GOT2* was demonstrated to be highly expressed in H292 and PC-9 cell lines (Figure III.2 C). These results are very important since CDO1 is not often considered in cancer metabolism as an intervenient in cysteine-derived pyruvate production, being only explored as a mediator of taurine synthesis in NSCLC [421].

These results, together with results reported previously[401], indicate two main cysteine metabolic profiles can be disclosed, considering the reliance on glucose *versus* glutamine and the way cysteine can contribute to fill metabolic gaps. NSCLC cells that present a more glycolytic profile (represented by the PC-9 cell line), use glucose mainly to supply biosynthesis with an intensive production of lactate, increasing the need for glutamine to supply bioenergetics. Thus, glutamate alternative sources are needed, and cysteine can fulfill this role, by following the catabolic route of CAT/MST or CDO1 and giving rise to pyruvate and glutamate. The oxidative metabolism through CDO1 does not generate H_2S and accounts for its global decreased levels. NSCLC cells presenting a more oxidative profile (represented by the A549 cell line) use glucose to supply bioenergetics and biosynthesis, the reliance on glutamine decreases and it works as the main source of glutamate. Cysteine catabolism occurs mainly through the H_2S-generating pathways dependent on CBS and CSE, accounting for global increased levels of H_2S.

Independently of the preferential cysteine catabolic pathway used by NSCLC cells, all of them are able to degrade cysteine, produce H_2S and maintain or increase ATP generation, even upon glycolysis inhibition (Figure III.1). Therefore, given that these cell lines are chemoresistant to the main drugs used in NSCLC conventional therapy, we tested the effect of SeChry, which we had published as an inhibitor of cysteine catabolism through CBS.[363] SeChry as a new therapy could be more effective in cancer cell lines with increased antioxidant capacity, such as those presenting resistance to conventional cytotoxic drugs, as we showed (Figure III. A), which are commonly more capable of scavenging ROS. All tested drugs still promote ROS generation according to published studies [422–425], even the ones that do not present the induction of ROS generation as the main mechanism of action. The platinum salts (carboplatin and cisplatin), temozolomide and cyclophosphamide are alkylating agents, directly reacting with proteins and DNA, inducing cell injury and DNA damage, as they also stimulate the generation of ROS (https://go.drugbank.com/drugs/DB00544).

The use of a dendrimer nanoparticle functionalized with folate to deliver SeChry (SeChry@PURE$_{G4}$-FA) was an attempt to more specifically direct nanoparticles to cancer cells, as they overall express higher levels of folate receptor.[426,427] Interestingly, the EC_{50} for SeChry@PURE$_{G4}$-FA was inversely proportional to the expression levels of FR-α (Figure III.3 B, C, and D). So, all NSCLC cell lines, except PC-9, were quite sensitive to SeChry and SeChry@PURE$_{G4}$-FA. PC-9 presented an EC_{50} for SeChry very close to non-cancer cell lines (Figure III.3 B and C), in line with PC-9's metabolic reliance on cysteine not depending on CBS. It remains to be clarified why in NSCLC cell lines free SeChry had slightly lower EC_{50} comparing to encapsulated SeChry, as we have previously described in ovarian cancer.[428] Despite this, the nanoformulation SeChry@PURE$_{G4}$-FA can still be a good option for a SeChry-based therapy since it protects the non-cancer cells from SeChry toxicity, as we saw by the lack of effect of SeChry@PURE$_{G4}$-FA on HK2 and HaCaT (Figure III.3 C). Moreover, free or encapsulated SeChry impaired the proliferation of NSCLC cell lines (Figure III.3 E), which constitutes an important feature in cancer therapy.

Bringing cysteine metabolic circuitries to the NSCLC context may open new perspectives on disease management with the identification of new and more specific targets and markers. Therefore, the expression of pivotal players in cysteine transport and catabolism was explored in the TCGA database. In LUAD and LUSC histotypes, comparing to normal lung tissue, *CBS*, *GOT1*, *GOT2* and *SLC7A11* are overexpressed,

SLC1A1 and *CDO1* are downregulated, and *MPST* expression is not altered. Additionally, *CTH* is overexpressed in LUAD but not LUSC, thereby representing a clear distinctive pattern between the two histotypes that can be further explored. The proteins encoded by the overexpressed genes can serve as therapeutic targets, as we demonstrated by using SeChry, a well-tolerated compound by non-cancer cells and an effective cytotoxic and growth controller in NSCLC depending on CBS activity, such as A549 and H292 cell lines. The proteins encoded by these genes can also be validated as therapy response markers, since cysteine metabolic reliance accounts for chemoresistance, and they will function as an important tool to predict disease prognosis. Downregulated genes, such as *SLC1A1* and *CDO1* can help finding specificities exhibited less frequently in NSCLC cases. This is the case of *CDO1*, whose dependence is shown by the PC-9 cell line that presents a versatile cysteine reliance pattern. Results suggest that PC-9 cells use CDO1 to oxidatively degrade cysteine in order to sustain pyruvate and glutamate levels, and MST to sustain cysteine-dependent H_2S generation and account for pyruvate yield.

Importantly, we addressed the expression profile of cysteine-related genes in a cohort of NSCLC patients characterized for the prevalent somatic mutations found in NSCLC, affecting *EGFR* and *KRAS* genes. Some *in vitro* profiles were reinforced by the expression levels of cysteine-related genes in NSCLC samples. *MPST* was the most expressed cysteine-degrading and H_2S-producing enzyme encoding gene (Figure III.4 C), and Spearman strong correlations ($0.4 > r < 0.69$), with statistical significance ($p < 0.01$), were observed between *MPST* expression with its metabolic partners *GOT1* and *GOT2*, as well as with *CDO1*, whose encoded enzyme acts sequentially with *GOT1* and *GOT2* encoded enzymes (Table III.3). This pattern of genes related to cysteine fits with the one observed in the PC-9 cell line. The relevance of MST action in cancer requires clarification[391], and our study gives one more step towards this. The significant correlations between *MPST* with *GOT2, SLC1A1* and *SLC7A11* and between *MPST* with *GOT1* and *SLC1A1* were also verified, respectively in tumors $EGFR^{Mut}$ and $KRAS^{Mut}$ (Table III.3), suggesting that cysteine catabolism routes through MST and CAT/GOT enzymes with the production of H_2S and through CDO1 and CAT/GOT enzymes are pivotal in some subsets of NSCLC. Moreover, *CDO1* was significantly more expressed in NSCLC metastases than in primary tumors (Figure III.4 D). Contrarily to what is shown by different studies indicating *CDO1* may be a tumor suppressor gene[255,299,429–431], our results point out that its function may contribute to more aggressive phenotypes. This indicates that there is an opportunity for therapeutical intervention by targeting CDO1 in

particular cancer contexts in which *CDO1* silencing is not occurring, since it was described in NSCLC that *CDO1* silencing by methylation was occurring preferentially in *KEAP1* mutated cases.[421] KEAP1 is a negative regulator of NRF2 the main controller of oxidative stress. Therefore, upon KEAP1 inactivation, the overexpression of genes regulated by NFR2 will occur, including *SLC7A11*.[432] No significant correlations were observed between the expression of *CDO1* and *SLC7A11* genes (Table III.3). Hence, more studies are needed to ensure CDO1 targeting can be a suitable strategy to treat some subsets of NSCLC.

Considering the EAAT3 and xCT transporters, their encoding genes (respectively, *SLC1A1* and *SLC7A11*) were expressed at similar levels, in NSCLC samples (Figure III.4 C), suggesting that cysteine enters the cell as a free amino acid and also as a dimer, cystine, since EAAT3 is a cysteine transporter and xCT is a glutamate/cystine antiporter .[197] Interestingly, the expression of *SLC1A1* presented a significantly strong Spearman correlation with the expression of *MPST* and *GOT1*, in the $EGFR^{Mut}$ group, while in all NSCLC cases and in $KRAS^{Mut}$ samples the correlation was significant only with *MPST* expression (Table III.3). The expression of *SLC7A11* in all NSCLC cases and in the $EGFR^{Mut}$ group presented a significantly strong correlation with *GOT1* expression, while in the $EGFR^{Mut}$ group a significantly strong correlation was also observed with *MPST* expression (Table III.3). A significant moderate correlation between *SLC7A11* and *CTH* expression was observed in all NSCLC cases (Table III.3). The relevance of xCT function in chemoresistance and cell death inhibition, namely through ferroptosis, is already set in NSCLC.[432,433] and our study is in accordance with this, reinforcing that xCT blockade can be a useful adjuvant therapy to improve the efficacy of conventional cancer therapy.

Besides our results highlighting MST and CDO1 role in cysteine metabolism, the correlations observed between *CBS* and *CTH* with other genes encoding enzymes and transporters support the role of CBS and CSE on cancer biology disclosed in other studies [279,434,435], as we also verified in our H_2S detection assays, using A549 and H292 cell lines (Figure III.1).

III.VI. Conclusion

The definition of cancer metabolome will very hardly allow clear-cut identification of markers for disease. However, the definition of profiles that fit certain clinical behaviors

and patients' subsets can constitute a powerful tool in the prognosis and stratification of patients who may benefit from new therapies. Heterogeneity defines individual profiles and the identification of new targets among metabolic players is also a step forward in cancer management towards personalized medicine.

Chapter IV

CBS Inhibition as a Therapeutic Approach in Colorectal Cancer

This chapter is based on the following publication:

Ana Hipólito, Cindy Mendes, Filipa Martins, *et al*. Cystathionine β-Synthase Inhibition: Pioneering a New Era in Colorectal Cancer Therapeutics with Selenium-Chrysin Polyurea Dendrimer Nanoformulation. Submitted for publication.

IV.I. Abstract

Colorectal cancer (CRC) remains a leading cancer-related cause of death worldwide. Although studies have been focused on disclosing CRC molecular features and novel therapies, resistance to therapy remains a major clinical obstacle to overcome.

This study investigates the potential of inhibiting CBS as a putative therapeutic strategy for CRC. A novel metabolism-based approach, SeChry@PURE$_{G4}$-FA, was employed to specifically target cystathionine-β-synthase (CBS), offering dual benefits of inhibiting CBS activity while selectively targeting cancer cells, thereby reducing toxicity effects.

By exploring CBS inhibition as a targeted therapeutic approach, this work contributes to advancing personalized therapy options for CRC patients and offers new insights into disrupting metabolic remodeling in cancer cells.

Keywords: Colorectal cancer, SeChry, Cystathionine-β-synthase, Targeted therapy

IV.II. Introduction

CRC is a leading cause of cancer-related deaths, accounting for about 10% of all annually diagnosed cancers worldwide, more frequently diagnosed in women and showing higher incidence rates in the most developed countries.[6,122] CRC etiology is related to sporadic and hereditary genetic alterations, with familial history accounting for about 10–20% of all patients.[123] However, risk factors as environmental aspects, such as dietary composition rich in saturated fats and red meat, excessive total energy intake, alcohol and tobacco consumption, and sedentary lifestyle are further described to account for CRC.[122,124] CRC treatment still greatly relies on chemotherapy regimens, including alkylating and oxidative agents.[122,133] However, chemoresistance to these drugs remains a major obstacle in CRC management, due to the plasticity of CRC cancer cells, which can adapt and find ways to metabolically surpass the effect of these agents.[134–140]

Increased cysteine metabolic reliance deeply linked with hydrogen sulfide (H_2S) metabolism have been growingly associated with cancer progression and aggressiveness

as well as chemoresistance in various cancer types (reviewed in [192,197,231]). Disturbed H_2S metabolism related to altered expression, localization and post-translational control of the enzymes that synthesize or detoxify H_2S has been reported to sustain neoangiogenesis and stimulate cell bioenergetics, among other physiological processes that underlie cancer progression[264]. In particular, cystathionine β-synthase (CBS), the first enzyme of the reverse transsulfuration pathway of methionine metabolism, has been demonstrated to be a key H_2S-generating enzyme with multiple roles in cancer (reviewed e.g. in [192,264]) CBS is thought to participate in CRC carcinogenesis, since its expression was found to increase significantly in the transition from healthy colonic tissue to adenocarcinoma formation.[280] Several studies described CBS overexpression in CRC tumors, comparing to surrounding healthy tissue[280–282], thus suggesting an important impact of CBS overexpression in tumor bioenergetics and growth.[283] Moreover, CBS upregulation is believed to be linked to cancer progression and metastasis[284], as demonstrated in CRC metastasis-competent circulating tumor cells[246], further reinforcing the significance of CBS in these processes. Szabo and colleagues[283] found that inhibiting CBS has a detrimental effect on tumor bioenergetics, hindering the capacity of cancer cells to proliferate, migrate, and infiltrate. Interestingly, their research also demonstrates that inhibiting CSE does not yield comparable outcomes, as it does not hinder cancer cell proliferation or suppress tumor growth. These results point the pivotal role of CBS, rather than CSE, in supporting growth and proliferation of CRC cells. In line with its established role, the potential in pharmacologically targeting CBS for cancer treatment has been firmly recognized[354,436] and has been the object of compound screening and development campaigns with mixed results concerning effectivity and selectivity.[277,327,415,437–441] Our groups have reported on the discovery of a selective CBS inhibitor (with respect to CSE and MST), a selenium-containing chrysin (SeChry) that proved cytotoxic towards ovarian cancer cells.[363] SeChry encapsulation with folate-targeted polyurea dendrimer generation four (SeChry@$PURE_{G4}$-FA) afforded specific targeting of SeChry to ovarian cancer cells, thereby circumventing cytotoxicity to non-malignant cells.

In this study, we explored the inhibition of CBS as a therapeutic approach in CRC, using a metabolism-based strategy (SeChry@$PURE_{G4}$-FA) specifically directed to CBS-dependent cancer cells, which not only allows the inhibition of CBS activity but also has

the potential to specifically target cancer cells overexpressing folate receptor alpha (FR-α), diminishing toxicity effects.

In this chapter, we explored the inhibition of CBS as a therapeutical approach in CRC, using a metabolism-based approach (SeChry@PURE$_{G4}$-FA) specifically directed to CBS-dependent cancer cells, which not only allows the inhibition of CBS activity but also has the potential to specifically target cancer cells overexpressing folate receptor alpha (FR-α), diminishing toxicity effects, as studied before (Chapter III).

IV.III. Materials and Methods

Cell lines and culture conditions

Human colorectal adenocarcinoma cell lines HCT15 (CCL-225™), HCT116 (CCL-247™), LoVo (CCL-229™) and SW48 (CCL-231™) were obtained from ATCC (Manassas, VA, USA).

The selected CRC cell lines represent distinct CRC molecular pathways with different mutations in critical genes (Table IV.1). Cells were cultured in Dulbecco's Modified Eagle's Medium 1× (DMEM) (41965-039, Gibco, Life Technologies) supplemented with 10% fetal bovine serum (FBS; S 0615, Merck), 1% Antibiotic-Antimycotic (AA; P06-07300, PAN Biotech) and 50 μg/mL Gentamicin (15750-060, Gibco, Life Technologies). Cells were maintained at 37°C in a humidified environment with 5% CO_2. Cells were cultured until an optical confluence of 75–100% and detachment was performed with 0.05% trypsin-EDTA 1× (25300-054, Invitrogen). Before *in vitro* experiment, cells were synchronized under starvation (FBS free culture medium) overnight, except for cytotoxic experiments. All experiments were then conducted using 1% FBS medium with the additional supplements stated above.

Table IV.1. – Molecular characteristics of the selected panel of CRC cell lines. Data adapted from Ahmed *et al*., 2013[442]

Cell line	CRC molecular pathway			Mutation status				
	CIN	MS status	CIMP	*KRAS*	*BRAF*	*PIK3CA*	*PTEN*	*TP53*
HCT15	-	MSI	+	G13D	WT	E545;D549N	WT	S241F
HCT116	-	MSI	+	G13D	WT	H1047R	WT	WT

LoVo	-	MSI	-	G13D; A14V	WT	WT	WT	WT
SW48	-	MSI	+	WT	WT	WT	WT	WT

Quantitative real-time PCR (qPCR)

Total RNA was extracted using RNeasy Mini Extraction kit (74104, Qiagen, Hilden, Germany) and cDNA synthesized from 1 µg RNA by SuperScript II Reverse Transcriptase (18080044, Thermo Fisher Scientific), both according to the manufacturer's protocol and cDNA was synthesized as mentioned above. qPCR was performed using SYBR Green PCR Master Mix (04707516001, Roche), according to the manufacturer's protocol and the specific primers and genes are presented in Table IV.2.

Real-time PCR was carried out during 40 amplification cycles, according to the manufacturer's instructions, using a Lightcycler® 480 System instrument (05015243001, Roche). *HPRT* was used as a housekeeping gene (Table IV.2). Experiments were performed in biological triplicates.

Table IV.2 - Primers used in gene expression analysis. Detailed characterization of the primers used in RT-qPCR assays.

Gene	Primer	Sequence (5'→3')	Length (nt)	AT (ºC)	GC %	Fragment (bp)
CBS	Forward	*GAGCTCTTGGCCAAGTGTG*	19	60	58	232
	Reverse	*GCACGTCCACCTTCTCGG*	18		67	
HPRT1	Forward	*TGACACTGGCAAAACAATGCA*	21	58	43	94
	Reverse	*GGTCCTTTTCACCAGCAAGCT*	21		52	

Immunofluorescence

Immunofluorescence was used to detect the expression of proteins. Cells (1×10^5 cells/well) were seeded in glass cover slips in 24-well plates coated with 0.2% gelatin from porcine skin (G-1890, Sigma-Aldrich) and then fixated with 2% paraformaldehyde for 15 min at 4ºC. After fixation, cells were incubated with 50 mM NH_4Cl for 10 min. Blocking and antibodies dilution were performed with PBS 1× - 0.5% BSA - 0.1% saponin-PBS (w/v/v). Between incubations, cells were rinsed twice with PBS

1×, for 5 min. After blocking for 1 h, cover slips were incubated with primary antibodies targeting FR- α (PA5-112130, Invitrogen) and CBS (WH0000875M1, Sigma-Aldrich), overnight at 4°C. Cells were incubated with secondary antibody for 2 h at room temperature (1:1000; Alexa Fluor® 488 goat anti-rabbit, A-11034, Thermo Fisher Scientific; 1:1000; Alexa Fluor® 488 goat anti-mouse, A-11001, Thermo Fisher Scientific).

The slides were mounted in VECTASHIELD media with DAPI (H-1200-10, Vector Labs) and examined by standard fluorescence microscopy under a Zeiss Imager.Z1 AX10 microscope. Images were acquired and processed with CytoVision software.

WST-1 assay for cell metabolic viability

The WST-1 based colorimetric assay (11 644 807 001, Roche Applied Science, Indianapolis, IN, USA) was performed to quantify cell metabolic viability. Cells were seeded in 96-well clear bottom tissue culture plates and treated at different concentrations (of common chemotherapeutic drugs or SeChry). For chemoresistance/sensitivity analysis, cells were exposed for 24 h to carboplatin (0.0025 mg/mL), cisplatin (0.0025 mg/mL), 5-fluorouracyl (5-FU, 0.0026 mg/mL), oxaliplatin (0.0008 mg/mL) or vehicle. To analyze the effect of SeChry, the free (SeChry) or encapsulated (SeChry@PURE$_{G4}$-FA) formulation were added to cells, as well as the empty PURE$_{G4}$-FA, in the 3-100 µM concentration range, and the metabolic viability measured after 24 h of exposure. At the selected time points, cells were incubated with WST-1 reagent for 1 h at 37 °C with 5% CO_2, according to the manufacturer's instructions. In actively metabolizing cells, the WST-1 reagent is cleaved to formazan by cellular enzymes. The presence of formazan was assessed through spectrophotometric quantification (450 nm) in a Bio-Rad Laboratories iMark™ Microplate Absorbance Reader (1681130).

Proliferation curves

Cell proliferation rate was determined by the establishment of proliferation curves. Cells were seeded in 24-well plates (5×10^4 cells/well) in complete DMEM, synchronized under starvation and exposed to the experimental conditions. At each time-point (0, 6, 10,

24, 32 and 48 h), cells were detached as described (supernatant was also collected) and cells were centrifuged for 5 min at 155 × *g*. The supernatant was discarded and cells were counted by staining with Trypan Blue Stain 0.4% (15250061, Thermo Fisher Scientific) to identify cells with a compromised cell membrane, hence indicating cell death, using a Neubauer improved cell counting chamber.

Statistical analysis

Statistical analysis and EC_{50} calculation were performed using GraphPad Prism 8.0 software (www.graphpad.com). Sample data were presented as mean (normal distribution) ± SD. Assays were performed with at least three biological replicates per treatment (with at least 3 independent n). Comparisons between data from each group were statistically analyzed by a two-tailed unpaired Student's t-test and multiple comparisons were performed using one-way or two-way ANOVA. Differences between experimental conditions were considered statistically significant at $p < 0.05$.

IV.IV. Results

CRC cell lines differentially express H_2S-synthesizing enzymes

As stated before, expression of H_2S-synthesizing enzymes is described to show alterations in CRC. In line with this, we studied the mRNA expression of *CBS*, *CTH* and *MPST*, respectively encoding CBS, CSE and MST to understand if our panel of CRC cell lines (representing different molecular CRC pathways listed in Table IV.1) presented altered expression (Figure IV.1 A). Despite being the gene amongst the three exhibiting lowest expression levels, *CBS* presented the most differential expression between the CRC cell lines studied, with significantly increased levels in HCT116 cell line comparing to the remaining. HCT15 and SW48 cell lines show similar levels of *CBS* expression, while LoVo cells show the lowest expression in this panel of CRC cell lines. While *CTH* expression was not found to significantly differ across this panel of cell lines, it seems to present lower levels in HCT15 cells. *MPST* was found significantly increased in LoVo cell line, while HCT15, HCT116 and SW48 showed similar *MPST* levels, with SW48 showing slightly lower expression levels (Figure IV.1 A). Since *CBS* was the gene

exhibiting the most differential expression in this panel of CRC cell lines, we then studied CBS protein expression in these cell lines (Figure IV.1 B). Overall, CBS showed high protein expression levels in all cell lines (Figure IV.1 B).

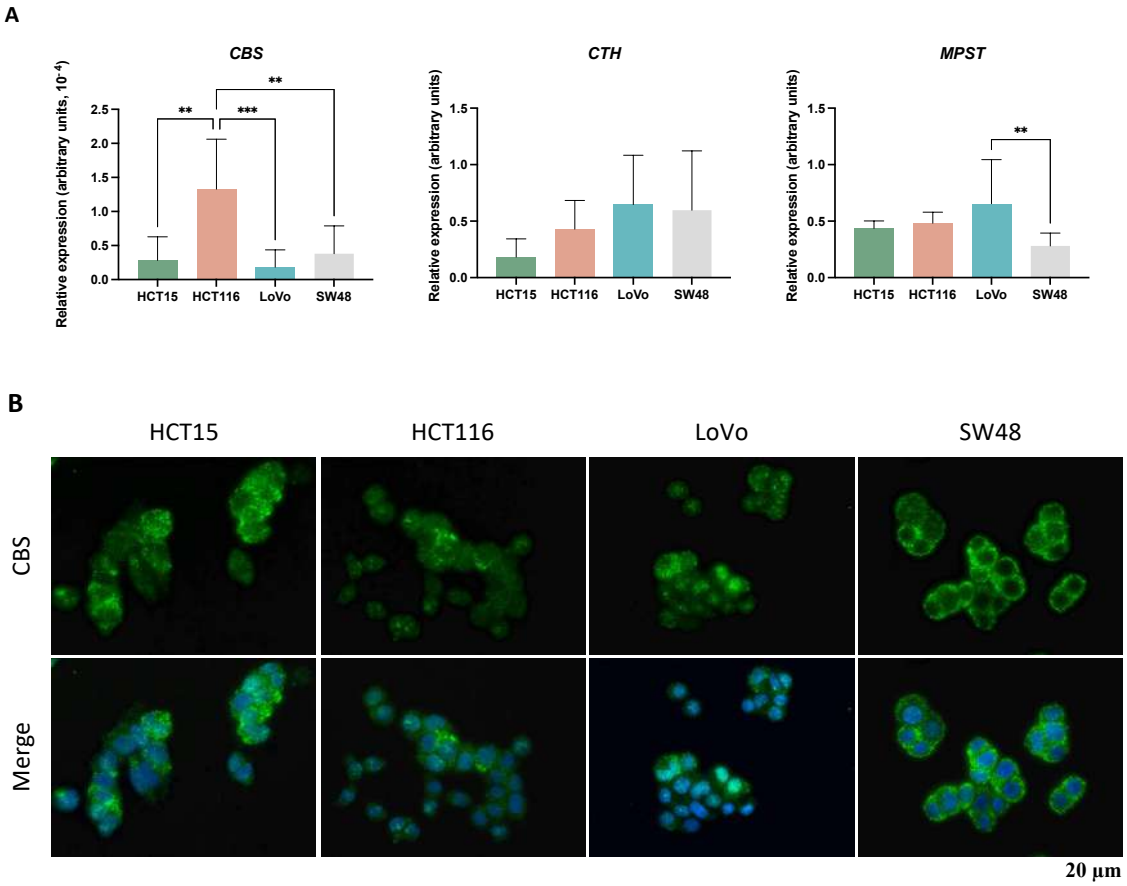

Figure IV.1 – CRC cell lines differentially express H_2S-synthesizing enzymes. **(A)** mRNA expression of H_2S-synthesizing enzymes CBS, CSE and MST show different patterns of expression between the CRC cell lines analyzed, with CBS showing significant different levels of expression between cell lines. **(B)** Immunofluorescence analysis show high expression of CBS protein in all CRC cell lines. Magnification 400 X, scale 20 µm. Statistical significance is represented as mean ± SD. *p<0.5, **p<0.01, ***p<0.001, ****p<0.0001.

CRC cell lines show different response to standard chemotherapy agents

Overexpression of H_2S-synthesizing enzymes, which underlies cysteine metabolic remodeling, has been associated to chemoresistance to conventional agents, mostly to platinum salts due to increased antioxidant potential[256]. Therefore, we tested the response of CRC cancer cells to standard agents used in CRC treatment regimens: carboplatin, cisplatin, 5-FU and oxaliplatin (Figure IV.2). Previously tested doses of these cytotoxic agents (data not shown) 0.025 mg/ml (carboplatin and cisplatin), 0.026 mg/ml (5-FU) and 0.008 mg/ml (oxaliplatin) were used to perform this study. In Figure IV.2, the metabolic viability of each cell line after 24 h exposure to each chemotherapeutic drug was

normalized for the respective control in the absence of drug. All cell lines appeared to be relatively insensitive to carboplatin, SW48 being the only one slightly affected (~15%). Conversely, all cell lines exhibited the highest degree of sensitivity to cisplatin. HCT15 cells were the only resistant to 5-FU, whereas HCT116 appeared particularly sensitive as compared to the other cell lines. HCT116 cells showed resistance to oxaliplatin, whereas LoVo and SW48 were slightly but significantly affected. Overall, the sensitivity profiles varied among the cell lines panel, HCT15 and SW48 globally presenting the opposite sensitivity profiles.

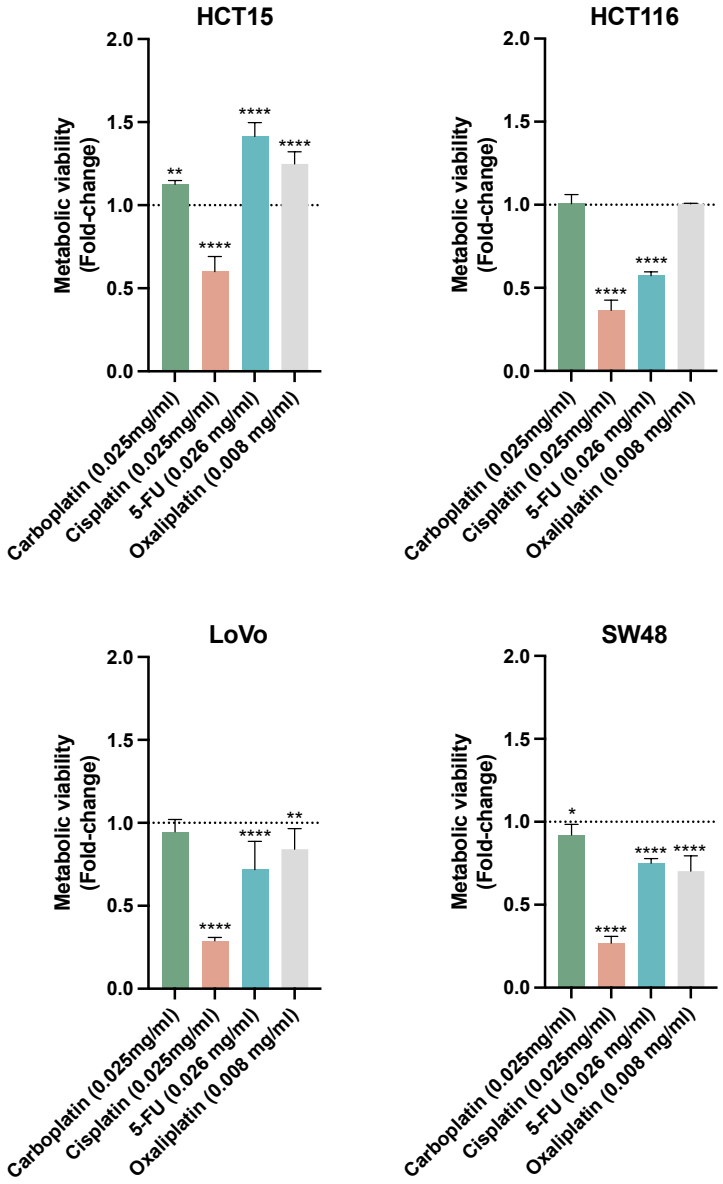

Figure IV.2 – CRC cell lines response to standard chemotherapy agents. Metabolic viability analysis show that HCT15 cell line show resistance to carboplatin, 5-FU and oxaliplatin but not to cisplatin; HCT116 show resistance to carboplatin and oxaliplatin but not to cisplatin and 5-FU; LoVo and SW48 cell lines respond to all agents tested. Statistical significance is represented as mean ± SD. *p<0.5, **p<0.01, ***p<0.001, ****p<0.0001.

SeChry induced decreased metabolic viability in CRC cells

Since *CBS* was differentially expressed in this CRC panel of cell lines (Figure IV.1) and these cells showed resistance to two of the tested platinum salts (Figure IV.2), we assessed exposure to SeChry and SeChry@PURE$_{G4}$-FA as a possible metabolism-targeting therapeutic approach. Encapsulation of SeChry in PURE$_{G4}$-FA was performed to increase specificity to target cancer cells and thus diminish possible toxic effects on non-cancer cells. We started by studying the expression of FR-α in all CRC cell lines and found that this receptor was overall highly expressed in all cell lines, though with apparent lower expression levels in LoVo and SW48 cell lines (Figure IV.3 A).

The effect of 24-h exposure to SeChry (free vs encapsulated) on cell metabolic viability displays cell-specific profiles (Figure IV.3 B). HCT15, HCT116 and LoVo were impaired by free SeChry with similar EC_{50} values (respectively, 12.3 ± 0.7 μM, 12.8 ± 1.4 μM and 7.8 ± 3.7 μM). However, only HCT15 and HCT116 were sensitive towards encapsulated SeChry (SeChry@PURE$_{G4}$-FA), although with higher EC_{50} than the free compound: 24 ± 60 μM and 19.0 ± 8.6 μM, respectively (the range of fitted values for HCT115 is too wide to be considered, hence the dashed green line representing the fit). SW48 cells were insensitive to both free and encapsulated SeChry. None of the cell lines were affected by the empty PURE$_{G4}$-FA nanoparticles.

Based on the effect of SeChry free and encapsulated on metabolic viability, we then analyzed cell proliferation. Cells were exposed to 12.5 μM SeChry or 25 μM SeChry@PURE$_{G4}$-FA, based on the EC_{50} values estimated for their effect on metabolic viability. Control cells were either devoid of any added compound or were exposed to 25 μM PURE$_{G4}$-FA. LoVo and SW48 cells were not exposed to SeChry@PURE$_{G4}$-FA (nor empty PURE$_{G4}$-FA) but only to free SeChry, as they had proven metabolically insensitive to encapsulated SeChry. As observed in Figure IV.3 C, SeChry and SeChry@PURE$_{G4}$-FA significantly decreased HCT15 and HCT116 proliferation, as compared to the respective controls. Notably, the anti-proliferative effect of encapsulated SeChry@PURE$_{G4}$-FA was similar (HCT116) or higher (HCT15) than free SeChry (contrarily to the effect on metabolic viability observed in Figure IV.3 B). In line with the metabolic impairment caused on LoVo cells observed in Figure IV.3 B, free SeChry significantly decreased LoVo proliferation upon 48 h treatment (Figure IV.3 C). Likewise, SeChry-insensitive SW48 cells were also not affected in terms of their proliferative capacity (Figure IV.3 C).

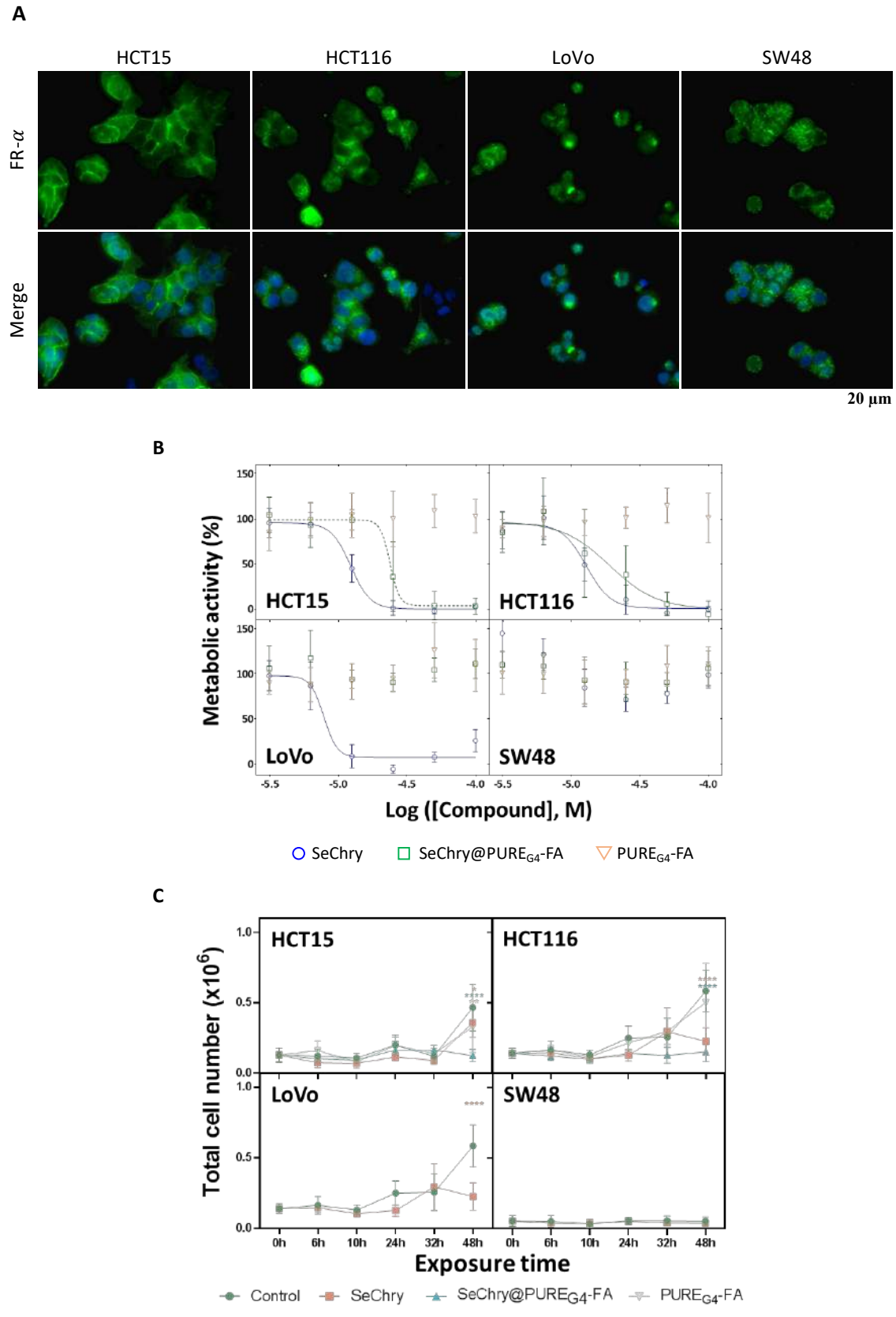

Figure IV.3 – SeChry/SeChry@PURE$_{G4}$-FA is and efficient metabolic therapeutic approach in CRC cell lines. (A) Immunofluorescence analysis show that FR-α is highly expressed in CRC cell lines. Magnification 400 X, scale 20 µm. **(B)** Metabolic activity of CRC cell lines after 24 h in the presence/absence of free SeChry (blue circles) or encapsulated SeChry (SeChry@PURE

G4 -FA, green squares) in the 3-100 μM range. Cells were also exposed to the empty $PURE_{G4}$ -FA (orange triangles) in the same concentration range. Data were analyzed in Graphpad and fitted with a log(inhibitor) vs.response -- Variable slope (four parameters) equation: Y = Bottom + (Top-Bottom) / (1 + 10^((LogEC50-X)*HillSlope)). **(C)** Effect of SeChry (12.5 μM) and SeChry@$PURE_{G4}$ -FA (25 μM) exposure on the proliferation of CRC cell lines, assessed by trypan blue staining. Cell proliferation assessed by trypan blue staining at various exposure time points, up to 48 h. Statistical significance is represented as mean ± SD. *p<0.5, **p<0.01, ***p<0.001, ****p<0.0001.

IV.V. Discussion

CRC remains a leading cause of cancer-related deaths worldwide[6,122], with late-stage diagnosis and therapy resistance being the main factors contributing to its high mortality rate.[134–140] CRC is a heterogeneous disease associated with various tumorigenic molecular pathways, which are not mutually exclusive and define the molecular characteristics of CRC tumors.[125–128] The heterogeneity and the prevalence of chemo-resistant CRC tumors highlight the need for personalized therapies and innovative approaches that can target key features of CRC and enhance the sensitivity of cancer cells to existing treatments. In this context, metabolic adaptations relying on cysteine emerge as a crucial factor supporting cancer cells' bioenergetics and biomass production while acting as a significant source of antioxidants, potentially abrogating the effects of oxidant agents commonly used in cancer therapy regimens.[244,256,318,319] In this context, cysteine metabolism is tightly linked with H_2S metabolism and associated signaling pathways. Indeed, cysteine is a priority substrate for generation of H_2S which regulates multiple cellular and physiological processes, while being generally endowed with antioxidant capacity.

In this study, we show that CRC cell lines with diverse sensitivity profiles to common chemotherapeutic drugs differ in their reliance on CBS as a key player in the metabolic remodeling centered on the cysteine/H_2S axis. The analysis of the expression of the genes encoding H_2S-synthesizing enzymes showed that *CBS* was the most differentially expressed in our CRC panel of cell lines (Figure IV.1), although the basal levels were much lower than those of two other genes encoding H_2S-synthesizing enzymes. This observation underlies a differential reliance on CBS which may correlate with distinct features of this CRC cell panel. In terms of protein levels, all cell lines appeared to abundantly express CBS. This discrepancy between mRNA and protein levels is a common observation, often related with relative stability of mRNA and protein in different cell lines under diverse growth conditions. While altered expression of all H_2S-synthesizing enzymes has been observed in different types of cancer specimens or cells,

in certain cases only inhibition of CBS seems to exert an effect on cancer-related phenotypes. In HCT116 cells, while chemical and shRNA-mediated CBS inhibition abrogated some of the enhanced cancer-associated features, no effect of shRNA-mediated CSE silencing was observed.[283]

In addition to a different reliance on CBS regarding metabolic adaptations, these CRC cell lines showed different response to the standard agents commonly used in CRC therapy: carboplatin, cisplatin, 5-FU and oxaliplatin. All cell lines showed significant sensitivity to cisplatin, as evaluated by the diminished metabolic viability. HCT15 cells, expressing high CBS protein levels (Figure IV.1 B), showed resistance to all the remaining agents (Figure IV. 2). HCT116 cells, which expressed the highest *CBS* mRNA and high CBS protein expression (Figure IV. 1 A and B), showed no response to exposure to carboplatin and oxaliplatin, while being sensitive to 5-FU (Figure IV.2). LoVo cell line, which expressed the lowest levels of CBS expression (Figure IV.1 A and B), showed only resistance to carboplatin, with a significant decrease in metabolic viability upon treatment with cisplatin, 5-FU and oxaliplatin (Figure IV.2). SW48 cells, which showed median levels of CBS mRNA expression but high levels of protein expression (Figure IV.1 A and B), showed sensitivity to all agents (Figure IV.2). Interestingly, although SW48 shows molecular features following similar CRC pathways as HCT15 and HCT116 (CIN^-, MSI, $CIMP^+$), shows WT genotype for all critical genes considered (*KRAS, BRAF, PIK3CA, PTEN* and *TP53*) (Table IV.1), which can explain the chemoresistance exhibited by this cell line to all agents studied. Since CBS was differentially expressed across this panel of cell lines and given the overall poor response to standard agents, we aimed to test a novel metabolic-driven pharmacological approach focused on a previously reported CBS inhibitor. Cells were exposed to free (SeChry) or encapsulated (SeChry@$PURE_{G4}$-FA) selenium-chrysin and their metabolic viability assessed. HCT15, HCT116 and LoVo were similarly sensitive to free SeChry. Interestingly, only HCT15 and HCT116 cells were metabolically impaired by encapsulated SeChry (SeChry@$PURE_{G4}$-FA), although the efficacy slightly decreased as compared to the free compound. This suggests that while nanoformulation of SeChry affords the desired specificity and delivery into cancer cells expressing high folate receptor levels, it may partially compromise its bioavailability. Still, the effect of metabolically impairing specific cell lines significantly expressing CBS was achieved. Conversely, the absent effect of encapsulated SeChry (SeChry@$PURE_{G4}$-FA) on LoVo cells indicates that the observed impairment with the free compound probably relates to

some off-target. SW48 cells were totally insensitive to free or encapsulated SeChry which again underlies the specificity of the drug targeting cell lines with diverse molecular and phenotypical signatures (Figure IV.3).

In line with the observed effects on metabolic viability, the anti-proliferative effect of free versus encapsulated SeChry was evaluated and overall corroborated the observed effects on metabolic viability. Neatly, in HCT15 and HCT116 cells, encapsulated SeChry (SeChry@PURE$_{G4}$-FA) exhibited higher anti-proliferative capacity than the free compound, both tested at concentrations derived from the EC_{50} for metabolic impairment. In LoVo cells free SeChry exhibited anti-proliferative activity, while SW48 cells were insensitive (resistant) (Figure IV.3).

Overall, these results validate the approach based on pharmacologically targeting phenotypically diverse CRC cell lines (with respect to their chemoresistance profiles and reliance on cysteine/H_2S metabolism enzymes) using a specific inhibitor of a key enzyme of this metabolic pathway. Moreover, encapsulation of this inhibitor affords a level of specificity and effectiveness that is of paramount importance to accomplish the desired anticancer effects.

Considering metabolic profiling in CRC clinical management represents a progressive stride towards CRC personalized therapy and should pave the path to the discovery of novel therapies that allow targeting metabolic remodeling and disrupt energetic and biomass sources that enable cancer cells to survive and thrive.

IV.VI. Conclusion

In conclusion, this chapter highlights the significance of cysteine metabolic remodeling as a central feature in CRC resistance and demonstrates the potential of metabolic approaches, such as SeChry(@PURE$_{G4}$-FA), to overcome chemoresistance in CRC therapy. The differential response of various CRC cell lines to standard agents and the identification of CBS as a potential target for treatment emphasize the need for personalized therapies. The findings underscore the importance of incorporating metabolic profiling in CRC clinical management to pave the way for the development of novel therapies that can disrupt metabolic remodeling. Overall, these insights open promising avenues for advancing CRC personalized therapy and enhancing treatment outcomes.

Chapter V

SeChry@PURE$_{G4}$-FA Elicits Distinct Cell Death Mechanisms by Disrupting Cysteine Metabolism in Breast Cancer Cells

This chapter is based on the following publication:

Ana Hipólito, Cindy Mendes, Isabel Lemos, *et al*. Cystathionine β-synthase (CBS) and xCT (*SLC7A11*) targeting by selenium-chrysin (SeChry) triggers different types of cell death in breast cancer. Manuscript in preparation.

V.I. Abstract

Breast cancer (BC) represents a heterogeneous and intricate disease encompassing diverse molecular and histological subtypes, each exhibiting distinct clinical behaviors and responses to therapy.

This study provides insights into the complex interplay between cysteine metabolism, BC progression, and potential therapeutic interventions. The overexpression of cystathionine-β-synthase (CBS) and the cystine/glutamate antiporter (xCT) in BC samples, particularly within aggressive subtypes, underscores their potential as therapeutic targets. Moreover, SeChry@PURE$_{G4}$-FA effect on BC cell lines further emphasizes its promise as an innovative therapeutic strategy.

Keywords: Breast cancer, Cystathionine-β-synthase, Cystine/glutamate antiporter, SeChry, Cancer therapy, Ferroptosis

V.II. Introduction

Breast cancer (BC) is a common cancer among women from all ages around the world, though it can also affect men.[141] BC is a heterogenous disease, with multiple molecular entities that define distinct phenotypes and clinical responses. Identification of primary tumor histological and molecular characteristics such as the expression of estrogen and progesterone receptor (ER and PR) and HER2 are key features with predictive value of response to therapy and prognosis.[142–145] Although it seems like a relatively poor characterization, this expression pattern remains one of the main indicatives for clinical management, with triple-negative tumors (TNBC) indicating a poorer prognosis.[141,157–160] Besides these markers, Ki-67, a proliferation marker which reflect tumor growth capacity, as well as expression and mutation profiling of other genes of interest are tools with clinical significance in stratifying invasive BC patients across the considered molecular subtypes. The molecular classification of BC tumors relies mainly on the expression of hormone receptors ER/PR and/or HER2 expression (when amplified), being TNBC classification attributed to BC tumors lacking ER, PR and HER2 expression [141,146,160–162].

Metastases remain the leading cause of death in BC patients, mostly affecting lung, liver, brain and bone tissue, though with different preference patterns according to the molecular subtype. [163,164]

BC therapy regimens are based on the molecular classification of the tumor as well as on the disease stage, and they are overall integrated protocols that can comprise (neo)adjuvant chemotherapy with cytotoxic agents as doxorubicin, paclitaxel and cyclophosphamide, platinum-based salts (eg. carboplatin, cisplatin), monoclonal antibodies (*e.g*. tocilizumab and trastuzumab), tyrosine kinase inhibitors (TKIs; *e.g*. tivozanib and lapatinib), histone deacetylase inhibitors (HDACis; *e.g*. vorinostat), radiotherapy, surgery and endocrine therapy (estrogen receptor inhibitors; *e.g.* tamoxifen).[163,165]

H_2S-synthesisizing enzymes are described to participate in BC promotion.[293,294] CBS is overexpressed in BC tissue comparing to adjacent normal tissue and, interestingly, expression score correlates with BC progression.[239,295] CBS expression in BC seems to associate with more aggressive phenotypes, suggesting a prognostic value.[239,293,295], cystine/glutamate antiporter xCT/*SLC7A11* is reported to be highly expressed in BC cells and to participate in BC pathogenesis.[443,444] As an antioxidant antiporter, xCT plays a fundamental role in cellular detoxification against ROS-induced damage, including ferroptosis.[445], Although first described as an iron-dependent cell death mechanism, ferroptosis is nowadays known to contribute for the regulation of both physiological and pathophysiological processes, including carcinogenesis.[322,323,446] Ferroptosis is stimulated by the accumulation of lipid peroxides generated by increased oxidative stress, which promotes the reduction of intracellular levels of glutathione (GSH) and glutathione peroxidase 4 (GPX4) activity. This, alongside with increasing ROS levels, impairs lipid peroxide reduction by GPX4 and promotes lipid oxidation by Fe^{2+}, in a Fenton-like manner, stimulating ferroptosis.[321,322,446]

This chapter is focused on the study of the feasibility of a metabolic approach targeting cysteine metabolism with SeChry@$PURE_{G4}$-FA as a way of sensitizing and/or inducing BC cells' death.

V.III. Materials and Methods

Cell lines and culture conditions

Human TNBC cell lines MDA-MB-231 (HTB-26™, ATCC) and HCC1806 (CRL-2335™, ATCC); ER^+ /PR^+ cell line MCF7 (HTB-22TM, ATCC), and PR^+/$HER2^+$ cell line BT-474 (HTB-20TM, ATCC), were obtained from American Type Culture Collection (ATCC, Manassas, VA, USA). Cells were maintained at 37°C in a humidified environment of 5% CO_2 in Dulbecco's modified eagle medium 1× (DMEM) (41965-039, Gibco, Life Technologies). Medium was supplemented with 10% fetal bovine serum (FBS; S 0615, Merck), 1% Antibiotic-Antimycotic (AA; P06-07300, PAN Biotech) and 50 µg/mL gentamicin (15750-060, Gibco, Life Technologies). Cells were cultured until an optical confluence of 75–100% before they were detached with 0.05% trypsin-EDTA 1X (25300-054, Invitrogen).

Measurement of H_2S in cell homogenates

Cells (5×10^5 cells/well) were seeded in 6-well plates, cultured in control condition and exposed to experimental conditions: 0.402 mM L-cysteine; 50 µM bromopyruvic acid (BPA; 16490, Sigma-Aldrich), and 30 µM sodium hydrosulfide (NaHS;161527, Sigma-Aldrich) for 24 h. Cells were scraped in PBS 1× and homogenized in NP40 lysis buffer (1% NP40, 150 mM NaCl, 50 mM Tris-Cl, pH 8.0) on ice for 30 min and centrifuged at 20000 g for 5 min at 4°C. Cell homogenates (20 µL) were incubated in black 96-well plates with 80 µL of 10 µM 7-azido-4-methylcoumarin (AzMC, L511455, Sigma-Aldrich) with and without 1 mM aminooxyacetic acid (AOAA, C13408, Sigma-Aldrich) and/or 3 mM DL-propargylglycine (PAG, P7888, Sigma-Aldrich), inhibitors of CBS and CSE enzymes. AOAA is an inhibitor of both CBS and CSE, whereas PAG is selective towards CSE.

Protein concentration was determined with the Bradford method (500-0006, Bio-Rad) against a BSA calibration curve. The H_2S measurements were subsequently normalized to total protein concentration and to a blank sample (cellular lysates with and without AOAA, PAG or both without a probe).

H_2S levels were monitored following the AzMC probe emission wavelength (λ_{exc}: 355 nm; λ_{em}: 460 nm) in a VICTOR3 instrument from PerkinElmer and using the *Wallac 1420 v3.0* software (Umbelliferone, 0.1 s protocol).

Quantitative real-time PCR (qPCR)

Total RNA was extracted using the RNeasy Mini Extraction kit (74104, Qiagen, Hilden, Germany) and cDNA synthesized from 1 μg RNA by SuperScript II Reverse Transcriptase (18080044, Thermo Fisher Scientific), according to the manufacturers' protocols and cDNA was synthesized as mentioned above. qPCR was performed using SYBR Green PCR Master Mix (04707516001, Roche), according to the manufacturer's protocol and the specific primers and genes are presented in Table V.1.

Real-time PCR was carried out during 40 amplification cycles, according to the manufacturer's instructions, using a Lightcycler® 480 System instrument (05015243001, Roche). *HPRT* was used as a housekeeping gene (Table V.1). Experiments were performed in biological triplicates.

Table V.1 - Primers used in gene expression analysis. Detailed characterization of the primers used in RT-qPCR assays.

Gene	Primer	Sequence (5'→3')	Length (nt)	AT (°C)	GC %	Fragment (bp)
CBS	Forward	*GAGCTCTTGGCCAAGTGTG*	19	60	58	232
	Reverse	*GCACGTCCACCTTCTCGG*	18		67	
SLC7A11	Forward	*GGTCCTGTCACTATTTGGAGC*	21	61	58	136
	Reverse	*GAGGAGTTCCACCCAGACTC*	20		59	
GSS	Forward	*GAGAGAGGGTGGAGGTAAC*	19	60	58	98
	Reverse	*CCATGAGGATGTAGGAGGCC*	20		60	
GPX4	Forward	*GCAGGAGCCAGGGAGTAAC*	19	60	63	137
	Reverse	*CCTTGGGTTGGATCTTCATCC*	21		52	
PTGS2	Forward	*CTGGCAGGGTTGCTGGTG*	18	59	67	83
	Reverse	*CATCTGCCTGCTCTGGTC*	18		61	
HPRT1	Forward	*TGACACTGGCAAAACAATGCA*	21	58	43	94
	Reverse	*GGTCCTTTTCACCAGCAAGCT*	21		52	

Immunofluorescence and Nile Red Staining

Cells (1×10^5 cells/well) were seeded in glass cover slips in 24-well plates coated with 0.2% gelatin from porcine skin (G-1890, Sigma-Aldrich) and then fixated with 2% paraformaldehyde for 15 min at 4 °C. After fixation, cells were incubated with 50 mM ammonium chloride (NH_4Cl) for 10 min. Blocking and antibodies dilution were performed with PBS 1× - 0.5% BSA - 0.1% saponin-PBS (w/v/v). Between incubations, cells were rinsed twice with PBS 1×, for 5 min. After blocking for 1 h, cover slips were incubated with primary antibodies (anti-CBS, WH0000875M1, Sigma-Aldrich; anti-xCT, ab175186, Abcam), overnight at 4 °C. Cells were incubated with secondary antibody for 2 h at room temperature (1:1000; Alexa Fluor® 488 goat anti-rabbit, A-11034, Thermo Fisher Scientific; 1:1000; Alexa Fluor® 488 goat anti-mouse, A-11001, Thermo Fisher Scientific). Nile Red staining was performed as previously reported.[447] Cells were incubated with Nile Red (1 μg/mL) for 5 min at room temperature. The slides were mounted in VECTASHIELD media with DAPI (4'-6-diamidino-2-phenylindole) (H-1200-10, Vector Labs) and examined by standard fluorescence microscopy under a Zeiss Imager.Z1 AX10 microscope. Images were acquired and processed with *CytoVision* software and quantified with *ImageJ* software.

Cell death analysis by flow cytometry

BC cells were seeded in 24-well plates (1×10^5 cells/well). After exposure to experimental conditions, cells were collected and labeling with FITC-labeled Annexin V (640906, BioLegend) and propidium iodide (PI; P4170, Sigma Aldrich Aldrich) was performed as described.[364] Results were analyzed by flow cytometry (BD FACSCanto II). FlowJo X v10.0.7 software (https://www.flowjo.com/) was used to analyze data.

Reactive oxygen species (ROS) quantification by flow cytometry

BC cells were seeded in 24-well plates (1×10^5 cells/well). The intracellular ROS levels were detected in cells previously incubated with 10 μM DCF-DA probe (D6883, Sigma Aldrich), at 37 °C for 30 min. Results were acquired through flow cytometry (BD FACSCanto II). FlowJo X v10.0.7 software (https://www.flowjo.com/) was used to analyze data.

Lipid peroxides quantification by flow cytometry

BC cells were seeded in 24-well plates (1 × 10^5 cells/well). After experimental conditions, cells were incubated with 2 µM C11-Bodipy 581/591 (D3861, Invitrogen), for 30 min at 37 °C in dark. Excessive dye was removed by washing with 2% FBS-1× PBS and cell pellets were resuspended in 2% FBS-1× PBS for the acquisition by flow cytometry (BD FACSCanto II). FlowJo X v10.0.7 software (https://www.flowjo.com/) was used to analyze data.

Immunohistochemistry assay

BC specimens (N= 52) were retrieved from the archive of the Pathology Department of IPOLFG with the approval of the Ethics Committee (Ref: UIC/1188). Immunohistochemical staining for xCT and CBS was performed on 4-µm-thick, formalin-fixed, paraffin-embedded tissue, after deparaffinization and rehydration according to the manufacturer's instructions. Slides were stained using anti–xCT (ab175186, Abcam) and anti-CBS (WH0000875M1, Sigma-Aldrich) with appropriate positive and negative controls samples, on the BenchMark ULTRA IHC/ISH Automatic staining platform (Ventana Medical Systems, Tucson, Arizona, USA) using OptiView DAB IHC Detection Kit with diaminobenzidine as the chromogen to detect antigen expression. Tissue sections were counterstained with Mayer's hematoxylin before mounting. Image acquisition was performed in Digital Microimaging Device Leica DMD108 (version 1.15 Build 704, Leica Microsystems).

Bioinformatics analysis

Breast invasive carcinoma (BRCA) RNA-Seq data from the The Cancer Genome Atlas (TCGA)[416] were analyzed using the cBio Cancer Genomics Portal (http://cbioportal.org)[417,418] to explore the genomic data set which included *CBS*, *CTH*, *MPST*, *SLC1A1*, and *SLC7A11*.

Statistical analysis

Statistical analysis was performed using GraphPad Prism 8.0 software (www.graphpad.com). Sample data were presented as mean (normal distribution) ± SD. Assays were performed with at least three biological replicates *per* treatment (with at least 3 independent n). Comparisons between data from each group were statistically analyzed by a two-tailed unpaired Student's t-test and multiple comparisons were performed using one-way or two-way ANOVA. To assess differences in gene expression levels in samples from BC tumors (BRCA cohort from TCGA and IPOLFG cohort), 2-sided independent samples Kruskal-Wallis One-way ANOVA with multiple comparisons or Mann-Whitney test was performed, where the adjusted significance was considered.

Differences between experimental conditions were considered statistically significant at $p < 0.05$.

V.IV. Results

Overexpression of CBS and *SLC7A11*/xCT in tumor samples and BC cell lines reinforces cysteine metabolism involvement in BC pathogenesis

We explored TCGA-BRCA transcriptomic data, considering primary tumor and metastasis comparing to normal breast tissue to evaluate the expression dynamics of genes involved in cysteine metabolism. Regarding the genes encoding enzymes, the analysis indicated that the expression of *CBS* is significantly increased in primary tumors comparing to normal tissue, while *CTH* presented significantly lower levels comparing tumor samples with normal tissue and *MPST* showed no significant differences (Figure V.1 A). Genes encoding the transporters xCT (*SLC7A11*) and EAAT3 (*SLC1A1*) were found differentially expressed in the BRCA cohort from TCGA. While *SLC7A11* showed significantly higher expression levels in both primary and metastatic tumors, *SLC1A1* did not show significant differences, comparing to normal tissue (Figure V.1 A).

Expression of CBS and xCT was then studied using immunohistochemistry in BC specimens obtained from Pathology Department of IPOLFG. In total, 52 cases were considered for this analysis, including 18 TNBC cases, 14 HER2-enriched cases and 20 luminal cases. However, due to sample availability, only a total of 29 samples were

considered for the simultaneous analysis of both proteins, which included 7 TBNC cases, 5 HER2-enriched cases and 17 luminal cases (Figure V.1 B). Although statistical analyses show no differences between the histological classes of BC regarding CBS expression, xCT expression is significantly increased in TNBC and HER2-enriched cases compared to luminal cases (Figure V.1 C). Moreover, it was possible to obtain normal tissue regarding some samples analyzed for xCT. Data show that *in situ* and invasive components in tumors significantly overexpress xCT comparing to normal tissue. Additionally, invasive components in tumors express significantly higher levels of xCT, comparing to *in situ* component in tumors (Figure V.1 D). Considering all samples analyzed for both CBS and xCT, data indicate there are no differences in CBS expression between *in situ* and invasive components in tumors. However, invasive areas present higher expression of xCT comparing to *in situ* areas (Figure V.1 E). Moreover, from the invasive tumor cases analyzed for both CBS and xCT, around 86% (n=25) of cases positively expressing CBS were found to positively express xCT, while around only 14% (n=4) of cases not expressing CBS were found to express xCT. In our analysis, we report no case expressing CBS but not xCT or without expression of both proteins. Additionally, in the TNBC group all cases were CBS^+ xCT^+; in the HER2-enriched samples most cases were CBS^+ xCT^+ and only 1 case was CBS^+ xCT^+; and in the luminal group most cases were CBS^+ xCT^+ (Figure V.1 F).

Next, we selected a panel of BC cell lines representative of distinct histological and molecular profiles (TNBC: MDA-MB-231 and HCC-1806; Luminal A: MCF7; Luminal B: BT-474) in order to further study the importance of cysteine metabolic remodeling across the different BC phenotypes. Expression of CBS and xCT mRNA and protein analysis indicated that both cysteine metabolic players are differentially expressed in our panel of cell lines. mRNA and protein analysis showed that MDA-MB-231 express low levels of CBS comparing to the remaining cell lines but significantly higher SLC7A11/xCT levels; HCC-1806 highly express both CBS and *SLC7A11*/xCT; MCF7 highly express CBS but present low expression levels of *SLC7A11*/xCT and BT-474 cell lines express the lowest levels of both CBS and *SLC7A11*/xCT (Figure V.1 G and H). Collectively, these findings suggest a significant involvement of cysteine metabolic intervenients CBS and xCT in BC, highlighting their potential as putative targets for therapeutic interventions and/or as stratification tools.

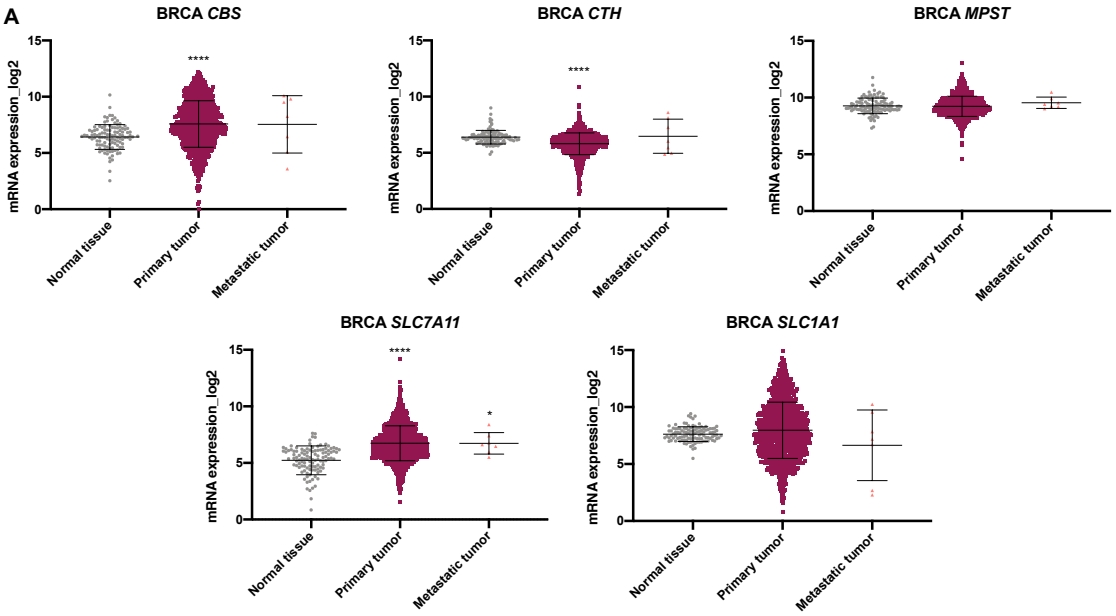
A
BRCA CBS
BRCA CTH
BRCA MPST
BRCA SLC7A11
BRCA SLC1A1
mRNA expression_log2
Normal tissue
Primary tumor
Metastatic tumor

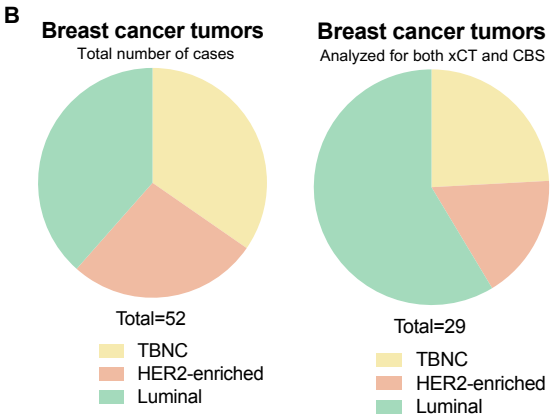
B
Breast cancer tumors
Total number of cases
Total=52
TBNC
HER2-enriched
Luminal
Breast cancer tumors
Analyzed for both xCT and CBS
Total=29
TBNC
HER2-enriched
Luminal

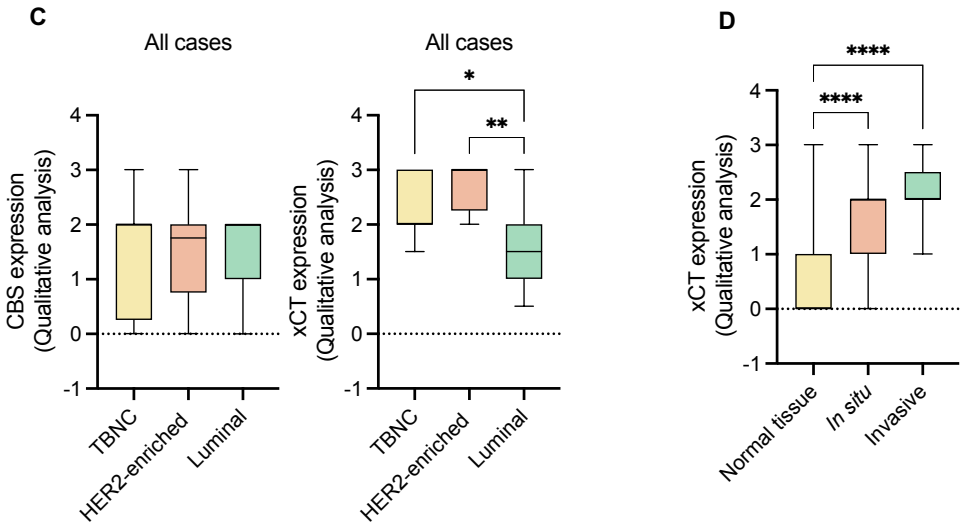
C
All cases
CBS expression (Qualitative analysis)
All cases
xCT expression (Qualitative analysis)
TBNC
HER2-enriched
Luminal
D
xCT expression (Qualitative analysis)
Normal tissue
In situ
Invasive

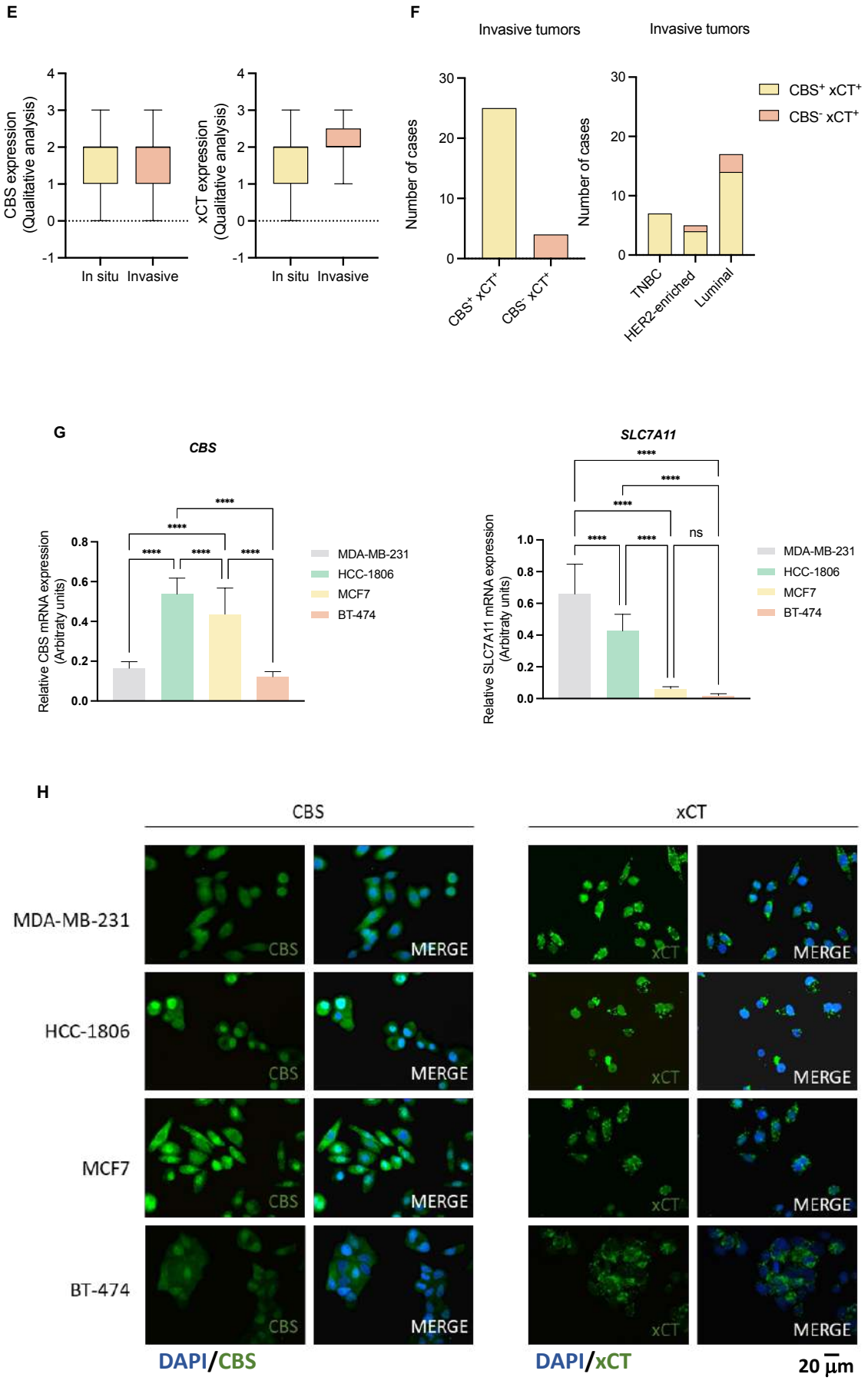
E
CBS expression (Qualitative analysis)
xCT expression (Qualitative analysis)
In situ
Invasive
F
Invasive tumors
Invasive tumors
Number of cases
CBS+ xCT+
CBS- xCT+
TNBC
HER2-enriched
Luminal
G
CBS
SLC7A11
Relative CBS mRNA expression (Arbitraty units)
Relative SLC7A11 mRNA expression (Arbitraty units)
MDA-MB-231
HCC-1806
MCF7
BT-474
ns
H
CBS
xCT
MERGE
DAPI/CBS
DAPI/xCT
20 µm

Figure V.1 – CBS and *SLC7A11*/xCT are overexpressed in BC tumors and cell lines (A) Bioinformatic analysis from BRCA cohort (TCGA) show overexpression of CBS and SLC7A11 in tumor tissue comparing to normal tissue. **(B)** Distribution of BC specimens obtained from Pathology Department of IPOLFG and studied by immunohistochemistry across the histological classifications. **(C)** Immunohistochemistry results regarding CBS and xCT and comparison between the different histological subtypes show differential expression of xCT between TNBC, HER2-enriched and luminal BC samples. **(D)** Immunohistochemistry analysis shows xCT overexpression correlated with invasive potential in BC, with overexpression in tumoral tissue comparing to normal tissue. **(E)** immunohistochemistry analysis shows a tendency for xCT overexpression in invasive comparing to *in situ* tumors. **(F)** Analysis of the distribution of BC specimens across the classes $CBS^{+/-}xCT^{+}$ and distribution of these classification across the histological subtypes shows that most invasive tumors studied presents CBS and xCT expression. **(G, H)** mRNA expression analysis **(G)** and immunofluorescence analysis **(H)** in BC cell lines shows differential expression of CBS and *SLC7A11*/xCT, with overexpression of CBS in HCC-1806 and MCF7 and overexpression of *SLC7A11*/xCT in MDA-MB-231 and HCC-1806, comparing to the remaining cell lines. Statistical significance is represented as mean ± SD. Magnification 400 X, scale 20 µm. *p<0.5, **p<0.01, ***p<0.001, ****p<0.0001.

BC cell lines present high cysteine metabolic activity

We then explored cysteine metabolic activity in the BC panel of cell lines studied in control conditions and in the presence of the H_2S synthesis inhibitors AOAA and/or PAG, in order to disclose the participation of the different H_2S-synthesizing enzymes for the measured H_2S values. Although there are no statistically significant differences among the studied cell lines, overall, HCC-1806 cells tend to present lower H_2S levels comparing to the remaining cell lines, followed by MDA-MB-231 cells (Figure V.2). Both MCF7 and BT-474 cell present similar levels of H_2S in control conditions or when exposed to CBS/CSE inhibitors. Interestingly, the exposure of these cells to AOAA and/or PAG did not induce significant differences when comparing to control (Figure V.2).

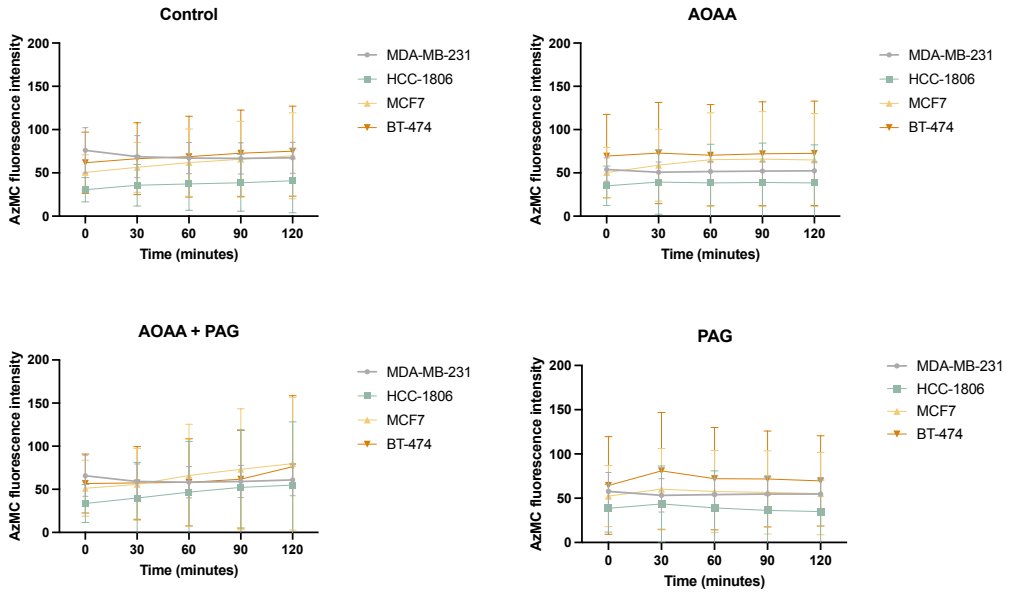

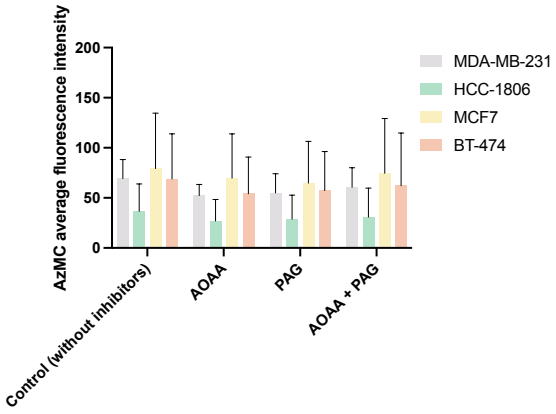

Figure V.2 – BC cell lines present high cysteine metabolic activity. No statistically differences were found across our BC panel of cell lines regarding H_2S production, however, HCC-1806 cells present lower H_2S levels comparing to the remaining cell lines. Statistical significance is represented as mean ± SD. *p<0.5, **p<0.01, ***p<0.001, ****p<0.0001.

SeChry@PURE$_{G4}$-FA induces cell death in BC cell lines and stimulates ferroptosis in BT-474

Given the clear and cell-dependent importance of CBS and xCT in BC, we then studied the effect of SeChry@PURE$_{G4}$-FA in our panel of BC cell lines. BC cell lines were exposed for 24 h to 30 μM (MCF7 and BT-474) or 160 μM of SeChry@PURE$_{G4}$-FA (MDA-MB-231 and HCC-1806). Both MDA-MB-231 and HCC-1806 were shown in previous assays to be resistant to lower concentrations of SeChry@PURE$_{G4}$-FA; data not shown). MDA-MB-231, MCF7 and BT-474 show significantly increased cell death levels comparing to control, while HCC-1806 did not show a statistically significant increase but rather a tendency for increased cell death upon exposure to SeChry@PURE$_{G4}$-FA (Figure V.3 A). In MDA-MB-231, cell death occurs mainly through apoptosis, while in HCC-1806, necrosis or necroptosis contribute for cell death. In MCF7, late apoptosis and necroptosis are the prevalent cell death processes. Next, and since SeChry is described as a CBS inhibitor, which, in theory, leads to imbalanced intracellular antioxidant potential, we studied the effect of exposure to SeChry@PURE$_{G4}$-FA regarding intracellular ROS and lipid peroxides levels. Treatment with SeChry@PURE$_{G4}$-FA significantly increased the intracellular ROS in MDA-MB-231 and HCC-1806 but not in MCF7 and BT-474 (Figure V.3 B). Interestingly, lipid peroxides levels were only found significantly increased upon exposure to SeChry@PURE$_{G4}$-FA in BT-474 cells (Figure V.3 C), indicating that this treatment induces a different kind of response in this cell line - ferroptosis. Taking this into account, we next evaluated the expression of genes involved in ferroptosis upon SeChry@PURE$_{G4}$-FA treatment. SeChry@PURE$_{G4}$-FA induced

significant overexpression of *GSS* in MDA-MB-23 and HCC-1806 but not in the remaining cell lines; *GPX4* expression was only found significantly increased in HCC-1806 and, interestingly, *PTGS2* was found highly overexpressed only in BT-474 cells (Figure V.3 D). Finally, staining with Nile Red, a marker for lipid droplets, indicates all BC cell lines studied except BT-474 produce high levels of lipid droplets (Figure V.3 E).

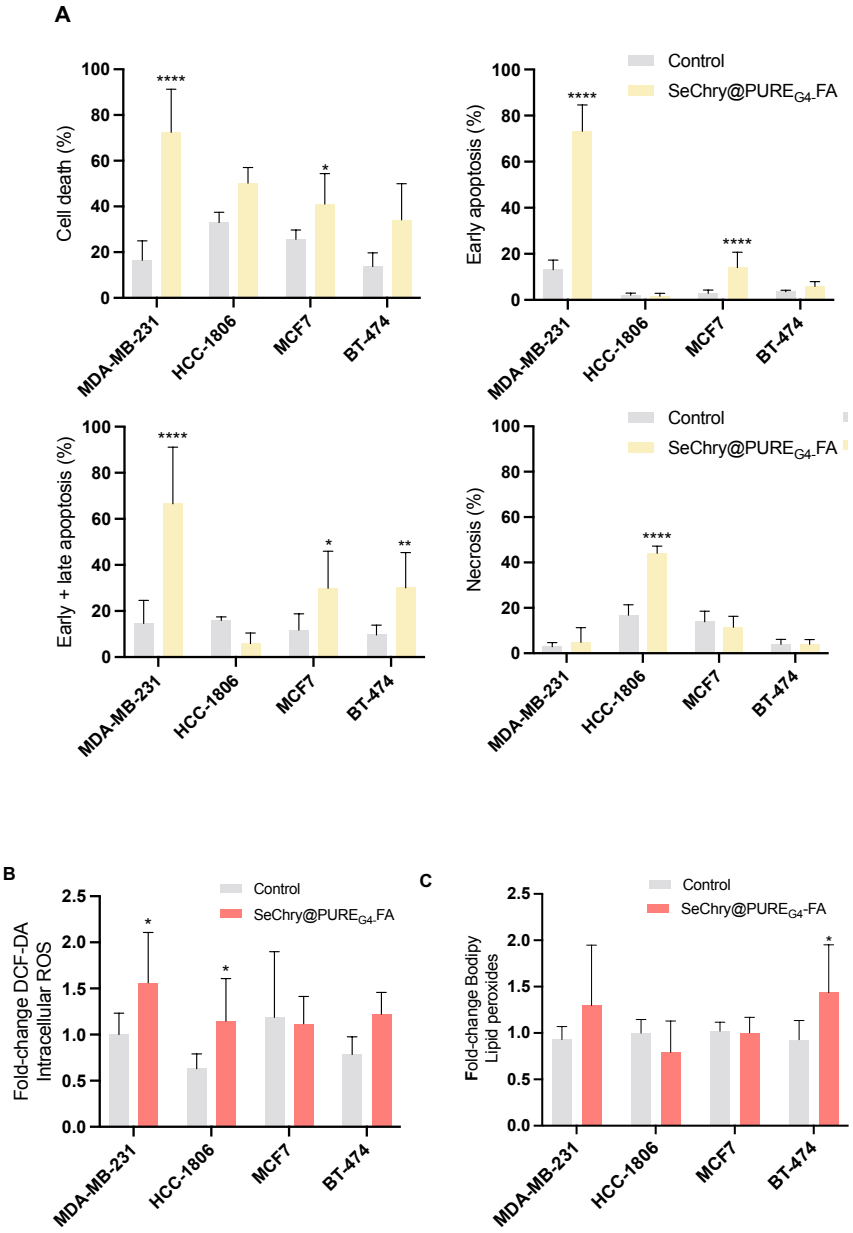

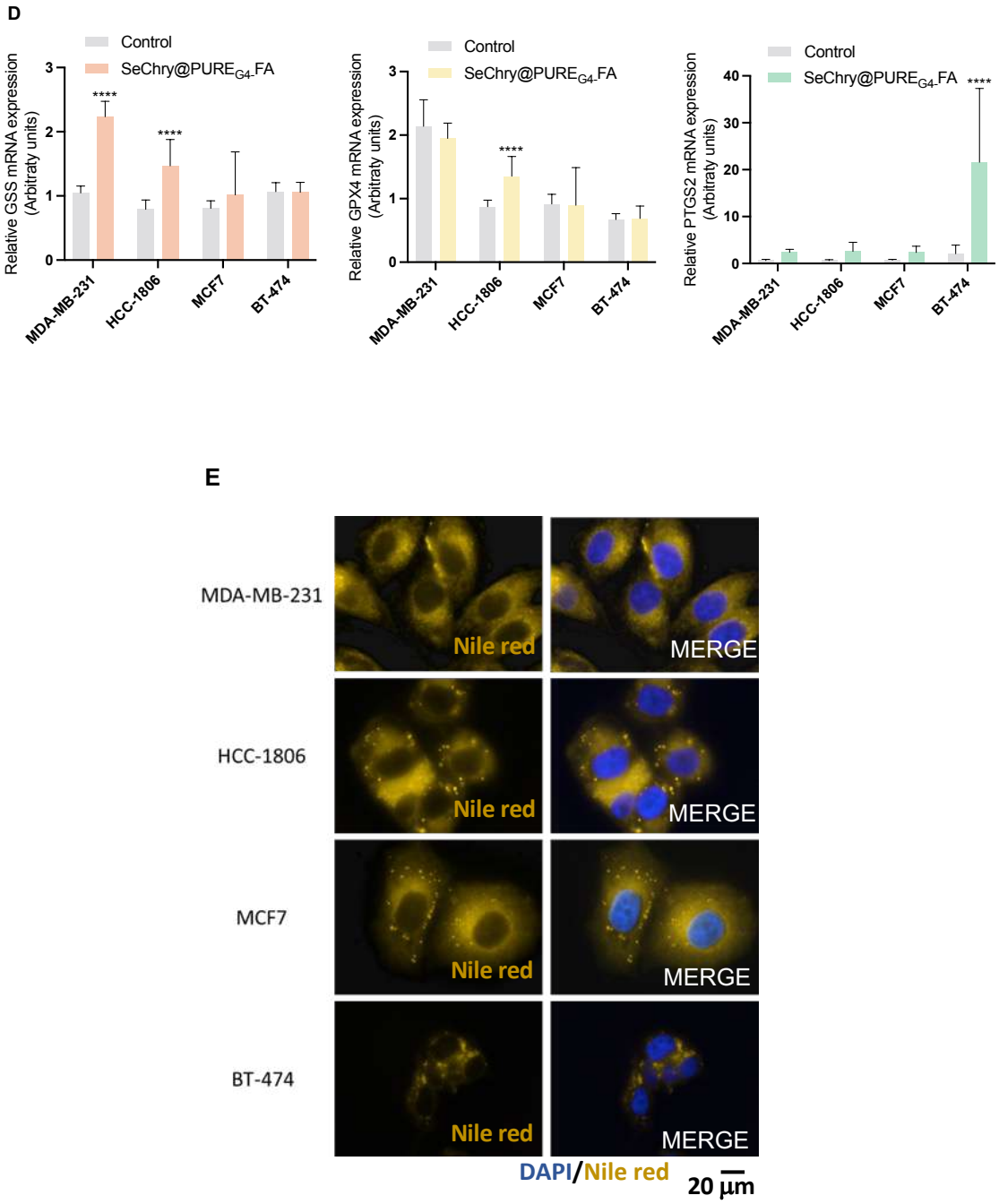

Figure V.3 – SeChry@PURE$_{G4}$-FA induces cell death in BC cell lines and stimulates ferroptosis in BT-474 cell line. (A) Cell death analysis of BC cells exposed for 24h to SeChry@PURE$_{G4}$-FA indicate this treatment induces significant increased early and/or late apoptosis or necrosis in BC cell lines. **(B)** Intracellular ROS analysis using DCF-DA marker indicates increased generation of intracellular ROS in MDA-MB-231 and HCC-1806 cell lines upon exposure to SeChry@PURE$_{G4}$-FA comparing to control. **(C)** Lipid peroxide analysis indicates increased generation of lipid peroxide levels in BT-474 upon exposure to SeChry@PURE$_{G4}$-FA comparing to control. **(D)** mRNA analysis of ferroptosis markers indicates significant increased GSS levels in MDA-MB-231 and HCC-1806 cell lines, increased GPX4 in HCC-1806 and highly increased PTGS2 in BT-474 cell line, when exposed to SeChry@PURE$_{G4}$-FA comparing to control. **(E)** Nile red staining in breast cancer cells shows BT-474 presents the lowest levels of lipid droplets. Magnification 400 X, scale 20 µm. Statistical significance is represented as mean ± SD. *p<0.5, **p<0.01, ***p<0.001, ****p<0.0001.

V.V. Discussion

BC is a complex and heterogeneous disease with various molecular and histological subtypes that have distinct clinical behaviors and therapeutic responses. Even though BC is a widely studied type of cancer, the heterogeneous nature of BC remains a major clinical issue to surpass, since it is deeply related to the development of resistance to currently available therapies. This study delved into the role of cysteine metabolism, specifically focusing on CBS and xCT, in BC pathogenesis, as well as the potential therapeutic impact of SeChry@PURE$_{G4}$-FA on BC cells.

The expression patterns of CBS and xCT in BC samples were investigated to elucidate their involvement in BC progression and to potentially identify new therapeutic targets. The results from both TCGA transcriptomic data analysis and immunohistochemistry on BC specimens from the Pathology Department of IPOLFG underscored the significant overexpression of CBS and xCT in BC tissues (Figure V.1). This overexpression, especially of xCT, was particularly pronounced in TNBC and HER2-enriched subtypes, implying potential therapeutic targets for these aggressive BC phenotypes (Figure V.1). These findings not only support the notion that cysteine metabolic pathways play a crucial role in BC pathogenesis but also suggest their potential utility as biomarkers for molecular subtype classification. Additionally, our study further shows a crucial role of cysteine metabolic remodeling in BC progression, since overexpression of xCT correlates with the invasive phenotypes and is present in metastatic (Figure V.1 A) and invasive components in tumors (Figure V.1 D), comparing to its expression in normal tissue, primary tumors and *in situ* components in tumors. Interestingly, from all cases analyzed retrieved from the Pathology Department of IPOLFG, xCT was expressed in invasive areas in tumors, which further highlights the central role of xCT and cysteine metabolic remodeling in BC progression (Figure V.1 F). Moreover, the differential expression of CBS and xCT in BC cell lines, representing the heterologous profile of BC, points cysteine metabolic remodeling as a potential tool to differentiate BC tumors. While CBS presents highest expression in HCC-1806 and MCF7, *SLC7A11*/xCT high expression is presented by MDA-MB-231 and HCC-1806, comparing to the remaining cell lines (Figure V.1 G and H).

In this study, we further evaluated the response of different BC cell lines representative of different histological BC classes to SeChry@PURE$_{G4}$-FA treatment, aiming to

understand the putative feasibility of a metabolic approach targeting cysteine metabolism as BC therapy. The observed cell death induction in multiple BC cell lines suggests that SeChry@PURE$_{G4}$-FA holds promise as a therapeutic intervention for BC. The variations in response across cell lines further emphasize the heterogeneity of BC and the importance of personalized treatment approaches. Notably, the induction of increased intracellular ROS and lipid peroxides in response to SeChry@PURE$_{G4}$-FA treatment, particularly in MDA-MB-231, HCC-1806 and BT-474 cells, indicates an induction of oxidative stress by SeChry@PURE$_{G4}$-FA in these cells, which is likely contributing to the observed increased cell death (Figure V.3 A, B, C). Moreover, significant increased lipid peroxides in BT-474 cell line upon treatment with SeChry@PURE$_{G4}$-FA indicates the involvement of ferroptosis, a cell death mechanism associated with lipid peroxidation and oxidative stress, which is further confirmed by the significantly increased expression of PTGS2 ferroptosis marker, comparing to control and comparing to the remaining cell lines (Figure V.3 D). Increased GSS expression in MDA-MB-231 and HCC-1806 further complies with increased oxidative stress induced by SeChry@PURE$_{G4}$-FA treatment (Figure V.3 D). Interestingly, Nile Red staining showed BT-474 produce the lowest levels of lipid droplets. These structures are major ways of storage and release of fatty acids and are known to play a critical role in suppressing ROS damage, including ferroptosis, in several types of cancers. This may explain the susceptibility showed by BT-474 cell to ferroptosis upon exposure to SeChry@PURE$_{G4}$-FA.[448,449]

The results of this study shed light on the intricate interplay between cysteine metabolism, BC progression, and potential therapeutic interventions. The overexpression of CBS and *SLC7A11*/xCT in BC samples, particularly in aggressive subtypes, highlights their potential as therapeutic targets for specific BC patient groups. The impact of SeChry@PURE$_{G4}$-FA on BC cell lines further underscore its potential as a novel therapeutic approach. However, further investigations are necessary to elucidate the exact molecular mechanisms underlying the effect of SeChry@PURE$_{G4}$-FA, especially in the context of ferroptosis induction.

V.VI. Conclusion

In conclusion, this study contributes to our understanding of the role of cysteine metabolic remodeling in BC pathogenesis and therapy. The overexpression of CBS and xCT in BC samples suggests their value as potential prognostic markers and therapeutic targets. SeChry@PURE$_{G4}$-FA shows promise as a therapeutic intervention, particularly in inducing cell death and potentially promoting ferroptosis in BC cells. The implications of this research extend to both personalized therapeutic strategies and the development of novel therapeutic agents targeting cysteine metabolism in BC treatment.

Chapter VI

General Discussion and Final Remarks

Cysteine metabolic remodeling remains a central topic in cancer biology, whose potential is not fully disclosed in the context of carcinogenesis and as a potential target. As scientific progress marches forward, oncobiology has shifted its attention toward personalized approaches, prompted by the remarkable heterogeneity observed in tumors. Metabolic remodeling has emerged as a focal point due to cancer cells' remarkable adaptability, enabling them to adjust their metabolism to meet novel metabolic demands and support the anomalous traits exhibited by malignant cells. This adaptive capacity plays a crucial role in fueling tumor growth, invasion, and development of resistance.

The present thesis aimed to disclose and demonstrate the crucial role of cysteine metabolic remodeling in highly frequent and mortal types of cancers worldwide, to which science and medicine could not yet find adequate therapeutic options that would allow to overcome resistance and prevent advanced disease. Important achievements were obtained concerning CM, NSCLC, BC and CRC.

Chapter II: The Metabolic Impact of Mutated *BRD9* in Cutaneous Melanoma

Overall, this thesis shows the relevance of cysteine metabolic rewiring, under the regulation of *BRD9* status, in CM aggressiveness, sustaining altered cellular metabolism and abnormal cellular features and point out MST as a putative marker for CM, since its overexpression correlated with a more invasive and migratory CM phenotype associated with decreased melanin production, thus introducing cysteine metabolic remodeling modulation dependent on *BRD9* status as a possible susceptibility factor for CM development as well (Chapter II).

Interestingly, and in line with our results, a recent study has disclosed the SWI/SNF subunit BRD9 as a melanogenesis major regulator. Selective inhibition of BRD9 induced decreased pigmentation and melanin synthesis through regulation of other pigmentation genes, including SMARCA4.[450] This suggests that alterations that could interfere with BRD9 activity, which seems to be the case of *BRD9* c.183 G>C mutation, can induce a disruption in melanogenesis not only by dysregulation of pigmentation genes but also by remodeling of important players in the melanin (pheomelanin) synthesis pathway, as cysteine. However, new studies are needed to determine the impact of c.183

G>C in BRD9 structure and function, in order to understand the way this BRD9 variant can interfere with SWI/SNF complex function and differentially modulate the expression of genes involved in this process.

Additionally, our results display an increased antioxidant potential in A375 *BRD9* WT and c.183 G>C cells through increased expression of the H_2S-generating enzyme MST[377] and EAAT3 transporter (Figure II.2 D, E and F). Moreover, A375 *BRD9* c.183G>C cells exhibit increased levels of H_2S comparing to A375 Empty, in control conditions. Interestingly, A375 *BRD9* WT, even though showing significant decreased expression of antioxidant enzymes and transporters, show similarly increased H_2S levels, comparing to A375 *BRD9* c.183G>C (Figure II.3 A). H_2S is described to act in two equally important ways: either as a potent antioxidant or as source of electron equivalents to the mETC, leading to ATP production.[264,378] In our results, increased H_2S levels do not translate in proportionally increased ATP levels (Figure II.3 B) but may rather be directed towards a more efficient detoxifying ability in these cells. In fact, oxidative stress is described to limit the metastatic potential of melanoma cells.[451–453] Thus, increasing their ability to respond to increased ROS is a necessary adaptation for cancer cells to invade surrounding tissues and metastasize. This further complies with our results showing that A375 *BRD9 WT/* c.183 G>C cells, besides increasing their redox potential, show a phenotypic shift from a proliferative to a migrative and invasive phenotype, comparing to control (Figure II.1 and II.5).

Our results thus suggest a crucial role for cysteine metabolism in CM, as an energy and antioxidant supplier for CM cancer cells, aiding its malignant traces and promoting more aggressive and invasive phenotypes, while being itself a susceptibility factor for CM by promoting imbalances in melanogenesis. Moreover, in a hereditary or familial cancer context, *BRD9* mutations can contribute for a higher susceptibility to radiation-related mutagenesis since the metabolic shift through cysteine reliance impacts the melanin production and therefore the DNA protection against radiation.

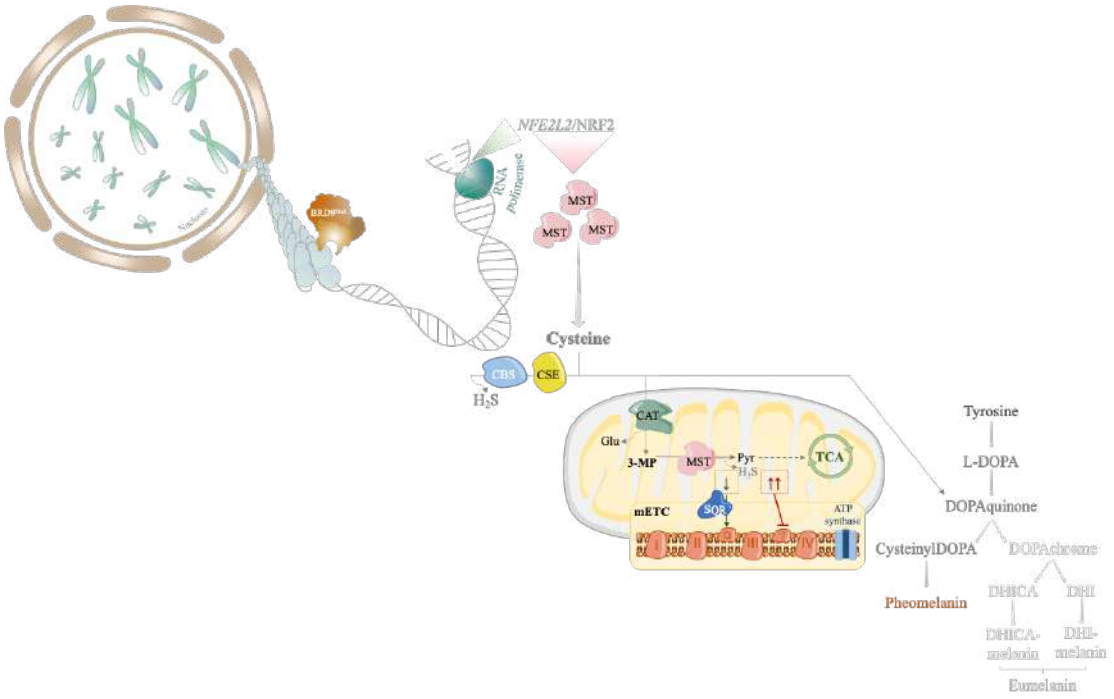

Figure VI.1 –*BRD9 status* regulates cysteine metabolic remodeling in cutaneous melanoma through NRF2. Overexpression of *BRD9* in its WT or c.183 G>C variants can induce cysteine metabolic remodeling, leading to altered cellular features as increased migratory and invasive potential, by inducing MST overexpression through the binding of the transcription factor NFR2. This leads to alterations in cysteine metabolism, which directly interferes with melanogenesis, leading to imbalances in melanin production, which accounts for an increased risk of accumulating mutations due to decreased DNA protection against radiation.

Chapter III: Cysteine Metabolic Profiling is a Putative Determinant in NSCLC Management and a Step Forward in Personalized Medicine

In the work developed within the context of this thesis we further showed the potential of metabolic profiling, specifically cysteine metabolism, as a powerful tool in stratifying patients for therapy alignment in NSCLC (Chapter III). The results obtained offer novel insights into how metabolic players adapt and the diverse nature of NSCLC cells, which are characterized by its high heterogeneity in terms of molecular and metabolic profiles.[401] This enhances our understanding of the different aspects of the disease. While common cancer traits can exist alongside specific characteristics of cancer cells, they provide valuable targets and markers. The cellular models used in this work represented distinct molecular profiles of NSCLC. However, interestingly, in all cell lines was found a dependency on cysteine metabolism to fulfill energetic needs, though using different paths (Chapter III). While A549 and H292 seem to rely mostly on CBS and CSE

to generate H_2S, PC-9 appears to rely mostly on the CAT:MST axis for H_2S and ATP levels maintenance (Figure III.1 and III.2).

Although *CDO1* is not often considered in the general panorama of cysteine metabolic remodeling[421], interestingly, PC-9 cells showed high expression of this gene (Figure III.2 C), suggesting an important role for this metabolic player in NSCLC. CDO1 can participate in the synthesis of pyruvate from cysteine and in the generation of glutamate from α-KG by CAT/GOT enzymes, thus complementing the MST role, since these two enzymes closely work in collaboration with CAT enzymes.[235,237,238] In fact, CDO1 has been linked to LC pathogenesis as a metabolic vulnerability for tumor growth, especially in tumors displaying NRF2 alterations by *KEAP1* mutations[254], however, CDO1 is preferentially found downregulated rather than overexpressed in NSCLC.[254,304] PC-9 cells are described to express wild-type genotype for *KEAP1*[254,454–456], which indicates a possible role for NRF2 in this molecular trait in PC-9 cells, enhancing the antioxidant response of these cells, which can be a distinguishing factor. In line with this, from the studied panel, PC-9 cells showed resistance to our metabolic approach targeting cysteine metabolism using SeChry, thus increasing cellular oxidant damage. All NSCLC cell lines, except PC-9, were quite sensitive to SeChry and SeChry@PURE$_{G4}$-FA, which presented an EC_{50} for SeChry very close to non-cancer cell lines (Figure III.3 B and C), also in line with our hypothesis that PC-9 cells do not metabolically rely on CBS. Within this chapter we further explored the expression of key players in cysteine metabolism in tumor samples (data retrieved from TCGA LUAD and LUSC cohorts and data obtained from tumor samples belonging to a cohort of NSCLC patients followed at IPOLFG). This study highlights the importance of considering cysteine metabolism in the identification of specific profiles. Regarding the TCGA data, comparing to normal lung tissue, *CBS*, *GOT1*, *GOT2* and *SLC7A11* are overexpressed, *SLC1A1* and *CDO1* are downregulated, and *MPST* expression is not altered. Additionally, *CTH* is overexpressed in LUAD but not LUSC, thereby representing a clear distinctive pattern between the two histotypes that can be further explored. mRNA expression of cysteine metabolic players in NSCLC tumor samples (IPOLFG cohort) reinforced the importance of *MPST* in NSCLC pathology, since this was the most expressed cysteine-degrading and H_2S-producing enzyme encoding gene (Figure III.4 C). Additionally, Spearman strong correlations ($0.4 > r < 0.69$), with statistical significance ($p < 0.01$), were observed between *MPST* expression with its metabolic partners *GOT1* and *GOT2*, as well as with *CDO1*, whose encoded enzyme acts sequentially with *GOT1* and *GOT2* encoded enzymes (Table III.3),

which lines up with PC-9 profile which was characterized by reliance on CDO1 expression, however, a deepened understanding in this profile, which represents an important and aggressive NSCLC histological and molecular group (LUAD; *EGFR* exon 19 deletion (Ex19Del; Glu746-Ala750 deletion) and *KRAS* WT), related with enzymatic activity and redox potential is further needed for better clarification of CDO1 and MST role in this context. The significant correlations between *MPST* with *GOT2, SLC1A1* and *SLC7A11* and between *MPST* with *GOT1* and *SLC1A1* were also verified, respectively in tumors $EGFR^{Mut}$ and $KRAS^{Mut}$, suggesting that cysteine catabolism routes through MST and CAT/GOT enzymes with the production of H_2S and through CDO1 and CAT/GOT enzymes are pivotal in some subsets of NSCLC. Interestingly, in $KRAS^{Mut}$ and WT tumor samples, a correlation was observed between *CBS* and *CTH* genes expression, corresponding to A549 and H292 genetic background, while the expression of *CBS* and *CTH* are not correlated in PC-9 cells ($EGFR^{Mut}$). Again, the genetic background of tumors must be explored and comprehensively correlated with metabolic profiles, in a perspective of finding mechanisms of resistance to target therapy applied in NSCLC.

Moreover, *CDO1* was significantly more expressed in NSCLC metastases than in primary tumors (Figure III.4 D). Contrarily to what is shown by different studies indicating *CDO1* may be a tumor suppressor gene[255,299,429–431], our results point out that its function may contribute to more aggressive phenotypes. This thus suggest *CDO1* as a putative target for therapeutical intervention in specific NSCLC profiles. However, and given the ambiguity of this findings comparing to what is described in the literature[255,299,429–431], further studies are needed to disclose this expression pattern and its effect in PC-9 phenotype and molecular and metabolic traits.

Chapter IV: CBS Inhibition as a Therapeutic Approach in Colorectal Cancer

Chapter IV focused on the study of the effect of SeChry@$PURE_{G4}$-FA as a suitable approach in CRC, which is a leading cause of cancer-related deaths worldwide[6,122] and therapy resistance is a major factor contributing to its high mortality.[134–140] Therefore, its crucial to disclose novel putative targets that can be helpful in overcoming this major issue. Expression analysis of H_2S-synthesizing enzymes showed CBS as the most differentially expressed enzyme in the chosen CRC panel of cell lines (Figure IV.1). Moreover, CRC cell lines showed different response to the standard agents commonly used in CRC therapy carboplatin, cisplatin, 5-FU and oxaliplatin

(Figure IV.2). All cell lines showed resistance to at least two tested drugs except for SW48 cells, which showed sensitivity to all agents (Figure IV.2) and, interestingly presented median levels of CBS mRNA expression but high levels of protein expression (Figure IV.1 A and B).

Treatment with SeChry@PURE$_{G4}$-FA, a nanoformulation previously described to specifically inhibit CBS among all H_2S-synthesizing enzymes[363], induced different responses: HCT15, HCT116 and LoVo showed similar response to SeChry, showing EC_{50} values ranging 8-13 μM (Figure IV.3 B). However, only HCT15 and HCT116 were sensitive towards encapsulated SeChry (SeChry@PURE$_{G4}$-FA), although with higher EC_{50} than the free compound: 24 ± 60 μM and 19.0 ± 8.6 μM, respectively. SW48 cells were insensitive to both free and encapsulated SeChry. (Figure IV.3 B). Besides impairing cell viability, treatment with SeChry or SeChry@PURE$_{G4}$-FA significantly reduced the proliferative capacity mostly of HCT15 and HCT116 (Figure IV.3 C).

CBS is in fact highly described to be associated with CRC carcinogenesis and its overexpression is widely described by several studies[280–282]. Alterations in CBS expression status is suggested to correlate with more aggressive phenotypes of CRC.[246,284] A recent study has identified CBS as a strong target for induction of sensitivity to CRC treatment, specifically to immunotherapy. Indeed, reducing H_2S production by abrogating CBS activity induced a more responsive immune microenvironment, thus highlighting the central role of CBS in CRC therapy resistance.[457] Our results on CBS expression in CRC are in line with the results described in the literature and the CBS inhibition by SeChry@PURE$_{G4}$-FA reinforce the efficacy of targeting cysteine metabolism was a way to disrupt CRC progression and sensitize CRC cell to therapy.

Consistent with the preceding chapters, the outcomes achieved within the scope of this study specifically focused on CRC, once more underscore the significance of metabolic profiling in clinical management as a groundbreaking step towards individualized treatment. Moreover, these results also unveil opportunities for exploring new therapeutic approaches that can allow better responses to current therapy regiments.

Chapter V: SeChry@PURE$_{G4}$-FA Elicits Distinct Cell Death Mechanisms by Disrupting Cysteine Metabolism in Breast Cancer Cells

Finally, Chapter V of this thesis aimed to test the effect of SeChry@PURE$_{G4}$-FA as a putative therapeutic option in BC cells. CBS is described to be overexpressed in BC and as a player in BC progression.[239,295] Moreover, CBS expression in BC is thought to correlate with more aggressive tumors[239,293,295,296], which led us to believe SeChry@PURE$_{G4}$-FA could be an interesting and effective approach in BC context. Interestingly, data retrieved from a BRCA TCGA cohort showed that *CBS* and *SLC7A11* (xCT) expression patterns stand out from the remaining cysteine metabolic players studied (Figure V.1 A). Both *CBS* and *SLC7A11* showed significant overexpression in tumors comparing to normal tissue, while *CTH*, *MPST*, and *SLC1A1* showed reduced expression (*CTH*) or no differences (Figure V.1 A). Complementing this analysis, we studied the expression of CBS and xCT by immunohistochemistry in a cohort of BC tumors of patients followed at IPOLFG. This analysis further emphasized the critical role of CBS and xCT in BC since, overall we found significant expression of CBS and xCT in BC tissues (Figure V.1), particularly for xCT in TNBC and HER2-enriched cases, two aggressive histologic subtypes of BC not expressing hormone receptors and therefore presenting less efficient therapeutic alternatives. xCT overexpression also correlated with invasive phenotypes since it was found in metastatic (Figure V.1 A) and invasive components in tumors (Figure V.1 D), comparing to its expression in normal tissue, primary tumors and *in situ* components in tumors. In line with current knowledge of the heterogeneous profile of BC, expression analysis of *CBS* and *SLC7A11* showed distinct expression patterns among the different cell lines studied, representative of different molecular and histologic subtypes of BC (Figure V.1 G and H). BC is described as a highly heterogeneous disease, with multiple molecular entities that define distinct phenotypes and clinical responses.[142–145] Analysis of cell death of BC cells upon SeChry@PURE$_{G4}$-FA treatment showed HCC-1806 did not presented an overall good response while MDA-MB-231, MCF7 and BT-474 show significantly cell death levels comparing to control (Figure V.3 A), which suggests SeChry@PURE$_{G4}$-FA may represent a putative effective approach in BC. Notably, the induction of increased intracellular ROS and lipid peroxides in response to SeChry@PURE$_{G4}$-FA treatment, particularly in MDA-MB-231, HCC-1806 and BT-474 cells, indicates an induction of oxidative stress by SeChry@PURE$_{G4}$-FA in these cells (Figure V.3 A, B, C). Different

patterns of cell death were observed amongst BC cell lines. MDA-MB-231 cells died mainly through apoptosis, MCF7 exhibit apoptosis activation and necrosis/necroptosis, and HCC-1806 cell death occurred mainly through necrosis/necroptosis. BT-474 cell line showed significant increased lipid peroxides upon treatment with SeChry@PURE$_{G4}$-FA, which point to the involvement of a distinct mechanism being induced in this cell line – ferroptosis. This was confirmed by significantly increased expression of PTGS2, encoding cycloxygenase 2 (COX2) a ferroptosis marker, comparing to control and comparing to the remaining cell lines (Figure V.3 D). Moreover, a mechanism underlying the protection against ferroptosis may be the accumulation of lipid droplets in the endoplasmic reticulum, which corroborates our observations since BT-474 cells present lower levels of lipid droplets comparing with the other cell lines (Figure V.3 E), thus lipids were more exposed to peroxidation. Increased LD accumulation appears to be a common characteristic in cancer, where they act as protective structures against toxicity resulting from excess of ROS and also as energy suppliers, favoring cell survival, aggressiveness and resistance to therapy.[458] Ferroptosis is in fact described in BC, especially for the most aggressive histological subtype TNBC and is shown to be an heterogeneous phenomenon, which can explain the results presented here regarding TBNC cell lines studied.[459] Our results underline the mechanism of ferroptosis as a possible response from luminal tumors as well. Even though further studies are needed to disclose the role of ferroptosis in BC, the induction of different cell death patterns can be used as a predictive tool to stratify responsive and non-responsive patients.[460] However, SeChry and CBS inhibition was proven to efficiently affect BC cell survival, even though BC cell lines present the activation of different mechanisms of cell death.

With the deepening of cancer metabolism understanding, we are uncovering the intricate ways in which cysteine intersects with other metabolic pathways and interfere with specific players, sustaining malignant abilities. This knowledge holds the potential to identify new therapeutic targets, unravel the complexities of drug resistance mechanisms, and pave the way for personalized treatment strategies that exploit the unique metabolic profiles of individual tumors.

A common feature in cancer metabolism of all the models studied in the present thesis is heterogeneity, which may be a gold clue for individual-related characteristics guiding towards personalized medicine. Albeit, more frequent patterns define and

characterize a group of patients, individual/personalized medicine relies on uncommon and specific alterations requiring the adjustment of the therapeutic protocol. As precision medicine gains *momentum*, the integration of cysteine metabolic remodeling insights into treatment paradigms offers a tantalizing prospect into tailored therapies. Therapies based on a tumor's specific metabolic profile could enhance treatment efficacy while minimizing side effects. Moreover, these strategies could, rather than substitute, combine with existing treatment modalities to create synergistic effects, providing a multi-pronged attack on cancer cells.

Chapter VII

Future Perspectives

The work presented in this thesis provides valid indications of the importance of considering cysteine metabolic remodeling and metabolic profiles in the discovery of new targets for cancer therapy. However, further steps are needed to further clarify efficient ways of taking advantage of cysteine metabolic remodeling and alterations in intervenients involved in the associated pathways as a tool to aid clinical decisions and stratify patients. In line with this, the initial plan for this work included the analysis of tumor samples from various types of aggressive and deadly cancers, in different stages of patient follow-up and the gathering of clinical information specifically focused on treatment regimens and tumor response. Even though this was not possible to perform for the present thesis, this is an essential step that would allow us to obtain thresholds for expression and activity of cysteine enzymes and transporters as well as study metabolic profiles, that could lead to the development of a platform focused on stratifying oncologic patients and predict the benefit of those patients in receiving specific drugs whose effect could or not be abrogated by cysteine metabolism. This would be an important tool to support clinical decisions and avoid patients' exposure to therapies which commonly induce side effects and diminish patient's quality of life, that would not be effective against their specific tumor and, rather, direct those patients towards therapy regimens that could offer better results.

Moreover, the study of the effect of metabolic approaches together with available drugs would be of interest. The effect of SeChry(@PURE$_{G4}$-FA) in combination with platinum salts has been studied for ovarian cancer. SeChry@PURE$_{G4}$-FA in combination with carboplatin induced increased cell death in ovarian cancer cells, comparing to carboplatin alone[363], which indicates our formulation as a putative adjuvant drug. However, it would be important to understand if other types of cancer cells resistant to platinum salts, could also be sensitized to regimens that include SeChry(@PURE$_{G4}$-FA) as adjuvant. Additionally, it would be crucial to study the pharmacodynamics and pharmacokinetics interactions between SeChry(@PURE$_{G4}$-FA) and other drugs that could be used in combined regimens. A future important step in this research line would also be the study of SeChry@PURE$_{G4}$-FA in animal models to disclose the *in vivo* effect of this approach since, until now, it has only been studied in 2D cell cultures. Because the feasibility of SeChry@PURE$_{G4}$-FA much depends on possible side effects and tissue toxicity that this drug could induce, it would be important to evaluate *in vivo* systemic toxicity, namely kidney and liver toxicity and the efficiency of cancer cell targeting by the PURE$_{G4}$-FA formulation. Combination of SeChry@PURE$_{G4}$-FA with available anti-

cancer therapies should also be evaluated *in vivo* to further evaluate the effect of this combined regimens considering the influence of a complex microenvironment and the involvement of the immune system.

References

1. Hanahan D, Weinberg RA. Hallmarks of cancer: the next generation. *Cell*. 2011;144(5):646-674.
2. Cree IA. Cancer biology. *Methods Mol Biol*. 2011;731:1-11.
3. Senga SS, Grose RP. Hallmarks of cancer-the new testament. *Open Biol*. 2021;11(1).
4. Hanahan D. Hallmarks of Cancer: New Dimensions. *Cancer Discov*. 2022;12(1):31-46.
5. Siegel RL, Miller KD, Wagle NS, et al. Cancer statistics, 2023. *CA Cancer J Clin*. 2023;73(1):17-48.
6. Sung H, Ferlay J, Siegel RL, et al. Global Cancer Statistics 2020: GLOBOCAN Estimates of Incidence and Mortality Worldwide for 36 Cancers in 185 Countries. *CA Cancer J Clin*. 2021;71(3):209-249.
7. Siegel RL, Miller KD, Fuchs HE, et al. Cancer statistics, 2022. *CA Cancer J Clin*. 2022;72(1):7-33.
8. Dyba T, Randi G, Bray F, et al. The European cancer burden in 2020: Incidence and mortality estimates for 40 countries and 25 major cancers. *Eur J Cancer*. 2021;157:308.
9. Santucci C, Carioli G, Bertuccio P, et al. Progress in cancer mortality, incidence, and survival: A global overview. *Eur J Cancer Prev*. 2020;29(5):367-381.
10. Patterson AD, Gonzalez FJ, Perdew GH, et al. Molecular Regulation of Carcinogenesis: Friend and Foe. *Toxicol Sci*. 2018;165(2):277-283.
11. Hipólito A, Martins F, Mendes C, et al. Molecular and Metabolic Reprogramming: Pulling the Strings Toward Tumor Metastasis. *Front Oncol*. 2021;11.
12. Hanahan D, Weinberg RA. The hallmarks of cancer. *Cell*. 2000;100(1):57-70.
13. Odenthal J, Takes R, Friedl P. Plasticity of tumor cell invasion: governance by growth factors and cytokines. *Carcinogenesis*. 2016;37(12):1117-1128.
14. Hanahan D, Coussens LM. Accessories to the crime: functions of cells recruited to the tumor microenvironment. *Cancer Cell*. 2012;21(3):309-322.
15. Gameiro PA, Struhl K. Nutrient Deprivation Elicits a Transcriptional and Translational Inflammatory Response Coupled to Decreased Protein Synthesis. *Cell Rep*. 2018;24(6):1415.
16. Skrypek N, Goossens S, De Smedt E, et al. Epithelial-to-Mesenchymal

Transition: Epigenetic Reprogramming Driving Cellular Plasticity. *Trends Genet*. 2017;33(12):943-959.

17. Serrano-Gomez SJ, Maziveyi M, Alahari SK. Regulation of epithelial-mesenchymal transition through epigenetic and post-translational modifications. *Mol Cancer*. 2016;15(1).
18. Cano A, Pérez-Moreno MA, Rodrigo I, et al. The transcription factor snail controls epithelial-mesenchymal transitions by repressing E-cadherin expression. *Nat Cell Biol*. 2000;2(2):76-83.
19. Batlle E, Sancho E, Francí C, et al. The transcription factor Snail is a repressor of E-cadherin gene expression in epithelial tumour cells. *Nat Cell Biol 2000 22*. 2000;2(2):84-89.
20. Javaid S, Zhang J, Anderssen E, et al. Dynamic Chromatin Modification Sustains Epithelial-Mesenchymal Transition following Inducible Expression of Snail-1. *Cell Rep*. 2013;5(6):1679.
21. Mohammadi H, Sahai E. Mechanisms and impact of altered tumour mechanics. *Nat Cell Biol*. 2018;20(7):766-774.
22. Ali Z, Yousaf N, Larkin J. Melanoma epidemiology, biology and prognosis. *EJC Suppl*. 2013;11(2):81.
23. Mihajlovic M, Vlajkovic S, Jovanovic P, et al. Primary mucosal melanomas: a comprehensive review. *Int J Clin Exp Pathol*. 2012;5(8):739.
24. Krantz BA, Dave N, Komatsubara KM, et al. Uveal melanoma: epidemiology, etiology, and treatment of primary disease. *Clin Ophthalmol*. 2017;11:279-289.
25. Vasalaki M, Fabian ID, Reddy MA, et al. Ocular oncology: advances in retinoblastoma, uveal melanoma and conjunctival melanoma. *Br Med Bull*. 2017;121(1):107-119.
26. Kuk D, Shoushtari AN, Barker CA, et al. Prognosis of Mucosal, Uveal, Acral, Nonacral Cutaneous, and Unknown Primary Melanoma From the Time of First Metastasis. *Oncologist*. 2016;21(7):848-854.
27. Bandarchi B, Ma L, Navab R, et al. From melanocyte to metastatic malignant melanoma. *Dermatol Res Pract*. 2010;2010(1).
28. Schadendorf D, Fisher DE, Garbe C, et al. Melanoma. *Nat Rev Dis Prim*. 2015;1.
29. Sang Y, Deng Y. Current insights into the epigenetic mechanisms of skin cancer. *Dermatol Ther*. 2019;32(4):e12964.
30. Parra LM, Webster RM. The malignant melanoma market. *Nat Rev Drug Discov*.

2022;21(7):489-490.

31. Alexandrov LB, Nik-Zainal S, Wedge DC, et al. Signatures of mutational processes in human cancer. *Nat 2013 5007463*. 2013;500(7463):415-421.
32. Hodis E, Watson IR, Kryukov G V., et al. A Landscape of Driver Mutations in Melanoma. *Cell*. 2012;150(2):251.
33. Pleasance ED, Cheetham RK, Stephens PJ, et al. A comprehensive catalogue of somatic mutations from a human cancer genome. *Nature*. 2010;463(7278):191-196.
34. Armstrong BK, Cust AE. Sun exposure and skin cancer, and the puzzle of cutaneous melanoma: A perspective on Fears et al. Mathematical models of age and ultraviolet effects on the incidence of skin cancer among whites in the United States. American Journal of Epidemiology 1977; . *Cancer Epidemiol*. 2017;48:147-156.
35. Dimitriou F, Krattinger R, Ramelyte E, et al. The World of Melanoma: Epidemiologic, Genetic, and Anatomic Differences of Melanoma Across the Globe. *Curr Oncol Rep*. 2018;20(11).
36. Sun X, Zhang N, Yin C, et al. Ultraviolet Radiation and Melanomagenesis: From Mechanism to Immunotherapy. *Front Oncol*. 2020;10:951.
37. Kobayashi N, Nakagawa A, Muramatsu T, et al. Supranuclear melanin caps reduce ultraviolet induced DNA photoproducts in human epidermis. *J Invest Dermatol*. 1998;110(5):806-810.
38. Slominski RM, Sarna T, Płonka PM, et al. Melanoma, Melanin, and Melanogenesis: The Yin and Yang Relationship. *Front Oncol*. 2022;12:1.
39. Nasti TH, Timares L. MC1R, eumelanin and pheomelanin: their role in determining the susceptibility to skin cancer. *Photochem Photobiol*. 2015;91(1):188-200.
40. Lin JY, Fisher DE. Melanocyte biology and skin pigmentation. *Nature*. 2007;445(7130):843-850.
41. Land EJ, Riley PA. Spontaneous redox reactions of dopaquinone and the balance between the eumelanic and phaeomelanic pathways. *Pigment cell Res*. 2000;13(4):273-277.
42. Land EJ, Ramsden CA, Riley PA. Pulse radiolysis studies of ortho-quinone chemistry relevant to melanogenesis. *J Photochem Photobiol B Biol*. 2001;64(2-3):123-135.

43. Ito S, Wakamatsu K. Melanin chemistry and melanin precursors in melanoma. *J Invest Dermatol*. 1989;92(5 Suppl):261S-265S.
44. LERNER AB, FITZPATRICK TB. Biochemistry of melanin formation. *Physiol Rev*. 1950;30(1):91-126.
45. Körner A, Pawelek J. Mammalian tyrosinase catalyzes three reactions in the biosynthesis of melanin. *Science*. 1982;217(4565):1163-1165.
46. Michaloglou C, Vredeveld LCW, Soengas MS, et al. BRAFE600-associated senescence-like cell cycle arrest of human naevi. *Nature*. 2005;436(7051):720-724.
47. Hussussian CJ, Struewing JP, Goldstein AM, et al. Germline p16 mutations in familial melanoma. *Nat Genet*. 1994;8(1):15-21.
48. Colombino M, Capone M, Lissia A, et al. BRAF/NRAS mutation frequencies among primary tumors and metastases in patients with melanoma. *J Clin Oncol*. 2012;30(20):2522-2529.
49. Bastian BC. The molecular pathology of melanoma: an integrated taxonomy of melanocytic neoplasia. *Annu Rev Pathol*. 2014;9:239-271.
50. Long G V., Menzies AM, Nagrial AM, et al. Prognostic and clinicopathologic associations of oncogenic BRAF in metastatic melanoma. *J Clin Oncol*. 2011;29(10):1239-1246.
51. Mann GJ, Pupo GM, Campain AE, et al. BRAF mutation, NRAS mutation, and the absence of an immune-related expressed gene profile predict poor outcome in patients with stage III melanoma. *J Invest Dermatol*. 2013;133(2):509-517.
52. Jakob JA, Bassett RL, Ng CS, et al. NRAS mutation status is an independent prognostic factor in metastatic melanoma. *Cancer*. 2012;118(16):4014-4023.
53. van 't Veer LJ, Burgering BM, Versteeg R, et al. N-ras mutations in human cutaneous melanoma from sun-exposed body sites. *Mol Cell Biol*. 1989;9(7):3114-3116.
54. Ellerhorst JA, Greene VR, Ekmekcioglu S, et al. Clinical correlates of NRAS and BRAF mutations in primary human melanoma. *Clin Cancer Res*. 2011;17(2):229-235.
55. Davies H, Bignell GR, Cox C, et al. Mutations of the BRAF gene in human cancer. *Nature*. 2002;417(6892):949-954.
56. Mazurenko NN. Molecular Profile of Cutaneous Melanoma. *Eurasian J Med Oncol*. 2022.

57. Gast A, Scherer D, Chen B, et al. Somatic alterations in the melanoma genome: a high-resolution array-based comparative genomic hybridization study. *Genes Chromosomes Cancer*. 2010;49(8):733-745.
58. Curtin JA, Fridlyand J, Kageshita T, et al. Distinct sets of genetic alterations in melanoma. *N Engl J Med*. 2005;353(20):2135-2147.
59. Griewank KG, Scolyer RA, Thompson JF, et al. Genetic alterations and personalized medicine in melanoma: Progress and future prospects. *J Natl Cancer Inst*. 2014;106(2).
60. Dasgupta B, Yi Y, Chen DY, et al. Proteomic analysis reveals hyperactivation of the mammalian target of rapamycin pathway in neurofibromatosis 1-associated human and mouse brain tumors. *Cancer Res*. 2005;65(7):2755-2760.
61. Johannessen CM, Reczek EE, James MF, et al. The NF1 tumor suppressor critically regulates TSC2 and mTOR. *Proc Natl Acad Sci U S A*. 2005;102(24):8573-8578.
62. Maertens O, Johnson B, Hollstein P, et al. Elucidating distinct roles for NF1 in melanomagenesis. *Cancer Discov*. 2013;3(3):339-349.
63. Whittaker SR, Theurillat JP, Van Allen E, et al. A genome-scale RNA interference screen implicates NF1 loss in resistance to RAF inhibition. *Cancer Discov*. 2013;3(3):351-362.
64. Ribeiro Moura Brasil Arnaut J, dos Santos Guimarães I, Evangelista dos Santos AC, et al. Molecular landscape of Hereditary Melanoma. *Crit Rev Oncol Hematol*. 2021;164.
65. Toussi A, Mans N, Welborn J, et al. Germline mutations predisposing to melanoma. *J Cutan Pathol*. 2020;47(7):606-616.
66. Goldstein AM, Chan M, Harland M, et al. Features associated with germline CDKN2A mutations: a GenoMEL study of melanoma-prone families from three continents. *J Med Genet*. 2007;44(2):99-106.
67. Eliason MJ, Larson AA, Florell SR, et al. Population-based prevalence of CDKN2A mutations in Utah melanoma families. *J Invest Dermatol*. 2006;126(3):660-666.
68. Bennett DC. How to make a melanoma: what do we know of the primary clonal events? *Pigment Cell Melanoma Res*. 2008;21(1):27-38.
69. Puntervoll HE, Yang XR, Vetti HH, et al. Melanoma prone families with CDK4 germline mutation: phenotypic profile and associations with MC1R variants. *J*

Med Genet. 2013;50(4):264-270.

70. Goldstein AM, Chan M, Harland M, et al. High-risk melanoma susceptibility genes and pancreatic cancer, neural system tumors, and uveal melanoma across GenoMEL. *Cancer Res*. 2006;66(20):9818-9828.
71. Deshpande A, Sicinski P, Hinds PW. Cyclins and cdks in development and cancer: a perspective. *Oncogene*. 2005;24(17):2909-2915.
72. Huang FW, Hodis E, Xu MJ, et al. Highly recurrent TERT promoter mutations in human melanoma. *Science*. 2013;339(6122):957-959.
73. Urso C. Melanocytic Skin Neoplasms: What Lesson From Genomic Aberrations? *Am J Dermatopathol*. 2019;41(9):623-629.
74. Sizemore GM, Pitarresi JR, Balakrishnan S, et al. The ETS family of oncogenic transcription factors in solid tumours. *Nat Rev Cancer*. 2017;17(6):337-351.
75. Toland AE. POT1 pathogenic variants: not all telomere pathway genes are equal in risk of hereditary cutaneous melanoma. *Br J Dermatol*. 2019;181(1):14-15.
76. Potrony M, Puig-Butille JA, Ribera-Sola M, et al. POT1 germline mutations but not TERT promoter mutations are implicated in melanoma susceptibility in a large cohort of Spanish melanoma families. *Br J Dermatol*. 2019;181(1):105-113.
77. Trigueros-Motos L. Mutations in POT1 predispose to familial cutaneous malignant melanoma. *Clin Genet*. 2014;86(3):217-218.
78. Calvete O, Garcia-Pavia P, Domínguez F, et al. The wide spectrum of POT1 gene variants correlates with multiple cancer types. *Eur J Hum Genet*. 2017;25(11):1278-1281.
79. Shain AH, Yeh I, Kovalyshyn I, et al. The Genetic Evolution of Melanoma from Precursor Lesions. *N Engl J Med*. 2015;373(20):1926-1936.
80. Andrés-Lencina JJ, Rachakonda S, García-Casado Z, et al. TERT promoter mutation subtypes and survival in stage I and II melanoma patients. *Int J cancer*. 2019;144(5):1027-1036.
81. Bristot IJ, Kehl Dias C, Chapola H, et al. Metabolic rewiring in melanoma drug-resistant cells. *Crit Rev Oncol Hematol*. 2020;153.
82. Zarei M, Giannikou K, Du H, et al. MITF is a driver oncogene and potential therapeutic target in kidney angiomyolipoma tumors through transcriptional regulation of CYR61. *Oncogene*. 2021;40(1):112-126.
83. Wolf Horrell EM, Boulanger MC, D'Orazio JA. Melanocortin 1 Receptor:

Structure, Function, and Regulation. *Front Genet*. 2016;7(MAY).

84. Saleha S, Khan TA, Zafar S. MC1R gene variants involvement in human OCA phenotype. *Open Life Sci*. 2016;11(1):142-150.
85. Fargnoli MC, Gandini S, Peris K, et al. MC1R variants increase melanoma risk in families with CDKN2A mutations: a meta-analysis. *Eur J Cancer*. 2010;46(8):1413-1420.
86. Robles-Espinoza CD, Harland M, Ramsay AJ, et al. POT1 loss-of-function variants predispose to familial melanoma. *Nat Genet*. 2014;46(5):478-481.
87. Horn S, Figl A, Rachakonda PS, et al. TERT promoter mutations in familial and sporadic melanoma. *Science*. 2013;339(6122):959-961.
88. Patel S, Wilkinson CJ, Sviderskaya E V. Loss of Both CDKN2A and CDKN2B Allows for Centrosome Overduplication in Melanoma. *J Invest Dermatol*. 2020;140(9):1837-1846.e1.
89. Campos C, Fragoso S, Luís R, et al. High-Throughput Sequencing Identifies 3 Novel Susceptibility Genes for Hereditary Melanoma. *Genes (Basel)*. 2020;11(4):403.
90. Landi MT, Bishop DT, MacGregor S, et al. Genome-wide association meta-analyses combining multiple risk phenotypes provide insights into the genetic architecture of cutaneous melanoma susceptibility. *Nat Genet*. 2020;52(5):494-504.
91. Wang X, Wang S, Troisi EC, et al. BRD9 defines a SWI/SNF sub-complex and constitutes a specific vulnerability in malignant rhabdoid tumors. 2019;10(1):1-11.
92. Smith JJ, Xiao Y, Parsan N, et al. The SWI/SNF chromatin remodeling assemblies BAF and PBAF differentially regulate cell cycle exit and cellular invasion in vivo. *PLoS Genet*. 2022;18(1).
93. Vaart A Van Der, Vaart A Van Der, Godfrey M, et al. Dose-dependent functions of SWI/SNF BAF in permitting and inhibiting cell proliferation in vivo. *Sci Adv*. 2020;6(21).
94. Wang X, Haswell JR, Roberts CWM. Molecular pathways: SWI/SNF (BAF) complexes are frequently mutated in cancer--mechanisms and potential therapeutic insights. *Clin Cancer Res*. 2014;20(1):21-27.
95. Garbe C, Amaral T, Peris K, et al. European consensus-based interdisciplinary guideline for melanoma. Part 2: Treatment - Update 2019. *Eur J Cancer*.

2020;126:159-177.

96. Coit DG, Thompson JA, Albertini MR, et al. Cutaneous Melanoma, Version 2.2019, NCCN Clinical Practice Guidelines in Oncology. *J Natl Compr Canc Netw*. 2019;17(4):367-402.
97. Ziogas DC, Theocharopoulos C, Koutouratsas T, et al. Mechanisms of resistance to immune checkpoint inhibitors in melanoma: What we have to overcome? *Cancer Treat Rev*. 2023;113.
98. Du W, Elemento O. Cancer systems biology: embracing complexity to develop better anticancer therapeutic strategies. *Oncogene*. 2015;34(25):3215-3225.
99. Davis LE, Shalin SC, Tackett AJ. Current state of melanoma diagnosis and treatment. *Cancer Biol Ther*. 2019;20(11):1366-1379.
100. Siegel RL, Miller KD, Jemal A. Cancer statistics, 2019. *CA Cancer J Clin*. 2019;69(1):7-34.
101. Schabath MB, Cote ML. Cancer Progress and Priorities: Lung Cancer. *Cancer Epidemiol Biomarkers Prev*. 2019;28(10):1563-1579.
102. Hipólito A, Mendes C, Serpa J. The Metabolic Remodelling in Lung Cancer and Its Putative Consequence in Therapy Response. *Adv Exp Med Biol*. 2020;1219:311-333.
103. Inamura K. Lung Cancer: Understanding Its Molecular Pathology and the 2015 WHO Classification. *Front Oncol*. 2017;7(AUG).
104. Hoseok I, Cho JY. Lung Cancer Biomarkers. *Adv Clin Chem*. 2015;72:107-170.
105. Lemjabbar-Alaoui H, Hassan OU, Yang Y-W, et al. Lung cancer: Biology and treatment options. *Biochim Biophys Acta - Rev Cancer*. 2015;1856(2):189-210.
106. Bade BC, Dela Cruz CS. Lung Cancer 2020: Epidemiology, Etiology, and Prevention. *Clin Chest Med*. 2020;41(1):1-24.
107. Gazdar AF, Shigematsu H, Herz J, et al. Mutations and addiction to EGFR: the Achilles “heal” of lung cancers? *Trends Mol Med*. 2004;10(10):481-486.
108. Dagogo-Jack I, Shaw AT. Tumour heterogeneity and resistance to cancer therapies. *Nat Rev Clin Oncol 2017 152*. 2017;15(2):81-94.
109. Salehi-Rad R, Li R, Paul MK, et al. The Biology of Lung Cancer: Development of More Effective Methods for Prevention, Diagnosis, and Treatment. *Clin Chest Med*. 2020;41(1):25-38.
110. Chen Z, Fillmore CM, Hammerman PS, et al. Non-small-cell lung cancers: a heterogeneous set of diseases. *Nat Rev Cancer 2014 148*. 2014;14(8):535-546.

111. Collisson EA, Campbell JD, Brooks AN, et al. Comprehensive molecular profiling of lung adenocarcinoma. *Nat 2014 5117511*. 2014;511(7511):543-550.
112. Hammerman PS, Voet D, Lawrence MS, et al. Comprehensive genomic characterization of squamous cell lung cancers. *Nature*. 2012;489(7417):519.
113. Govindan R, Ding L, Griffith M, et al. GENOMIC LANDSCAPE OF NON-SMALL CELL LUNG CANCER IN SMOKERS AND NEVER SMOKERS. *Cell*. 2012;150(6):1121.
114. Pao W, Wang TY, Riely GJ, et al. KRAS Mutations and Primary Resistance of Lung Adenocarcinomas to Gefitinib or Erlotinib. *PLoS Med*. 2005;2(1):0057-0061.
115. Mittal V, El Rayes T, Narula N, et al. The Microenvironment of Lung Cancer and Therapeutic Implications. *Adv Exp Med Biol*. 2016;890:75-110.
116. Hirsch FR, Scagliotti G V., Mulshine JL, et al. Lung cancer: current therapies and new targeted treatments. *Lancet (London, England)*. 2017;389(10066):299-311.
117. Fehrenbacher L, Spira A, Ballinger M, et al. Atezolizumab versus docetaxel for patients with previously treated non-small-cell lung cancer (POPLAR): a multicentre, open-label, phase 2 randomised controlled trial. *Lancet (London, England)*. 2016;387(10030):1837-1846.
118. Rizvi NA, Brahmer JR, Ou S-HI, et al. Safety and clinical activity of MEDI4736, an anti-programmed cell death-ligand 1 (PD-L1) antibody, in patients with non-small cell lung cancer (NSCLC). *https://doi.org/101200/jco20153315_suppl8032*. 2015;33(15_suppl):8032-8032.
119. Gettinger SN, Horn L, Gandhi L, et al. Overall Survival and Long-Term Safety of Nivolumab (Anti-Programmed Death 1 Antibody, BMS-936558, ONO-4538) in Patients With Previously Treated Advanced Non-Small-Cell Lung Cancer. *J Clin Oncol*. 2015;33(18):2004-2012.
120. Herbst RS, Soria JC, Kowanetz M, et al. Predictive correlates of response to the anti-PD-L1 antibody MPDL3280A in cancer patients. *Nature*. 2014;515(7528):563.
121. Garon EB, Rizvi NA, Hui R, et al. Pembrolizumab for the treatment of non-small-cell lung cancer. *N Engl J Med*. 2015;372(21):2018-2028.
122. Dekker E, Tanis PJ, Vleugels JLA, et al. Colorectal cancer. *Lancet*. 2019;394(10207):1467-1480.

123. Henrikson NB, Webber EM, Goddard KA, et al. Family history and the natural history of colorectal cancer: systematic review. *Genet Med*. 2015;17(9):702-712.
124. Thanikachalam K, Khan G. Colorectal Cancer and Nutrition. *Nutrients*. 2019;11(1).
125. Nguyen LH, Goel A, Chung DC. Pathways of Colorectal Carcinogenesis. *Gastroenterology*. 2020;158(2):291.
126. Church J. Molecular genetics of colorectal cancer. *Semin Colon Rectal Surg*. 2016;27(4):172-175.
127. Colussi D, Brandi G, Bazzoli F, et al. Molecular pathways involved in colorectal cancer: implications for disease behavior and prevention. *Int J Mol Sci*. 2013;14(8):16365-16385.
128. Pino MS, Chung DC. The chromosomal instability pathway in colon cancer. *Gastroenterology*. 2010;138(6):2059-2072.
129. Vogelstein B, Papadopoulos N, Velculescu VE, et al. Cancer genome landscapes. *Science*. 2013;339(6127):1546-1558.
130. Grady WM, Carethers JM. Genomic and epigenetic instability in colorectal cancer pathogenesis. *Gastroenterology*. 2008;135(4):1079-1099.
131. De'angelis GL, Bottarelli L, Azzoni C, et al. Microsatellite instability in colorectal cancer. *Acta Bio Medica Atenei Parm*. 2018;89(Suppl 9):97.
132. Ashktorab H, Brim H, Dc W. DNA Methylation and Colorectal Cancer.
133. Marques RP, Duarte GS, Sterrantino C, et al. Triplet (FOLFOXIRI) versus doublet (FOLFOX or FOLFIRI) backbone chemotherapy as first-line treatment of metastatic colorectal cancer: A systematic review and meta-analysis. *Crit Rev Oncol Hematol*. 2017;118:54-62.
134. Van Der Jeught K, Xu HC, Li YJ, et al. Drug resistance and new therapies in colorectal cancer. *World J Gastroenterol*. 2018;24(34):3834.
135. Yan D, Tu L, Yuan H, et al. WBSCR22 confers oxaliplatin resistance in human colorectal cancer. *Sci Rep*. 2017;7(1).
136. Gnoni A, Russo A, Silvestris N, et al. Pharmacokinetic and metabolism determinants of fluoropyrimidines and oxaliplatin activity in treatment of colorectal patients. *Curr Drug Metab*. 2011;12(10):918-931.
137. de Man FM, Goey AKL, van Schaik RHN, et al. Individualization of Irinotecan Treatment: A Review of Pharmacokinetics, Pharmacodynamics, and Pharmacogenetics. *Clin Pharmacokinet*. 2018;57(10):1229-1254.

138. Nielsen DL, Palshof JA, Brünner N, et al. Implications of ABCG2 Expression on Irinotecan Treatment of Colorectal Cancer Patients: A Review. *Int J Mol Sci*. 2017;18(9).
139. Abdallah EA, Fanelli MF, Buim MEC, et al. Thymidylate synthase expression in circulating tumor cells: a new tool to predict 5-fluorouracil resistance in metastatic colorectal cancer patients. *Int J cancer*. 2015;137(6):1397-1405.
140. Douillard JY, Cunningham D, Roth AD, et al. Irinotecan combined with fluorouracil compared with fluorouracil alone. as first-line treatment for metastatic colorectal cancer: a multicentre randomised trial. *Lancet*. 2000;355(9209):1041-1047.
141. Barzaman K, Karami J, Zarei Z, et al. Breast cancer: Biology, biomarkers, and treatments. *Int Immunopharmacol*. 2020;84:106535.
142. Abderrahman B, Jordan VC. Steroid receptors in breast cancer. *Breast Compr Manag Benign Malig Dis*. 2018:272-281.e2.
143. Purdie CA, Quinlan P, Jordan LB, et al. Progesterone receptor expression is an independent prognostic variable in early breast cancer: a population-based study. *Br J Cancer*. 2014;110(3):565-572.
144. Yip CH, Rhodes A. Estrogen and progesterone receptors in breast cancer. *Futur Oncol*. 2014;10(14):2293-2301.
145. Mohammed H, Russell IA, Stark R, et al. Progesterone receptor modulates estrogen receptor-α action in breast cancer. *Nature*. 2015;523(7560):313.
146. Orrantia-Borunda E, Anchondo-Nuñez P, Acuña-Aguilar LE, et al. Subtypes of Breast Cancer. *Breast Cancer*. August 2022:31-42.
147. Hicks DG, Lester SC. Hormone Receptors (ER/PR). *Diagnostic Pathol Breast*. January 2016:430-439.
148. Yu K-D, Cai Y-W, Wu S-Y, et al. Estrogen receptor-low breast cancer: Biology chaos and treatment paradox. 2021.
149. Iqbal N, Iqbal N. Human Epidermal Growth Factor Receptor 2 (HER2) in Cancers: Overexpression and Therapeutic Implications. *Mol Biol Int*. 2014;2014:1-9.
150. Burstein HJ. The distinctive nature of HER2-positive breast cancers. *N Engl J Med*. 2005;353(16):1652-1654.
151. Park K, Han S, Kim HJ, et al. HER2 status in pure ductal carcinoma in situ and in the intraductal and invasive components of invasive ductal carcinoma determined

by fluorescence in situ hybridization and immunohistochemistry. *Histopathology*. 2006;48(6):702-707.

152. Hackshaw MD, Danysh HE, Henderson M, et al. Prognostic factors of brain metastasis and survival among HER2-positive metastatic breast cancer patients: a systematic literature review. *BMC Cancer*. 2021;21(1).
153. Gusterson BA, Gelber RD, Goldhirsch A, et al. Prognostic importance of c-erbB-2 expression in breast cancer. International (Ludwig) Breast Cancer Study Group. *J Clin Oncol*. 1992;10(7):1049-1056.
154. Andrulis IL, Bull SB, Blackstein ME, et al. neu/erbB-2 amplification identifies a poor-prognosis group of women with node-negative breast cancer. Toronto Breast Cancer Study Group. *J Clin Oncol*. 1998;16(4):1340-1349.
155. Ross JS, Fletcher JA. The HER-2/neu oncogene in breast cancer: Prognostic factor, predictive factor, and target for therapy. *Stem Cells*. 1998;16(6):413-428.
156. Slamon DJ, Clark GM, Wong SG, et al. Human breast cancer: correlation of relapse and survival with amplification of the HER-2/neu oncogene. *Science*. 1987;235(4785):182-191.
157. Veronesi U, Boyle P, Goldhirsch A, et al. Breast cancer. *Lancet*. 2005;365(9472):1727-1741.
158. Liedtke C, Mazouni C, Hess KR, et al. Response to neoadjuvant therapy and long-term survival in patients with triple-negative breast cancer. *J Clin Oncol*. 2008;26(8):1275-1281.
159. Hilton HN, Clarke CL, Graham JD. Estrogen and progesterone signalling in the normal breast and its implications for cancer development. *Mol Cell Endocrinol*. 2018;466:2-14.
160. Rakha EA, Green AR. Molecular classification of breast cancer: what the pathologist needs to know. *Pathology*. 2017;49(2):111-119.
161. Gupta P, Rai NN, Agarwal L, et al. Comparison of Molecular Subtypes of Carcinoma of the Breast in Two Different Age Groups: A Single Institution Experience. *Cureus*. 2018;10(6).
162. Ignatov A, Eggemann H, Burger E, et al. Patterns of breast cancer relapse in accordance to biological subtype. *J Cancer Res Clin Oncol*. 2018;144(7):1347-1355.
163. Park M, Kim D, Ko S, et al. Breast Cancer Metastasis: Mechanisms and Therapeutic Implications. *Int J Mol Sci*. 2022;23(12).

164. Liang Y, Zhang H, Song X, et al. Metastatic heterogeneity of breast cancer: Molecular mechanism and potential therapeutic targets. *Semin Cancer Biol*. 2020;60:14-27.
165. Fisusi FA, Akala EO. Drug Combinations in Breast Cancer Therapy. *Pharm Nanotechnol*. 2019;7(3):3.
166. Lyssiotis CA, Kimmelman AC. Metabolic Interactions in the Tumor Microenvironment. *Trends Cell Biol*. 2017;27(11):863-875.
167. Nunes SC. Tumor Microenvironment - Selective Pressures Boosting Cancer Progression. *Adv Exp Med Biol*. 2020;1219:35-49.
168. Xiao Y, Yu D. Tumor microenvironment as a therapeutic target in cancer.
169. Gupta S, Roy A, Dwarakanath BS. Metabolic cooperation and competition in the tumor microenvironment: Implications for therapy. *Front Oncol*. 2017;7(APR):68.
170. Cairns RA, Harris IS, Mak TW. Regulation of cancer cell metabolism. *Nat Rev Cancer 2011 112*. 2011;11(2):85-95.
171. Lunt SJ, Chaudary N, Hill RP. The tumor microenvironment and metastatic disease. *Clin Exp Metastasis*. 2009;26(1):19-34.
172. Warburg O, Minami S. Versuche an Überlebendem Carcinom-gewebe. *Klin Wochenschr*. 1923;2(17):776-777.
173. Warburg O. Über den Stoffwechsel der Carcinomzelle. *Naturwissenschaften*. 1924;12(50):1131-1137.
174. Warburg O. On the origin of cancer cells. *Science*. 1956;123(3191):309-314.
175. Pascale RM, Calvisi DF, Simile MM, et al. The Warburg Effect 97 Years after Its Discovery. *Cancers (Basel)*. 2020;12(10):1-33.
176. Serpa J. Metabolic Remodeling as a Way of Adapting to Tumor Microenvironment (TME), a Job of Several Holders. *Adv Exp Med Biol*. 2020;1219:1-34.
177. Gaglio D, Metallo CM, Gameiro PA, et al. Oncogenic K-Ras decouples glucose and glutamine metabolism to support cancer cell growth. *Mol Syst Biol*. 2011;7(523):523.
178. Altman BJ, Stine ZE, Dang C V. From Krebs to Clinic: Glutamine Metabolism to CancerTherapy. *Nat Rev Cancer*. 2016;16(10):619.
179. Wellen KE, Lu C, Mancuso A, et al. The hexosamine biosynthetic pathway couples growth factor-induced glutamine uptake to glucose metabolism. *Genes*

Dev. 2010;24(24):2784-2799.

180. Ge T, Yang J, Zhou S, et al. The Role of the Pentose Phosphate Pathway in Diabetes and Cancer. *Front Endocrinol (Lausanne)*. 2020;11:507678.
181. Yen WC, Wu YH, Wu CC, et al. Impaired inflammasome activation and bacterial clearance in G6PD deficiency due to defective NOX/p38 MAPK/AP-1 redox signaling. *Redox Biol*. 2020;28.
182. Traverso N, Ricciarelli R, Nitti M, et al. Role of glutathione in cancer progression and chemoresistance. *Oxid Med Cell Longev*. 2013;2013.
183. Mayers JR, Vander Heiden MG. Famine versus feast: understanding the metabolism of tumors in vivo. *Trends Biochem Sci*. 2015;40(3):130-140.
184. Lacey JM, Wilmore DW. Is glutamine a conditionally essential amino acid? *Nutr Rev*. 1990;48(8):297-309.
185. Curthoys NP, Watford M. Regulation of glutaminase activity and glutamine metabolism. *Annu Rev Nutr*. 1995;15:133-159.
186. Yelamanchi SD, Jayaram S, Thomas JK, et al. A pathway map of glutamate metabolism. *J Cell Commun Signal*. 2016;10(1):69.
187. Shuvalov O, Petukhov A, Daks A, et al. One-carbon metabolism and nucleotide biosynthesis as attractive targets for anticancer therapy. *Oncotarget*. 2017;8(14):23955.
188. Asantewaa G, Harris IS. Glutathione and its precursors in cancer. *Curr Opin Biotechnol*. 2021;68:292-299.
189. Yang M, Vousden KH. Serine and one-carbon metabolism in cancer. *Nat Rev Cancer*. 2016;16(10):650-662.
190. Locasale JW. Serine, glycine and the one-carbon cycle: cancer metabolism in full circle. *Nat Rev Cancer*. 2013;13(8):572.
191. Weinberg F, Hamanaka R, Wheaton WW, et al. Mitochondrial metabolism and ROS generation are essential for Kras-mediated tumorigenicity. *Proc Natl Acad Sci U S A*. 2010;107(19):8788-8793.
192. Bonifácio VDB, Pereira SA, Serpa J, et al. Cysteine metabolic circuitries: druggable targets in cancer. 2021;124(5):862.
193. Liu J, Xia X, Huang P. xCT: A Critical Molecule That Links Cancer Metabolism to Redox Signaling. *Mol Ther*. 2020;28(11):2358-2366.
194. Nunes SC, Ramos C, Santos I, et al. Cysteine Boosts Fitness Under Hypoxia-Mimicked Conditions in Ovarian Cancer by Metabolic Reprogramming. *Front*

cell Dev Biol. 2021;9.

195. Oshimura E, Sakamoto K. Amino acids, peptides, and proteins. *Cosmet Sci Technol Theor Princ Appl*. March 2017:285-303.
196. Safrhansova L, Hlozkova K, Starkova J. Targeting amino acid metabolism in cancer. *Int Rev Cell Mol Biol*. 2022;373:37-79.
197. Serpa J. Cysteine as a Carbon Source, a Hot Spot in Cancer Cells Survival. 2020;10:533316.
198. Arensman MD, Yang XS, Leahy DM, et al. Cystine-glutamate antiporter xCT deficiency suppresses tumor growth while preserving antitumor immunity. *Proc Natl Acad Sci U S A*. 2019;116(19):9533-9542.
199. Gout PW, Buckley AR, Simms CR, et al. Sulfasalazine, a potent suppressor of lymphoma growth by inhibition of the x(c)- cystine transporter: a new action for an old drug. *Leukemia*. 2001;15(10):1633-1640.
200. Badgley MA, Kremer DM, Carlo Maurer H, et al. Cysteine depletion induces pancreatic tumor ferroptosis in mice. *Science*. 2020;368(6486).
201. Daher B, Parks SK, Durivault J, et al. Genetic Ablation of the Cystine Transporter xCT in PDAC Cells Inhibits mTORC1, Growth, Survival, and Tumor Formation via Nutrient and Oxidative Stresses. *Cancer Res*. 2019;79(15):3877-3890.
202. Lo M, Wang YZ, Gout PW. The x(c)- cystine/glutamate antiporter: a potential target for therapy of cancer and other diseases. *J Cell Physiol*. 2008;215(3):593-602.
203. Liu R, Blower PE, Pham AN, et al. Cystine-glutamate transporter SLC7A11 mediates resistance to geldanamycin but not to 17-(allylamino)-17-demethoxygeldanamycin. *Mol Pharmacol*. 2007;72(6):1637-1646.
204. Huang Y, Dai Z, Barbacioru C, et al. Cystine-glutamate transporter SLC7A11 in cancer chemosensitivity and chemoresistance. *Cancer Res*. 2005;65(16):7446-7454.
205. Okuno S, Sato H, Kuriyama-Matsumura K, et al. Role of cystine transport in intracellular glutathione level and cisplatin resistance in human ovarian cancer cell lines. *Br J Cancer*. 2003;88(6):951-956.
206. Tarragó-Celada J, Foguet C, Tarrado-Castellarnau M, et al. Cysteine and Folate Metabolism Are Targetable Vulnerabilities of Metastatic Colorectal Cancer. *Cancers (Basel)*. 2021;13(3):1-22.

207. Zhao X, Li Y, Wu H. A novel scoring system for acute myeloid leukemia risk assessment based on the expression levels of six genes. *Int J Mol Med*. 2018;42(3):1495-1507.
208. Tang B, Zhu J, Liu F, et al. xCT contributes to colorectal cancer tumorigenesis through upregulation of the MELK oncogene and activation of the AKT/mTOR cascade. *Cell Death Dis*. 2022;13(4).
209. Robert SM, Buckingham SC, Campbell SL, et al. SLC7A11 expression is associated with seizures and predicts poor survival in patients with malignant glioma. *Sci Transl Med*. 2015;7(289).
210. Shin SS, Jeong BS, Wall BA, et al. Participation of xCT in melanoma cell proliferation in vitro and tumorigenesis in vivo. *Oncogenesis*. 2018;7(11).
211. Zhong W, Weiss HL, Jayswal RD, et al. Extracellular redox state shift: A novel approach to target prostate cancer invasion. *Free Radic Biol Med*. 2018;117:99-109.
212. Ji X, Qian J, Rahman SMJ, et al. xCT (SLC7A11)-mediated metabolic reprogramming promotes non-small cell lung cancer progression. *Oncogene*. 2018;37(36):5007-5019.
213. Yin F, Yi S, Wei L, et al. Microarray-based identification of genes associated with prognosis and drug resistance in ovarian cancer. *J Cell Biochem*. 2019;120(4):6057-6070.
214. Briggs KJJ, Koivunen P, Cao S, et al. Paracrine Induction of HIF by Glutamate in Breast Cancer: EglN1 Senses Cysteine. *Cell*. 2016;166(1):126-139.
215. Lanzardo S, Conti L, Rooke R, et al. Immunotargeting of Antigen xCT Attenuates Stem-like Cell Behavior and Metastatic Progression in Breast Cancer. *Cancer Res*. 2016;76(1):62-72.
216. Hanigan MH, Ricketts WA. Extracellular glutathione is a source of cysteine for cells that express gamma-glutamyl transpeptidase. *Biochemistry*. 1993;32(24):6302-6306.
217. Davidson SM, Jonas O, Keibler MA, et al. Direct evidence for cancer-cell-autonomous extracellular protein catabolism in pancreatic tumors. *Nat Med*. 2017;23(2):235-241.
218. Mosharov E, Cranford MR, Banerjee R. The quantitatively important relationship between homocysteine metabolism and glutathione synthesis by the transsulfuration pathway and its regulation by redox changes. *Biochemistry*.

2000;39(42):13005-13011.

219. Margaritelis N V., Chatzinikolaou PN, Bousiou F V., et al. Dietary Cysteine Intake is Associated with Blood Glutathione Levels and Isometric Strength. *Int J Sports Med*. 2021;42(5):441-447.
220. Scalise M, Console L, Galluccio M, et al. Exploiting Cysteine Residues of SLC Membrane Transporters as Targets for Drugs. *SLAS Discov Adv life Sci R D*. 2019;24(9):867-881.
221. Jiang Y, Cao Y, Wang Y, et al. Cysteine transporter SLC3A1 promotes breast cancer tumorigenesis. *Theranostics*. 2017;7(4):1036-1046.
222. Bianchi MG, Bardelli D, Chiu M, et al. Changes in the expression of the glutamate transporter EAAT3/EAAC1 in health and disease. *Cell Mol Life Sci*. 2014;71(11):2001-2015.
223. Pedraz-Cuesta E, Christensen S, Jensen AA, et al. The glutamate transport inhibitor DL-Threo-β-Benzyloxyaspartic acid (DL-TBOA) differentially affects SN38- and oxaliplatin-induced death of drug-resistant colorectal cancer cells. *BMC Cancer*. 2015;15(1).
224. Fan H, Lu S, Wang S, et al. Identification of critical genes associated with human osteosarcoma metastasis based on integrated gene expression profiling. *Mol Med Rep*. 2019;20(2):915-930.
225. Xiong J, Wang N, Zhong HJ, et al. SLC1A1 mediated glutamine addiction and contributed to natural killer T-cell lymphoma progression with immunotherapeutic potential. *EBioMedicine*. 2021;72.
226. Akaike T, Ida T, Wei FY, et al. Cysteinyl-tRNA synthetase governs cysteine polysulfidation and mitochondrial bioenergetics. *Nat Commun 2017 81*. 2017;8(1):1-15.
227. Renga B. Hydrogen sulfide generation in mammals: The molecular biology of cystathionine-β-synthase (CBS) and cystathionine-γ-lyase (CSE). *Inflamm Allergy - Drug Targets*. 2011;10(2):85-91.
228. Bełtowski J. Synthesis, Metabolism, and Signaling Mechanisms of Hydrogen Sulfide: An Overview. *Methods Mol Biol*. 2019;2007:1-8.
229. Shibuya N, Kimura H. Production of hydrogen sulfide from d-cysteine and its therapeutic potential. *Front Endocrinol (Lausanne)*. 2013;4(JUL).
230. Tomisawa H, Ichimoto N, Takanohashi Y, et al. Purification and characterization of cysteine conjugate transaminases from rat liver. *Xenobiotica*.

1988;18(9):1015-1028.

231. Hipólito A, Nunes SC, Vicente JB, et al. Cysteine Aminotransferase (CAT): A Pivotal Sponsor in Metabolic Remodeling and an Ally of 3-Mercaptopyruvate Sulfurtransferase (MST) in Cancer. *Molecules*. 2020;25(17).
232. Shibuya N, Tanaka M, Yoshida M, et al. 3-Mercaptopyruvate sulfurtransferase produces hydrogen sulfide and bound sulfane sulfur in the brain. *Antioxid Redox Signal*. 2009;11(4):703-714.
233. Nagahara N. Multiple role of 3-mercaptopyruvate sulfurtransferase: antioxidative function, H2 S and polysulfide production and possible SOx production. *Br J Pharmacol*. 2018;175(4):577-589.
234. Yadav PK, Yamada K, Chiku T, et al. Structure and kinetic analysis of H2S production by human mercaptopyruvate sulfurtransferase. *J Biol Chem*. 2013;288(27):20002-20013.
235. Bella DL, Hirschberger LL, Hosokawa Y, et al. Mechanisms involved in the regulation of key enzymes of cysteine metabolism in rat liver in vivo. *Am J Physiol*. 1999;276(2).
236. Stipanuk MH. Sulfur amino acid metabolism: pathways for production and removal of homocysteine and cysteine. *Annu Rev Nutr*. 2004;24:539-577.
237. Lee JI, Londono M, Hirschberger LL, et al. Regulation of cysteine dioxygenase and γ-glutamylcysteine synthetase is associated with hepatic cysteine level. *J Nutr Biochem*. 2004;15(2):112-122.
238. Bella DL, Hahn C, Stipanuk MH. Effects of nonsulfur and sulfur amino acids on the regulation of hepatic enzymes of cysteine metabolism. *Am J Physiol*. 1999;277(1).
239. Sen S, Kawahara B, Gupta D, et al. Role of cystathionine β-synthase in human breast Cancer. *Free Radic Biol Med*. 2015;86:228-238.
240. Poisson LM, Munkarah A, Madi H, et al. A metabolomic approach to identifying platinum resistance in ovarian cancer. *J Ovarian Res*. 2015;8(1).
241. Panza E, De Cicco P, Armogida C, et al. Role of the cystathionine γ lyase/hydrogen sulfide pathway in human melanoma progression. 2015;28(1):61-72.
242. Xu M, Zhang L, Song S, et al. Hydrogen sulfide: Recent progress and perspectives for the treatment of dermatological diseases. *J Adv Res*. 2020;27:11-17.

243. Ascenção K, Szabo C. Emerging roles of cystathionine β-synthase in various forms of cancer. *Redox Biol*. 2022;53.
244. Bhattacharyya S, Saha S, Giri K, et al. Cystathionine beta-synthase (CBS) contributes to advanced ovarian cancer progression and drug resistance. *PLoS One*. 2013;8(11).
245. Sekiguchi F, Sekimoto T, Ogura A, et al. Endogenous Hydrogen Sulfide Enhances Cell Proliferation of Human Gastric Cancer AGS Cells. *Biol Pharm Bull*. 2016;39(5):887-890.
246. Alix-Panabières C, Cayrefourcq L, Mazard T, et al. Molecular Portrait of Metastasis-Competent Circulating Tumor Cells in Colon Cancer Reveals the Crucial Role of Genes Regulating Energy Metabolism and DNA Repair. *Clin Chem*. 2017;63(3):700-713.
247. Turbat-Herrera EA, Kilpatrick MJ, Chen J, et al. Cystathione β-Synthase Is Increased in Thyroid Malignancies. *Anticancer Res*. 2018;38(11):6085-6090.
248. You J, Shi X, Liang H, et al. Cystathionine- γ-lyase promotes process of breast cancer in association with STAT3 signaling pathway. *Oncotarget*. 2017;8(39).
249. Wang L, Shi H, Zhang XX, et al. I157172, a novel inhibitor of cystathionine γ-lyase, inhibits growth and migration of breast cancer cells via SIRT1-mediated deacetylation of STAT3. *Oncol Rep*. 2019;41(1):427-436.
250. Kaczor-Kamińska M, Kaminski K, Wróbel M. The Expression and Activity of Rhodanese, 3-Mercaptopyruvate Sulfurtransferase, Cystathionine γ-Lyase in the Most Frequently Chosen Cellular Research Models. *Biomolecules*. 2021;11(12).
251. Jurkowska H, Placha W, Nagahara N, et al. The expression and activity of cystathionine-γ-lyase and 3-mercaptopyruvate sulfurtransferase in human neoplastic cell lines. 2011;41(1):151-158.
252. Harada H, Hosoda K, Moriya H, et al. Cancer-specific promoter DNA methylation of Cysteine dioxygenase type 1 (CDO1) gene as an important prognostic biomarker of gastric cancer. *PLoS One*. 2019;14(4).
253. Jeschke J, O'Hagan HM, Zhang W, et al. Frequent inactivation of cysteine dioxygenase type 1 contributes to survival of breast cancer cells and resistance to anthracyclines. *Clin Cancer Res*. 2013;19(12):3201-3211.
254. Kang YP, Torrente L, Falzone A, et al. Cysteine dioxygenase 1 is a metabolic liability for non-small cell lung cancer. *Elife*. 2019;8.
255. Hao S, Yu J, He W, et al. Cysteine Dioxygenase 1 Mediates Erastin-Induced

Ferroptosis in Human Gastric Cancer Cells. *Neoplasia*. 2017;19(12):1022-1032.
256. Nunes SC, Ramos C, Lopes-Coelho F, et al. Cysteine allows ovarian cancer cells to adapt to hypoxia and to escape from carboplatin cytotoxicity. 2018;8(1).
257. Módis K, Coletta C, Erdélyi K, et al. Intramitochondrial hydrogen sulfide production by 3-mercaptopyruvate sulfurtransferase maintains mitochondrial electron flow and supports cellular bioenergetics. *FASEB J*. 2013;27(2):601-611.
258. Módis K, Ju YJ, Ahmad A, et al. S-Sulfhydration of ATP synthase by hydrogen sulfide stimulates mitochondrial bioenergetics. *Pharmacol Res*. 2016;113(Pt A):116-124.
259. Kabil O, Banerjee R. Enzymology of H2S biogenesis, decay and signaling. *Antioxid Redox Signal*. 2014;20(5):770-782.
260. Filipovic MR, Zivanovic J, Alvarez B, et al. Chemical Biology of H2S Signaling through Persulfidation. *Chem Rev*. 2018;118(3):1253-1337.
261. Cuevasanta E, Möller MN, Alvarez B. Biological chemistry of hydrogen sulfide and persulfides. *Arch Biochem Biophys*. 2017;617:9-25.
262. Jiang J, Chan A, Ali S, et al. Hydrogen Sulfide--Mechanisms of Toxicity and Development of an Antidote. *Sci Rep*. 2016;6.
263. Vicente JB, Malagrinò F, Arese M, et al. Bioenergetic relevance of hydrogen sulfide and the interplay between gasotransmitters at human cystathionine β-synthase. *Biochim Biophys Acta*. 2016;1857(8):1127-1138.
264. Giuffrè A, Tomé CS, Fernandes DGF, et al. Hydrogen Sulfide Metabolism and Signaling in the Tumor Microenvironment. *Adv Exp Med Biol*. 2020;1219:335-353.
265. Zhen Y, Pan W, Hu F, et al. Exogenous hydrogen sulfide exerts proliferation/anti-apoptosis/angiogenesis/migration effects via amplifying the activation of NF-κB pathway in PLC/PRF/5 hepatoma cells. *Int J Oncol*. 2015;46(5):2194-2204.
266. Tiong CX, Lu M, Bian JS. Protective effect of hydrogen sulphide against 6-OHDA-induced cell injury in SH-SY5Y cells involves PKC/PI3K/Akt pathway. *Br J Pharmacol*. 2010;161(2):467.
267. Rose P, Moore PK, Ming SH, et al. Hydrogen sulfide protects colon cancer cells from chemopreventative agent β-phenylethyl isothiocyanate induced apoptosis. *World J Gastroenterol*. 2005;11(26):3990.
268. Wu D, Li M, Tian W, et al. Hydrogen sulfide acts as a double-edged sword in

human hepatocellular carcinoma cells through EGFR/ERK/MMP-2 and PTEN/AKT signaling pathways. *Sci Rep*. 2017;7(1).

269. Tao BB, Cai WJ, Zhu YC. H2S Is a Promoter of Angiogenesis: Identification of H2S "Receptors" and Its Molecular Switches in Vascular Endothelial Cells. *Handb Exp Pharmacol*. 2015;230:137-152.
270. Wang M, Yan J, Cao X, et al. Hydrogen sulfide modulates epithelial-mesenchymal transition and angiogenesis in non-small cell lung cancer via HIF-1α activation. *Biochem Pharmacol*. 2020;172.
271. Wu D, Li J, Zhang Q, et al. Exogenous Hydrogen Sulfide Regulates the Growth of Human Thyroid Carcinoma Cells. *Oxid Med Cell Longev*. 2019;2019.
272. Cai F-F, Xu H-R, Yu S-H, et al. ADT-OH inhibits malignant melanoma metastasis in mice via suppressing CSE/CBS and FAK/Paxillin signaling pathway.
273. Leikam C, Hufnagel A, Walz S, et al. Cystathionase mediates senescence evasion in melanocytes and melanoma cells. *Oncogene*. 2014;33(6):771-782.
274. Jurkowska H, Placha W, Nagahara N, et al. The expression and activity of cystathionine-γ-lyase and 3-mercaptopyruvate sulfurtransferase in human neoplastic cell lines. *Amino Acids*. 2011;41(1):151-158.
275. Szczesny B, Marcatti M, Zatarain JR, et al. Inhibition of hydrogen sulfide biosynthesis sensitizes lung adenocarcinoma to chemotherapeutic drugs by inhibiting mitochondrial DNA repair and suppressing cellular bioenergetics. *Sci Rep*. 2016;6.
276. Anderson S, Bankier AT, Barrell BG, et al. Sequence and organization of the human mitochondrial genome. *Nature*. 1981;290(5806):457-465.
277. Asimakopoulou A, Panopoulos P, Chasapis CT, et al. Selectivity of commonly used pharmacological inhibitors for cystathionine β synthase (CBS) and cystathionine γ lyase (CSE). 2013;169(4).
278. Han YQ, Zhang ZB, Wang K, et al. Cystathionine β-synthase expression correlates with tumor development and poor prognosis in lung squamous cell carcinoma patients. *Neoplasma*. 2022;69(4):868-876.
279. Russo A, Saide A, Cagliani R, et al. rpL3 promotes the apoptosis of p53 mutated lung cancer cells by down-regulating CBS and NFκB upon 5-FU treatment. *Sci Rep*. 2016;6.
280. Phillips CM, Zatarain JR, Nicholls ME, et al. Upregulation of Cystathionine-β-

Synthase in Colonic Epithelia Reprograms Metabolism and Promotes Carcinogenesis. *Cancer Res*. 2017;77(21):5741-5754.

281. Chen S, Yue T, Huang Z, et al. Inhibition of hydrogen sulfide synthesis reverses acquired resistance to 5-FU through miR-215-5p-EREG/TYMS axis in colon cancer cells. *Cancer Lett*. 2019;466:49-60.
282. Oláh G, Módis K, Törö G, et al. Role of endogenous and exogenous nitric oxide, carbon monoxide and hydrogen sulfide in HCT116 colon cancer cell proliferation. *Biochem Pharmacol*. 2018;149:186-204.
283. Szabo C, Coletta C, Chao C, et al. Tumor-derived hydrogen sulfide, produced by cystathionine-β-synthase, stimulates bioenergetics, cell proliferation, and angiogenesis in colon cancer. *Proc Natl Acad Sci U S A*. 2013;110(30):12474-12479.
284. Guo S, Li J, Huang Z, et al. The CBS-H2S axis promotes liver metastasis of colon cancer by upregulating VEGF through AP-1 activation. *Br J Cancer*. 2022;126(7):1055-1066.
285. Yue T, Zuo S, Bu D, et al. Aminooxyacetic acid (AOAA) sensitizes colon cancer cells to oxaliplatin via exaggerating apoptosis induced by ROS. *J Cancer*. 2020;11(7):1828-1838.
286. Zhao H, Ming T, Tang S, et al. Wnt signaling in colorectal cancer: pathogenic role and therapeutic target. *Mol Cancer*. 2022;21(1).
287. Fan K, Li N, Qi J, et al. Wnt/β-catenin signaling induces the transcription of cystathionine-γ-lyase, a stimulator of tumor in colon cancer. *Cell Signal*. 2014;26(12):2801-2808.
288. Ascenção K, Lheimeur B, Szabo C. Regulation of CyR61 expression and release by 3-mercaptopyruvate sulfurtransferase in colon cancer cells. *Redox Biol*. 2022;56.
289. Bantzi M, Augsburger F, Loup J, et al. Novel Aryl-Substituted Pyrimidones as Inhibitors of 3-Mercaptopyruvate Sulfurtransferase with Antiproliferative Efficacy in Colon Cancer. *J Med Chem*. 2021;64(9):6221-6240.
290. Zuhra K, Tomé CS, Masi L, et al. N-Acetylcysteine Serves as Substrate of 3-Mercaptopyruvate Sulfurtransferase and Stimulates Sulfide Metabolism in Colon Cancer Cells. *Cells*. 2019;8(8).
291. Augsburger F, Randi EB, Jendly M, et al. Role of 3-Mercaptopyruvate Sulfurtransferase in the Regulation of Proliferation, Migration, and Bioenergetics

in Murine Colon Cancer Cells. *Biomolecules*. 2020;10(3).

292. Ramasamy S, Singh S, Taniere P, et al. Sulfide-detoxifying enzymes in the human colon are decreased in cancer and upregulated in differentiation. *Am J Physiol Gastrointest Liver Physiol*. 2006;291(2).
293. Youness RA, Gad AZ, Sanber K, et al. Targeting hydrogen sulphide signaling in breast cancer. *J Adv Res*. 2021;27:177.
294. Knethen V, Sousa Santos S, de Oliveira Cavalcanti Peres Rodrigues L, et al. Role of Cystathionine β-Synthase and 3-Mercaptopyruvate Sulfurtransferase in the Regulation of Proliferation, Migration, and Bioenergetics of Murine Breast Cancer Cells. 2023.
295. Peng J, Zhang D. Potentials of CCL21 and CBS as Therapeutic Approaches for Breast Cancer. *Eur Surg Res*. 2022;63(4):211-223.
296. Khan NH, Wang D, Wang W, et al. Pharmacological Inhibition of Endogenous Hydrogen Sulfide Attenuates Breast Cancer Progression. *Molecules*. 2022;27(13).
297. Wang L, Shi H, Liu Y, et al. Cystathionine-γ-lyase promotes the metastasis of breast cancer via the VEGF signaling pathway. *Int J Oncol*. 2019;55(2):473.
298. Bronowicka-adamska P, Bentke A, Lasota M, et al. Effect of S-Allyl –L-Cysteine on MCF-7 Cell Line 3-Mercaptopyruvate Sulfurtransferase/Sulfane Sulfur System, Viability and Apoptosis. *Int J Mol Sci*. 2020;21(3).
299. Brait M, Ling S, Nagpal JK, et al. Cysteine dioxygenase 1 is a tumor suppressor gene silenced by promoter methylation in multiple human cancers. *PLoS One*. 2012;7(9).
300. Chen M, Zhu JY, Mu WJ, et al. Cysteine dioxygenase type 1 (CDO1): Its functional role in physiological and pathophysiological processes. *Genes Dis*. 2023;10(3):877.
301. Kojima K, Nakamura T, Ohbu M, et al. Cysteine dioxygenase type 1 (CDO1) gene promoter methylation during the adenoma-carcinoma sequence in colorectal cancer. 2018;13(5):e0194785.
302. Vedeld HM, Andresen K, Eilertsen IA, et al. The novel colorectal cancer biomarkers CDO1, ZSCAN18 and ZNF331 are frequently methylated across gastrointestinal cancers. *Int J Cancer*. 2015;136(4):844.
303. Yokoi K, Harada H, Yokota K, et al. Epigenetic Status of CDO1 Gene May Reflect Chemosensitivity in Colon Cancer with Postoperative Adjuvant

Chemotherapy. *Ann Surg Oncol*. 2019;26(2):406-414.

304. Yin W, Wang X, Li Y, et al. Promoter hypermethylation of cysteine dioxygenase type 1 in patients with non-small cell lung cancer. *Oncol Lett*. 2020;20(1):967.
305. Ohta T, Iijima K, Miyamoto M, et al. Loss of Keap1 function activates Nrf2 and provides advantages for lung cancer cell growth. *Cancer Res*. 2008;68(5):1303-1309.
306. Denicola GM, Karreth FA, Humpton TJ, et al. Oncogene-induced Nrf2 transcription promotes ROS detoxification and tumorigenesis. *Nature*. 2011;475(7354):106-110.
307. Minatani N, Waraya M, Yamashita K, et al. Prognostic Significance of Promoter DNA Hypermethylation of cysteine dioxygenase 1 (CDO1) Gene in Primary Breast Cancer. *PLoS One*. 2016;11(1).
308. Bai Y, Yuan F, Yu J, et al. A BIRC5High COD1Low Cancer Tissue Phenotype Indicates Poorer Prognosis of Metastatic Breast Cancer Patients. *Cancer Inform*. 2022;21.
309. Tanaka Y, Kosaka Y, Waraya M, et al. Differential Prognostic Relevance of Promoter DNA Methylation of CDO1 and HOPX in Primary Breast Cancer. *Anticancer Res*. 2019;39(5):2289-2298.
310. Dietrich D, Krispin M, Dietrich J, et al. CDO1 promoter methylation is a biomarker for outcome prediction of anthracycline treated, estrogen receptor-positive, lymph node-positive breast cancer patients. *BMC Cancer*. 2010;10.
311. Fodale V, Pierobon M, Liotta L, et al. Mechanism of Cell Adaptation: When and How Do Cancer Cells Develop Chemoresistance? *Cancer J*. 2011;17(2):89.
312. Chapal N, Molina L, Molina F, et al. Pharmacoproteomic approach to the study of drug mode of action, toxicity, and resistance: applications in diabetes and cancer. *Fundam Clin Pharmacol*. 2004;18(4):413-422.
313. Lopes-Coelho F, Gouveia-Fernandes S, Gonçalves LG, et al. HNF1β drives glutathione (GSH) synthesis underlying intrinsic carboplatin resistance of ovarian clear cell carcinoma (OCCC). *Tumour Biol*. 2016;37(4):4813-4829.
314. Zanotto-Filho A, Pragathi Masamsetti V, Loranc E, et al. Alkylating Agent-Induced NRF2 Blocks Endoplasmic Reticulum Stress-Mediated Apoptosis via Control of Glutathione Pools and Protein Thiol Homeostasis. *Mol Cancer Ther*. 2016;15(12):3000-3014.
315. Lien EC, Lyssiotis CA, Juvekar A, et al. Glutathione biosynthesis is a metabolic

vulnerability in PI(3)K/Akt-driven breast cancer. *Nat Cell Biol*. 2016;18(5):572-578.

316. Harris IS, Treloar AE, Inoue S, et al. Glutathione and thioredoxin antioxidant pathways synergize to drive cancer initiation and progression. *Cancer Cell*. 2015;27(2):211-222.
317. Colla R, Izzotti A, De Ciucis C, et al. Glutathione-mediated antioxidant response and aerobic metabolism: two crucial factors involved in determining the multi-drug resistance of high-risk neuroblastoma. *Oncotarget*. 2016;7(43):70715-70737.
318. Untereiner AA, Pavlidou A, Druzhyna N, et al. Drug resistance induces the upregulation of H2S-producing enzymes in HCT116 colon cancer cells. *Biochem Pharmacol*. 2018;149:174-185.
319. Stokes E, Shuang T, Zhang Y, et al. Efflux inhibition by H2S confers sensitivity to doxorubicin-induced cell death in liver cancer cells. *Life Sci*. 2018;213:116-125.
320. Shackelford RE, Mohammad IZ, Meram AT, et al. Molecular Functions of Hydrogen Sulfide in Cancer. *Pathophysiology*. 2021;28(3):437.
321. Yang WS, Sriramaratnam R, Welsch ME, et al. Regulation of ferroptotic cancer cell death by GPX4. *Cell*. 2014;156(1-2):317-331.
322. Li J, Cao F, Yin H liang, et al. Ferroptosis: past, present and future. *Cell Death Dis*. 2020;11(2).
323. Lopes-Coelho F, Martins F, Hipólito A, et al. The Activation of Endothelial Cells Relies on a Ferroptosis-Like Mechanism: Novel Perspectives in Management of Angiogenesis and Cancer Therapy. *Front Oncol*. 2021;11:656229.
324. Dixon SJ, Lemberg KM, Lamprecht MR, et al. Ferroptosis: an iron-dependent form of nonapoptotic cell death. *Cell*. 2012;149(5):1060-1072.
325. Koppula P, Zhuang L, Gan B. Cystine transporter SLC7A11/xCT in cancer: ferroptosis, nutrient dependency, and cancer therapy. *Protein Cell*. 2021;12(8):599.
326. Nunes SC, Lopes-Coelho F, Gouveia-Fernandes S, et al. Cysteine boosters the evolutionary adaptation to CoCl2 mimicked hypoxia conditions, favouring carboplatin resistance in ovarian cancer. *BMC Evol Biol*. 2018;18(1).
327. Sandru A, Voinea S, Panaitescu E, et al. Survival rates of patients with metastatic malignant melanoma. *J Med Life*. 2014;7(4):572.

328. Santourlidis S, Schulz WA, Araúzo-Bravo MJ, et al. Epigenetics in the Diagnosis and Therapy of Malignant Melanoma. *Int J Mol Sci*. 2022;23(3):23.
329. Wasif N, Bagaria SP, Ray P, et al. Does metastasectomy improve survival in patients with Stage IV melanoma? A cancer registry analysis of outcomes. *J Surg Oncol*. 2011;104(2):111.
330. Palmer SR, Erickson LA, Ichetovkin I, et al. Circulating serologic and molecular biomarkers in malignant melanoma. *Mayo Clin Proc*. 2011;86(10):981-990.
331. Eggermont AMM, Blank CU, Mandalà M, et al. Adjuvant pembrolizumab versus placebo in resected stage III melanoma (EORTC 1325-MG/KEYNOTE-054): distant metastasis-free survival results from a double-blind, randomised, controlled, phase 3 trial. *Lancet Oncol*. 2021;22(5):643-654.
332. Franken MG, Leeneman B, Aarts MJB, et al. Trends in survival and costs in metastatic melanoma in the era of novel targeted and immunotherapeutic drugs. *ESMO Open*. 2021;6(6):100320.
333. Kamb A, Shattuck-Eidens D, Eeles R, et al. Analysis of the p16 gene (CDKN2) as a candidate for the chromosome 9p melanoma susceptibility locus. *Nat Genet*. 1994;8(1):22-26.
334. Shi J, Yang XR, Ballew B, et al. Rare missense variants in POT1 predispose to familial cutaneous malignant melanoma. *Nat Genet*. 2014;46(5):482-486.
335. Bassoli S, Pellegrini C, Longo C, et al. Clinical, dermoscopic, and confocal features of nevi and melanomas in a multiple primary melanoma patient with the MITF p.E318K homozygous mutation. *Melanoma Res*. 2018;28(2):166-169.
336. Adler NR, Kelly JW, Haydon A, et al. Clinicopathological characteristics and prognosis of patients with multiple primary melanomas. *Br J Dermatol*. 2018;178(1):e44-e45.
337. Tran KD, Chakravarty T, Garzon JL, et al. Hypoxic response is driven by the BAF form of SWI/SNF.
338. Gatchalian J, Malik S, Ho J, et al. A non-canonical BRD9-containing BAF chromatin remodeling complex regulates naive pluripotency in mouse embryonic stem cells. *Nat Commun 2018 91*. 2018;9(1):1-16.
339. Huang H, Wang Y, Li Q, et al. miR-140-3p functions as a tumor suppressor in squamous cell lung cancer by regulating BRD9. *Cancer Lett*. 2019;446:81-89.
340. Lou W, Gao K, Xu C, et al. Bromodomain-containing protein 9 is a prognostic biomarker associated with immune infiltrates and promotes tumor malignancy

through activating notch signaling pathway in negative HIF-2α clear cell renal cell carcinoma. *IUBMB Life*. 2021;73(11):1334-1347.

341. Dou C, Sun L, Wang L, et al. Bromodomain-containing protein 9 promotes the growth and metastasis of human hepatocellular carcinoma by activating the TUFT1/AKT pathway. *Cell Death Dis*. 2020;11(9).
342. Fang D, Wang MR, Guan JL, et al. Bromodomain-containing protein 9 promotes hepatocellular carcinoma progression via activating the Wnt/β-catenin signaling pathway. *Exp Cell Res*. 2021;406(2).
343. Barma N, Stone TC, Echeverria LMC, et al. Exploring the value of BRD9 as a biomarker, therapeutic target and co-target in prostate cancer. *Biomolecules*. 2021;11(12).
344. Bishop DT, Demenais F, Iles MM, et al. Genome-wide association study identifies three loci associated with melanoma risk. *Nat Genet*. 2009;41(8):920-925.
345. Nguyen NT, David F. MITF and UV responses in skin: from pigmentation to addiction.
346. Jara JR, Aroca P, Solano F, et al. The role of sulfhydryl compounds in mammalian melanogenesis: the effect of cysteine and glutathione upon tyrosinase and the intermediates of the pathway. *Biochim Biophys Acta - Gen Subj*. 1988;967(2):296-303.
347. RORSMAN H, ALBERTSSON E, EDHOLM LE, et al. Thiols in the Melanocyte. *Pigment Cell Res*. 1988;1:54-60.
348. Luís R, Brito C, Pojo M. Melanoma Metabolism: Cell Survival and Resistance to Therapy. *Adv Exp Med Biol*. 2020;1219:203-223.
349. Kalinina E V., Chernov NN, Novichkova MD. Role of glutathione, glutathione transferase, and glutaredoxin in regulation of redox-dependent processes. *Biochem*. 2014;79(13):1562-1583.
350. Zuhra K, Tomé CS, Forte E, et al. The multifaceted roles of sulfane sulfur species in cancer-associated processes. *Biochim Biophys acta Bioenerg*. 2021;1862(2).
351. Cano-Galiano A, Oudin A, Fack F, et al. Cystathionine-γ-lyase drives antioxidant defense in cysteine-restricted IDH1-mutant astrocytomas. *Neuro-oncology Adv*. 2021;3(1).
352. Liu Y, Wang L, Zhang X, et al. A novel cystathionine γ-lyase inhibitor, I194496,

inhibits the growth and metastasis of human TNBC via downregulating multiple signaling pathways. *Sci Rep*. 2021;11(1).

353. Wang Y, Huang J, Chen W, et al. Dysregulation of cystathionine γ-lyase promotes prostate cancer progression and metastasis. *EMBO Rep*. 2019;20(10).
354. Zuhra K, Augsburger F, Majtan T, et al. Cystathionine-β-Synthase: Molecular Regulation and Pharmacological Inhibition. *Biomolecules*. 2020;10(5).
355. Feist M, Schwarzfischer P, Heinrich P, et al. Cooperative STAT/NF-κB signaling regulates lymphoma metabolic reprogramming and aberrant GOT2 expression. *Nat Commun*. 2018;9(1).
356. Hong R, Zhang W, Xia X, et al. Preventing BRCA1/ZBRK1 repressor complex binding to the GOT2 promoter results in accelerated aspartate biosynthesis and promotion of cell proliferation. *Mol Oncol*. 2019;13(4):959-977.
357. Corsello T, Komaravelli N, Casola A. Role of Hydrogen Sulfide in NRF2- and Sirtuin-Dependent Maintenance of Cellular Redox Balance. *Antioxidants*. 2018;7(10).
358. Itoh K, Chiba T, Takahashi S, et al. An Nrf2/small Maf heterodimer mediates the induction of phase II detoxifying enzyme genes through antioxidant response elements. *Biochem Biophys Res Commun*. 1997;236(2):313-322.
359. Escartin C, Won SJ, Malgorn C, et al. Nuclear Factor Erythroid 2-Related Factor 2 Facilitates Neuronal Glutathione Synthesis by Upregulating Neuronal Excitatory Amino Acid Transporter 3 Expression. *J Neurosci*. 2011;31(20):7392.
360. Song S, Nguyen V, Schrank T, et al. Loss of SWI/SNF Chromatin Remodeling Alters NRF2 Signaling in Non-Small Cell Lung Carcinoma. *Mol Cancer Res*. 2020;18(12):1777-1788.
361. Jin J, Chen F, He W, et al. YAP-Activated SATB2 Is a Coactivator of NRF2 That Amplifies Antioxidative Capacity and Promotes Tumor Progression in Renal Cell Carcinoma. *Cancer Res*. 2023;83(5).
362. Hu X, Zhang Y, Wang H, et al. BRD9 Facilitates Oncogenic Nrf2 Pathway and Dampens Venetoclax Sensitivity By Remodeling Chromatin Accessibility in Chronic Lymphocytic Leukemia. *Blood*. 2022;140(Supplement 1):356-357.
363. Santos I, Ramos C, Mendes C, et al. Targeting Glutathione and Cystathionine β-Synthase in Ovarian Cancer Treatment by Selenium-Chrysin Polyurea Dendrimer Nanoformulation. *Nutrients*. 2019;11(10).
364. Mendes C, Lopes-Coelho F, Ramos C, et al. Unraveling FATP1, regulated by

ER-β, as a targeted breast cancer innovative therapy. *Sci Rep*. 2019;9(1).

365. Serpa J, Mesquita P, Mendes N, et al. Expression of Lea in gastric cancer cell lines depends on FUT3 expression regulated by promoter methylation. *Cancer Lett*. 2006;242(2):191-197.
366. Silva LS, Goncalves LG, Silva F, et al. STAT3:FOXM1 and MCT1 drive uterine cervix carcinoma fitness to a lactate-rich microenvironment. *Tumour Biol*. 2016;37(4):5385-5395.
367. Hu DN. Methodology for Evaluation of Melanin Content and Production of Pigment Cells in Vitro†. *Photochem Photobiol*. 2008;84(3):645-649.
368. Hall MJ, Lopes-Ventura S, Neto M V., et al. Reconstructed human pigmented skin/epidermis models achieve epidermal pigmentation through melanocore transfer. *Pigment Cell Melanoma Res*. 2022;35(4):425-435.
369. Zoio P, Lopes-Ventura S, Oliva A. Barrier-on-a-chip with a modular architecture and integrated sensors for real-time measurement of biological barrier function. *Micromachines*. 2021;12(7):816.
370. Uslu U, Schliep S, Schliep K, et al. Comparison of the Serum Tumor Markers S100 and Melanoma-inhibitory Activity (MIA) in the Monitoring of Patients with Metastatic Melanoma Receiving Vaccination Immunotherapy with Dendritic Cells. *Anticancer Res*. 2017;37(9):5033-5037.
371. Harpio R, Einarsson R. S100 proteins as cancer biomarkers with focus on S100B in malignant melanoma. *Clin Biochem*. 2004;37(7):512-518.
372. Xavier R, Ferreira A. BRD9 as a Novel Susceptibility Gene for Familial Cutaneous Melanoma. 2021.
373. Bamford S, Dawson E, Forbes S, et al. The COSMIC (Catalogue of Somatic Mutations in Cancer) database and website. *Br J Cancer*. 2004;91(2):355.
374. Dankort D, Curley DP, Cartlidge RA, et al. BRafV600E cooperates with Pten silencing to elicit metastatic melanoma. *Nat Genet*. 2009;41(5):544.
375. Hsu MY, Meier FE, Nesbit M, et al. E-cadherin expression in melanoma cells restores keratinocyte-mediated growth control and down-regulates expression of invasion-related adhesion receptors. *Am J Pathol*. 2000;156(5):1515-1525.
376. Nunes SC, Serpa J. Glutathione in Ovarian Cancer: A Double-Edged Sword. *Int J Mol Sci*. 2018;19(7).
377. Nagahara N, Tanaka M, Tanaka Y, et al. Novel Characterization of Antioxidant Enzyme, 3-Mercaptopyruvate Sulfurtransferase-Knockout Mice: Overexpression

of the Evolutionarily-Related Enzyme Rhodanese. *Antioxidants (Basel, Switzerland)*. 2019;8(5).

378. Giuffrè A, Vicente JB. Hydrogen Sulfide Biochemistry and Interplay with Other Gaseous Mediators in Mammalian Physiology. *Oxid Med Cell Longev*. 2018;2018.
379. Matés JM, Pérez-Gómez C, De Castro IN, et al. Glutamine and its relationship with intracellular redox status, oxidative stress and cell proliferation/death. *Int J Biochem Cell Biol*. 2002;34(5):439-458.
380. Sahuri-Arisoylu M, Mould RR, Shinjyo N, et al. Acetate Induces Growth Arrest in Colon Cancer Cells Through Modulation of Mitochondrial Function. *Front Nutr*. 2021;8:588466.
381. Moffett JR, Puthillathu N, Vengilote R, et al. Acetate Revisited: A Key Biomolecule at the Nexus of Metabolism, Epigenetics, and Oncogenesis – Part 2: Acetate and ACSS2 in Health and Disease. *Front Physiol*. 2020;11:1451.
382. Mori N, Wildes F, Takagi T, et al. The tumor microenvironment modulates choline and lipid metabolism. *Front Oncol*. 2016;6(DEC):262.
383. Bagnoli M, Granata A, Nicoletti R, et al. Choline metabolism alteration: A focus on ovarian cancer. *Front Oncol*. 2016;6(JUN):153.
384. Meiser J, Schuster A, Pietzke M, et al. Increased formate overflow is a hallmark of oxidative cancer. *Nat Commun*. 2018;9(1).
385. de la Cruz-López KG, Castro-Muñoz LJ, Reyes-Hernández DO, et al. Lactate in the Regulation of Tumor Microenvironment and Therapeutic Approaches. *Front Oncol*. 2019;9:1143.
386. Napolitano A, Panzella L, Monfrecola G, et al. Pheomelanin-induced oxidative stress: Bright and dark chemistry bridging red hair phenotype and melanoma. *Pigment Cell Melanoma Res*. 2014;27(5):721-733.
387. Chedekel MR, Smith SK, Post PW, et al. Photodestruction of pheomelanin: role of oxygen. *Proc Natl Acad Sci U S A*. 1978;75(11):5395-5399.
388. Panzella L, Szewczyk G, D'Ischia M, et al. Zinc-induced structural effects enhance oxygen consumption and superoxide generation in synthetic pheomelanins on UVA/visible light irradiation. *Photochem Photobiol*. 2010;86(4):757-764.
389. Wenczl E, Van Der Schans GP, Roza L, et al. (Pheo)melanin photosensitizes UVA-induced DNA damage in cultured human melanocytes. *J Invest Dermatol*.

1998;111(4):678-682.

390. Hu DN, Wakamatsu K, Ito S, et al. Comparison of eumelanin and pheomelanin content between cultured uveal melanoma cells and normal uveal melanocytes. *Melanoma Res*. 2009;19(2):75-79.

391. Augsburger F, Szabo C. Potential role of the 3-mercaptopyruvate sulfurtransferase (3-MST)-hydrogen sulfide (H2S) pathway in cancer cells. *Pharmacol Res*. 2020;154.

392. Ostrakhovitch EA, Akakura S, Sanokawa-Akakura R, et al. Dedifferentiation of cancer cells following recovery from a potentially lethal damage is mediated by H2S-Nampt. *Exp Cell Res*. 2015;330(1):135-150.

393. Knethen V, Sousa Santos S, de Oliveira Cavalcanti Peres Rodrigues L, et al. Role of Cystathionine β-Synthase and 3-Mercaptopyruvate Sulfurtransferase in the Regulation of Proliferation, Migration, and Bioenergetics of Murine Breast Cancer Cells. *Antioxidants 2023, Vol 12, Page 647*. 2023;12(3):647.

394. Planchard D, Popat S, Kerr K, et al. Metastatic non-small cell lung cancer: ESMO Clinical Practice Guidelines for diagnosis, treatment and follow-up. *Ann Oncol Off J Eur Soc Med Oncol*. 2018;29(Suppl 4):iv192-iv237.

395. Molina JR, Yang P, Cassivi SD, et al. Non-small cell lung cancer: epidemiology, risk factors, treatment, and survivorship. *Mayo Clin Proc*. 2008;83(5):584-594.

396. Lin JJ, Shaw AT. Resisting Resistance: Targeted Therapies in Lung Cancer. *Trends in cancer*. 2016;2(7):350-364.

397. Esposito L, Conti D, Ailavajhala R, et al. Lung Cancer: Are we up to the Challenge? *Curr Genomics*. 2010;11(7):513-518.

398. Schiliro C, Firestein BL. Mechanisms of Metabolic Reprogramming in Cancer Cells Supporting Enhanced Growth and Proliferation. *Cells*. 2021;10(5).

399. Vander Heiden MG, DeBerardinis RJ. Understanding the Intersections between Metabolism and Cancer Biology. *Cell*. 2017;168(4):657-669.

400. García-Cañaveras JC, Lahoz A. Tumor Microenvironment-Derived Metabolites: A Guide to Find New Metabolic Therapeutic Targets and Biomarkers. *Cancers (Basel)*. 2021;13(13).

401. Mendes C, Lemos I, Francisco I, et al. NSCLC presents metabolic heterogeneity, and there is still some leeway for EGF stimuli in EGFR-mutated NSCLC. *Lung Cancer*. 2023;182:107283.

402. Mendes C, Serpa J. Revisiting lactate dynamics in cancer-a metabolic expertise

or an alternative attempt to survive? *J Mol Med (Berl)*. 2020;98(10):1397-1414.
403. Sonveaux P, Végran F, Schroeder T, et al. Targeting lactate-fueled respiration selectively kills hypoxic tumor cells in mice. *J Clin Invest*. 2008;118(12):3930.
404. Boidot R, Vegran F, Meulle A, et al. Regulation of monocarboxylate transporter MCT1 expression by p53 mediates inward and outward lactate fluxes in tumors. *Cancer Res*. 2012;72(4):939-948.
405. Faubert B, Li KY, Cai L, et al. Lactate Metabolism in Human Lung Tumors. *Cell*. 2017;171(2):358-371.e9.
406. Hui S, Ghergurovich JM, Morscher RJ, et al. Glucose feeds the TCA cycle via circulating lactate. *Nature*. 2017;551(7678):115-118.
407. Schnelldorfer T, Gansauge S, Gansauge F, et al. Glutathione Depletion Causes Cell Growth Inhibition and Enhanced Apoptosis in Pancreatic Cancer Cells. 2000.
408. Balendiran GK, Dabur R, Fraser D. The role of glutathione in cancer. *Cell Biochem Funct*. 2004;22(6):343-352.
409. Pan Y, Zhou C, Yuan D, et al. Radiation Exposure Promotes Hepatocarcinoma Cell Invasion through Epithelial Mesenchymal Transition Mediated by H2S/CSE Pathway. *Radiat Res*. 2016;185(1):96-105.
410. Gai JW, Qin W, Liu M, et al. Expression profile of hydrogen sulfide and its synthases correlates with tumor stage and grade in urothelial cell carcinoma of bladder. *Urol Oncol*. 2016;34(4):166.e15-166.e20.
411. Zivanovic J, Kouroussis E, Kohl JB, et al. Selective Persulfide Detection Reveals Evolutionarily Conserved Antiaging Effects of S-Sulfhydration. *Cell Metab*. 2019;30(6):1152-1170.e13.
412. Stipanuk MH. Sulfur amino acid metabolism: pathways for production and removal of homocysteine and cysteine. *Annu Rev Nutr*. 2004;24:539-577.
413. Yin J, Ren W, Yang G, et al. L-Cysteine metabolism and its nutritional implications. *Mol Nutr Food Res*. 2016;60(1):134-146.
414. Cao X, Ding L, Xie Z-Z, et al. A Review of Hydrogen Sulfide Synthesis, Metabolism, and Measurement: Is Modulation of Hydrogen Sulfide a Novel Therapeutic for Cancer? *Antioxidants Redox Signal*. 2019;31(1).
415. Chao C, Zatarain JR, Ding Y, et al. Cystathionine-beta-synthase inhibition for colon cancer: Enhancement of the efficacy of aminooxyacetic acid via the prodrug approach. *Mol Med*. 2016;22:361-379.

416. Weinstein JN, Collisson EA, Mills GB, et al. The Cancer Genome Atlas Pan-Cancer analysis project. *Nat Genet*. 2013;45(10):1113-1120.
417. Cerami E, Gao J, Dogrusoz U, et al. The cBio Cancer Genomics Portal: An Open Platform for Exploring Multidimensional Cancer Genomics Data. *Cancer Discov*. 2012;2(5):401-404.
418. Gao J, Aksoy BA, Dogrusoz U, et al. Integrative analysis of complex cancer genomics and clinical profiles using the cBioPortal. *Sci Signal*. 2013;6(269).
419. Borisov VB, Forte E. Impact of Hydrogen Sulfide on Mitochondrial and Bacterial Bioenergetics. *Int J Mol Sci*. 2021;22(23).
420. Cruz A, Mota P, Ramos C, et al. Polyurea Dendrimer Folate-Targeted Nanodelivery of l-Buthionine sulfoximine as a Tool to Tackle Ovarian Cancer Chemoresistance. *Antioxidants (Basel, Switzerland)*. 2020;9(2).
421. Kang YP, Torrente L, Falzone A, et al. Cysteine dioxygenase 1 is a metabolic liability for non-small cell lung cancer. *Elife*. 2019;8.
422. Jeelani R, Khan SN, Shaeib F, et al. Cyclophosphamide and acrolein induced oxidative stress leading to deterioration of metaphase II mouse oocyte quality. *Free Radic Biol Med*. 2017;110:11.
423. Chien CH, Hsueh WT, Chuang JY, et al. Dissecting the mechanism of temozolomide resistance and its association with the regulatory roles of intracellular reactive oxygen species in glioblastoma. *J Biomed Sci*. 2021;28(1):18.
424. He PJ, Ge RF, Mao WJ, et al. Oxidative stress induced by carboplatin promotes apoptosis and inhibits migration of HN-3 cells. *Oncol Lett*. 2018;16(6):7131.
425. Kleih M, Böpple K, Dong M, et al. Direct impact of cisplatin on mitochondria induces ROS production that dictates cell fate of ovarian cancer cells. *Cell Death Dis*. 2019;10(11).
426. Palakurthi S, Yellepeddi VK, Vangara KK. Recent trends in cancer drug resistance reversal strategies using nanoparticles. *Expert Opin Drug Deliv*. 2012;9(3):287-301.
427. Rizzo A, Napoli A, Roggiani F, et al. One-Carbon Metabolism: Biological Players in Epithelial Ovarian Cancer. *Int J Mol Sci*. 2018;19(7).
428. Mendes C, Lopes-Coelho F, Ramos C, et al. Unraveling FATP1, regulated by ER-β, as a targeted breast cancer innovative therapy. *Sci Rep*. 2019;9(1).
429. Kojima K, Nakamura T, Ooizumi Y, et al. Clinical significance of cancer specific

methylation of the CDO1 gene in small bowel cancer. *PLoS One*. 2019;14(1).

430. Deckers IAG, Schouten LJ, Van Neste L, et al. Promoter Methylation of CDO1 Identifies Clear-Cell Renal Cell Cancer Patients with Poor Survival Outcome. *Clin Cancer Res*. 2015;21(15):3492-3500.
431. Ushiku H, Yamashita K, Katoh H, et al. Promoter DNA methylation of CDO1 gene and its clinical significance in esophageal squamous cell carcinoma. *Dis esophagus Off J Int Soc Dis Esophagus*. 2017;30(2).
432. Li Y, Yan H, Xu X, et al. Erastin/sorafenib induces cisplatin-resistant non-small cell lung cancer cell ferroptosis through inhibition of the Nrf2/xCT pathway. *Oncol Lett*. 2020;19(1):323-333.
433. Jian Bagherpoor A, Shameem M, Luo X, et al. Inhibition of Lung Adenocarcinoma by Combinations of Sulfasalazine (SAS) and Disulfiram-copper (DSF-Cu) in Cell Line Models and Mice. *Carcinogenesis*. April 2023.
434. Szabo C. Gasotransmitters in cancer: from pathophysiology to experimental therapy. *Nat Rev Drug Discov*. 2016;15(3):185-203.
435. Ascenção K, Szabo C. Emerging roles of cystathionine β-synthase in various forms of cancer. *Redox Biol*. 2022;53.
436. Hellmich MR, Coletta C, Chao C, et al. The therapeutic potential of cystathionine β-synthetase/hydrogen sulfide inhibition in cancer. *Antioxid Redox Signal*. 2015;22(5):424-448.
437. Thorson MK, Majtan T, Kraus JP, et al. Identification of cystathionine β-synthase inhibitors using a hydrogen sulfide selective probe. *Angew Chem Int Ed Engl*. 2013;52(17):4641-4644.
438. Zhou Y, Yu J, Lei X, et al. High-throughput tandem-microwell assay identifies inhibitors of the hydrogen sulfide signaling pathway. *Chem Commun*. 2013;49(100):11782-11784.
439. Zuhra K, Sousa PMF, Paulini G, et al. Screening Pyridine Derivatives against Human Hydrogen Sulfide-synthesizing Enzymes by Orthogonal Methods. *Sci Reports 2019 91*. 2019;9(1):1-14.
440. Fantel AM, Myrianthopoulos V, Georgoulis A, et al. Screening of Heteroaromatic Scaffolds against Cystathionine Beta-Synthase Enables Identification of Substituted Pyrazolo[3,4-c]Pyridines as Potent and Selective Orthosteric Inhibitors. *Mol 2020, Vol 25, Page 3739*. 2020;25(16):3739.
441. Druzhyna N, Szczesny B, Olah G, et al. Screening of a composite library of

clinically used drugs and well-characterized pharmacological compounds for cystathionine β-synthase inhibition identifies benserazide as a drug potentially suitable for repurposing for the experimental therapy of colon cancer. *Pharmacol Res*. 2016;113(Pt A):18-37.

442. Ahmed D, Eide PW, Eilertsen IA, et al. Epigenetic and genetic features of 24 colon cancer cell lines. *Oncog 2013 29*. 2013;2(9):e71-e71.
443. Wang D, Wei G, Ma J, et al. Identification of the prognostic value of ferroptosis-related gene signature in breast cancer patients. *BMC Cancer*. 2021;21(1).
444. Yang Y, Yee D. IGF-I regulates redox status in breast cancer cells by activating the amino acid transport molecule xC−. *Cancer Res*. 2014;74(8):2295.
445. Stockwell BR, Friedmann Angeli JP, Bayir H, et al. Ferroptosis: A Regulated Cell Death Nexus Linking Metabolism, Redox Biology, and Disease. *Cell*. 2017;171(2):273-285.
446. Stockwell BR, Friedmann Angeli JP, Bayir H, et al. Ferroptosis: a regulated cell death nexus linking metabolism, redox biology, and disease. *Cell*. 2017;171(2):273.
447. Lopes-Coelho F, André S, Félix A, et al. Breast cancer metabolic cross-talk: Fibroblasts are hubs and breast cancer cells are gatherers of lipids. *Mol Cell Endocrinol*. 2018;462(Pt B):93-106.
448. Bezawork-Geleta A, Dimou J, Watt MJ. Lipid droplets and ferroptosis as new players in brain cancer glioblastoma progression and therapeutic resistance. *Front Oncol*. 2022;12:1085034.
449. Klasson TD, LaGory EL, Zhao H, et al. ACSL3 regulates lipid droplet biogenesis and ferroptosis sensitivity in clear cell renal cell carcinoma. *Cancer Metab*. 2022;10(1).
450. Basuroy T, Dreier M, Baum C, et al. Epigenetic and pharmacological control of pigmentation via Bromodomain Protein 9 (BRD9). *Pigment Cell Melanoma Res*. 2023;36(1):19.
451. Piskounova E, Agathocleous M, Murphy MM, et al. Oxidative stress inhibits distant metastasis by human melanoma cells. *Nature*. 2015;527(7577):186-191.
452. Gal K Le, Ibrahim MX, Wiel C, et al. Antioxidants can increase melanoma metastasis in mice. *Sci Transl Med*. 2015;7(308).
453. Kashif M, Yao H, Schmidt S, et al. ROS-lowering doses of vitamins C and A accelerate malignant melanoma metastasis. *Redox Biol*. 2023;60.

454. Kang YP, Torrente L, Falzone A, et al. Erratum: Correction: Cysteine dioxygenase 1 is a metabolic liability for non-small cell lung cancer (eLife (2019) 8 PII: e52671). *Elife*. 2019;8.
455. Tate JG, Bamford S, Jubb HC, et al. COSMIC: the Catalogue Of Somatic Mutations In Cancer. 2019;47(D1):D941-D947.
456. Fahrmann JF, Tanaka I, Irajizad E, et al. Mutational Activation of the NRF2 Pathway Upregulates Kynureninase Resulting in Tumor Immunosuppression and Poor Outcome in Lung Adenocarcinoma. *Cancers (Basel)*. 2543;2022:2543.
457. Yue T, Li J, Zhu J, et al. Hydrogen Sulfide Creates a Favorable Immune Microenvironment for Colon Cancer. *Cancer Res*. 2023;83(4):595-612.
458. Tirinato L, Pagliari F, Di Franco S, et al. ROS and Lipid Droplet accumulation induced by high glucose exposure in healthy colon and Colorectal Cancer Stem Cells. *Genes Dis*. 2019;7(4):620-635.
459. Yang F, Xiao Y, Ding JH, et al. Ferroptosis heterogeneity in triple-negative breast cancer reveals an innovative immunotherapy combination strategy. *Cell Metab*. 2023;35(1):84-100.e8.
460. Zou Y, Xie J, Zheng S, et al. Leveraging diverse cell-death patterns to predict the prognosis and drug sensitivity of triple-negative breast cancer patients after surgery. *Int J Surg*. 2022;107.